Electronic Thesis and Dissertation Repository

12-14-2010 12:00 AM

A Step towards Continuous Production of NaY Zeolite in Amorphous Silica Particles using a Dry Process

Syed Sameen Ali Zaidi, *The University of Western Ontario*

Supervisor: Sohrab Rohani, *The University of Western Ontario*
A thesis submitted in partial fulfillment of the requirements for the Doctor of Philosophy degree in Chemical and Biochemical Engineering
© Syed Sameen Ali Zaidi 2010

A Step towards Continuous Production of NaY Zeolite in Amorphous Silica Particles using a Dry Process

(Spine title: Synthesis of NaY Zeolite in Amorphous Silica Particles using a Dry Process)

(Thesis Format: Integrated Article)

By:

Syed Sameen Ali Zaidi

Graduate program in Engineering Science
Department of Chemical and Biochemical Engineering

A thesis submitted in partial fulfillment
of the requirement for the degree of
Doctor of Philosophy

School of Graduate and Postdoctoral Studies
The University of Western Ontaio
London, Ontario, Canada

THE UNIVERSITY OF WESTERN ONTARIO
School of Graduate and Postdoctoral Studies

CERTIFICATE OF EXAMINATION

Supervisor

_____
Dr. Sohrab Rohani

Supervisory Committee

_____
Dr. Anand Prakash

_____
Dr. Dimitre Karamanev

Examiners

_____
Dr. Anand Prakash

_____
Dr. Shahzad Barghi

_____
Dr. Ronald Martin

_____
Dr. David Ward

The thesis by

Syed Sameen Ali Zaidi

entitled:

A Step towards Continuous Production of NaY Zeolite in Amorphous Silica Particles using a Dry Process

is accepted in partial fulfillment of the
requirements for the degree of
Doctor of Philosophy

Date_____   _____
                                              Chair of the Thesis Examination Board

ABSTRACT

This thesis is focused on the synthesis of nano-size $(50-100nm)$ NaY zeolite crystals inside the micro/meso pores of preshaped amorphous silica particles of size $50\mu m$ using a dry process, which reduced several operational steps and the zeolite synthesis time that are generally required for current in-practice processes. Three types of reactors namely; polypropylene bottles, a stainless steel tubular reactor, and a novel vibrated baffles fluidized bed (VBFB) reactor coupled with infrared radiation emitters were used to evaluate the effects of different operating parameters on the synthesis of NaY zeolite. The synthesis process took place without using any structure directing agent and, due to using a dry synthesis technique, no significant chemical waste was generated. A parametric study revealed that an SiO_2/Al_2O_3 ratios above 6.6 did not produce any appreciable zeolite within the time frame of 24 h at $100^{\circ}C$. The optimal SiO_2/Al_2O_3 ratio was found to be 6.1 for 16 h of synthesis at $100^{\circ}C$ in polypropylene bottles. The use of a stainless steel tubular reactor reduced the synthesis time to 8 h owing to its higher thermal conductivity as compared to polypropylene. Synthesis in the stainless steel tubular reactor reduced the synthesis time to 15 min while operating at $170^{\circ}C$ without any zeolite phase transformation. An operating temperature beyond $170^{\circ}C$ was not recommended due to NaY zeolite phase transformation to analcime. The effects of different concentrations of NaOH revealed that concentrations below $20wt\%$ retarded the synthesis process whereas higher concentrations up to $32wt\%$, not only accelerated the synthesis but also resulted in the production of smaller crystals, less than $50nm$ in size. An NaOH concentration beyond $32wt\%$ was not recommended due to dissolution and loss of structure of silica particles. The novel VBFB reactor produced single crystals in the size range of $300-600nm$ at $100^{\circ}C$ in 5 min. Using IR radiation for fast heat transfer accelerated the surface integration mechanism and led to the growth of crystals in 5 min. The synthesized NaY zeolite was tested for FCC reaction in a riser simulator after an ion-exchange with NH_4NO_3. A high conversion of 1,3,5-tri-isopropylbenzene in the range of 55-65% was obtained with a loss in conversion by 10% after regeneration. The as-synthesized

NaY zeolite within silica particles was also tested for desulfurization of model hydrocarbons containing thiophene. The desulfurization through adsorption was achieved by removing thiophene from 500 ppmw to less than 15 ppmw in hexanes and a mixture of p-xylene in hexanes. The removal of 500 ppmw thiophene could not be achieved below 300 ppmw while using the mixture of toluene in hexanes. The as-synthesized NaY zeolite performed better for thiophene removal as compared to other adsorbents like silica, commercial NaX and NaY pellets, and commercial NaY fine powder.

Statement of Co-Authorship

Chapter 2: The author drafted the original draft of this chapter. Dr. S. Rohani reviewed it and made revisions for improvements. A version of this chapter has been published in the following journal:

- Syed Sameen Ali Zaidi and Sohrab Rohani, "Progress Towards a Dry Process for the Synthesis of Zeolite - A Review", *Reviews in Chemical Engineering*, 2005, 21(5), pp. 265-306.

ACKNOLEDGEMENTS

I would like to extend my heartfelt thanks to my advisor, Dr. Sohrab Rohani, for guidance throughout my doctoral study and research at The University of Western Ontario. He continually inspired and motivated me with his enthusiasm and energy in research.

I would like to thank Dr. Anand Prakash and Dr. Dimitre Karamanev as the members of my advisory committee for providing me valuable advice from time to time.

My special thanks go to Dr. Maurice Bergougnou who not only helped me in designing the fluidized bed reactor system but also provided me valuable professional tips.

I am further thankful to Dr. Prakash for providing me all possible help during desulfurization study. I am also grateful to Dr. Amarjeet Bassi for allowing me to use his gas chromatograph for carrying out analysis for desulfurization study.

I extend my thanks to Dr. Hugo deLasa for providing me his facility of CREC riser simulator to conduct FCC reaction study.

My sincere thanks go to the team of The University of Western Ontario Engineering Machine Services for making my drawing board sketches into reality.

I am grateful to Joanna Bloom, the graduate affairs coordinator for helping the department to run smoothly and for assisting me in many different ways.

My deepest gratitude goes to my parents and family for their continuous love and support throughout my life. This thesis would have been simply impossible without them. I am indebted to my loving wife Deenaz for her perpetual support, love, and patience for me. She also did proof reading of my thesis and provided me with valuable tips. Most importantly, I wish to thank my adorable daughter Manaal for being the integral part of my life.

I would like to thank all people who have helped and inspired me during my doctoral study.

TABLE OF CONTENTS

CHAPTER 3: SYNTHESIS OF NaY ZEOLITE IN PRESHAPED

          AMORPHOUS SILICA PARTICLES THROUGH

CHAPTER 4: EFFECTS OF VARIOUS OPERATING CONDITIONS

          ON THE DRY SYNTHESIS OF NANOSIZED NaY

List of Tables

List of Figures

NOMENCLATURE

Abbreviations

$AlPO_4$	aluminum phosphate molecular sieve
ANA	analcime
BEA	beta zeolite
BET	Brunauer-Emmett-Teller
BJH	Barett-Joyner-Halenda
CHA	Chabazite
CREC	Chemical Reactor Engineering Centre
DGC	dry gel conversion
DTG	differential thermogravimetry
EDA	ethylenediamine
EDP	electron diffraction pattern
EDX	energy dispersion x-ray
EMT	EMC-2
EPA	US Environmental Protection Agency
EUER	European Union Emission Regulations
EXAFS	X-Ray Absorption Fine Structure
FAU	Faujasite Structure
FCC	fluid catalytic cracking
FER	Ferrierite
FPD	flame photometric detector
FTIR	Fourier Transform Infrared
HDS	hydrodesulfurization
HMBr	hexamethonium bromide
HRTEM	high resolution transmission electron microscopy
HTS	hydrothermal synthesis
HZSM-5	ZSM-5 with H^+
IR	infrared
IZA	International Zeolite Association

MAPO	aluminophosphate molecular sieve
MAS NMR	Magic Angle Spinning Nuclear Magnetic Resonance
MFI	zsM(Five) zeolite
MOR	Mordenite
MTW	ZSM-12
PI	Proportional and Integral (Chap. 5)
PXRD	Powder X-Ray Diffraction
SAC	steam-assisted conversion
SAPO-5	Silico-Alumino-Phosphate zeolite
SAXS	Small Angle X-ray Scattering
SEM	scanning electron microscope
TAA	tetraalkylammonium ions, TAA^+
T-atoms	Si or Al atoms
TEA	tetraethylammonium
TEAOH	tetraethylammonium hydroxide
TEM	transmission electron microscopy
TMA	tetramethylammonium
TPA	tetrapropylammonium
TPABr	tetrapropylammonium bromide
TS	titanosilicalite
USY	Ultrastable Y Zeolite
UWO	University of Western Ontario
VBFB	vibrated baffles fluidized bed
VPT	vapor-phase transport
XANES	X-ray Absorption Near Edge Structure
XRA	X-Ray Amorphous
XRD	X-Ray Diffraction
XRF	x-ray florescence
ZSM	Zeolite Scony Mobil

Symbols

A	bed cross-section area, m^2

Ar	Archimedes Number
B	*Barometric pressur ,mmHg*
c	solution concentration, $kmol/m^3$ (Chap. 2)
c^*	equilibrium concentration, $kmol/m^3$ (Chap. 2)
c	speed of light, $3X10^8$ m/s
C_D	drag coefficient, dimensionless
d_p	diameter of particle, m or $\mu m = 1X10^{-6} m$
e	*vapour pressure of moisture in air, mmHg*
E_b	emissive power of a black body, W/m^2
f_z	fraction of zeolite formed
F_{ij}	shape or view factor between surfaces i and j
h	Plank's constant, $6.625X10^{-34}$ J.s (Chap.5)
H	bed height, m
k	Boltzmann constant, $1.38066X10^{-23}$ J/molecule.K (Chap. 5)
K	proportionality constant (Appen. A)
Q	flowrate, m^3/s (Appen. A)
Q_r	radiation heat transfer, W (Chap. 5)
r_c	critical radius, m
Re	Renolds Number, $\dfrac{\rho_g v_g d_p}{\mu_g}$
S	super-saturation ratio
t_g	time required for nuclei to grow to detectable size, s or h
t_n	time required for stable nuclei, s or h
t_r	relaxation time, s or h
T	*Temperatur e, K*
T	Si or Al
u_{mf}	minimum fluidization velocity , m/s
υ	molecular volume or molar volume, m^3/mol (Chap. 2)

W	weight, kg
z	distance, m,
α	absorptivity (Chap. 5)
ΔP	pressure drop, N/m^2 or Pa
ε	emissivity (Chap. 5)
ε	porosity, (Appen. A)
λ	wavelength, m or $\mu m = 1 X 10^{-6} m$
μ	dynamic viscosity, cP, or Pa.s
$v = \dfrac{\mu}{\rho}$	Kinematic viscosity, m^2/s
ρ	reflectivity (Chap. 5)
ρ	density, kg/m^3 (Appen. A)
ρ_{air}	density of air, kg/m^3
σ	Stefan-Boltzmann constant, $5.669 X 10^{-8}$ $W/m^2.K^4$ (Chap. 5)
σ	interfacial tension (surface energy per unit area), J/m^2 or N/m[Chap. 2]
τ	induction time, s or h (Chap. 2)
τ	transmissivity (Chap. 5)
ϕ	sphericity of the particle

Subscripts

g	gas, or air
mf	minimum fluidization
o	orifice
p	particle
t	terminal

CHAPTER 1: INTRODUCTION

_____

1.1   INTRODUCTION

Zeolites are crystalline aluminosilicates with a three dimensional fully cross-linked open framework structure that forms uniformly sized pores of molecular dimensions. These crystalline aluminosilicates are made up of corner-sharing SiO_4 and AlO_4 tetrahedra. The pore size of the zeolite plays an important role for adsorbing molecules of different sizes like a molecular sieve. Therefore, molecules of a certain size are adsorbed by the zeolites and others which are larger than the pore size are not adsorbed. A naturally occurring zeolite called stilbite was discovered by Cronstedt who observed that this mineral started to lose water upon heating, thus the term zeolite (boiling stone) was coined. The framework of zeolite containing Si^{4+} is replaced by Al^{3+} at many places in the framework thus making the framework carry a net negative charge. The negative charge is balanced by a non-framework loosely attached alkali metal cation which sits within the cavities and maintains an overall electroneutrality of the zeolite. These alkali metal cations are capable to ion-exchange with other cations which make them to react reversibly with polar molecules. The reaction properties of zeolites have made them commercially viable for several industrial applications.

The diversification in industrial application was first realized by R.M. Barrer in the area of adsorption which triggered the synthesis era of synthesized zeolites. The commercially viable synthetic zeolites A, X, and Y were synthesized by R.M. Milton and D.W. Breck in the 1940's and early 1950's. Since then more than 150 types of synthetic zeolites have been synthesized. Many, but not all, find useful industrial applications in the areas of petroleum refining and chemical process industries as selective adsorbents, catalyst and ion-exchangers, thus building an estimated more than two billion dollar industry (Flanigen 2001).

The Y zeolite has drawn a lot of attention in the petroleum industry due to its application in the area of fluidized catalytic cracking (FCC) as about 40% of the gasoline production is obtained through FCC process. The generally used crystal size is in the

range of 1-2 micrometer. The pore size of the Y zeolite is sufficient to allow gas oil molecule to enter the pore and react, though the gas oil molecule size is bigger than the pore size (Scherzer 1989). The molecules are flexible to snuggle into the pore but pose a diffusion resistance. The diffusion resistance can be reduced by using smaller size crystals in the range of sub-micrometer to nanometer size so that the reactants may easily reach the active sites for reaction. In general, the crystal size of 100 nm or smaller falls under the category of nano-sized particles.

The petroleum products which are used in everyday consumption especially in the automobile industry pose several threats to environment. These threats are the production of acid rain, smog, and green house gases emissions. So far several steps have been taken by governments to reduce such threats. One of the steps includes the reduction in sulfur compounds emissions which are the main source of acid rain. To enforce sulfur emission reduction, North America has implemented a policy of a maximum of 30 ppmw sulfur compounds in gasoline, and 15 ppmw sulfur compounds in diesel fuel since 2006. According to European Union emission regulations the sulfur-free diesel and gasoline fuels with 10 ppm of sulfur was available since from 2005, and became mandatory from 2009 (EPA 1999; Internet 2010b; Internet 2010a). The existing process to address sulfur compounds reduction is called hydrotreating or hydrodesulfurization process. This process involves stringent process conditions of high temperature and pressure, and consumption of valuable hydrogen (Avidan *et al.* 2001; Babich and Moulijn 2003). To meet the current challenge of low sulfur emission and also to reduce the cost, the process of desulfurization of hydrocarbons is focusing on the use of Y zeolite for selective removal of sulfur compounds. The use of Y zeolite in desulfurization of hydrocarbons has potential as an alternative, or supplement, to the existing hydrodesulfurization process.

The zeolites are normally synthesized through hydrothermal process by reacting silica alumina gel in alkaline solution under mild conditions with temperatures in the range of $100 - 200^\circ C$ (Bhatia 1990; Szostak 1998). An expensive structure directing agent (SDA) may or may not be used to get the desired zeolite phase. The solution based synthesis produces waste at the end of the synthesis process. Also, it takes days to get the finished product in a batch process. Many excellent studies have been performed to meet

the challenges of reducing the synthesis time, particle size, and the waste production, in addition to change the process to a continuous production facility. The synthesis in confined space, synthesis from clear solution, microwave heating, parallel processing of batches are some of the examples which have been tried to handle some of the difficulties face by the zeolite synthesis process (Arafat *et al.* 1993; Rollmann and Valyocsik 1983; Schmidt *et al.* 2000; Serrano and Grieken 2001; Valyocsik 1983; Koegler and Yeh 2003; Li *et al.* 2002; Murrell *et al.* 1999; Park *et al.* 2001; Schoeman *et al.* 1994; Slangen *et al.* 1997).

The synthesis of NaY zeolite in a confined space has been the focus of this study to address the existing limitations of the commercial Y zeolite due to the crystal size, narrower particle size distribution, and to minimize the waste generation. Special attention is paid to the synthesis using an almost dry process instead of using the conventional solution based method. The dry process is lucrative in the sense that it produces negligible waste. All the reactants including source of silica and source of alumina are precisely used and do not generate any waste. The dry synthesis process provides a better control on the reactants selection and adjusting the desired ratios. The confined space methodology provides a narrower particle size distribution and better crystal size control through carefully selecting the quantity and concentration of source of alkali metal cation. The other focal point of this study is the reduction of synthesis time. Different types of reactors with different heating modes are used to reduce the synthesis time. The combination of dry synthesis process and the use of different types of reactors with different heating modes is pivotal in reducing the synthesis time from days to hours, and from hours to minutes. The developed synthesis techniques are further translated into real situation by testing the finished product for different applications such as FCC process, and the desulfurization of hydrocarbons.

1.2   SCOPE OF THE RESEARCH

The aims of this research are to investigate the synthesis of NaY zeolite crystals inside the micro/meso pores of pre-shaped amorphous silica particles with an average particle size of $50 \mu m$ in polypropylene bottles, stainless steel tubular reactor, and a novel vibrated baffles fluidized bed (VBFB) reactor coupled with infrared radiation using a batch process. The concept of using infrared radiation for the synthesis reaction is implemented for the first time. The batch synthesis is further analyzed for parametric sensitivity studies to optimize the operating conditions for the process. The ultimate aim of this study is to make the synthesis of nano-sized NaY zeolite possible in the size range of $50 - 100 nm$ and reduce the synthesis time from 24 hours to 5 minutes. The information obtained from batch process may be utilized to transform the batch process into a continuous process. The synthesized product is tested for fluid catalytic cracking reaction in a fluidized bed riser simulator using a model compound. The product is further tested for desulfurization of hydrocarbons using a model compound. The results are compared with the performance of commercial Y zeolite.

These aims are achieved in various chapters of the thesis:

- In Chapter 2 a comprehensive literature review is carried out to understand the basics of zeolites, their general structures, and some applications. The review further focuses on the synthesis methods and describes various stages by which the zeolite synthesis progresses starting from the amorphous phase solution followed by induction, nucleation, and crystal growth. The effects of several parameters on crystal growth such as ageing, alkali metal cation type, and organic templates are also reviewed. The possibility of two types of crystal growth mechanisms i.e. homogeneous and heterogeneous mechanisms are reviewed and the focus is shifted towards the heterogeneous mechanism which is due to solid-solid transformation. The heterogeneous mechanism leads to the dry gel synthesis. A comparison is made between the dry gel synthesis and the conventional solution based hydrothermal synthesis. It also describes the advantages of dry process over the solution based process in terms of product

purity and the possibility of certain product which is not achievable through solution based process. Also the role of water in dry synthesis is reviewed.

- Chapter 3 comprises the synthesis of NaY zeolite using a modified adapted technique. For the synthesis, pre-shaped silica particles with an average size of $50\,\mu m$ are embedded with alumina in three stages and finally NaOH is added to carry out the synthesis at $100^{\circ}C$ for 16 h using polypropylene bottles. The process takes place on dry basis as the silica particles do not lose their shape or form a paste during the various stages of the synthesis process. This technique is able to produce NaY zeolite crystals in the size range of $100-200nm$ with a cluster size around 1-2 micrometer. The crystals are embedded inside the silica particles.

- Chapter 4 focuses on the effects of various operating conditions on the synthesis of nano-sized NaY zeolite within pre-shaped silica particles of size $50\,\mu m$ using two different types of reactors i.e. polypropylene bottles and a stainless steel tubular reactor. The general synthesis technique is the same as described in Chapter 3; however, the quantities and concentrations of different chemicals are changed. The operating conditions include SiO_2/Al_2O_3 ratio, ageing and synthesis time, synthesis temperature, type of reactor, and concentration of NaOH. The effects of operating conditions reveal how different SiO_2/Al_2O_3 ratios may affect the synthesis rate. It also discusses why a higher SiO_2/Al_2O_3 ratio may slow down the synthesis process. The positive effect of the rise in synthesis temperature on the zeolite formation is shown. It also discusses the limit of higher temperature of $170^{\circ}C$ and why a higher synthesis temperature may cause more harm than to produce any improvement in the synthesis rate. Due to dry synthesis, the role of concentration the of NaOH becomes important. It discusses why beyond the $32wt\%$ concentration of NaOH a desired product is not possible. Also, concentrations lower than $20wt\%$ of NaOH make the synthesis process very slow. Further the NaOH concentration is linked with the size of the crystal. It is possible to obtain crystals smaller than 50 nm by using higher NaOH concentrations. The use of

different types of reactors reveals some interesting results. The stainless steel reactor surpasses the polypropylene reactor in acquiring higher synthesis rate and significant reduction in synthesis time. The higher heat transfer rate in stainless steel reactors is believed to be important, which suggests developing a reactor system with fast heat transfer rates.

- Chapter 5 includes the detailed design calculations of a novel vibrated baffles fluidized bed (VBFB) reactor. The reactor is coupled with infrared radiation emitters for fast heating. The novel idea of using infrared radiation for fast synthesis is discussed and compared with another fast zeolite synthesis technique using microwaves as the primary source of heating. It further discusses the advantage of infrared radiation under dry synthesis conditions as compared to a microwave synthesis technique which is being tested in solution based synthesis. The design conditions are changed in the novel reactor system; therefore, a different zeolite synthesis technique is developed. This technique includes the adjustment of the SiO_2 / Al_2O_3 in two steps instead of three, used in the previous chapters. The effects of different operating conditions in the novel reactor system are studied. These include the time of reaction, and quantity of NaOH solution in the pores of silica particles.

- The NaY zeolite synthesized in the laboratory is further tested for two different applications. The first application is in the field of the fluidized catalytic cracking (FCC) reaction. For this purpose, the NaY zeolite is subjected to ion-exchange to replace Na^+ with H^+ in order to behave as FCC catalyst. Since the laboratory prepared zeolite is embedded in silica particles no further processing is needed and it is directly used for FCC reaction. Chapter 6 discusses the catalyst preparation and its testing for FCC reaction using a riser simulator (CREC-RISER simulator, The University of Western Ontario). Chapter 6 further discusses the role of as-synthesized laboratory NaY zeolite for the removal of thiophene from different hydrocarbons at room temperature. It describes the design of the experimental setup for this purpose. It further shows how quick or slow thiophene removal is possible from different hydrocarbons. The ambient temperature has a significant effect on desulfurization as compared

to the conventional hydrodesulfurization process. A comparison is also made with different adsorbents including commercially available NaX and NaY zeolites.

- Chapter 7 sheds light on our findings. The NaY zeolite synthesis and parametric studies using different types of reactors under different heating modes are able to reduce the crystal size from 200nm to less than 50 nm with a reduction in synthesis time from 24 h to 5 min. The idea of using IR radiation in novel vibrated baffles fluidized bed (VBFB) reactor system is successful in reducing the synthesis time to 5 min. The testing of lab synthesized zeolite for FCC reaction in riser simulator results in high conversion. Also, the testing of the as-synthesized NaY zeolite for desulfurization of thiophene from hydrocarbons is very successful. A 500 ppmw concentration of thiophene in hydrocarbons is reduced to less than 15 ppm in a matter of 5 min.

1.3   THE MOST IMPORTANT CONTRIBUTION OF THE THESIS

The most important contribution of this research study is that we are successful in not only reducing the size of the NaY zeolite from 200nm to less than 50 nm, but at the same time, the dry synthesis process reduces the synthesis time from 24 h to 5 min. The idea of synthesizing NaY zeolite within the amorphous silica particles works well with a fluidized bed system. It will be useful to all those applications where pressure drop is a concern e.g. packed bed system. Basically using Y zeolite synthesized in silica particles not only eliminates the step of loading zeolites in an inert matrix e.g. FCC catalyst but at the same time it will provide a direct application of submicometer to nano-sized crystals in industry. The direct application of submicron to nano-sized crystals is not suitable for industry unless a certain treatment is given to raw crystals e.g. making pellets in millimeters size. The diffusion resistance is an inherent issue with pellets and when used in packed bed they cause pressure drop as well. In this view, one quick example of our synthesized zeolite can be taken as the desulfurization of hydrocarbons where using our zeolite arrangement in silica particle can be used in fluidized bed system without any further treatment of small sized crystals and it will eliminate the use of packed bed system for any such application.

For the first time we are able to use IR radiation for fast synthesis reaction. The novel vibrated baffles fluidized bed (VBFB) reactor system is designed to take $50\,\mu m$ silica particles for reaction and the IR radiation reduce the synthesis time to 5 min. The reduction in synthesis time will be a key step towards a continuous process for zeolite synthesis.

1.4   REFERENCES

EPA (US Environmental Protection Agency). Report EPA420-F-99-051. 1999. EPA.

Arafat, A., Jansen, J. C., Ebaid, A. R., van Bekkum, H. "Microwave Preparation of Zeolite Y and ZSM 5." *Zeolites*, 1993, *13* (3), 162-165.

Avidan, A., Klein, B., Ragsdale, R. "Improved planning can optimize solutions to produce clean fuels." *Hydrocarbon Process., Int.Ed.*, 2001, *80* (2), 47-50, 53.

Babich, I. V. and Moulijn, J. A. "Science and technology of novel processes for deep desulfurization of oil refinery streams: a review." *Fuel*, 2003, 82(6), 607-631.

Bhatia, S. *Zeolite Catalysis Principles and Applications*. Fla.: CRC Press Boca Raton, 1990.

Flanigen, E. M. "Zeolites and molecular sieves: An historical perspective." *Stud.Surf.Sci.Catal.*, 2001, *137* (Introduction to Zeolite Science and Practice (2nd Edition)), 11-35.

Internet. EPA (US Environmental Protection Agency) Tier 2 Regulations., http://www.dieselnet.com/standards/us/ld_t2.php , 2010a.

Internet. European Union emission regulations., http://www.dieselnet.com/standards/eu/ld.php , 2010b.

Koegler, J. H., and Yeh, C. "Nanocrystalline inorganic based zeolite and method for making same." (ABB Lummus Global Inc. 2002-67719(20030147805), 12. 8-7-2003. US. 2-5-2002.

Li, Q., Creaser, D., Sterte, J. "An Investigation of the Nucleation/Crystallization Kinetics of Nanosized Colloidal Faujasite Zeolites." *Chem.Mater.*, 2002, *14* (3), 1319-1324.

Murrell, L. L., Overbeek, R. A., Chang, Y.-F., Puil, N. V. D., and Yeh, C. Y. "Method for Making Molecular Sieves and Novel Molecular Sieve Compositions." (6,004,527). 1999. USA.

Park, S.-E., Kim, D. S., Chang, J. S., and Kim, J. M. "Continuous Process and Apparatus for Preparing Inorganic Materials Employing Microwave." (US Patent 2001054549). 2001. USA.

Rollmann, L. D. and Valyocsik, E. W. "Continuous-Stream Upflow Zeolite Crystallization Apparatus." (US Patent 4,374,093). 1983.

Scherzer, J. "Octane-enhancing, zeolitic FCC catalysts: scientific and technical aspects." *Catal.Rev.- Sci.Eng.*, 1989, 31(3), 215-354.

Schmidt, I., Madsen, C., Jacobsen, C. J. H. "Confined space synthesis. A Novel Route to Nanosized Zeolites." *Inorg.Chem.*, 2000, *39* (11), 2279-2283.

Schoeman, B. J., Sterte, J., Otterstedt, J.-E. "Colloidal Zeolite Suspensions." *Zeolites*, 1994, *14* (2), 110-116.

Serrano, D. P., Van Grieken, R. "Heterogeneous Events in the Crystallization of Zeolites." *J.Mater.Chem.*, 2001, *11* (10), 2391-2407.

Slangen, P. M., Jansen, J. C., van Bekkum, H. "The effect of ageing on the microwave synthesis of zeolite NaA." *Microporous Mater.*, 1997, *9* (5,6), 259-265.

Szostak, R. *Molecular Sieves*. London. UK: Blackie Academic & Professional, 1998.

Valyocsik, E. W. "Apparatus for a continuous down-flow zeolite production." (US Patent 4,368,174). 1983.

CHAPTER 2.   LITERATURE REVIEW

2.1 INTRODUCTION

Zeolites were first recognized as a new type of minerals in 1756 by a Swedish mineralogist, A. Cronstedt. He named this mineral "zeolite" (Greek word: meaning boiling stone) as it seemed to boil at high temperature due to high water content (Serrano and Grieken 2001). Since then, many types of naturally occurring zeolites have been found, such as: chabazite, erionite, faujasite, mordenite, etc. (Othmer 1984). Zeolites consist of microporous crystalline aluminosilicates and possess properties of adsorption, reaction, and ion-exchange. The first industrially important zeolite was produced in 1942. Since then, more than 150 synthetic zeolites have been reported. At present, over 130 types of zeolite structures are approved by the International Zeolite Association (IZA). Currently only a few are of commercial importance such as, type A, X, Y, Z, L, ZSM-5, etc. (Corma and Wojciechowski 1985). The primary building block of all zeolites is a tetrahedron of four oxygen anions that surround a silicon or aluminum ion, as shown in Figure 2.1(a).

These tetrahedra are arranged in such a way that each of the four oxygen anions is further shared by another silica or alumina tetrahedron. The crystalline framework extends in three dimensions, therefore the -2 oxidation state of each oxygen is accounted for. The $+4$ charge on each silicon ion is balanced by the four tetrahedral oxygen making the silica tetrahedral electrostatically neutral. On the other hand, the $+3$ charge on aluminum is not balanced by the surrounding four tetrahedral oxygens, leaving a residual charge of -1 on each alumina tetrahedron. Thus each alumina tetrahedron requires a $+1$ charge from a cation in the structure to be electrostatically neutral, as shown in Figure 2.1(b). The cations providing electric stability to alumina tetrahedron are generally sodium in the zeolite where they occupy non-framework positions.
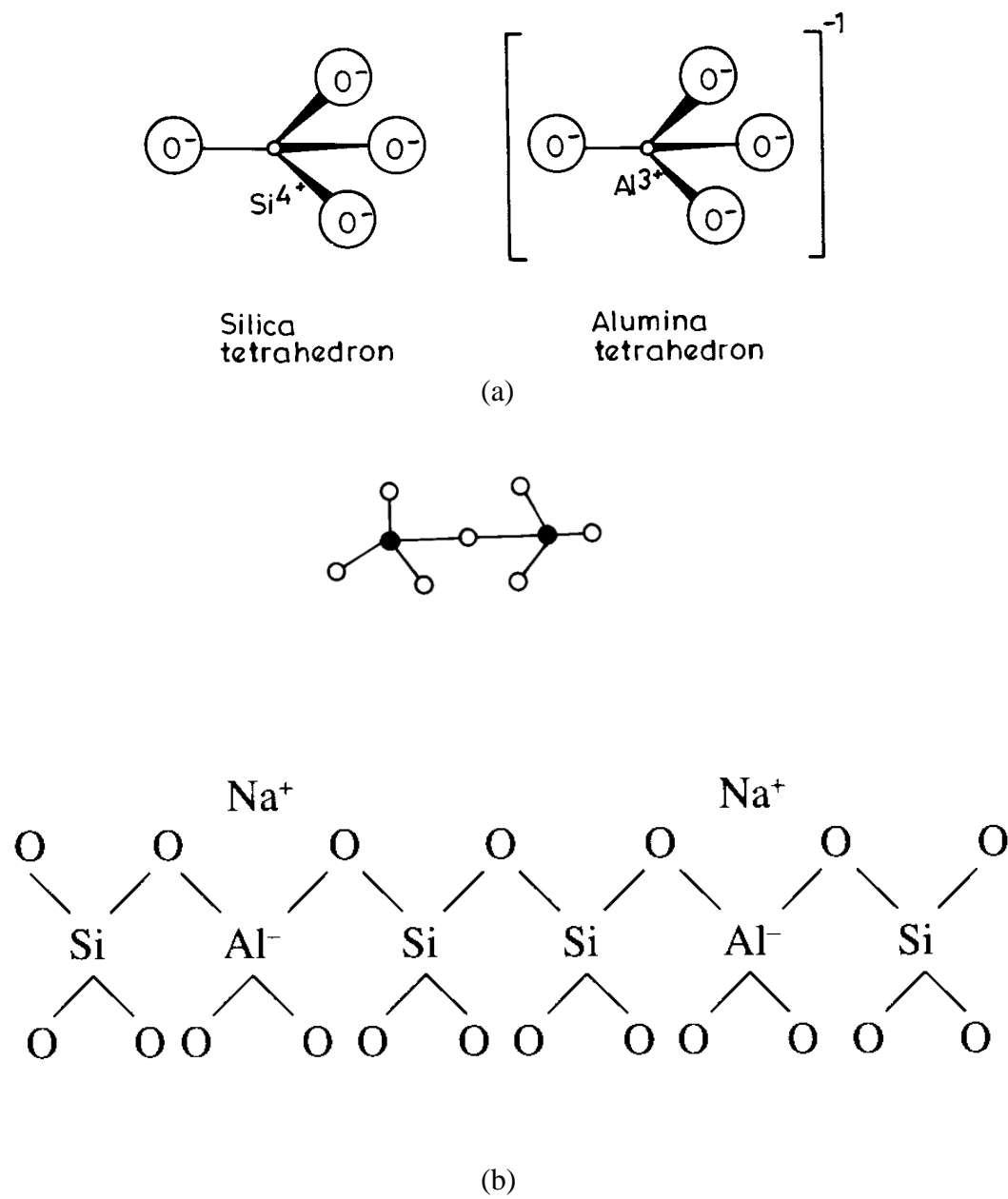
Figure 2.1: (a) Primary building blocks of zeolites, (b) Simplified surface structure of zeolite

For any specific application, the cations can be replaced by ion exchange, which is the most direct and useful method to change the properties of zeolites. The building block of the zeolite crystal structure is formed by the combination of silica and alumina tetrahedra into more complicated secondary units. The silica and alumina tetrahedral are geometrically arranged with the exception of Al-O-Al bonds. The unit cell formula is generally written as:

$$M_{2/n}O \cdot Al_2O_3 \cdot xSiO_2 \cdot YH_2O \tag{2.1}$$

where M represents the exchangeable cations, generally from group I or II ions, although other metallic, non-metallic, or organic cations may be used to balance the charge on framework; n represents the cation valence. These cations are present either during the synthesis or through post-synthesis ion-exchange. The value of x is equal to or greater than 2, as alumina tetrahedron does not occupy adjacent tetrahedral sites. Y value represents the degree of hydration.

The tetrahedra are arranged in such a way that the zeolites have an open framework structure with a large surface area. The pore structure varies from zeolite to zeolite. The pore diameters in all zeolites are determined by the free aperture resulting from 4-, 6-, 8-, 10- or 12-membered rings of oxygen atoms, and their maximum values are calculated to be 2.6, 3.6, 4.2, 6.3, and 7.4 $\overset{o}{A}$, respectively. As an example, Figure 2.2 depicts the structure and pore size of Y zeolite. However, due to some elongation of the oxygen ring or the presence of cations near or within the pore apertures, the effective free aperture of the pore may be reduced, and the aperture may be elliptical. The zeolites with 8- and 12-membered oxygen ring or more are used in major catalytic applications rather than small aperture size as it places unacceptable size limitations on the molecules to be adsorbed. Many of the zeolites formed are not in the equilibrium state but only in the metastable state, which in time may convert to other more stable zeolitic phases or other mineral phases. In principle, zeolites are prepared from alumina silicate gels, which in turn are prepared from aqueous solutions of sodium aluminate, sodium silicate, and
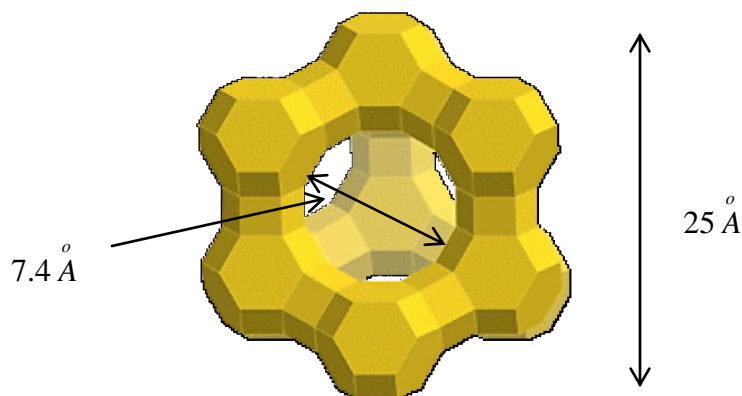
Figure 2.2: Perspective view of Y zeolite structure. The silicon or aluminum ions are located at the corners and the oxygen ions near the edges. The aperture opening is 7.4 $\overset{o}{A}$ and unit cell size is about 25 $\overset{o}{A}$

sodium hydroxide. The process employed is called hydrogel or hydrothermal process. (Bhatia 1990; Gates *et al.* 1979; Szostak 1998)

One of the major applications of zeolites is in the oil industry, especially in the process of catalytic cracking, where Y zeolite is frequently used in fluid catalytic cracking (FCC) process (Breck and Flanigen 1967; Breck 1974). The large-scale production of zeolites currently uses a batch process and the synthesis procedure takes days to obtain the finished product. Several researchers have devoted their efforts to improve the batch process and have tried to achieve a continuous process (Rollmann and Valyocsik 1983; Valyocsik 1983). Many zeolite synthesis operating variables have been identified and optimized to improve the quality of zeolites and reduce the synthesis time (Wang and Jacobson 2001; Xu *et al.* 1997). Microwave heating (Arafat *et al.* 1993; Jansen *et al.* 1992; Slangen *et al.* 1997; Cundy 1998; Kim *et al.* 2000; Park *et al.* 2001) and controlling the nucleation and crystal growth rates (Cundy *et al.* 1995c; Cundy *et al.* 1995b) have been tried.

The synthesis of small crystallite Y zeolite has been contributed in improving the catalytic activity for FCC reaction (Camblor *et al.* 1989; Rajagopalan *et al.* 1986).

Studies have been conducted to synthesize nano-size zeolites in colliodal solutions (Li *et al.* 2002; Schoeman *et al.* 1994). Efforts have also been carried out to produce nano-size zeolites in confined space using inert/amorphous materials (Murrell *et al.* 1999; Schmidt *et al.* 2000). Several researchers have successfully reported the synthesis of zeolites on a non-aqueous/dry basis (Dong *et al.* 1992; Dong *et al.* 1999; Fan *et al.* 1996; Hari Prasad Rao *et al.* 1998; Kim *et al.* 1993; Matsukata *et al.* 1993; Matsukata *et al.* 1996; Xu *et al.* 1989; Xu *et al.* 1990; Yamazaki and Tsutsumi 2000).

This Chapter mainly covers the mechanisms that are followed during nucleation and crystal growth of zeolite particles. The role of several variables that may influence the crystallization of zeolites will be addressed. Also, the transformation from the hydrothermal process to a dry process is discussed in detail.

2.2 SYNTHESIS OF ZEOLITE

Zeolites are crystallized under mild temperature and pressure, by a hydrothermal synthesis process (Barrer 1982). The nature of zeolite is determined by the specific synthesis conditions, i.e., reactant concentration, pH, reaction time, temperature, etc. The important factors affecting zeolite synthesis include: the nature of reactants chemical composition and pretreatment, the method of reactant mixture preparation, the overall, homogeneity or heterogeneity of the mixture, pH of the mixture, low temperature ageing of the gel, nucleation, seeding, addition of additives, temperature, pressure, and organic template.

The amorphous reactants containing silica and alumina are mixed together in presence of a cation source, usually with a high pH. The reactants for the source of alumina are generally sodium aluminate, aluminum nitrate, or aluminum phosphate. For the source of silica, generally sodium silicate, amorphous silica, or silica sol are used. Sodium hydroxide is normally used for the control of pH. The aqueous reaction mixture is heated to 100 ˚C or above in a sealed reactor. For some time after achieving the reaction temperature, the reactants remain amorphous. After this "induction period" the zeolite synthesis begins from the hydrous aluminosilicate amorphous gel. The carefully controlled conditions of the crystallization for the gel, gradually replaces all the amorphous phase into the desired zeolite phase. This sequence is shown as follows:

$$NaOH(aq) + NaAl(OH)_4(aq) + Na_2SiO_3 \xrightarrow{25^0 C} \underset{gel\ phase}{Na_a(AlO_2)_b(SiO_2)_c \cdot NaOH \cdot H_2O}$$

$$\xrightarrow{25-175^o C} \underset{zeolite\ phase}{Na_j(AlO_2)_j(SiO_2)_y \cdot zH_2O} + solution \tag{2.2}$$
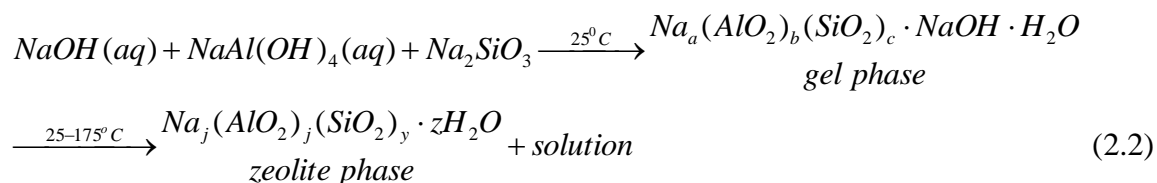
The resultant zeolite is then removed from the mother liquor, washed, and dried before any application (Bhatia 1990; Szostak 1998).

The steps involved in zeolite synthesis are depicted in Figure 2.3. The key elements, i.e. Si and Al, which make up the microporous framework of zeolite, are imported in an oxide form. These oxides and generally amorphous precursors contain Si-O and Al-O bonds. During the hydrothermal reaction in presence of a mineralizing agent, which is most likely an alkali metal hydroxide (e.g. NaOH), the crystalline zeolite product containing Si-O-Al linkages is created. Since the type of the bond of the product is very similar to that present in the precursor oxides, no considerable enthalpy change is anticipated. (Corma and Davis 2004; Cundy and Cox 2003; Navrotsky *et al.* 1995; Piccione *et al.* 2002; Van Santen *et al.* 1989).
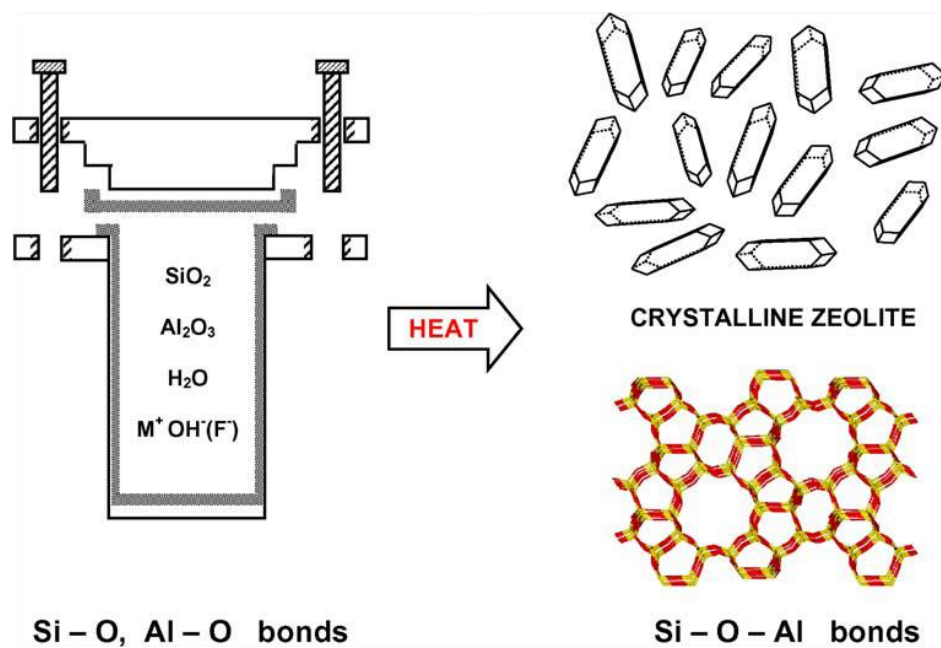
Figure 2.3: Hydrothermal zeolite synthesis. The starting materials (Si-O and Al-O bonds) are transformed by an aqueous mineralizing medium, such as OH$^-$ and/or F$^-$, into the crystalline product (Si-O-Al bonds). (Cundy and Cox 2005)

2.3 ZEOLITE SYNTHESIS MECHANISMS

Inspite of the advances in zeolite synthesis, the mechanism of crystallization is not well understood. Zeolites can be synthesized using solid-containing gels and also from clear solutions. In this chapter, crystallization from solid-containing gels is covered in more depth for the reason that the commercial synthesis of zeolite uses an amorphous gel phase with high solid content as the starting material. The gel phase is formed by mixing silicate and aluminate solutions, at basic pH in which the source of silicon and aluminum is either polymeric or monomeric. The synthesis generally takes place in the temperature range of 60-200ºC. Depending upon the operating conditions, the gel starts to dissolve in the solution and an intermediate in the form of an oligomeric aluminosilicate starts to grow. The intermediate crystallization phase is very complex process that cannot be described by a single crystallization mechanism. Finally, a crystalline phase starts to grow after an induction time (Serrano and Grieken 2001). In a nutshell, the most probable pathway to describe zeolite synthesis is a sequence of induction period, followed by nucleation and then crystal growth.

2.3.1   The Induction Period

The induction period is a time interval (τ) between the start of the reaction and the time when the first crystalline product is observed. Generally this period is taken as the interval between the time at which the reactants reach the reaction temperature and the time when a method of analysis detects the first solid product. For precipitation reactions, the classical nucleation theory (Mullin 2001) divides this period (τ) into three subunits:

$$\tau = t_r + t_n + t_g \tag{2.3}$$

Where, t_r is considered as the relaxation time, which is the time required "for the system to achieve a quasi-steady-state distribution of molecular clusters". In case of zeolites, this may be considered as the equilibration reactions that take place upon mixing the reactants and allowing them to reach reaction temperature. During this period, a distribution of

silicate and aluminate ions, and other species is established. The other subunits t_n and t_g are defined as the time required for the formation of a stable nuclei and the time required for the nucleus to grow to a detectable size, respectively. It is apparent from the above that the induction period covers all the important events in zeolite formation. Before the induction period, there are only individual reactant molecules; and after the induction period, the reaction mixture contains a large number of small and stable zeolite crystals, which are on the path of further growth.

2.3.2　The Nature of Amorphous Phase

It was initially considered that the reactants, which were composed of an amorphous phase, remained essentially unchanged throughout the synthesis. Such an approach is normally adopted for reaction modeling purpose (Lowe 1983; Thompson and Dyer 1985a; Thompson and Dyer 1985b; Thompson 1992). On the other hand, the dynamic nature of the amorphous phase was first pointed out by several mechanistic studies. Flanigen and Breck (Flanigen and Breck 1960a; Flanigen and Breck 1960b) found that the transformation of amorphous phase takes place through polymerization and depolymerization catalyzed by excess hydroxyl ion. At the same time Zhdanov (Zhdanov 1971) and Kerr (Kerr 1966) found that the initial amorphous phase comes to an equilibrium phase with the liquid phase and releases active soluble species into the solution. Such transformations in the amorphous phase are important in the early stages of synthesis reaction.

2.3.2.1 Primary and Secondary Amorphous Phase

When the synthesis reactants are mixed together, a visible gel is generally formed. This gel is considered as the primary amorphous phase. In some cases, e.g. synthesis from clear solution, this primary phase is colloidal and is invisible to naked eye. But its behavior and function are essentially the same. The primary amorphous phase is basically the initial and intermediate product from mixing the reactants. It is non-equilibrium and heterogeneous in nature and may contain precipitated amorphous aluminosilicates, coagulated silica and alumina that are precipitated from the starting material which is destabilized by change in pH and increase in salt content, and some unchanged reactants

(Cundy and Cox 2005). Upon standing at room temperature for some time or heating the reactants to reaction temperature, the above amorphous phase undergoes changes due to equilibration reactions and is converted into a pseudo-steady-state intermediate called the secondary amorphous phase. In the equilibration reaction, the relationship between solid and solution phases approaches equilibrium and a characteristic distribution of silicate and aluminosilicate anions is established. Figure 2.4 depicts this scenario. In case of high silica zeolite synthesis the pH measurements start to change as the primary amorphous phase undergoes transformation into secondary amorphous phase, thus by monitoring pH changes one can monitor the course of this transformation. In the final stage of synthesis reaction at an elevated temperature for a prolonged period of time, the secondary amorphous phase is converted into crystalline zeolite product, as shown in Figure 2.5.

Zhdanov (Zhdanov 1971) clearly represented the concept of equilibrated intermediate phase in synthesis process. He measured for the first time the effect of temperature in increasing the crystal growth rate, and observed that the crystal grew at a nearly constant rate over most of the synthesis period for zeolite A. Based on his measurement, Zhdanov was able to deduce the nucleation rate profile over the course of reaction. This reflects that the solid and liquid phases are connected through the solubility equilibrium, and the condensation reactions give rise to primary aluminosilicate blocks (4- and 6-membered rings) and crystal nuclei. The crystal growth takes place until the dissolution of amorphous phase is complete.

In 1981, the synthesis of X-ray amorphous (XRA) zeolites was reported by Jacobs et al. (Jacobs *et al.* 1981), which exhibited the properties typical for ZSM-5 zeolites. They used the procedure for ZSM-5 synthesis (Argauer and Landold 1972) with some modifications in the operating parameters. The synthesis was carried out in the presence of tetrapropylammonium (TPA) ion as a template with reaction temperature of 150 ℃ for 6 hr to 10 days. The resulting material was air-dried, calcined at 550 ℃, and ammonium exchanged. For crystallinity, both techniques of X-ray diffraction (XRD) and IR spectroscopy were used. The IR spectrum was followed for a typical ZSM-5 skeleton vibration at 550 cm^{-1}, and a sum of the area of the typical diffraction peaks between $2\theta = 22°$ and $25°$ (Cu-K$_\alpha$ radiation) was calculated for crystallinity.

SiO$_2$ source   Al$_2$O$_3$ source

M$^+$OH$^-$ Q$^+$OH$^-$

Partly-reacted, heterogeneous
non-equilibrium mixture:

Solution + **solid**

PRIMARY AMORPHOUS PHASE

-H$_2$O

Si(OH)$_4$ Si$_x$O$_y$(OH)$_2$

EQUILIBRATED
SOLUTION

OH$^-$ OH$^-$

-H$_2$O

ionized monomers   ionized polymers

Al(OH)$_4^-$

Colloidal and gel   Colloidal and gel
silicates   aluminosilicates

SECONDARY AMORPHOUS PHASE
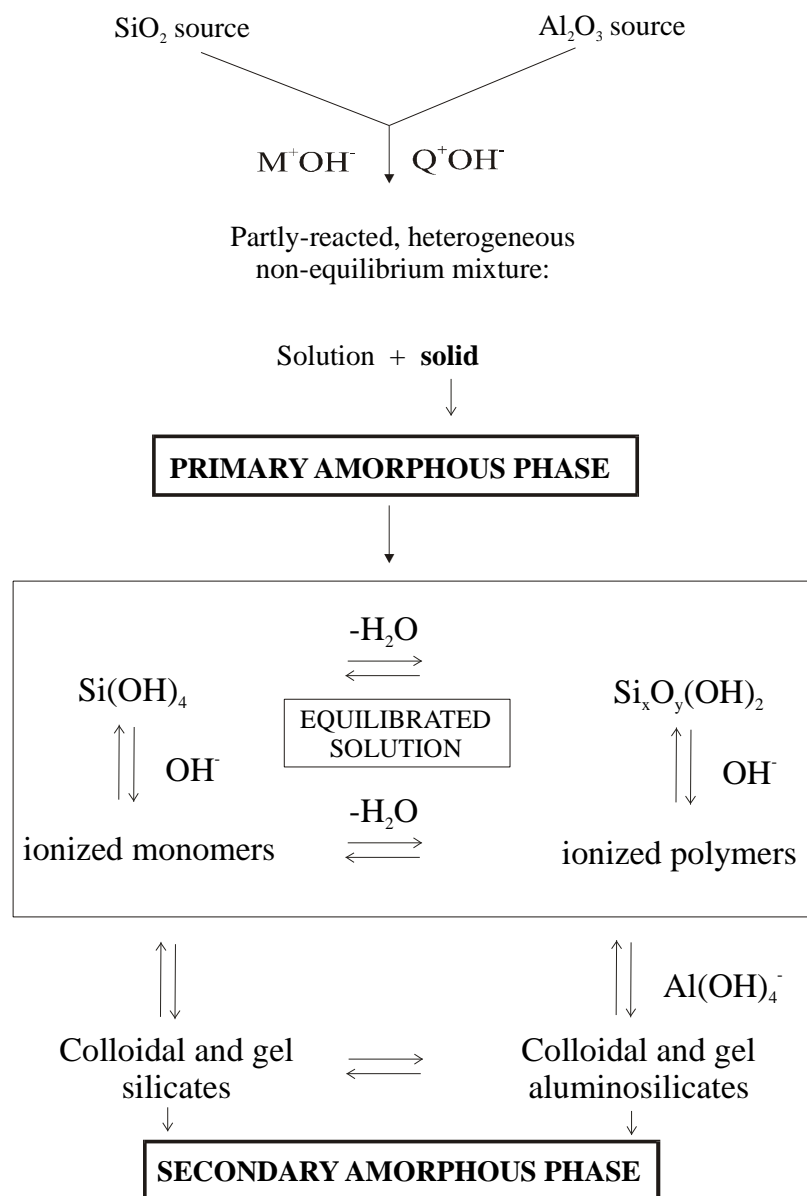
Figure 2.4: Equilibration of the starting mixture to establish a partly ordered secondary amorphous phase and a characteristic distribution of solution species. (Cundy and Cox 2005)
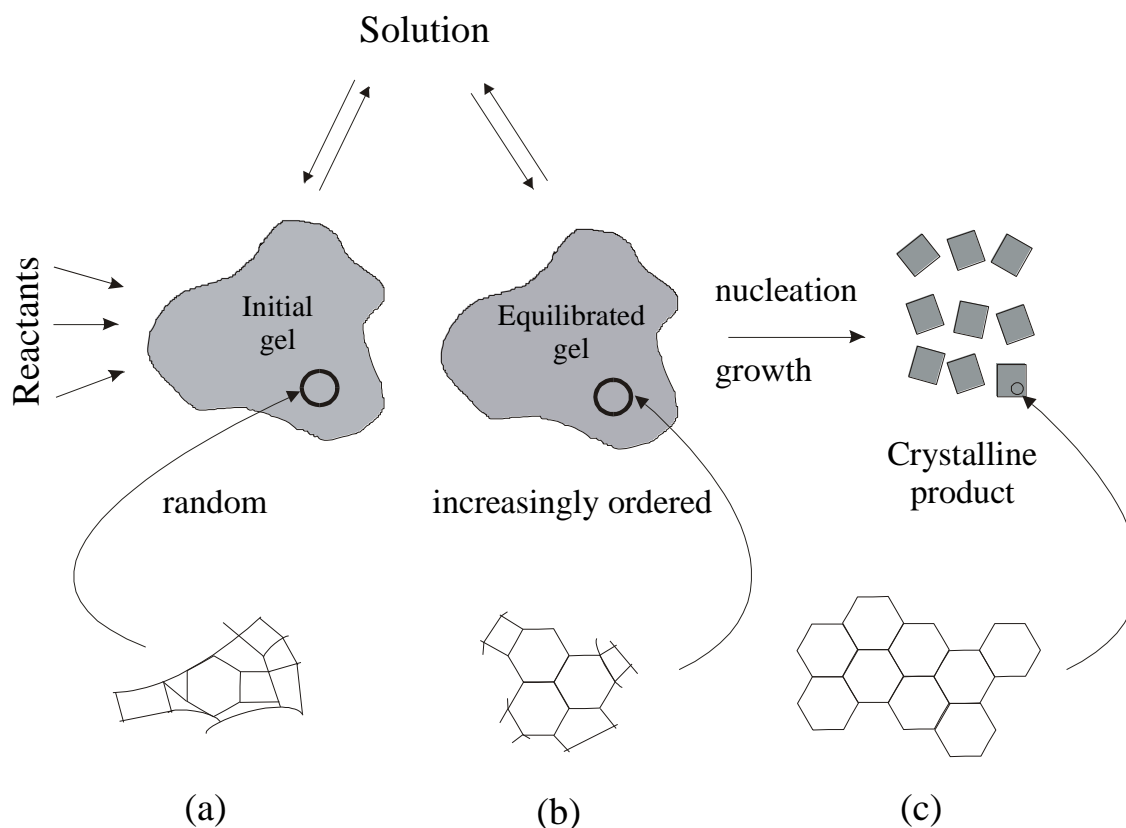
Figure 2.5: The emergence of order, from the primary amorphous phase (a) through the secondary amorphous phase (b) to the crystalline product (c). (Cundy and Cox 2005)

The conventional sigmoidal plot, as shown in Figure 2.6, indicated a typical crystallization mechanism of induction-nucleation period (about 3 days) followed by a crystal growth period (about 3-7 days) when examined with the XRD. On the other hand, the curve on the sigmoidal plot for IR crystallinity showed a completely different pattern. It showed that for a short span of synthesis time (i.e. 6 hr), the IR spectrum detected larger than 60% crystallinity. The XRD, on the other hand, showed amorphous phase up to 6 hrs of operation and 97% of crystallinity after 3 days of reaction. To explain the marked difference between the two analyses, they used Scherrer formula and found that crystallite size below 8 nm was not detectable on the XRD machine, which led them to conclude that the XRA zeolite must have crystals with less than 4 unit cells. They did not report the crystallinity under IR spectrometery for synthesis time less than 6 hr. The XRA

zeolite was loaded with Pt and tested for the hydro-conversion of n-decane, and compared with activities of HZSM-5, USY, and silica-alumina catalysts. They found that XRA zeolite showed an activity very similar to that of HZSM-5 significantly higher activity when compared to silica-alumina catalyst (Jacobs *et al.* 1981).
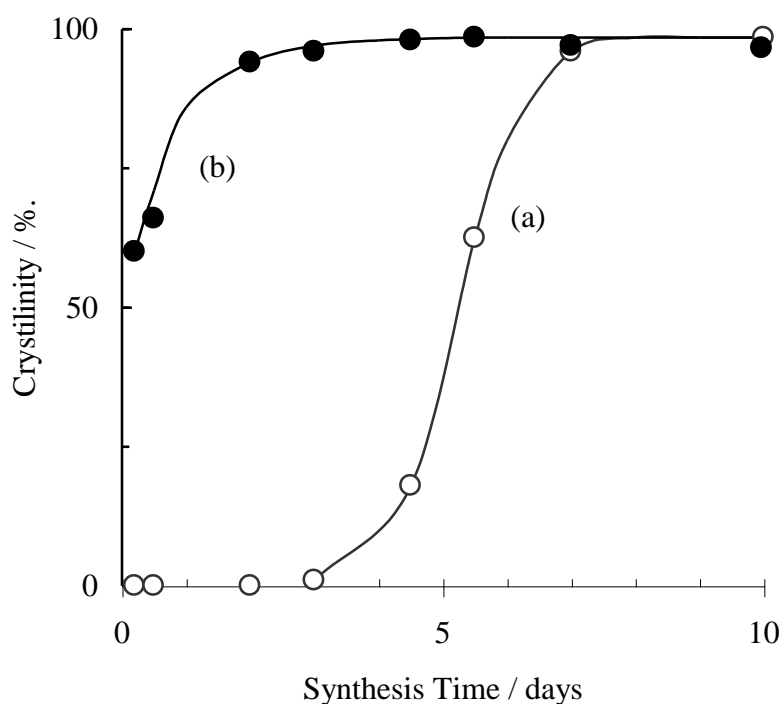
Figure 2.6. Change of the crystallinity of ZSM-5 materials with synthesis time: (a) X-ray crystallinity derived from peak summation between $2\theta = 22$ and $25°$; (b) IR crystallinity using the 550 cm^{-1} skeleton vibration in a KBr pellet technique with the 2200 cm^{-1} vibration of KCN as internal standard. Redrawn with permission from Jacobs et al. (Jacobs *et al.* 1981).

The crystal growth mechanism has been described to occur in two different ways. The first mechanism was reported as crystallization by solid hydrogel transformation during the nucleation and growth process of various zeolites (Breck and Flanigen 1967; McNicol *et al.* 1973). The second mechanism, in contrast to the first, demonstrated the role of liquid phase ion transportation in the growth of different zeolite nuclei.
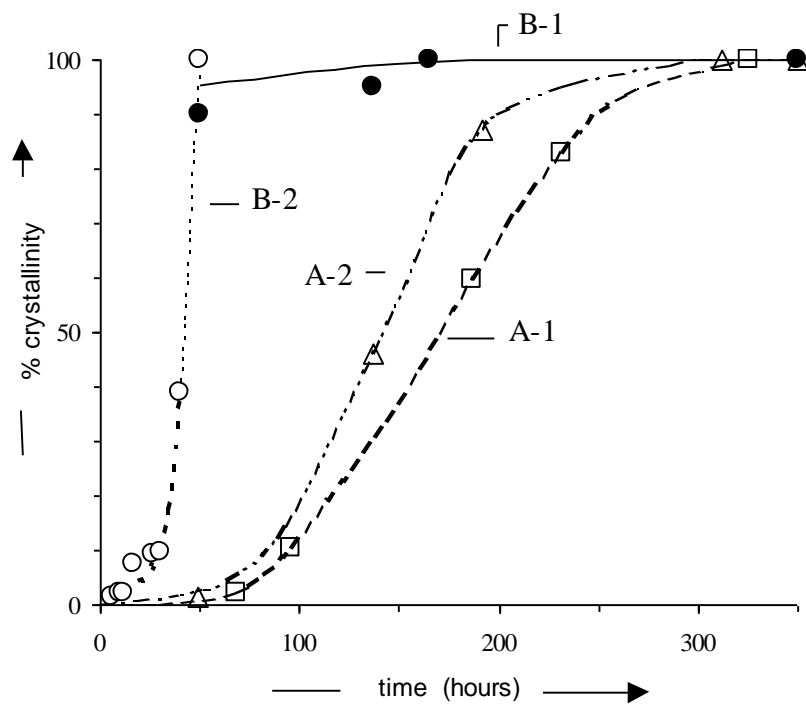
Figure 2.7. Crystallization curves for typical type A and type B syntheses. Redrawn with permission from Derouane et al. (Derouane *et al.* 1981).

Derouane et al. (Derouane *et al.* 1981) made a major contribution by proposing a theory to explain the mechanism of crystal growth through two distinct processes. They synthesized pentasil (ZSM) zeolites in the presence of TPA as structure-directing agent by two different methods (Argauer and Landold 1972; Chen *et al.* 1978). For ZSM-5 zeolite type A, Si/Al and Na/Si ratios were low and the source of silica was a solution of active silica (solid, polymeric), and the synthesis was found to take place by liquid phase ion transportation. For type B, Si/Al and Na/Si ratios were high and the source of silica was a solution of sodium silicate (liquid, mono- and poly-silicate anions), and the synthesis appeared to be solid hydrogel transformation. The sigmoidal plot, as shown in Figure 2.7, shows that 100% crystallinity is achieved in 300-330 hr for type A and in 45-50 hr for type B, thus indicating a distinct role of the type of silica.

Figure 2.8 depicts a schematic presentation of both mechanisms. In type A synthesis, solid (active) silica, initially present as colloidal silica particles dissolves in highly alkaline medium that leads to a depolymerization-hydration process that ultimately forms soluble monomeric silicate anions. As a result, a mixture of silica sol, dissolved silicate, and polysilicate ions is formed. The aluminum entities remain in solution in monomeric form. The silica monomers are continuously produced on the surface of the colloidal silica particles and condensed with aluminate ions to form alumino-silicate complexes, which transforms the colloidal silica particles into a silica-alumina sol. Changes occur on the surface of the silica-alumina sol and this restructuring moves inward as further depolymerization occurs. As the aluminum supply is progressively depleted, the inner core of the colloidal silica particles contains less aluminum than the surface, which leads to a non-homogeneous aluminum distribution. The inner core may be depolymerized at a lower rate than the outer shell, thus rendering the low depolymerization rate as the rate limiting step. As a result, gel composition remains low in the beginning and progressively increases with depolymerization. Thus nucleation takes place at a limited rate from the available siliceous monomers and crystal growth takes place at a faster rate because its activation energy is less than nucleation (Erdem and Sand 1979). The low depolymerization rates lead to small number of nuclei formation and hence large crystallites.

(A) **SOLID PHASE**   **LIQUID PHASE**

SiO₂

TPAOH
NaOH

Silica
Sol

Silica-alumina
Gel

Alkali cations

Polysilicate
and
Monosilicate

Anions

Aluminate

Dissolution

ZSM-5 nuclei

TPAOH

Dissolution

Silica-alumina
Sol

Zeolite
Crystallites

○ Silica phase

▦ Silica-alumina phase

(B)

LIQUID PHASE   **SOLID PHASE**

Aluminate
Polysilicate
and
Monosilicate

Anions

NaOH
TPAOH

Hydrous
Silica-alumina
Gel

TPAOH

$Al\text{-}(O\text{-}SiO_3)_4^{13-}$

Gel +
Zeolite nuclei
Microcrystallites

○ Pure silica phase

▦ Silica-alumina phase

Polycrystalline
ZSM-5 aggregates

Al free
Outer shell

Figure 2.8. Zeolite crystallization mechanisms: (a) solution mediated process (type A); (b) hydrogel reconstruction (type B). Redrawn with permission from Derouane et al. (Derouane *et al.* 1981).

In type B synthesis, sodium silicate provides momomers in the presence of some small oligomer species and aluminate species in monomeric form (Moolenaar *et al.* 1970). A mixture of both species immediately yields a hydrous alumino-silicate gel within the solution with high Na content and some TPA cations. Since the supply of silicate anions is not limited by depolymerization of Si reagent, the composition of the gel (Si/Al) throughout the synthesis process is therefore not much different from the reagent ratio. The high Si/Al and Na/SiO_2 molar ratio, and a uniform Al radial distribution throughout the gel favour a rapid nucleation rate with the help of TPA cations that are present throughout the gel. As a result, a rapid crystal growth yields a large number of small crystallites, which are not apparent in the SEM images until nearly 100% crystallinity is achieved. Under these conditions, a direct crystallization process is postulated involving a solid hydrogel transformation. The constant Si/Al molar ratio throughout the crystallization process shows that the growing crystallites and their gel precursors maintain the same composition, which further strengthen the direct hydrogel transformations through internal rearrangements. Studies of the syntheses of zeolite Y and mordenite further confirmed the mechanism of solid hydrogel transformations as low molecular weight species of Si were absent in the analysis of the solution by liquid ^{29}Si NMR (Bodart *et al.* 1986). It was also observed that solid hydrogel transformation process yielded polycrystalline aggregates instead of individual crystals. Furthermore, no evidence of crystal growth was observed for synthesis time less than 4 hours (Derouane *et al.* 1981).

Many other groups have reported the existence of the secondary amorphous phase. Angell and Frank (Angell and Flank 1977) reported for zeolite A synthesis that the initially formed sodium aluminosilicate gel was converted to an amorphous aluminsilicate intermediate through solution transport. This material was further converted to crystal via basic medium dissolution. Fahlke in 1987 (Fahlke *et al.* 1987) also observed for Y zeolite synthesis that there was an immediate precipitation of silica-rich primary amorphous gel, followed by its slow dissolution and then precipitation to a secondary amorphous gel having a similar Si/Al ratio to that of final zeolite product. Among these groups, Montpellier group (Nicolle *et al.* 1993) performed a very informative study. Their study clearly indicates the multistage-nature of the zeolite

synthesis reaction as shown in Figure 2.5. They prepared several samples of Na, TEA-aluminosilicate gels with different compositions (TEA=tetraethylammonium), and heated to 150 ˚C for two sets of duration, i.e. for a short time and for a longer period of time. The solid products from each reaction time were removed and analyzed. The aim of using different heating times for a particular composition was to obtain an equilibrated gel and the final crystalline zeolite product. The four chosen compositions (A-D) were finally crystallized to (A) zeolite beta, (B) mordenite, (C) ZSM-12, and (D) ZSM-5. The most interesting findings were obtained by analyzing the initial and equilibrated products.

X-ray diffraction showed only the broad spectrum indicative of local ordering but no sharp peaks for crystalline structure. Analysis under ^{27}Al MAS NMR spectroscopy showed only tetrahedral coordination in aluminum and no zeolitic bands in their infrared spectra. Chemical analysis indicated that the hydrothermal treatment had largely changed the composition of the solid phase as compared to that before heating for the case when Na^+ cation was replaced by TEA^+. It was found that the TEA content was almost constant, i.e. one organic cation per 12-16 T-atoms, whatever the method of preparation or Si/Al ratio was used. They also found after the calcination of equilibrated samples A and B that the cation exchange capacities were in close agreement with their aluminum content (i.e. ≈85 mmol NH_4^+/100 g). They also found that the calcination of equilibrated samples A-C generated a micropore system having about 60% volume capacity as shown by zeolite beta crystallized from composition A.

The authors concluded that the equilibrated, amorphous samples were different from the gel that was initially precipitated at room temperature, and had been formed by dissolution or rearrangement within gel and reprecipitation. These secondary amorphous products were silicoaluminates and shared several properties with high-silica zeolites. For both durations of reaction time, the clusters of silica or alumina tetrahedral had gathered around the bulky TEA molecule, whose decomposition upon calcinations left a micropore system. The essential difference between the two classes of solids (equilibrated and zeolite) was defined by the dispersion of cluster geometry. Zeolites show well-defined and repeatable site geometries, whereas the equilibrated amorphous products show irregular, aperiodical, and locally organized geometries. It has been also observed by other data that the above general observation is not only associated with the synthesis of

zeolites templated by quaternary ammonium ion, but also similar phenomena is further observed in preparation of aluminous zeolites without using an organic template (Angell and Flank 1977; Fahlke *et al.* 1987).

In another study, Tsuruta et al. (Tsuruta *et al.* 1986) investigated the initial product formation during the synthesis of zeolite A from concentrated solutions in the presence of an anionic surfactant. From the results of X-ray and electron diffraction, they found that the amorphous aluminosilicate, which was isolated from the solution under mild reaction conditions (i.e. 60 ºC, 15 min), contained a short-range order of Si and Al atoms similar to that in crystalline zeolite A. Subotic and coworkers (Subotic *et al.* 1994; Krznaric *et al.* 1998) also investigated the structural properties of X-ray amorphous sodium and potassium aluminosilicate gels using electron diffraction, thermal analysis, and FTIR spectroscopy. They found that the X-ray amorphous material contained structurally ordered region or particles of a partially crystalline phase inside an amorphous matrix. A further hydrothermal treatment in 2M NaOH at 80 ºC formed the zeolite A and X. With the help of EXAFS and XANES spectroscopy, Walton and O'Hare (Walton and O'Hare 2001) examined the amorphous gallium silicates, which were separated in the early stages of hydrothermal synthesis of Ga-hydroxysodalite. They found that Ga and Si K-edge EXAFS showed some degree of medium range order, indicative of an extended network of $Ga(OSi)_4$ and $Si(OGa)_4$ units, which resembled the structure of crystalline product. Yang et al. (Yang *et al.* 2004) carried out a related study on the amorphous zeolite A precursors using multinuclear MAS NMR and neutron diffraction techniques. They detected changes in the medium order before the crystallization as the Al in the presence of Na^+ cations was incorporated into the Si network. At the same time, diffraction and spectroscopic techniques did not indicate the presence of well-defined structural units before the formation of zeolite crystals. Very similar results were obtained in an earlier study of various zeolite syntheses using ^{129}Xe NMR technique (Ito *et al.* 1989). The gel structuring (large cavities) was found evident for Na,TPA-ZSM5, and NaY zeolites but not for Na,TEA-ZSM20. The NMR measurements for NaY only showed any appreciable microcrystalline formation in the absence of XRD crystallinity.

The presence of pre-crystalline structure in MFI-type synthesis has been also investigated. Burkett and Davis (Burkett and Davis 1994) demonstrated by ^{1}H-^{29}Si CP MAS NMR spectroscopic results that TPA molecules and silicate species were close to each other in the heated gel before XRD and IR indicated any evidence of crystalline silicalite formation. However, no such demonstration was observed for unheated gel. This result was further supported by an in-site multinuclear NMR investigation at 80 ºC (Gougeon *et al.* 1998). It was found that the hydrogen bonds between the organic template and water-clathrated molecules were replaced by silica species as the hydrophobic interactions between the organic template and silica species progressed. The organic template occlusion is also evident from SAXS (small angle X-ray scattering) (Regev *et al.* 1994), and SANS (small angle neutron scattering) (Watson *et al.* 1997; Watson *et al.* 1998) measurements. Many groups of researchers have reported FTIR bands at 550-560 cm^{-1} for the isolated material, which is XRD amorphous (Schoeman 1997; Jacobs *et al.* 1981; Ravishankar *et al.* 1999; Watson *et al.* 1997; Watson *et al.* 1998; Mintova *et al.* 2002). These bands indicate the presence of material having MFI structure.

To wrap up the above discussion, it can be summarized that initially the reaction mixture for zeolite synthesis contains a non-equilibrium combination of components that is heterogeneous or may be partly reacted, and thus called primary amorphous phase. With time (t_r) and especially upon heating the reaction mixture, the silicate and aluminosilicate equilibration reactions start to take place that lead to a redistribution of species between the solid and the liquid phase as they approach equilibrium with each other. Cations play a very important role of structure directing agent in the organization of the solid phase. The newly generated solid phase, created in the presence of cations, has a similar chemical composition that is attributed to the final zeolite product, but it lacks long-range periodical organization and hence remains X-ray amorphous, and thus called secondary amorphous phase.

2.4 ROLE OF ALKALI METAL CATION (Na$^+$or K$^+$)

It is widely accepted that hydrothermal treatment is affected by the composition and structure of the starting aluminosilicate gels. Studies have been carried out to

understand the mechanism governing zeolite formation by characterizing the aluminosilicate gels prior to the hydrothermal treatment.

The role and effect of alkali metal cations on the properties of aluminosilcate gels as the starting material, during zeolite synthesis, has been investigated by different spectroscopic techniques. Ivanova et al. (Ivanova *et al.* 1994) investigated the aluminosilicate gel obtained by mixing the alkali-silicate and aluminate clear solutions using multinuclear NMR. They found that the tetrahedrally coordinated Al was homogeneously dispersed throughout the gel, irrespective of the type of alkali metal cation. However, when the textural properties of the gel were investigated using ^{129}Xe NMR, they found a dependence on the type of the alkali metal cation present in the material.

Subotic et al. (Subotic *et al.* 1994) used two types of dry amorphous aluminosilicate gel containing Na^+ and K^+ cations. A part of the gel was heated to 500ºC for 1 hr and finally stirred in 2M NaOH solution at 80ºC to reach complete crystallization. The samples were investigated before heating, after heating, and after complete crystallization using XRD, FTIR, and differential thermogravimetry (DTG). It was found that the sample containing the "structure-forming" Na^+ cation showed a similar endotherm which was observed for the sample after complete crystallization and without being exposed to high temperature. This led to a postulation that the presence of Na^+ induced the formation of structural subunits or complex structures in the range of 5-20 nm, which were also present in the complete crystalline product and were beyond the detection limits of XRD. On the other hand, the sample containing "structure-breaking" K^+ cation did not show any endotherm at a similar location, which led to an assumption that structural subunits were either not formed or formed in a considerably lower quantity in the presence of K^+ inside the X-ray amorphous solid aluminosilicate gel. This was further confirmed by the electron diffraction pattern (EDP). The effect of heating the sample before crystallization was investigated through FTIR for both types of samples and it was found that the formation of structural subunits was further deteriorated, which affected the rate of hydrothermal transformations of X-ray amorphous solid aluminosilicate gel into the crystalline product. An interesting observation was made when the samples were crystallized at high temperature. The sample containing Na^+

cation showed deterioration in the formation of structural subunits as expected, but K^+ containing sample formed pure zeolite, small crystal size, large number of crystals and the shortest time of synthesis which remained a question beyond explanation.

The production of side products such as zeolite A and zeolite P may also occur along with zeolite Y as the main product. It has been established that the production of side products is dependent on different factors such as; alkali concentration, Si/Al ratio, ageing time, and hydrothermal treatment (Den Ouden and Thompson 1991; Lechert and Kacirek 1991). Li et al. (Li *et al.* 2002) shed some light on the role of addition of NaOH on the synthesis of zeolite Y. They used a molar composition of 2.46 $(TMA)_2$:x Na_2O:1.0 Al_2O_3:3.4 SiO_2:370 H_2O:13.6 EtOH from clear solution. The concentration of NaOH ranged between (0.03 < x < 0.43). They found that with a larger Na_2O/Al_2O_3 ratio (0.43) the synthesis favored the formation of zeolite A with a high yield and a shorter crystallization time. On the other hand, using a lower Na_2O/Al_2O_3 ratio (0.03), the synthesis favored the formation of zeolite Y with a lower yield and a longer crystallization time. They found that the sodium was the growth-limiting factor in the synthesis of zeolite Y. They also tested a mid-synthesis addition of sodium to observe changes, if any, in zeolite yield with zeolites A and Y as final product. They have also reported that the addition of sodium before the completion of nucleation did not produce a single-crystalline phase even when the amount and rate of mid-synthesis addition of sodium was kept low (Li *et al.* 2001). So they tested the addition of sodium after the completion of nucleation and found that the addition of 1M NaOH after a nucleation time of 6.5 days highly influenced the zeolite phase. A one-time addition of NaOH still produced a mixture of zeolites Y and A, which was indicative of excessive sodium concentration forcing nucleation of zeolite A. To control sodium concentration, its addition was divided in several equal portions and added into the synthesis mixture at different time intervals. They found that the sodium addition with small number of equal portions and shorter time intervals produced a mixture of zeolites A and Y with higher concentration of zeolite Y. On the other hand, a large number of equal portions and longer time intervals indicated that the crystalline phase in the final product was strongly dependent on the addition frequency. A pure zeolite Y with a slightly increased size and an increase in yield of more than 6-fold, was synthesized by the addition of NaOH in

eight equal portions with addition time interval of 8 hr. Thus, they concluded that the synthesis of pure zeolite Y, the mid-synthesis addition of sodium with controlled amount and rate of addition was pivotal.

2.5 ROLE OF ORGANIC TEMPLATES

The effect of structure-directing agents (tetraalkylammonium ions, TAA^+) on the structural and physiochemical properties of aluminosilicate gels was investigated in-depth by Bodart et al. and Nagy et al. using various NMR (Bodart *et al.* 1986; Nagy *et al.* 1995). The gel was obtained by mixing $Al(OH)_3$ solution with fumed silica, which is typically used in the synthesis as starting material. The role of the structure-directing agents (TAA^+) was determined by varying the aluminosilicate gel composition in their preparation under different operating conditions. When the TAA-Br was added at neutral pH in the absence of Na^+ cation (gel I), it was found that the tetrahedral Al atoms were not well dispersed throughout the gel. Due to the presence of TAA-Br crystallites, some large (40-60 °A) and medium (21 °A) cavities were detected. On the other hand, when TAA-OH was used in absence of Na^+ cation (gel II), it was found that tetrahedral Al atoms were very well dispersed throughout the gel and TAA^+ cations took the place of counter cations of the negatively charged gel. When TAA-Br was added to the gel containing NaOH (gel IV), it was observed that Al atoms were better dispersed but the counter cation for the gel remained essentially the sodium ions, this caused less dispersion of TAA^+ cation within the gel. The textural characterization of the gels using ^{129}Xe NMR showed a monomeric high dispersion of structure-directing agent when TAA-OH was use in gel formation. Hence, this suggested a direct role of TAA cations in zeolite synthesis.

2.6 EFFECT OF AGEING

For the synthesis of Y zeolite, the use of colloidal silica sol was a preferred source of silica. When colloidal silica was used, ageing of the synthesis gel was carried out before heating for synthesis of NaY zeolite (Breck 1974). Ginter et al. (1992a, 1992b) studied the ageing of the starting gel as another feature, which is related to the nucleation step in the synthesis of zeolites (Ginter *et al.* 1992b; Ginter *et al.* 1992a). They performed

two different studies; to quantify the physical and chemical transformations occurring during the ageing of aluminosilcate gel produced from colloidal silica, and to investigate the effects of ageing on the synthesis of NaY zeolite. For both studies, they used colloidal silica and sodium aluminate solutions as starting materials. In the first study, they found that upon mixing of colloidal silica sol and sodium aluminate solutions, a gel was immediately formed due to the flocculation of silica particles in the sol. By mixing, the gel was homogenized into small granules in the order of 1 mm in diameter. However, no chemical transformation was observed upon mixing, but during ageing, the silica particles were slowly dissolved and released silicate anions into the surrounding solution. These species reacted with aluminate anions and formed aluminum silicate species, which precipitated due to their low solubility. The solid amorphous aluminosilicate thus formed was rich in Al and hydrated Na^+ cations. The precipitation of aluminosilicate consumed the dissolved Al and prevented the accumulation of Si in solution. When the entire dissolved Al was consumed in aluminosilicate formation, the remaining colloidal silica started to dissolve in the solution, which decreased the basic pH and started to release silicate anions in the solution. The aluminosilicate slowly reacted with the silicate anions in solution, which resulted in an increase in Si/Al ratio and a decrease in Na/Al ratio. In their second study, as shown in Figure 2.9, they found that room-temperature ageing of colloidal silica gel strongly affected the kinetics of NaY crystallization at 100 ºC. With ageing, the crystallization was accelerated and the final crystal size was decreased, especially ageing up to 12 hours.

Their results are consistent with the generally accepted hypothesis that ageing enables the formation of nuclei from which crystals subsequently grow (Barrer 1982). They found that high pH and Al content in the solution during the first 12 hours lead to the formation of amorphous aluminosilicate gel with Si/Al = 1 and Na/Al = 2. They proposed that this amorphous phase coexists with un-dissolved silica, and upon heating of aged gel, the remaining colloidal silica dissolves quickly and releases silicate anions into solution. The silicate anions react with amorphous aluminosilicate gel and form NaY nuclei under high concentration of hydrated Na^+ cations in amorphous aluminosilicate gel.
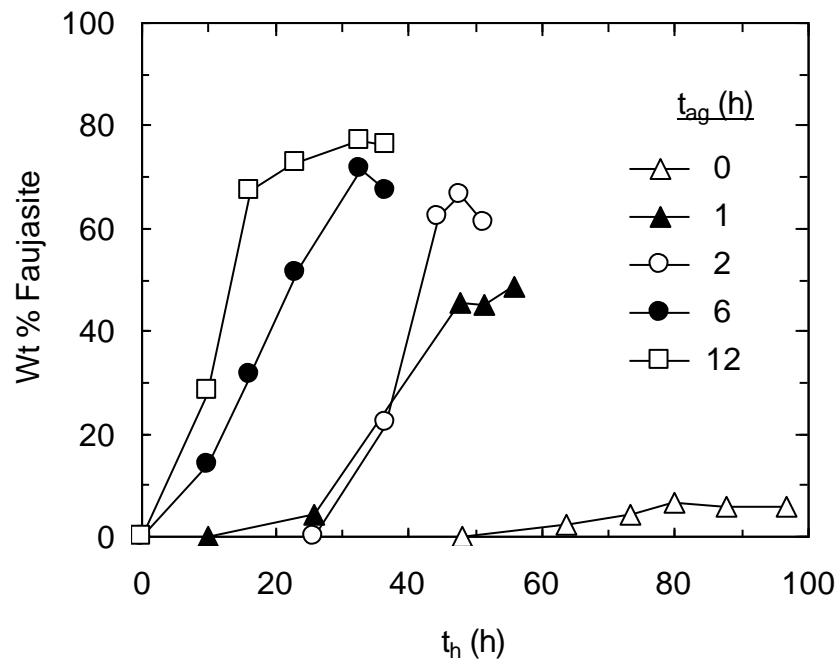
Figure 2.9. Effect of ageing of starting gel on the synthesis of zeolite NaY; wt% of NaY in the solid phase isolated from synthesis gels as a function of heating time for ageing time up to 12 h as determined by powder X-ray diffraction. Redrawn with permission from Ginter et al. (Ginter *et al.* 1992a).

They found that the high concentration of Na^+ cations in the amorphous aluminosilcate seemed to stabilize the faujasite structure. It was further confirmed that by crystallization of the gel, fewer NaY nuclei were formed and a denser structure such as NaS and NaR was produced. Ageing beyond 12 hours incorporated more Si into the aluminosilcate, which led to a decrease in the size of Al-rich zones in the gel. Upon heating the gel, aged for more than 24 hours, smaller and single crystals were formed.

2.7 MECHANISM OF NUCLEATION AND CRYSTAL GROWTH

Two extreme alternatives; homogeneous and heterogeneous mechanisms have been suggested to explain the nucleation and crystal growth during zeolite synthesis. In the homogeneous mechanism, the nucleation is supposed to occur directly from the liquid phase. Once the embryos reach a critical size, they grow into crystals by progressive incorporation of soluble species. If any amorphous solid phase is present in the solution, it may serve as a reservoir of nutrients for the growing crystals. In the heterogeneous mechanism, it is assumed that zeolite crystallization proceeds by reorganization of the amorphous phase hydrogel which is present in the solution from the beginning of synthesis. Therefore, the nucleation takes place within the hydrogel and the crystals are formed by solid-solid transformation (Szostak 1998).

Nucleation is basically the next step after the formation of the gel and ageing in a conventional crystallization process before crystal growth. The crystallization of zeolites from aluminosilicate gels and their transformation from metastable phase to a more stable phase is a solution-mediated process. In this process, the metastable phase is the precursor of the aluminosilicate species that is required for the formation and growth of a stable phase. As mentioned earlier, the induction period (τ) composed of three components i.e. t_r, t_n, t_g. Among these t_n is the time required to form a stable nucleus. Figure 2.10 depicts the classical concept of critical nuclear radius, which is explained by change in free energy (ΔG) during nucleation process.
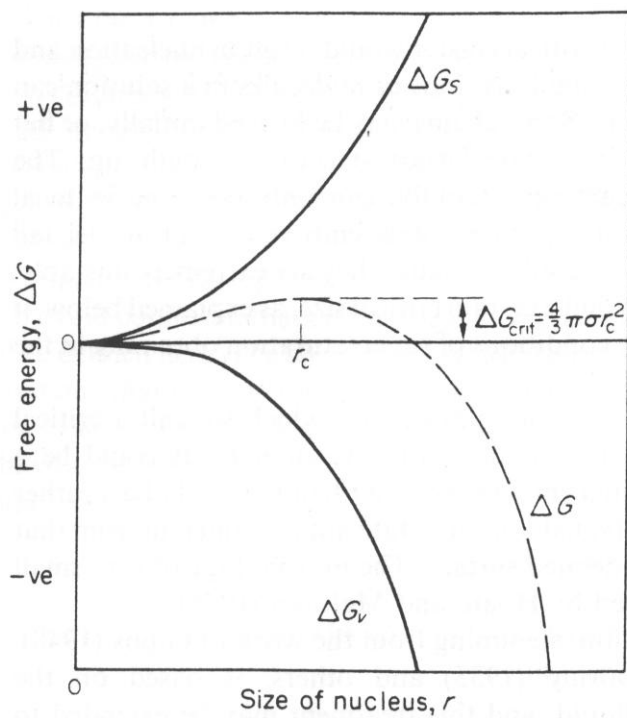
Figure 2.10: The energetics of nucleation, illustrating the concept of a critical nucleus of radius rc; beyond this size, the net energy gain from the resultant (ΔG) of cohesive (ΔG_v) and surface (ΔG_s) terms is favourable to growth (Mullin 1993).

The overall change in the free energy (ΔG) between a small solid particle of solute and the solute in the solution is equal to the sum of change in surface free energy (ΔG_S) and the change in the volume free energy (ΔG_V). Whereas, the surface free energy (ΔG_S) is the change in the free energy between the surface of the particle and the bulk of the particle. On the other hand, the volume free energy (ΔG_V) is the change in change in the free energy between a very large particle ($r = \infty$) and the solute in solution (Mullin 2001). Figure 2.10 shows that when the nuclear radius reaches the critical size (i.e. r = r$_c$), a sufficient amount of matter comes together in an ordered way that the cohesive energy (ΔG_V) of the matter becomes stronger than the energy (ΔG_S) which is expended in creating a surface dividing the nucleus from continuum. This makes a stable unit to be formed as stable nuclei capable of further growth. In zeolites, the critical size is estimated around 1-8 unit cells by Thompson and Dyer (Thompson and Dyer 1985a). At the same time, the chemical and physical processes which govern the formation of critical size are subjected to the experimental conditions. If these conditions are changed, then r$_c$ will also vary. This phenomenon can generally be expressed as below:

$$r = \frac{2\sigma\upsilon}{kT \ln S} \tag{2.4}$$

where σ is the interfacial tension (surface energy per unit area), υ is the molecular volume and S is the super-saturation ratio (i.e. $S = \frac{c}{c^*}$) (Mullin 2001). In general, the nucleation rate (J) can be defined as the rate of production of unit cells having radius $r \geq r_c$. It has generally be assumed that $J \propto \frac{1}{\tau}$ (Cundy and Cox 2003; Culfaz and Sand 1973), but this scenario may hold true if t_n is greater than t_r and t_g (Subotic *et al.* 1999; Warzywoda *et al.* 1989). It can safely be assumed that though the formation of nuclei for zeolite crystal formation is more complex due to its complex assembly as compared to simpler substances whose unit cells are smaller and contain fewer molecules, but there may be no difference in the basic principle of nucleation (Cundy and Cox 2005).

The direct experimental data on nucleation is very difficult to obtain since an extremely small fraction of the total mass is involved. Also, it is very difficult to distinguish the nuclei from the surrounding reactants of similar nature and composition. Furthermore, more reliable information is available for the early stages of crystal growth behavior rather than nucleation. So far only cryo-TEM (Regev *et al.* 1994) and HRTEM studies (Mintova *et al.* 1999b; Mintova *et al.* 1999a; Mintova *et al.* 2002) have provided direct evidence of nucleation phenomena. Other studies estimated the nucleation rate based on crystal growth rate (Culfaz and Sand 1973). Zhdanov and Samulevich (Zhdanov and Samulevich 1980) further improved the approach and were able to determine the isothermal nucleation rate profiles from the crystal growth rate and its size distribution. This method was first used in the analyses of NaA (Zhdanov 1971) and NaX (Zhdanov and Samulevich 1980) crystallization, and subsequently used for other zeolite systems including silicalite (Golemme *et al.* 1991; Cundy *et al.* 1990). In this method, it was assumed that all the crystals in a batch possess the same growth rate behavior, thus making it possible to calculate the total growth time for each crystal. Based on these findings the nucleation point for each crystal can be obtained by linearly extrapolating the time to zero. Thus the nucleation profile for the whole batch can be determined.

Adding seed crystals to zeolite reaction mixtures provide an effective way of reducing synthesis time and a direction towards a desired product with consequent reduction in impurities (Cundy *et al.* 1995a; Cundy *et al.* 2003; Kacirek and Lechert 1975; Verduijn 1993). Basically, the seed crystals provide a surface area upon which the product can grow. This step eliminates the need of the surface which is required to be generated through primary nucleation (t_n), thus reduces the induction time (τ). The seed crystals added to synthesis mixture may behave in different ways. They may remain inert, or dissolved, or act as pure seeds upon which the mass is deposited and start to grow. They can also lead to secondary nucleation and hence another crop of crystals. Therefore, it is generally required that a sufficient area is available to have an effect. It is rare for a very small quantity of large crystals to cause any significant change in the synthesis reaction rate. They remain inert or may show some signs of attack, which are due to dissolution in solution. If they show the signs of dissolution then their contribution will mainly be in changing the stoichiometry of the reactants. The balance between seed

growth and the secondary nucleation depends upon the quantity of the seed crystals added and the degree of agitation. If the surface of the added seeds is sufficient to absorb most of the flux of the growth species and prevents the supersaturation of the solution from reaching high levels, then most of the crystal growth will take place on the seed crystals. In this way, the crystal size and the growth rate can be controlled (Cundy *et al.* 1995a; Kacirek and Lechert 1975; Kacirek and Lechert 1976; Thompson and Dyer 1985a; Thompson and Dyer 1985b; Thompson 1992). On the other hand, if the quantity of the added seed crystals is reduced (i.e. reducing the available surface area), then supersaturation and self-nucleation will not be suppressed anymore, thus allowing a variety of crystal sizes to grow, and a better control on crystal size and growth rate may be difficult to achieve. A further aspect of using seed crystals was viewed by Bronic and co-workers. The syntheses of zeolites Y and P (Dutta and Bronic 1994) and zeolite A (Bronic *et al.* 1999) were investigated using a 2-compartment reactor in which the seed crystals and reactant gel were separated by a submicron membrane. The crystal growth took place in both compartments, but zeolite Y was formed on seed crystal side of the membrane and zeolite P were observed on the gel side of the membrane. This difference was indicative of the fact that seed crystals were the major participants in modifying the crystallization process when they were in physical contact with the gel. It can be deduced that the growth species travel freely through the membrane, and the nucleation is better controlled locally.

So far in this section, the nucleation is considered from an experimental point of view. A nucleation mechanism will be discussed now in the light of the above information. In a typical reaction sol, it may contain amorphous material, a solution phase, and one or more crystalline phases. It is relatively easy to identify crystalline phase. Whereas, the distinction between amorphous material and solution phase is less clear and is a subject of misunderstanding. Considering a simple case of traditional synthesis of zeolite X or Y in which amorphous material is visibly solid in nature. At the low Si/Al ratio and high pH of the precipitation nearly all the Si,Al-derived nutrients are present in solid gel phase, and the balance of the nutrients exist as monomers or oligomers in highly alkaline (Na^+OH^-) solution phase (Barrer 1982). The separation of the two phases through filtration or centrifugation makes it possible to acquire a division

of the reaction mixture into a liquid phase containing mainly true solution species, and a solid phase from which a proportion of crystalline to amorphous material can be determined through XRD analysis. The situation becomes complicated when a higher Si/Al ratio with lower pH is used for high molecular weight silicate and aluminosilicate components. It becomes difficult to distinguish between colloidal material and solution-related polymers (Andersson *et al.* 1982; Iler 1982; Otterstedt *et al.* 1987; Iler 1979). At the same time the polymeric species e.g. $Si_1, Si_2, \ldots Si_n$ cannot be considered as a continuum because the larger components may behave like particulate and can be phase-separated, thus resembling an invisible precipitate. The end result is that a part of the silicate and aluminosilicate reactants in the liquid phase behaves a true solution species, and at the same time the colloidal part of the reactant species resembles a separate amorphous phase. The colloidal phase is equal, in term of energetics, to solid phase that is amorphous and visible, but it is invisible to optical detection and is inseparable from the liquid phase by filtration and centrifugation. Figure 2.11 depicts such scenario. Therefore, in the systhesis of zeolites using "clear solution", all the amorphous feedstock is stored in the solution in this manner and provides the driving force for the crystallization of zeolite product (Andersson *et al.* 1982; Cundy *et al.* 1990; Iler 1982; Otterstedt *et al.* 1987; Schoeman *et al.* 1994; Watson *et al.* 1997; Thompsonand Dyer 1985c; Iler 1979; Ueda *et al.* 1980). Thus it may be emphasized that during the nucleation and crystal growth in hydrothermal synthesis of zeolite, the role of amorphous components at all levels should be accounted for.

In the light of above explanations it becomes easier to explain how the equilibration reactions lead to the formation of semi-ordered secondary amorphous phase, and how the related processes further form the zeolite nuclei. As shown in Figure 2.5, that the primary amorphous phase does not show any order in elements. Thus a driving force for zeolite formation may depend upon the ratio of the solubility constants (K_s) of the precursor and the final product. Since this is directly related to the solution supersaturation, therefore, the driving force for the zeolite crystallization reaction (i.e., change in free energy, ΔG) may be expressed as:
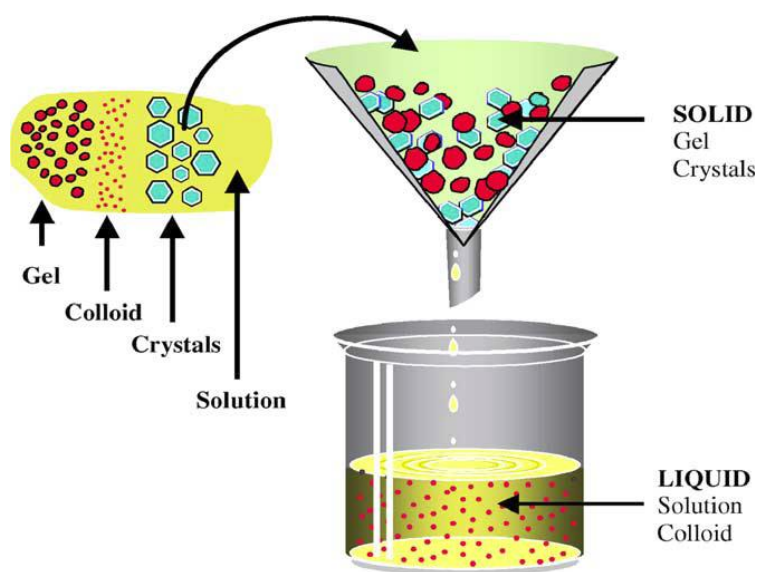
Figure 2.11: The liquid phase resulting from conventional solid-liquid separation methods (filtration or centrifugation) contains both true solution species and colloidal amorphous material (Cundy and Cox 2005).

$$\Delta G = -RT \ln\left(\frac{K_{s,gel}}{K_{s,zeolite}}\right) \tag{2.5}$$

The above equation and Figure 2.4 elaborate that the negative sign in the equation signifies a trend for the primary amorphous phase to become more and more ordered as the phase transforms toward secondary phase and so on. Flanigen and Breck (Flanigen and Breck 1960a; Flanigen and Breck 1960b), and also Chang and Bell (Chang and Bell 1991) focused on the chemical route by which the progressive transformation from amorphous phase to ordered phase took place. The breaking and re-making of Si, Si—O—Al, Al (T—O—T) bonds under the catalytic action of hydroxyl ion (-OH$^-$) with a related condensation reaction are expressed as follows:

$$T - OH + {}^-O - T \Leftrightarrow T - O - T + OH^- \tag{2.6}$$

$$T - OH + HO - T \Leftrightarrow T - O - T + H_2O \tag{2.7}$$

It should be noted that anions are not the only ones to take part in breaking and remaking of bonds but they are accompanied by cations (e.g. Na$^+$) that play a crucial role in the ordering of process. The cations will gather around themselves energetically favorable coordination spheres of oxy-species and will generate certain preferred geometries. In doing so the cation dependent elements, which will finally form the zeolite product, are gradually be assembled. This idea was originally came from Breck (Breck 1964), and was further refined by Brunner (Brunner 1992). The structuring of silicate and aluminosilicate units by electrostatic force (in case of organic templates) and van der Waals force (in case of inorganic material e.g. NaOH) has also been proposed by Fanigen (Flanigen *et al.* 1978; Flanigen 1980), Chang and Bell (Chang and Bell 1991), and Burkett and Davis (Burkett and Davis 1994; Burkett and Davis 1995b; Burkett and Davis

1995a). Based upon above ideas and proposals, Cundy and Cox (Cundy and Cox 2005) developed an argument to suggest a specific mechanism for the zeolite lattice construction.

According to his proposed scheme, as shown in Figure 2.12, first of all a cation (e.g. Na^+) migrates to a temporary site in a developing structure for nuclei where the coordination geometry may be suitable but not ideal. The cation initially maintains a hydrated shell (i.e. surrounded by water molecules). Once settled on this site, it starts to mediate the acquisition of T-units from the solution, which are formed through condensation reactions as mentioned above. The cation guides the new acquired T-units into more favorable coordination geometry, thus generates a periodic regular local structure. In due time, either most of the cation hydration shell is gradually replaced by lattice oxygen donors making it a fixture at the newly created site, or the cation may move to any other more suitable location to do the similar function. For this reason, some areas of the overall structure are more ordered as compared to others. Therefore, in due time, particular "islands of order" are established randomly throughout the newly developed semi-ordered network, as shown in Figure 2.5. These islands of order are dynamic, and at any time such islands are being created, up-graded, or even destroyed by dissolution. However, the overall effect will be a trend that moves towards a more

$Building\ UnitO\ Network \equiv T(OH)_3O^- (becomes: -OT(OH)_3, -OT(OH)_2O - etc)$
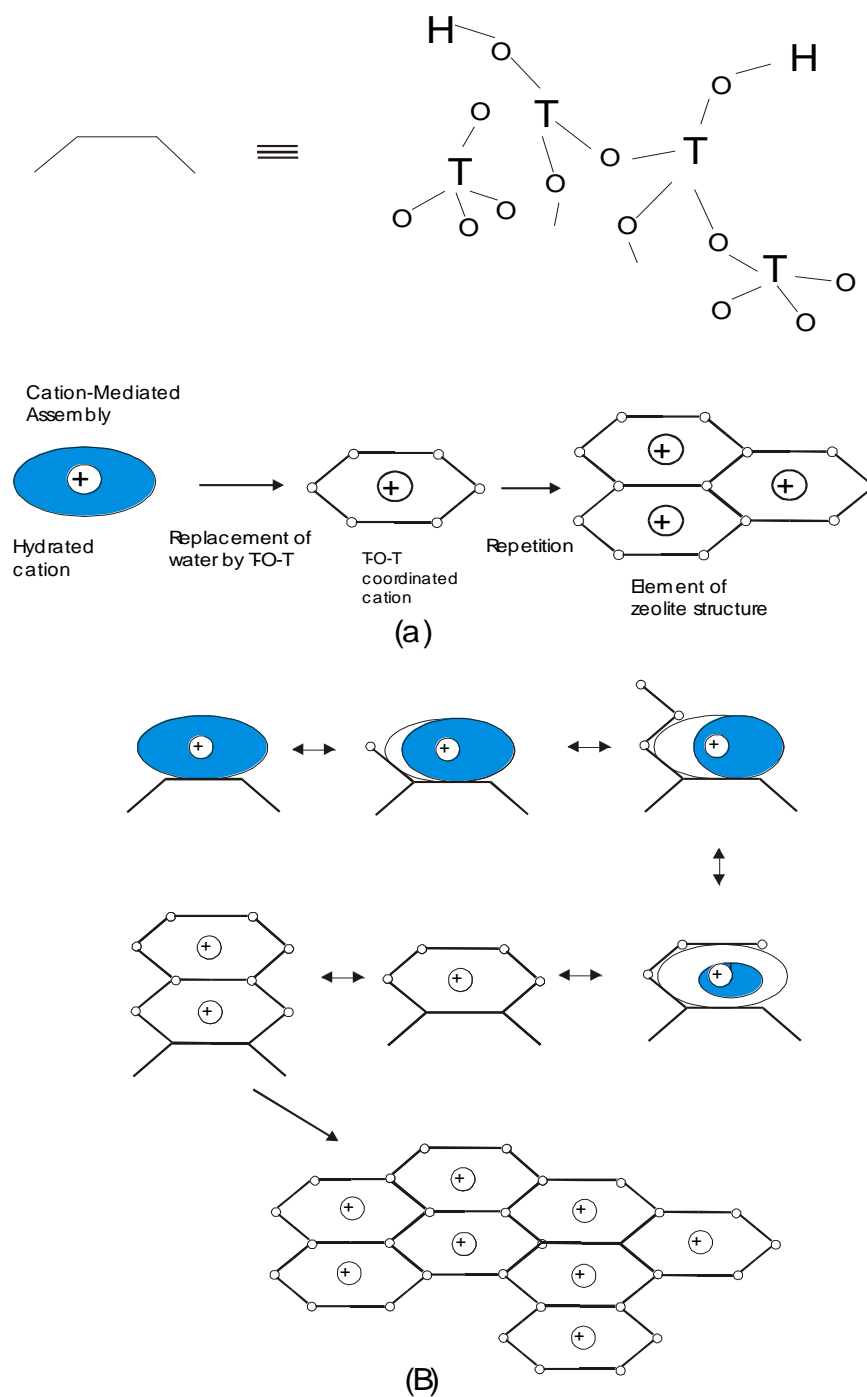
Figure 2.12: The basic mechanism for the cation-mediated assembly of ordered regions: (a) nomenclature and symbolism; (B) details of in-situ construction process by addition of solution units to a surface site. The same mechanism can be applied to zeolite crystal growth. (Cundy and Cox 2005)

ordered system. Ultimately, some areas of the newly ordered system will be able to make a periodic lattice that can propagate further, i.e. the nucleation has started to occur. Such transformation can be taken as a first order phase transition, and corresponds to the formation of critical radius (r_c) as mentioned earlier. From this point, the kinetics of the growth in increasing order become dominant as compared to the kinetics of the dissolution resulting in a net growth. As a result, the reversible equilibration reactions which correspond to the t_r component of induction period (τ) are superceded by the initial net growth (t_g). At the same time, the underlying chemistry remains the same and the reactions still maintain a significant reverse component of dissolution.(Cundy and Cox 2005)

The nucleation in zeolite may be considered as a discreet event which could be defined as "a phase transition whereby a critical volume of a semi-ordered gel network is transformed into a structure which is sufficiently well ordered to form a viable growth centre from which the crystal lattice can propagate". Cundy further added comments to the above definition. The critical volume in above definition corresponds to the requirement that the initial structure needs to be of a certain minimum size which refers to the critical radius (r_c) as explained earlier. Following this requirement, it is further assumed that the potential nucleus may not need to be perfect in its structure; rather it may be "good enough" to function as a nucleus in prevailing circumstances. This indicates the condition that r_c is not a fixed quantity but may vary, depending upon the other operating conditions such as temperature and supersaturation. Thus under such variable environment a rather defective potential nucleus may remain dormant or even dissolve under quasi-equilibrium conditions but may start to grow into a crystal under a high supersaturation driving force. The logic of gradual evolution of such a nucleus can further be explained by cutting a new key for a tumbler lock. Initially, there are no chances that the key will function to open the lock. As the machining of the key progresses, the key will become more and more perfect and a point will reach when it will open the lock. If the new key is compared with the original master key, it will show errors and imperfections in new key but within a certain tolerance it will perform the required function in the prevailing circumstances. It is good enough to do the function of opening the lock, but if the circumstances are changed (e.g. lock becomes hot and

expands) then it is possible that the imperfect key may not function any further to open the lock (Cundy and Cox 2005).

Experimental results of zeolite crystallization and transformation can be mathematically described by a simple kinetic relation (Subotic *et al.* 1980; Zhdanov 1971):

$$f_z = Kt_c^q \tag{2.8}$$

where f_z is the fraction of zeolite formed at time t_c, and K and q are constants. Generally q is a function of nucleation and crystal growth mechanism. For example, in a solid-crystal transforming system with constant supersaturation, q = 3 and nucleation is most likely heterogeneous. If q = 4, nucleation is homogeneous in the case of linear and size-independent growth. However, in a real solid-crystal transforming system, the value of q is less than 4. On the other hand, in the case of crystallization of zeolites from gel (i.e. gel-crystal transformations), the value q could be greater than 4, which shows that the nucleation rate increases during the crystallization process. Zhdanov (Zhdanov 1971) explained such an increase in the nucleation rate as autocatalytic nucleation by postulating "that not only the aluminosilicate blocks formed in the liquid phase, but also the blocks with an ordered structure occurring in the gel skeleton can be nuclei of crystals".

Based on Zhdanov's work, Subotic and Graovac, and Golemme et al. developed a theory to support the presence of non-solution mediated nucleation processes (Golemme *et al.* 1991; Subotic and Graovac 1985). They developed a kinetic model for zeolite growth, homogeneous nucleation, heterogeneous nucleation, and autocatalytic nucleation. They compared experimental results with numerical solution of their model and found that the particles of zeolites were formed by heterogeneous and autocatalytic nucleation. The role of homogeneous nucleation was insignificant. They also found that the gel-crystal transformation followed an exponential dependence on synthesis time with an increase in nucleation rate during the crystallization process. They postulated not only the formation of heterogeneous nuclei in the liquid phase (i.e. on the surface of gel and liquid interface), but also the formation of similar entities inside the amorphous gel with ordered

structures and called quasi crystalline zeolite. According to them, the growth of the quasi crystalline phase is not possible inside the gel phase but may take place when the gel is dissolved during the progress of crystallization and releasing it into the liquid phase. They also found that the ageing of the gel increased quasi crystalline phase (ordered structural entities) at room temperature. They concluded that the crystallization of zeolites could be explained by their kinetic model where the nucleation takes place at the external surface of the gel i.e. heterogeneous nucleation, or in the inside the pockets of the gel i.e. autocatalytic nucleation. What was missing was the contribution of homogeneous nucleation under the conditions of synthesis. They also concluded from the experimental evidence that the increase in the rate of nuclei formation during synthesis, production of a large portion of fine particles towards the end of synthesis, and the influence of gel ageing on the crystallization process could not be explained by the surface heterogeneous nucleation. Therefore, they suggested that a significant contribution from autocatalytic nucleation exists during zeolite crystallization.

Thompson 1992 and Gonthier et al. in 1993 showed that the autocatalytic nucleation model did not fit all the experimental data (Gonthier *et al.* 1993; Thompson 1992). Literature (Golemme *et al.* 1991; Subotic and Graovac 1985) suggested that the number of crystals formed by autocatalytic nucleation would be approximately 20 times greater than the number formed by the heterogeneous nucleation. Thompson and Gonthier et al. found that the nucleation began very early in the synthesis process and the fraction of crystals formed by the heterogeneous nucleation mechanism was low. They also found that the nucleation of all crystals was essentially complete before the crystallinity of ZSM-5 had reached 10%. This behaviour was not expected as more than 95% nuclei were still contained in the amorphous gel and were yet to be released by the dissolution of 90% of the remaining amorphous gel. They modified the original autocatalytic hypothesis model based on the hypothesis that the nuclei formed by autocatalytic nucleation mechanism were located preferentially near the outer surface of the amorphous gel particles rather than being uniformly distributed throughout the gel phase. The results of their model agreed well with the experimental data. However, the agreement did not necessarily prove the conceptual validity of the model but suggested the possible existence of a nuclei source other than from the solution (homogeneous

nucleation) and solid surface (heterogeneous nucleation) (Gonthier *et al.* 1993; Thompson 1992).

Homogeneous nucleation is frequently assumed as a possible process for the formation of primary zeolite particles in the liquid phase. It has been shown during the crystallization of different types of zeolites from clear solutions that nucleation may take place in the liquid without the presence of a solid amorphous gel. Using the classical theory of homogeneous nucleation, Bronic and Subotic tested the kinetics of homogeneous nucleation of zeolite A and Y. They found that the time required for the first nuclei to appear through the process of homogeneous nucleation was infinite. This was because supersaturation, which is typical for most of the zeolites, was considerably lower than the critical supersaturation required for homogeneous nucleation. So, it is realistic to expect that heterogeneous and autocatalytic nucleation mechanisms are dominant for the crystallization from gels (Bronic and Subotic 1995).

Mintova et al. (Mintova *et al.* 1999b; Mintova *et al.* 1999a) have reported, for the first time, the direct imageing of nucleation mechanism of zeolite Y and A using high-resolution transmission electron microscopy (HR-TEM) at 100 ˚C and room temperature, respectively. They studied the synthesis mechanism of nano-sized zeolites from a clear solution. They found by HR-TEM images that the freshly prepared solution at room temperature contained the aggregates of amorphous gel particles in the size of 25-35 nm having sharp edges, whereas x-ray diffraction indicated that these colloidal particles were amorphous. After heating the solution for different times at 100 ˚C, the colloidal gel particles of aluminosilicate remained amorphous for 24 hrs and then the first sign of crystal formation appeared after 28 hr of heating. They captured the images and found that the crystals always nucleated at the periphery of the amorphous gel aggregates which supported the nucleation mechanism discussed by Gonthier et al. (Gonthier *et al.* 1993). They also found that from each aggregate of amorphous gel only a single crystal formed and the particles were rather uniform. Their visualization was confirmed by a further analysis under dynamic light scattering (DLS) technique. As the synthesis time increased to 48 hr, it was observed that the size of the zeolite-gel particles remained the same suggesting that the nutrients for the crystal growth were primarily provided by the gel particles. This was further confirmed by the mass balance under several conditions of

operation. Upon further heating to 100 hr, the crystal size was further increased, suggesting that the extended growth of crystals was due to colloidal zeolites themselves as no gel particles remained in the solution after 48 h. These colloidal zeolites were able to grow to bigger crystals through the dominant mechanism of mass transfer in solution over macroscopic distances. Figure 2.13 shows all the stages of zeolite nucleation and crystal growth which were captured as a direct evidence using HR-TEM (Mintova 1999a).

Li et al. (Li *et al.* 2002) used two different synthesis temperatures, and a two-stage varying-temperature technique to further elucidate the mechanism of the nucleation kinetics of zeolite Y. They prepared two solutions containing source of alumina and source of silica separately and mixed them together before the hydrothermal treatment. In their one-stage synthesis at 100 ℃, they observed 30-40 nm particles before and during the first three days of hydrothermal treatment. The particles were characterized using dynamic light scattering (DLS). Both solutions were separately analyzed and it was found that only the silica-based solution contained particles of 5nm, which was consistent with their other study (Li *et al.* 1999). Thus, the 30-40 nm particles were amorphous aluminosilicate, which were formed after mixing the two solutions. Similar findings were also reported by Mintova et al. (Mintova *et al.* 1999b). The amorphous particles were observed for the first 4 days of hydrothermal treatment and then slowly decreased to the size of 20nm before a second larger population of zeolite Y was detected after 4 days. This population increased and grew linearly to a size of 75nm after 7 days. A similar pattern was observed at a temperature of 130 ℃ with the exception that the crystal size increased to 137 nm, reaction time reduced to 3 days, the crystal concentration was reduced to one-quarter as compared to the operation at 100 ℃, and the yield was slightly increased. In order to determine the nucleation time for zeolite Y at 100 ℃, they used a two-stage varying-temperature process. The crystallization was started at 100 ℃ and the temperature was changed to 130 ℃ to stop further nucleation. In the initial first two days of synthesis the crystal size was unaffected by the temperature. However, for a longer reaction time the effect of change in temperature was prominent. Therefore, the number of crystals nucleated in the final

hydrothermal
treatment

(100°C, 28 h)

amorphous gel particles, 25-35 nm
after 24 h aging at RT

nucleation and crystallization
of zeolite Y single crystals
(10 to 30 nm) at periphery of
gel particles

48 h at 100 ˚C

extended crystal growth, up to 50 nm
after 75 h at 100 ˚C

gel particles convert into zeolite Y
nanocrystals (25 to 35 nm)
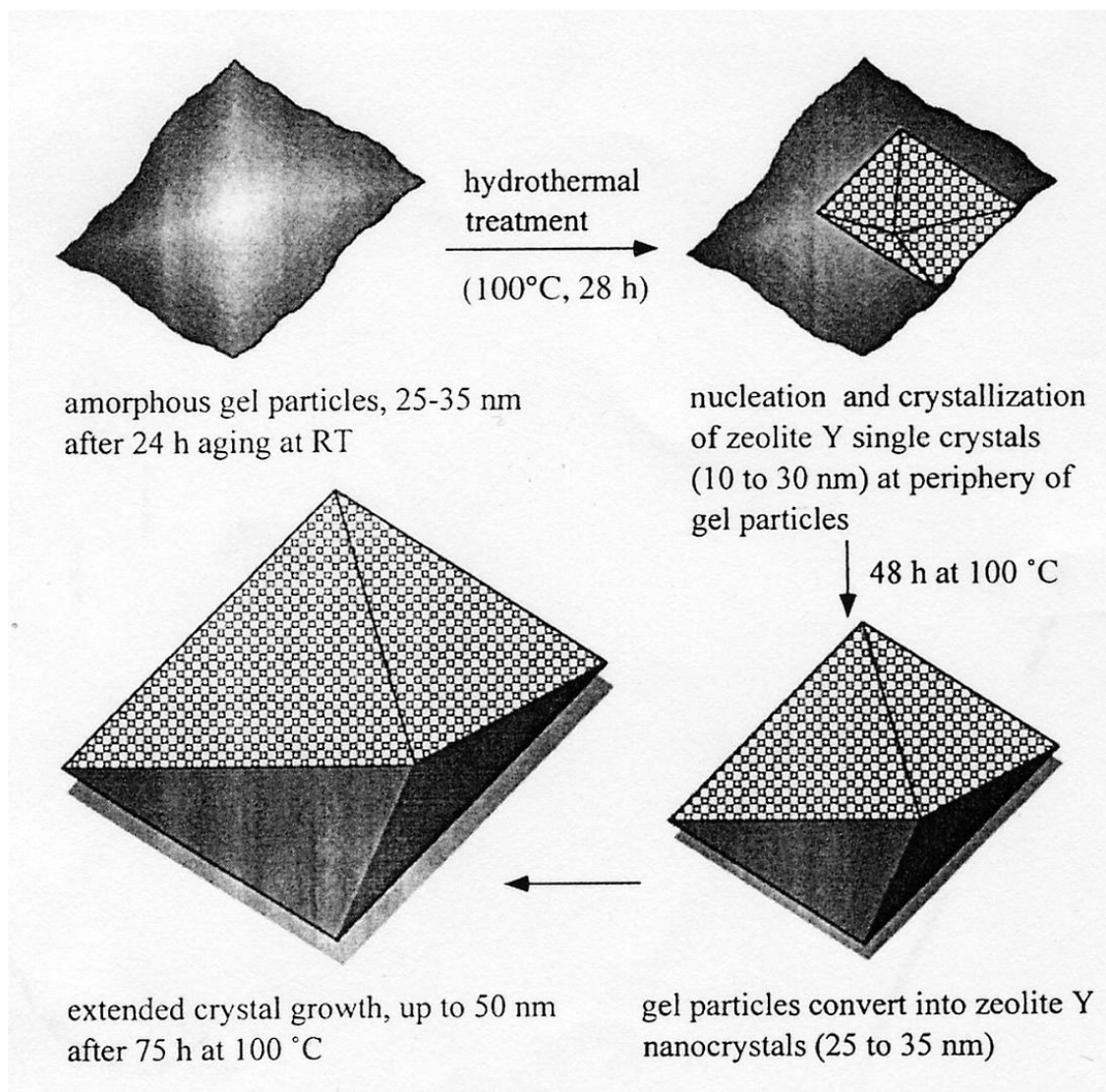
Figure 2.13. Proposed reaction scheme for the zeolite growth mechanism in colloidal solution. Reprinted with permission from Mintova et al. (Mintova *et al.* 1999a).

product (crystal concentration), influenced by the temperature variation were used to determine the time when nucleation was completed. Figure 2.14 shows that the process of nucleation continued until the crystal concentration reached a constant value.

Figure 2.14 also shows that for the first-stage of temperature at 100 ºC, the crystal concentration gradually increased to a constant value in 6.5 days and switching to the second-stage at 130 ºC did not reduce the crystal concentration, it only hindered further nucleation. They concluded that the nucleation period was extended over the entire period of crystal growth.

2.8 NON-AQUEOUS AND DRY GEL SYNTHESIS

2.8.1   Non-Aqueous Synthesis

Zeolites are conventionally synthesized by hydrothermal methods using excess of water. On the other hand, Bibby and Dale (Bibby and Dale 1985) in 1985 were the first to report the synthesis of silica sodalite from ethylene glycol solvent. However, recent results for many zeolite syntheses indicate that the nucleation and crystal growth proceed through heterogeneous transformations involving amorphous and/or pseudocrystalline particles (Serrano and Van Grieken 2001). The mechanism of solid-solid transformation during nucleation and crystal growth led to studies of non-aqueous synthesis of zeolite, which enhanced the conversion of dry gel to zeolite (Kim *et al.* 1993; Matsukata *et al.* 1993). Commercially, zeolite synthesis mostly involves the use of amorphous gel with high solid content (Serrano and Van Grieken 2001).

The concept of solid-solid transformation was successfully demonstrated by Xu et al. (Xu *et al.* 1989) in 1989 who synthesized ZSM-5 and ZSM-35 on a non-aqueous basis. They made aluminosilicate gel by preparing a solution of sodium silicate and sulphuric acid, and then adding a solution of $Al_2(SO4)_3$ and $NH_3.H_2O$. The resultant gel was then dehydrated at 823 K. The solid dehydrated gel was mixed in a solution of two amines (ethylenediamine and triethyleamine) for the synthesis reaction.
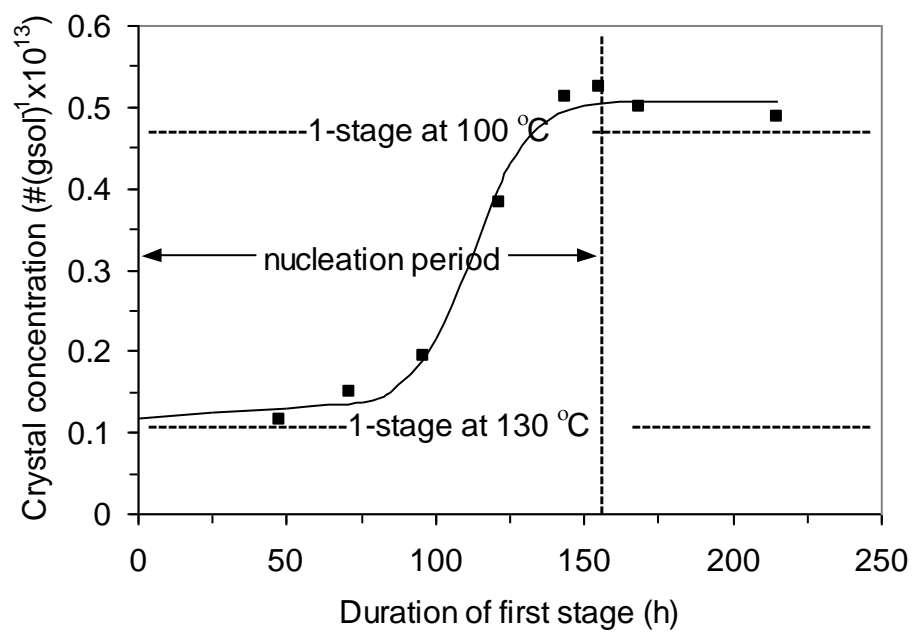
Figure 2.14. Crystal concentration of zeolite Y after two-stage syntheses. Redrawn with permission from Li et al. (Li *et al.* 2002).

Throughout the crystallization neither SiO_2 nor Al_2O_3 were dissolved in a mother liquid mixture of ethylenediamine and triethylamine. There was a constant molar SiO_2 / Al_2O_3 ratio in the solid phase, which strongly supports the solid-solid mass-transformation mechanism. It was found that the effect of Na_2O was very similar to the effect in aqueous synthesis. No effect of Na_2O was observed on the selectivity of ZSM-5 or ZSM-35. However, the initial molar ratio of SiO_2 / Al_2O_3 was crucial in determining the type of zeolite as the ratio did not change during the crystallization. A lower molar ratio (SiO_2 / Al_2O_3 = 18) led to the formation of ZSM-35. Likewise, lower molar ratios of $C_2H_8N_2$/Na_2O favored ZSM-35 synthesis. The most significant effect was the molar percent of triethlyamine and SiO_2 that determined formation of ZSM-35 or ZSM-5. A subsequent study performed by Li et al. (Li *et al.* 1995) in the absence of water further supported the solid phase transformation. They synthesized ZSM-48 zeolite using dried and dealuminated alumina-silica microspheres (aluminosilicate gel) mixed with solid NaOH, 1,6-hexanediamine, and quantities of seed crystals. The mixture was kept in a stainless steel autoclave at 100 ºC overnight and then crystallization was carried out at 180-200 ºC for 18-26 days. Finally the solid product was removed and washed with water. It was found that the ratio of 1,6-hexanediamine / SiO_2 and the size and shape of the autoclave reactor were decisive for the synthesis of the desired product. However, they did not discuss the role of 1,6-hexanediamine as an organic template. In a subsequent study (Fan *et al.* 1996) on the same zeolite, they investigated the effect of MCl (M = Li, Na, K, Rb, Cs) on the synthesis while keeping the M^+/Na^+ ratio the same. It was found that the presence of different alkali metal chlorides greatly slowed down the crystallization rate with the exception of NaCl. It is well known that Na^+ is the most effective structure-directing agent of all the alkali metal cations. The stronger the capability of the structure-directing cation is, the shorter is the induction time, and higher is the crystallization rate. Actually Na^+ forms a double five-member ring, essential for ZSM-48. Other alkali metal cations showed structure-breaking effects due to their lower polarizability. It was also observed that the presence of Cl^- anion affected the crystallization rate in the non-aqueous system. The morphology and the size of ZSM-48 were greatly influenced by the use of different metal alkali chlorides. However, the bulk composition of SiO_2 / Al_2O_3 did not vary, owing to the mechanism of heterogeneous

crystallization. On the other hand, XPS analysis showed significant changes in the surface composition. This was due to the non-homogeneous distribution of Al from the surface to the crystal core. This was attributed to the structure-directing or breaking abilities of alkali metal cations.

2.8.2   Dry Gel Synthesis

A deviation from the commonly practiced hydrothermal method for zeolite synthesis was reported by Xu et al. in 1990 (Xu *et al.* 1990) who described a new technique of vapor-phase transport (VPT) method. This study further bolstered the solid-solid transformation mechanism. In this technique, a dry gel of aluminosilicate was transformed into zeolite ZSM-5 by contacting with mixed vapor of water, ethylenediamine, and triethylamine. The amorphous aluminosilicate gel was obtained by mixing solutions of aluminum sulphate, sodium silicate, and sodium hydroxide; and then filtered and washed. The solid gel was placed in bottom-sieved container, which in turn was placed inside the top of an autoclave whose bottom contained ethylenediamine-triethylamine aqueous solution, as shown in Figure 2.15. Upon heating, only the mixed vapor of water, ethylenediamine, and triethylamine came in direct contact with the gel, and not the solution. The product was found damp upon completion of reaction. After washing and drying, and XRD analysis, the product was found to exhibit the pattern of ZSM-5 even if a dried gel was used for synthesis. The composition of SiO_2 / Al_2O_3 for the amorphous gel and the crystal product remained the same, suggesting the prevalence of solid-phase transformation. A further study in 1993 by Matsukata et al. and Kim et al. (Kim *et al.* 1993; Matsukata *et al.* 1993) confirmed the vapor-phase transport (VPT) technique for conversion of dry gel. They found it useful for synthesizing different types of zeolites such as; ANA, FER, ZSM, MOR, CHA, etc. In all these syntheses the dry gel never came in direct contact with the aqueous solution. Only the vapor with or without organic template came in contact with the amorphous gel. The excess water was not essential for the zeolite synthesis, however, it enhanced crystallization in some cases. Complete conversion to zeolite under appropriate
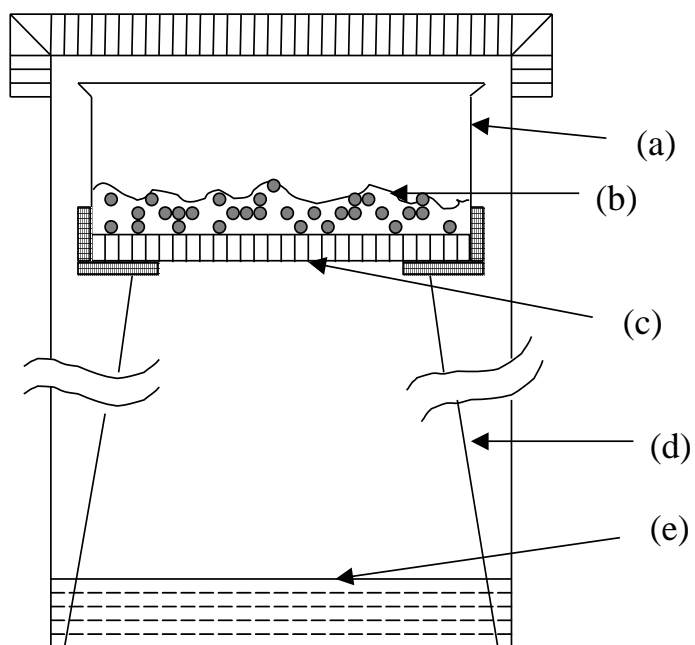
Figure 2.15. Schematic view of the dry process autoclave used in the zeolite synthesis by VPT method: (a) container; (b) amorphous gel; (c) porous sieve plate; (d) stainless steel support; (e) solution phase. Redrawn with permission from Xu et al. (Xu *et al.* 1990).

preparation conditions was found to be possible.

Althoff and coworkers (Althoff *et al.* 1994; Althoff *et al.* 1995) synthesized zeolite ZSM-5 by gradually decreasing the water content and ending up with a reaction mixture with absolutely dry reactants in the form of a powder. The aluminosilicate dry gel was prepared by mixing aluminum sulfate and fumed silica, and dehydrated by calcination. The silica-alumina precursor was mixed with ammonium floride (NH_4F) and tetrapropylammonium bromide (TPABr), used as an organic template. Initially the reaction was carried out in a 50 mL Teflon-lined stainless steel autoclave using different amounts of water in a hydrothermal synthesis. Further synthesis was devoid of any additional water. The NH_4F and TPABr were vacuum-dried and added to the precursor. But during the reaction, water vapor was produced due to the following reaction:

$$SiO_2 + 4NH_4F \rightarrow SiF_4 + 2H_2O + 4NH_3 \tag{2.9}$$
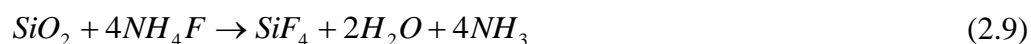
The pressure due to the production of water vapor was further eliminated by reducing the amount of NH_4F and using a larger size autoclave of size 200 mL. In all the cases, pure ZSM-5 was formed and its morphology for non-aqueous or aqueous methods remained the same. The X-ray fluorescence analysis indicated a pronounced difference in the composition of Si/Al in precursor and in the crystalline form as no aluminum was found in the samples obtained from dry synthesis. This observation led to the assumption that AlF_3 could be formed as a side reaction, which was later confirmed by ^{27}Al MAS-NMR. This gave rise to high Si/Al ratio and gave credence to the idea of gas phase transport mechanism with SiF_4 as the mobile species. AlF_3 due to its high melting and sublimation point was not mobile under reaction condition. Thus, formation of a zeolite in the absence of a solution phase was due to vapor phase mass transfer process with SiF_4, which acted as transporting species between the solid phase containing the unreacted precursor and the ZSM-5 crystals. The presence of water during the reaction was not ruled out; however, its amount was insufficient to reach saturation pressure under reaction conditions.

Dong and coworkers (Dong *et al.* 1999) synthesized zeolite B-Al-ZSM-5 using boron-aluminum-silicon porous glasses as dry gel and ethylamine-water as source of

vapor. A highly crystalline zeolite was formed with almost uniform composition of gel and final product, which also supported the heterogeneous crystallization mechanism. A similar study in 1998 was performed by Bandyopadhyay and coworkers (Bandyopadhyay *et al.* 1998) for boron based zeolite synthesis. The crystallization of dry gel with composition of SiO_2: 0.002-0.033 B_2O_3: 0.056-0.1 NaOH: 0.36-1.2 TEAOH was carried out at 448 K for 72 h. The phase of the borosilicates was strongly dependent on the dry gel composition, e.g. B-BEA was formed with TEAOH/SiO_2 ratios of 0.8-1.2 and SiO_2/ B_2O_3 ratios of 30-50, B-MTW was formed with TEAOH/SiO_2 ratios of 0.8-1.0 and SiO_2/ B_2O_3 ratios of 50-100, and B-MFI was formed with SiO_2/ B_2O_3 ratios of 100-200.

2.8.2.1 Classification of Dry Gel Synthesis

Matsukuta and coworkers (Matsukata *et al.* 1999) in a review paper classified the zeolite synthesis mechanisms in different categories. One is the conventional hydrothermal synthesis method where the hydrogel contains all the ingredients such as; silicon, aluminum, water, sodium, and/or organic structure-directing agent (SDA). Synthesis is performed in a confined space, usually an autoclave, to maintain autogeneous pressure, which is needed when reaction proceeds above 373 K. The other process is called dry gel conversion (DGC), which is sub-classified into two categories. When using SDA such as ethylenediamine (EDA), a mixture of water and EDA is placed in the bottom of autoclave (Figure 2.15) and the dry gel with no EDA is placed in the middle. Upon heating, EDA and water vaporize, reach the gel and start the crystallization. This method is called "vapor-phase transport" by Kim et al. (Kim *et al.* 1993). When quaternary non-volatile amines, such as tetrapropylamine hydroxide (TPA OH) are used as structure directing agents, they incorporate into the dry gel. Only water is placed in the bottom of the autoclave to supply steam for the gas phase. Matsukata et al. called this method as "steam-assisted conversion" (SAC). However, they did not categorize a complete dry gel method as demonstrated by Althoff et al. (Althoff *et al.* 1994; Althoff *et al.* 1995) in which no liquid was added to the autoclave.

2.8.2.2 Characteristics of Dry Gel Conversion (DGC) Process and its Advantages over
   Hydrothermal Synthesis (HTS) Process

Matsukuta et al. (Matsukata *et al.* 1999) also reviewed other issues such as efficient synthesis, high crystallinity, higher Si/Al ratios, thermal stability, and phase transformation. The DGC process for the syntheses of various zeolites e.g. MFI, FER, MOR, BEA, MTW, OU-1, FAU, and EMT was reviewed. The syntheses of hexagonal faujasite (EMT), and cubic faujasite (FAU) through SAC method using crown ethers [1,4,7,10.13,16-hexaoxacyclooctadecane, (18-crown-6) and 1,4,7,10,13-pentaoxacyclopentadecane, (15-crown-5)] as SDA instead of amines, was also studied. It was previously demonstrated that crown ethers can fit well in the super-cage of faujasite and give a selective product while using hydrothermal method (Delprato *et al.* 1990). They employed both methods for synthesis using colloidal silica and aluminum hydroxide with the composition of 10 SiO_2: Al_2O_3: xNa_2O: 0.75 R: 140 H_2O (x = 2.1-3.3, R= 18-crown-6 or 15-crown-5). The hydrogel was aged at 308 K for 24 h, and hydrothermally crystallized in an autoclave at 388 K for 7 days. In SAC method, the gel was dried and crushed into powder after ageing, and crystallized in steam at 388 K at autogeneous pressure. Both methods were found to be in agreement with each other. The SEM observations indicated that the EMT synthesized through hydrothermal process consisted of hexagonal plates and had facets randomly aligned at the edges of the plates. Such morphology was in agreement with layer-by-layer growth mechanism, which was proposed by Khouw and Davis (Khouw and Davis 1995). On the other hand, EMT crystals synthesized by SAC method showed a different morphology. The crystals were in the form of stripes indicating steps with smooth edges which suggested a spiral growth mechanism.

The dry gel process has many advantages over the conventional hydrothermal process such as saving of organic template (Xu *et al.* 1990). Another advantage of dry gel process was observed when Hari Prasad Rao et al. (Hari Prasad Rao *et al.* 1998) who were able to synthesize high-silica beta (BEA) zeolite with SiO_2/Al_2O_3 ratio in the range of 30–730. The conventional hydrothermal process can only achieve a maximum of SiO_2/Al_2O_3 ratio of 250 (Lohse *et al.* 1996; Perez-Pariente *et al.* 1988). The gel was

made by making a solution of aluminum sulfate, distilled water, NaOH, tetraethylammonium hydroxide (TEAOH, organic template or structure-directing agent), and fumed silica. The mixture was heated, dried, crushed to powder, and placed in an autoclave with only water in the bottom. The schematic diagram of the process is shown in Figure 2.15. Since the kinetics of the crystallization depended on SiO_2/Al_2O_3 ratio, the gel with the highest Al content was fully crystallized in 3 hr as shown in Figure 2.16.

The chemical composition of the starting gel and the crystalline form remained the same. The rate of crystallization and relative crystallinity decreased as the SiO_2/Al_2O_3 ratio was increased to 730. The relative crystallinity was improved to 100% by addition of $NaHSO_4$ to the parent gel, which supported an earlier finding that anions such as sulfates can improve the rate of crystallization in hydrothermal synthesis (Kumar *et al.* 1996). Hari Prasad Rao et al. (Hari Prasad Rao *et al.* 1998) found in their study that the concentration of Na^+ cation also increased by the addition of $NaHSO_4$, so they were unable to clarify which ion (Na^+ or SO_4^{+2}) was responsible for increase in crystallinity. However, when a higher concentration of Na^+ ion was used for higher SiO_2/Al_2O_3 ratios in the range of 380-480, the presence of Na^+ ion promoted the pure beta zeolite. Two interesting findings were reported; a uniform size of 60 nm was obtained with no amorphous phase present in the final product, and the water was absolutely required to get the crystalline product. In the absence of water vapor, an amorphous product was obtained. A similar method was employed successfully for the synthesis of zeolite ZSM-5 in another study (Matsukata *et al.* 1993) and in the preparation of unsupported zeolite ZSM-5 and ZSM-35 membranes by Dong et al. (Dong *et al.* 1992).

The wide application of NaY zeolite as a fluid catalytic cracking (FCC) catalyst led to its production using two different methods. One is the conventional synthesis using hydrothermal process and then loading the zeolite on an inert matrix of silica/alumina for final use as FCC catalyst. Another route is called "in-situ" process (Breck 1974). The starting phase includes the solid kaolinite microspheres which are transformed to NaY zeolite using hydrothermal synthesis method.
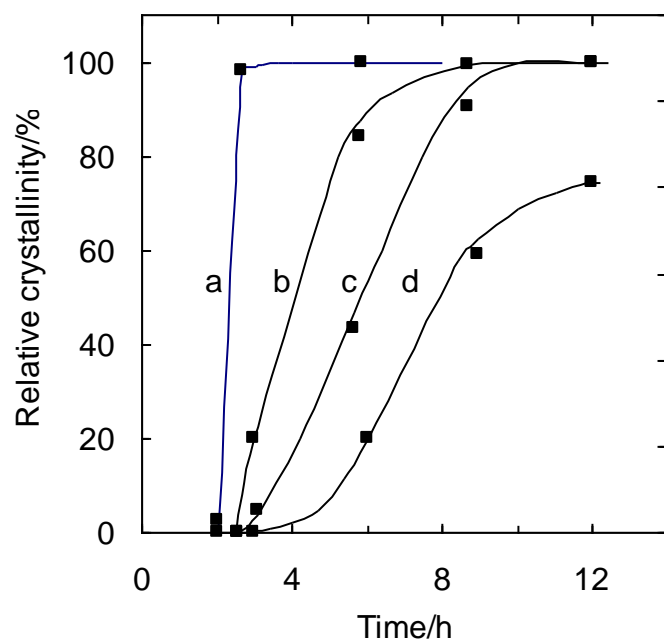
Figure 2.16. Crystallization curves of BEA with different chemical compositions at 453 K. SiO_2/Al_2O_3, SiO_2/Na_2O and SiO_4^{2-}/SiO_2 ratios: (a) 30, 23.8 and 20.9; (b) 380, 23.8 and 528; (c) 730, 10.9 and 10; (d) 730, 23.8 and 0, respectively. Redrawn with permission from Hari Prasad Rao et al. (Hari Prasad Rao *et al.* 1998).

Basaldella et al. (Basaldella *et al.* 1993) used a similar approach to grow NaY zeolite crystals on the internal and external surfaces of kaolinite microspheres using hydrothermal synthesis in which the reaction medium consisted of a solid phase (clay calcined microspheres) in contact with an alkaline mother liquor. Murrell et al. (Murrell *et al.* 1999) tried a different approach, in which the starting solid phase was silica gel particles of 50 microns that were gradually loaded with alumina to adjust the SiO_2/Al_2O_3 ratio followed by drying and calicination. Finally, NaOH solution with or without organic SDA was added through incipient wetness and the solid gel remained in semi-dry form giving a composition of 2.94 SiO_2 : 0.49 Al_2O_3 : Na_2O : 17.8 H_2O. The reaction was carried out in an autoclave or a polypropylene bottle and the final product contained 100% crystalline product. This process was similar to the DGC process with the exception that no additional water was added. The water within the gel pores was sufficient to carry out the crystallization.

Bhaumik and Tatsumi (Bhaumik and Tatsumi 2000) synthesized pure silica NU-1 and Na- and Al-free Ti-NU-1 zeolite successfully using the DGC method. These zeolites were previously synthesized through a hydrothermal method and posed lot of difficulties, especially in the dispersion of tetrahedral Ti species in the crystal (Ahedi *et al.* 1997). The starting materials tetrabutyl orthotitanate (TBOT), H_2O_2, tetramethylammonium hydroxide (TMA-OH), and fumed silica were mixed and prepared in the composition of 30 SiO_2 : TiO_2 : 7.5 $(TMA)_2O$, and then dried, powdered and loaded to an autoclave with 10g of water in the bottom of autoclave. The synthesis took 5-6 days at 170 ℃. They found highly dispersed isolated tetrahedral Ti species in Ti-NU-1 with a uniform needle like morphology. On the other hand, hydrothermal synthesis showed a non-uniform spherical morphology. A shorter synthesis time was possible with the DGC method without the need of any seeds or promoters. A similar problem was faced for the synthesis of metal-substituted aluminophosphate MAPO-36 (ATS topology) zeolite using hydrothermal synthesis (HTS) method. The product (MAPO-36) was contaminated due to co-crystallization of MAPO-5 (AFI topology). This problem was resolved by Saha et al. (Saha *et al.* 2003) using DGC method. They used both techniques i.e. SAC and VTP, but reported only VPT. The dry gel was used with a composition of 0.92 Al_2O_3 : 0.17 MgO : 1.0 P_2O_5 : 45 H_2O. Pr_3N (structure directing agent) was mixed

with water (0.3 g per 1.0 g of dry gel) and placed in the bottom of autoclave. The dried gel was placed in the middle of autoclave. The temperature and time were set in two steps, i.e. T = 105 ºC for 48 h followed by T = 140 ºC for 24 h. A deviation from the set temperature condition, especially in the first step led to a mixed product. However, a pure ATS was obtained using the above-mentioned set of conditions. This suggested that no phase transformation took place. However, there was a competition in nuclei formation between the two phases of ATS and AFI. Also, the MgO/ Al_2O_3 ratio affected the phase formation. When the ratio was 0.1-0.25, the ATS was the only product. On the other hand the ratio below 0.1 and above 0.25 produced contaminated product (ATS and AFI). Thus using the DGS method an exact synthesis protocol was devised for pure ATS. When similar conditions were applied to the HTS method, a contaminated product resulted. Therefore, a clear advantage of the DGS method was seen over the HTS method.

Bandyopadhyay et al. (Bandyopadhyay *et al.* 2001) successfully synthesized pure [Al]-SSZ-31 zeolite using the DGC method. 1,1,1,8,8,8-hexaethyl-1,8-diazoniaoctane dihydroxide $R^{2+}(OH)^-)_2$ was used as the structure directing agent. A gel with composition of SiO_2 : $0.2R^{2+}(OH)^-)_2$:0.084 NaOH : 0.0026 Al_2O_3 was mixed, dried, powdered and added to an autoclave generally used for the DGC method with 0.2-0.3 g of water per g of dry gel. It was found that the alkali to silica ratio ($NaOH/SiO_2$) was mainly responsible for the different phases. A $NaOH/SiO_2$ = 0.05-0.12 ratio produced pure SSZ-31 product, while $0.15< NaOH/SiO_2<0.03$ produced MFI phase. On the other hand, an optimum ratio of 0.084 caused phase transformation from BEA to SSZ-31. It was further identified that the synthesis time and phase transformation time were shorter, i.e. 12 h, which was not possible in hydrothermal synthesis. Also the yield of Al-SSZ-31 was higher (75-90%) using the DGC method than that of B-SSZ-31 (65%) using hydrothermal process. In another study (Bandyopadhyay *et al.* 2002), they were able to synthesize $AlPO_4$-5, $AlPO_4$-11, SAPO-5, and SAPO-11 zeolites by using the DGC method in two ways, i.e. steam assisted conversion (SAC) and vapor-phase transport (VPT). They found that the VPT was a slightly slower as compared to the SAC process and conventional hydrothermal synthesis (HTS) methods. In all cases, the need of water was mandatory to carry out crystallization. Two advantages were found in the DGC as compared to the HTS; the yield (75-90%) was 10% higher, and wastewater disposal was minimal.

Arnold et al. (Arnold *et al.* 2004) synthesized zeolite [Al]EU-1 and [Ga]EU-1 (EUO framework) with high purity using hexamethonium bromide (HMBr) as an organic template. Previously, the same zeolite was synthesized using the HTS method in Si/Al ratio in the range of 20-60 for [Al]EU-1 using HMBr, and 27<Si/Ga<50 for [Al]EU-1. However, impurities such as EU-2 were also formed when 60<Si/Al<120 was used for [Al]EU-1 synthesis. These problems were resolved when the DGS method was used. High composition range Si/Al = 18-142, and Si/Ga = 12-86 were successfully used to obtain pure products. Silica sol was added with HMBr solution, which in turn added to sodium silicate, NaOH and water for [Al]EU-1 synthesis, and Ga_2O_3, NaOH and water for [Ga]EU-1 synthesis. All ingredients were mixed, dried, and put in an autoclave of volume 100 ml with different amounts of water in the bottom. The desired product was obtained at T = 453 K for 7 days. In a parametric study, they found that sodium with Na/Si>0.3 and a high Ga content (Si/Ga $\leq$ 27) favored a pure [Ga] EU-1 over an amorphous phase. However, at Si/Ga $\geq$ 63 some extra-framework silicon species were easily washed out. The effects of template and water were also investigated. It was found that for a composition of $81.4SiO_2$: Al_2O_3 : xNa_2O : yHMBr (x = 10.9-18.6, y = 2.2-11.0) a high crystallinity was obtained with HMBr/Si $\geq$ 0.11 and Na/Si = 0.3. However, a decrease in template content led to the production of α-quartz as an impurity which was not removed even by increasing the Na content in the gel. The effect of the quantity of water in the autoclave on the conversion of dry gel with a molar composition of $61.0 SiO_2$: Al_2O_3 : $9.1 Na_2O$: 7.4 HMBr is depicted in Figure 2.17. The XRD patterns indicate that a minimum amount of water is needed for synthesizing highly crystalline zeolite EU-1. It can be seen that the zeolite EU-1 can be obtained over a large range of water content, which is in variance with the dry gel synthesis of zeolite Beta where the amount of water was very critical for synthesis (Matsukata *et al.* 1999). According to their calculations using van der Waals equation, a mass of liquid water more the 0.52 g (water/Si $\geq$ 0.67) in a 100 mL autoclave at 453 K would cause presence of liquid water in the autoclave.
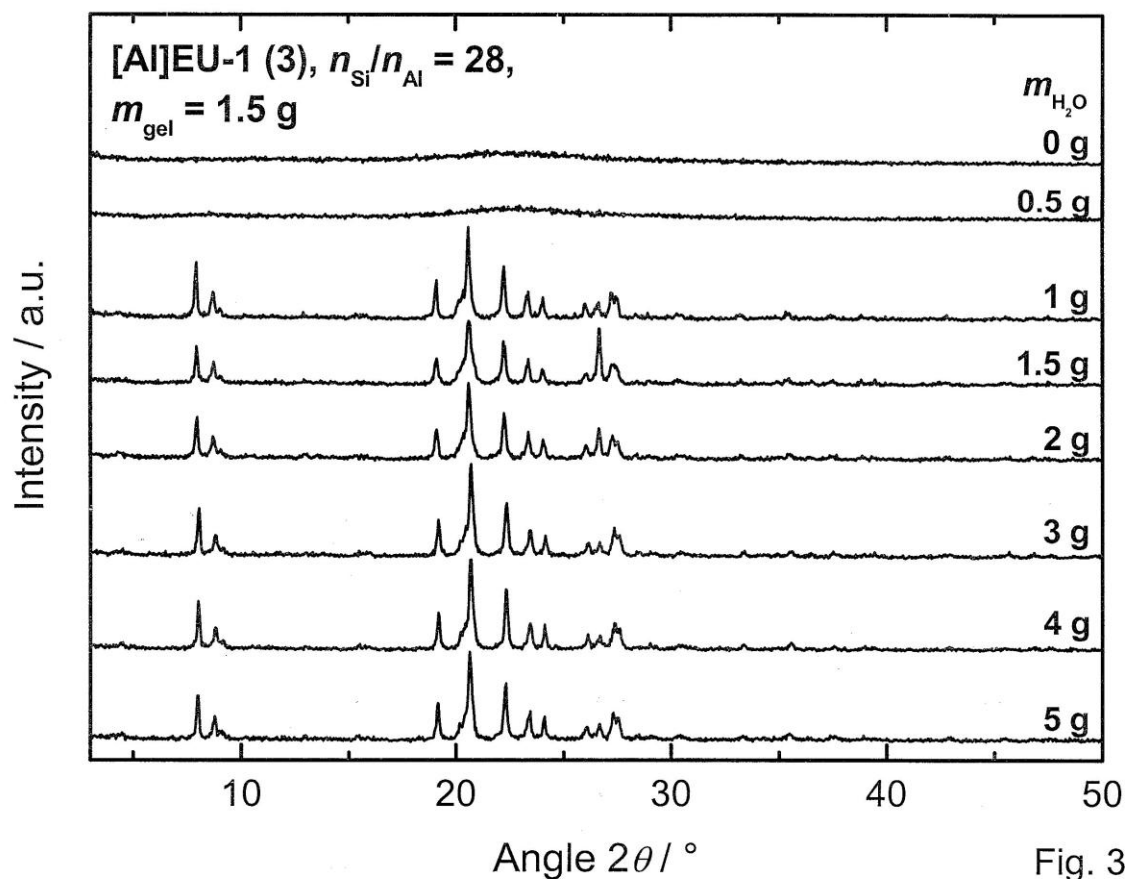
Figure 2.17. XRD patterns of as-synthesized samples obtained from a dry gel with an nSi = nAl ratio of 31 showing the influence of the water content on the dry-gel conversion process. Reprinted with permission from Arnold et al. (Arnold *et al.* 2004).

This led to a finding that the liquid water was present in the bottom of the autoclave or in the pores of the gel, therefore the presence of liquid water was a pre-requisite for successful crystallization. This finding was slightly different in comparison with dry gel synthesis of zeolite Beta where water amount in the range of saturation pressure was sufficient for desired product synthesis (Matsukata *et al.* 1999).

2.9 ROLE OF WATER IN DRY SYNTHESIS

Matsukuta et al. (Matsukata *et al.* 1999) tried to analyze a profound question about the role of water in SAC method. They conducted a study on the crystallization of TEA-containing dry gel at 453 K using different amounts of water for the production BEA zeolite as the final product. Figure 2.18 shows XRD patterns of as-synthesized products. It can be noticed that various amounts of water greatly influence the final product, therefore presence of water is of importance. Without the addition of water in the bottom of autoclave no crystallization took place which was in agreement with previous synthesis of Ti-BEA (Tatsumi *et al.* 1997), and B-BEA (Bandyopadhyay *et al.* 1998). When 0.22 ml of water was used, sufficient to produce saturation steam pressure at 453 K, no crystallization was observed after 24 h of reaction. However, increasing the amount of water resulted in the formation of BEA and it reached to maximum crystallinity when 1 ml of water was added to the autoclave. Further addition of water to 2.5 ml did not produced any crystalline phase. The water content in dry gel was typically 3-10% but it seems that it did not contribute to the water content in the bottom of autoclave even if all of it evaporates. This showed that saturated vapor pressure of steam was not enough to initiate crystallization. Adsorption and condensation of water in/on the dry gel were essential for crystallization. At the same time, excess water was detrimental for the crystallization. The requirement of a certain amount of water to keep the saturated vapor pressure results in the condensation of water would take place in the pores of dry gel. Such condensation would lead the SAC process to behave like a hydrothermal synthetic method.

It was also noticed that the SDA (TEA$^+$) remained stable and did not degrade at 423 K in dry gel, which was not possible even at 363 K in hydrothermal method due to the presence of alkaline aqueous solution. It was concluded that the TEA$^+$ cations in a dry

gel were forced to interact with (alumino) silicious species in the absence of a continuous phase of water by forming stable $Al-O^- TEA^+$ and $Si-O^- TEA^+$ bonds. Such stable bonds are not possible in a conventional hydrothermal synthesis above 400 K. Therefore, the zeolite synthesis under SDA could be considered as competitive reactions between the degradation of SDA, and zeolite-forming reactions. Such zeolite-forming reactions include hydrolysis of silicious species to produce intermediates and then their further dehydro-condensation to give rise to T-O-T networks. Hence, at high temperature of 453 K, a rapid crystallization in 1 day was possible due to the stabilization of TEA^+ cations in the dry gel, which is not possible with the excess amount of water due to the TEA^+ degradation that takes place when water condenses in the dry gel and forms a continuous layer. This was the case observed in Figure 2.18(f).

Hence, it was concluded that for the crystallization in the DGC method, the SDA has to be stable by keeping the amount of water as little as possible. Also the requirement of saturated vapor pressure was essential for zeolite-forming reactions, but excess amount of water should be avoided due to its condensation in the gel which degrades SDA in the aqueous phase.

Thoma and Nenoff (Thoma and Nenoff 2000) further explained the role of water in the DGC process. During gel rehydration, the water in the system readily breaks siloxane (Si-O-Si) bonds while organic SDA cations adsorb on the surface acid sites. Therefore, a molecular rearrangement takes place in the covalently bonded gel network due to the breaking of silane (and/or Si-O-Al) bonds. In turn, the bond cleavage creates free surface for adsorption from vapor phase. In this view, it was suggested that the role of water in the VPT process was twofold: rehydration of siloxane (Si-O-Si) groups to form hydroxyl groups that can become adsorption sites for organic SDA cations, and to facilitate bond breakage required for molecular rearrangement. This is consistent with the observation in Figure 2.18(a-d) that the increased water content up to certain extent leads to higher percent crystallinity.
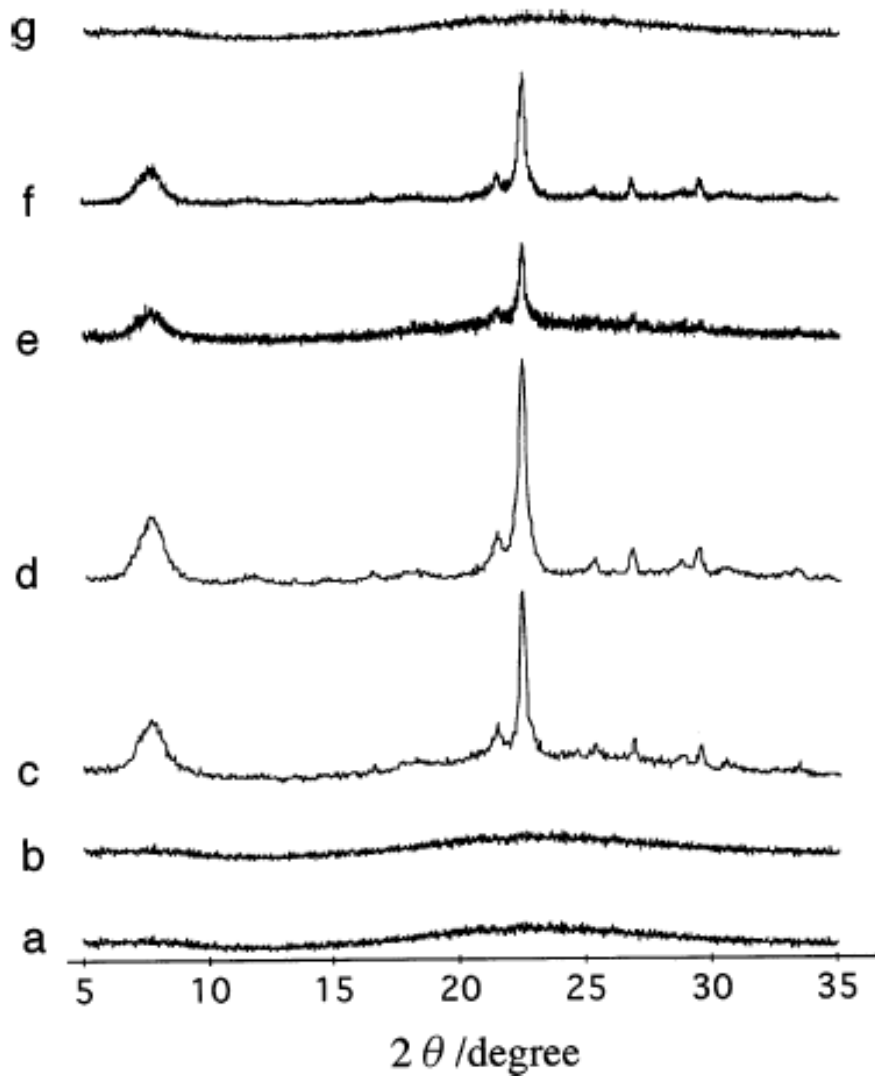
Figure 2.18. Effect of the amount of water at the bottom of autoclave in the synthesis of BEA by the SAC method. The composition of dry gel, SiO_2 : 0.033 Al_2O_3 : 0.036 Na_2O: 0.37 TEAOH, the inner volume of autoclave, 45 ml; the amount of dry gel used for crystallization, 1.50 g; crystallization temperature, 453 K; crystallization time, 24 h. The amount of water used in ml: (a) 0; (b) 0.22; (c) 0.5; (d) 1.0; (e) 1.5; (f) 2.0; (g) 2.5. Reprinted with permission from Matsukata et al. (Matsukata *et al.* 1999).

2.10   CONCLUSIONS

The crystallization of various structures and types of zeolites is possible depending upon the gel composition and the synthesis conditions. For many years it was assumed that the crystallization of zeolites was a solution-mediated phenomenon, but many studies suggested a heterogeneous transformation. It was evidenced that solid phases were involved in nucleation and crystal growth. The active participation of initially amorphous solid phase as the starting solid containing gel has been established in the crystallization of zeolites. It has been suggested that the nucleation takes place on the surface or within the solid gel phase through the autocatalytic mechanism. It has also been observed in some cases that the formation of zeolite crystals takes place by reorganization of amorphous phase hydrogel through solid-solid transformations with little contribution of soluble species. It has also been proposed that nanometer size units of amorphous particles are responsible for aggregation leading to the formation and growth of zeolite crystals. In some cases, the amorphous hydrogel is formed by nanometer size non-isolated entities, which through the process of densification forms zeolite crystals.

Heterogeneous nucleation of zeolites has successfully been demonstrated by synthesizing a wide variey of zeolites using a dry process. The dry gel conversion could be an alternative to conventional hydrothermal process. All the species that take part in forming the microporous crystal remain essentially in solid form. This is in contrast to hydrothermal synthesis where the species are dispersed in aqueous and solid phases. A better explanation of hydrothermal synthesis would be achieved by understanding of crystallization mechanisms involved in dry gel synthesis.

Some direct advantages of dry gel synthesis process over the hydrothermal process include:

- the composition of the starting gel remains the same as the composition of the synthesized crystals,
- reduction in crystallization time,
- possibility of replacing the batch synthesis process with a continuous one,
- reduction in the use of expensive structure directing organic agents,
- no generation of waste materials owing to high yield,

- no treatment of wastewater is needed in the SAC method,

- better control on a selective phase of zeolite, and

- a variation in operating parameters can easily be accommodated without affecting the desired zeolite phase, which may be difficult to handle in hydrothermal process.

It is, therefore, expected that the future studies will be more focused on a dry process.

2.11   REFERENCES

Ahedi, R. K, Shevade, S. S, Kotasthane, A. N. "Titanosilicate Derivative of the NU-1 Framework Zeolites (TS-NU-1)." *Zeolites* , 1997, *18* (5-6), 361-367.

Althoff, R., Reitmaier S., Schmidt W., Zibrowius, B., Unger K., Schuth, F. "The Synthesis of Zeolites From Dry Powders." *Stud.Surf.Sci.Catal.*, 1995, *98,* 36-37.

Althoff, R., Unger K., Schuth, F. "Is the Formation of a Zeolite From a Dry Powder Via a Gas Phase Transport Process Possible?" *Microporous Mater.*, 1994, *2* (6), 557-562.

Andersson, K. R., Dent, G., Lesley, S., Smith, D. N. "Polymerization and colloid formation in silicate solutions." *ACS Symp.Ser.*, 1982, *194* (Soluble Silic.), 115-131.

Angell, C. L., Flank, W. H. "Mechanism of zeolite A synthesis." *ACS Symp.Ser.*, 1977, *40* (Mol. Sieves-2, Int. Conf., 4th), 194-206.

Arafat, A., Jansen, J. C., Ebaid A.R., van Bekkum, H. "Microwave Preparation of Zeolite Y and ZSM 5." *Zeolites*, 1993, *13* (3), 162-165.

Argauer, R. J. and Landold, G. R. "Crystalline Zeolite ZSM-5 and Method of Preparing the Same." (3,702,886), 1972.

Arnold, A., Hunger, M., Weitkamp, J. "Dry-gel synthesis of zeolites [Al]EU-1 and [Ga]EU-1." *Microporous and Mesoporous Mater.* , 2004, *67* (2-3), 205-213.

Bandyopadhyay, R., Bandyopadhyay, M., Kubota, Y., Sugi, Y. "Synthesis of AlPO4 Molecular Sieves with AFI and AEL Structures by Dry-Gel Conversion Method and Catalytic Application of Their SAPO Counterparts on Isopropylation of Biphenyl." *J.Porous Mater.*, 2002, *9* (2), 83-95.

Bandyopadhyay, R., Kubota, Y., Sugi, Y. "Synthesis of Borosilicate Zeolites by Dry Gel Conversion (DGC) Method." *Chem.Lett.*, 1998, *8* 813-814.

Bandyopadhyay, R. K., Ahedi, R., Kubota, Y., Ogawa, M., Goto, Y. "Synthesis of High-silica [Al]-SSZ-31 by a Steam-assisted Conversion Method and its Catalytic Performance in the Isopropylation of Biphenyl." *J.Mater.Chem.*, 2001, *11* (7), 1869-1874.

Barrer, R. M. *Hydrothermal Chemistry of Zeolites*. New York: Academic Press, 1982.

Basaldella, E. I., Bonetto, R., Tara, J. C. "Synthesis of NaY Zeolite on Preformed Kaolinite Spheres. Evolution of Zeolite Content and Textural Properties With the Reaction Time." *Ind.Eng.Chem.Res.*, 1993, *32* (4), 751-752.

Bhatia, S. *Zeolite Catalysis Principles and Applications*. Fla.: CRC Press Boca Raton, 1990.

Bhaumik, A., Tatsumi, T. "Pure Silica NU-1 and Na- and Al-free Ti-NU-1 Synthesized by the Dry Gel Conversion Method." *Microporous Mesoporous Mater.*, 2000, *34* (1), 1-7.

Bibby, D. M., Dale, M. P. "Synthesis of Silica-Sodalite From Non-Aqueous Systems." *Nature*, 1985, *317* (6033), 157-158.

Bodart, P., Nagy, J. B., Gabelica, Z., Derouane, E. G. "Factors Governing the Synthesis of Zeolites From Silicoaluminate Hydrogels: A Comparative Study of the Crystallization Mechanisms of Zeolites Y, Mordenite, and ZSM-5." *J.Chim.Phys.Biol.*, 1986, *83* (11-12), 777-790.

Breck, D. W. "Crystalline molecular sieves." *J.Chem.Educ.*, 1964, *41* (12), 678-689.

Breck, W. D., *Zeolite Molecular Sieves*. New York: Wiley, 1974.

Breck, W. D., Flanigen, E. M. "Synthesis and Properties of Union Carbide Zeolites L, X, and Y." *Molcular Sieves Pap.Conf.*, 1967, 47-61.

Bronic, J., Subotic, B. "Role of Homogeneous Nucleation in the Formation of Primary Zeolite Particles." *Microporous Mater.*, 1995, *4* (2-3), 239-242.

Bronic, J., Subotic, B., Skreblin, M. "Investigation of the influence of seeding on the crystallization of zeolite A in the membrane-type reactor." *Microporous Mesoporous Mater.*, 1999, *28* (1), 73-82.

Brunner, G. O. "A proposal for a mechanism of nucleation in zeolite synthesis.", *Zeolites*, 1992, *12* (4), 428-430.

Burkett, S. L., Davis, M. E. "Mechanism of Structure Direction in the Synthesis of Si-ZSM-5: An Investigation by Intermolecular 1H-29Si CP MAS NMR." *J.Phys.Chem.*, 1994, *98* (17), 4647-4653.

Burkett, S. L., Davis, M. E. "Mechanism of Structure Direction in the Synthesis of Pure-Silica Zeolites. 2. Hydrophobic Hydration and Structural Specificity." *Chem.Mater.*, 1995a, *7* (8), 1453-1463.

Burkett, S. L., Davis, M. E. "Mechanisms of Structure Direction in the Synthesis of Pure-Silica Zeolites. 1. Synthesis of TPA/Si-ZSM-5." *Chem.Mater.*, 1995b, *7* (5), 920-928.

Camblor, M. A., Corma, A., Martinez, A., Mocholi F.A., Perez Pariente, J. "Benefits in Activity and Selectivity of Small Y Zeolite Crystallites Stabilized by a Higher Silicon-to-Aluminium Ratio by Synthesis." *Appl.Catal.*, 1989, *55* (1), 65-74.

Chang, C. D., and Bell, A. T. "Studies on the mechanism of ZSM-5 formation." *Catal.Lett.*, 1991, *8* (5-6), 305-316.

Chen, N. Y., Miale, J. N., and Reagan, N. Y. "Preparation of zeolites." (4,112,056). 1978.

Corma, A., Wojciechowski, B. W. "The chemistry of catalytic cracking." *Catal.Rev.-Sci.Eng.*, 1985, *27* (1), 29-149.

Corma, A., Davis, M. E. "Issues in the synthesis of crystalline molecular sieves: towards the crystallization of low framework-density structures." *ChemPhysChem*, 2004, *5* (3), 304-313.

Culfaz, A., and Sand, L. B. "Mechanism of nucleation and crystallization of zeolites from gels." *Advan.Chem.Ser.*, 1973, *121* (Mol. Sieves, Int. Conf., 3rd), 140-151.

Cundy, C. S. "Microwave Techniques in the Synthesis and Modification of Zeolite Catalysts. A Review." *Collect.Czech.Chem.Commun.*, 1998, *63* (11), 1699-1723.

Cundy, C. S., Henty, M. S., Plaisted, R. J. "Zeolite Synthesis Using a Semicontinuous Reactor. Part 1. Controlled Nucleation and Growth of ZSM-5 Crystals Having Well-Defined Morphologies." *Zeolites*, 1995a, *15* (4), 353-372.

Cundy, C. S., Henty, M. S., Plaisted, R. J. "Zeolite Synthesis Using a Semicontinuous Reactor. Part 1. Controlled Nucleation and Growth of ZSM-5 Crystals Having Well-Defined Morphologies." *Zeolites*, 1995b, *15* (4), 353-372.

Cundy, C. S., Henty, M. S., Plaisted, R. J. "Zeolites Synthesis Using a Semicontinuous Reactor. 2. Synthesis at High Nucleation Rates." *Zeolites*, 1995c, *15* (2), 400-407.

Cundy, C. S., Cox, P. A. "The Hydrothermal Synthesis of Zeolites: History and Development from the Earliest Days to the Present Time." *Chem.Rev.(Washington, DC, U.S.)*, 2003, *103* (3), 663-701.

Cundy, C. S., Cox, P. A. "The hydrothermal synthesis of zeolites: Precursors, intermediates and reaction mechanism." *Microporous Mesoporous Mater.*, 2005, *82* (1-2), 1-78.

Cundy, C. S., Forrest, J. O., Plaisted, R. J. "Some observations on the preparation and properties of colloidal silicalites. Part I: synthesis of colloidal silicalite-1 and titanosilicalite-1 (TS-1)." *Microporous Mesoporous Mater.*, 2003, *66* (2-3), 143-156.

Cundy, C. S., Lowe, B. M., Sinclair, D. M. "Direct measurements of the crystal growth rate and nucleation behavior of silicalite, a zeolitic silica polymorph." *J.Cryst.Growth*, 1990, *100* (1-2), 189-202.

Delprato, F., Delmotte, L., Guth, J. L., Huve, L. "Synthesis of New Silica-Rich Cubic And Hexagonal Faujasites Using Crown-Ether-Based Supramolecules As Templates." *Zeolites*, 1990, *10* (6), 546-552.

Den Ouden, C. J. J., Thompson, R. W. "Analysis of the Formation of Monodisperse Populations by Homogeneous Nucleation." *J.Colloid Interface Sci.*, 1991, *143* (1), 77-84.

Derouane, E. G., Detremmerie, S., Gabelica, Z., Blom, N. "Synthesis and Characterization of ZSM-5 Type Zeolites. I. Physicochemical Properties of Precursors and Intermediates." *Appl.Catal.*, 1981, *1* (3-4), 201-224.

Dong, J., Dou, T., Zhao, X., Gao, L. "Synthesis of Membranes of Zeolites ZSM-5 and ZSM-35 by the Vapor Phase Method." *J.Chem.Soc., Chem.Commun.*, 1992, (15), 1056-1058.

Dong, W.-Y, Sun, Y.-J., He, H.-Y., Long, Y.-C. "Synthesis and Structural Characterization of B-Al-ZSM-5 Zeolite From Boron-Silicon Porous Glass in the Vapor Phase." *Microporous Mesoporous Mater.*, 1999, *32* (1-2), 93-100.

Dutta, P. K., Bronic, J. "Mechanism of zeolite formation: seed-gel interaction." *Zeolites*, 1994, *14* (4), 250-255.

Erdem, A., Sand, L. B. "Crystallization and Metastable Phase Transformations of Zeolite ZSM-5 in the (TPA)2O-Sodium Oxide-Potassium Oxide-Aluminum Oxide-Silicon Dioxide-Water System." *J.Catal.*, 1979, *60* (2), 241-256.

Fahlke, B., Starke, P., Seefeld, V., Wieker, W., Wendlandt, K. P. "On the intermediates in zeolite Y synthesis." *Zeolites*, 1987, *7* (3), 209-213.

Fan, W., Li, R., Fan, B., Ma, J., Cao, J. "Effects of Introduction of Different Alkali Metal Halides on Crystallization and Characteristics of ZSM-48 in a Solid Reaction Mixture System Effects of Alkali Metal Chlorides[1]." *Appl.Catal.A:General*, 1996, *143* (2), 299-308.

Flanigen, E. M., Bennett, J. M., Grose, R. W., Cohen, J. P., Patton, R. L., Kirchner, R. M., Smith, J. V. "Silicalite, a new hydrophobic crystalline silica molecular sieve." *Nature (London)*, 1978, *271* (5645), 512-516.

Flanigen, E. M. and Breck, D. W. 137th Meeting of the ACS, Division of Inorganic Chemistry, Cleveland, OH, April 1960a, Abstracts, p.33-M.

Flanigen, E. M. and Breck, D. W. Paper No. 82: "Crystalline zeolites, V-Growth of zeolite crystals from gels." 1960b, 137th Meeting of the ACS, Division of Inorganic Chemistry, 4-19-1960b.

Flanigen, E. M., "Molecular sieve zeolite technology - the first twenty-five years." *Proc. Int. Conf. Zeolites*, 5th (1980), 760-780.

Gates, B. C., Katzer, J. R., Schuit, G. C. A. *Chemistry of Catalytic Processes*. New York: McGraw-Hill, 1979.

Ginter, D. M., Bell, A. T., Radke, C. J. "The Effects of Gel Aging on the Synthesis of NaY Zeolite From Colloidal Silica." *Zeolites*, 1992a, *12* (6), 742-749.

Ginter, D. M., Went, G. T., Bell, A. T., Radke, C. J. "A physicochemical study of the aging of colloidal silica gels used in zeolite Y synthesis." *Zeolites*, 1992b, *12* (6), 733-741.

Golemme, G., Crea, F., Nastro, A., Nagy, J. B., Subotic, B., Aiello, R. "Kinetic Study on the Nucleation of (Na,TPA)ZSM-5 Zeolite." *Zeolites*, 1991, *11* (8), 776-783.

Gonthier, S., Gora, L., Guray, I., Thompson, R. W. "Kinetic Study on the Nucleation of (Na,TPA)ZSM-5 Zeolite." *Zeolites*, 1993, *13* (6), 414-418.

Gougeon, R., Delmotte, L., Le Nouen, D., Gabelica, Z. "The early stages in the behavior of tetrapropylammonium cations in the synthesis of gel precursor to pure siliceous MFI zeolite: an in situ multinuclear NMR study." *Microporous Mesoporous Mater.*, 1998, *26* (1-3), 143-151.

Hari Prasad Rao, P. R., Ueyama, K., Matsukata, M. "Crystallization of High Silica BEA by Dry Gel Conversion." *Appl.Catal.A*, 1998, *166* (1), 97-103.

Iler, R. K. *The Chemistry of Silica : Solubility, Polymerization, Colloid and Surface Properties, and Biochemistry*. Wiley, New York, 1979.

Iler, Ralph K. "Colloidal components in solutions of sodium silicate." *ACS Symp.Ser.*, 1982, *194* (Soluble Silic.), 95-114.

Ito, T., Fraissard, J., Nagy, J. B., Dewaele, N., Nastro, E. G., and Derouane, E. G. "Zeolites: Facts, Figures, Future.", *Studies in Surface Science and Catalysis*, 1989, Ed. Jacobs, P. A. and Van Santen, R. A. (49), 579.

Ivanova, I. I., Aiello, R., Nagy, J. B., Crea, F., Derouane, E. G., Dumont, N., Nastro, A., Subotic, B., Testa, F. "Influence of Cations on the Physicochemical and Structural Properties of Aluminosilicate Gel Precursors. II. Multinuclear Magnetic Resonance Characterization." *Microporous Mater.*, 1994, *3* (3), 245-257.

Jacobs, P. A., Derouane, E. G., Weitkamp, J. "Evidence for X-Ray-Amorphous Zeolites." *J.C.S.Chem.Comm.*, 1981, (12), 591-593.

Jansen, J. C., Arafat, A., Barakat, A. K., and van Bekkum, H. "Microwave techniques in zeolite synthesis. Synthesis of Microporous Materials: Molecular Sieves" (1), 507-521. 1992. New York, Van Nostrand Reinhold.

Kacirek, H., and Lechert, H. "Growth of the zeolite type NaY." *J.Phys.Chem.*, 1975, *79* (15), 1589-1593.

Kacirek, H., Lechert, H. "Rates of crystallization and a model for the growth of sodium-Y zeolites." *J.Phys.Chem.*, 1976, *80* (12), 1291-1296.

Kerr, G. T. "Chemistry of crystalline aluminosilicates. I. Factors affecting the formation of zeolite A." *J.Phys.Chem.*, 1966, *70* (4), 1047-1050.

Khouw, C. B., Davis, M. E. "Catalytic Activity of Titanium Silicates Synthesized in the Presence of Alkali Metal and Alkaline Earth Ions." *J.Catal.*, 1995, *151* (1), 77-86.

Kim, D. S., Park S.-E., Kang, S. O. "Microwave Synthesis of Micro-Mesoporous Composite Material." *Stud.Surf.Sci.Catal.*, 2000, *129* 107-116.

Kim, M. H., Li, H. X., Davis, M. E. "Synthesis of Zeolites by Water-Organic Vapor-Phase Transport." *Microporous Mater.*, 1993, *1* (3), 191-200.

Krznaric, I., Antonic, T., Subotic, B., Babic-Ivancic, V. "Results of thermal and hydrothermal treatment of the aluminosilicate gels prepared at different batch concentrations." *Thermochim.Acta*, 1998, *317* (1), 73-84.

Kumar, R., Bahumik, A., Ahedi, R. K., Ganapathy, S. "Promoter-Induced Enhancement of the Crystallization Rate of Zeolites and Related Molecular Sieves." *Nature*, 1996, *381* (6580), 298-300.

Lechert, H., Kacirek, H. "Investigations on the Crystallization of X-Type Zeolites." *Zeolites*, 1991, *11* (7), 720-728.

Li, Q., Creaser, D., Sterte, J. "The nucleation period for TPA-silicalite-1 crystallization determined by a two-stage varying-temperature synthesis." *J.Microporous Mesoporous Mater*, 1999, *31* (1-2), 141-150.

Li, Q., Creaser, D., and Sterte, J. 13th International Zeolite Conference (13IZC). Paper 02-O-03. 2001, 8-7-2001.

Li, Q., Creaser, D., Sterte, J. "An Investigation of the Nucleation/Crystallization Kinetics of Nanosized Colloidal Faujasite Zeolites." *Chem.Mater.*, 2002, *14* (3), 1319-1324.

Li, R., Fan, W., Ma, J., Fan, B., Cao, J. "Synthesis and Characterization of ZSM-48 in the Pure Solid System." *Zeolites*, 1995, *15* (1), 73-76.

Lohse, U., Altrichter, B., Donath, R., Fricke, R., Janke, K., Parlitz, B., Schreier, E. "Synthesis of Zeolite Beta. Part 1. Using Tetraethylammonium Hydroxide/Bromide With Addition of Chelates as Templating Agents." *J.Chem.Soc.Faraday Trans.*, 1996, *92* (1), 159-165.

Lowe, B. M. "An equilibrium model for the crystallization of high silica zeolites." *Zeolites*, 1983, *3* (4), 300-305.

Matsukata, M., Nishiyama, N., Ueyama, K. "Synthesis of Zeolites Under Vapor Atmosphere. Effect of Synthetic Conditions on Zeolite Structure." *Microporous Mater.*, 1993, *1* (3), 219-222.

Matsukata, M., Nishiyama, N., Ueyama, K. "Crystallization of FER and MFI Zeolites by a Vapor-Phase Transport Method." *Microporous Mater.*, 1996, *7* (2-3), 109-117.

Matsukata, M., Ogura, M., Osaki, T., Hari Prasad Rao, P. R., Nomura, M., Kikuchi, E. "Conversion of Dry Gel to Microporous Crystals in Gas Phase." *Topics in Catalysis*, 1999, *9* (1-2), 77-92.

McNicol, B. D., Pott, G. T., Loos, R. K., Mulder, N. "Spectroscopic Studies of Zeolite Synthesis. Evidence for a Solid-State Mechanism." *Adv.Chem.Ser.*, 1973, *121* 152-161.

Mintova, S., Olson, N. H., Bein, T. "Electron Microscopy Reveals the Nucleation Mechanism of Zeolite Y from Precursor Colloids." *Angew.Chem.Int.Ed.*, 1999a, *38* (21), 3201-3204.

Mintova, S., Olson, N. H., Valtchev, V., Bein, T. "Mechanism of Zeolite a Nanocrystal Growth from Colloids at Room Temperature." *Science*, 1999b, *283* (5404), 958-960.

Mintova, S., Olson, N. H., Senker, J., Bein, T. "Mechanism of the transformation of silica precursor solutions into Si-MFI zeolite." *Angew.Chem., Int.Ed.*, 2002, *41* (14), 2558-2561.

Moolenaar, R. L., Evans, J. C., McKeever, L. D. "Structure of the Aluminate Ion in Solutions at High pH." *J.Phy.Chem.*, 1970, *74* (20), 3629-3636.

Mullin, J. K. *Crystallization*. 2001.

Murrell, L. L., Overbeek, R. A., Chang, Y.-F., Puil, N. V. D., and Yeh, C. Y. "Method for Making Molecular Sieves and Novel Molecular Sieve Compositions." (6,004,527). 1999. USA.

Nagy, J. B., Ivanova, I., Aiello, R., Crea, F., Nastro, A., Nesta, F. "Multinuclear Magnetic Resonance Characterization of Various Aluminosilicate Gels in the Presence of Tetraalkylammonium Ions." *Zeolites*, 1995, *15* (5), 421-430.

Navrotsky, A., Petrovic, I., Hu, Y., Chen, C. Y., Davis, M. E. "Little energetic limitation to microporous and mesoporous materials." *Microporous Mater.*, 1995, *4* (1), 95-98.

Nicolle, M. A., Di Renzo, F., Fajula, F., Espiau, P., and Des Courieres, T. "A microporous tetraethylammonium permutite as synthesis intermediate of the zeolite beta." *Proc. Int. Zeolite Conf.*, 9th (1993), 1, 313-320.

Othmer, K. *Encyclopaedia of Chemical Technology*. New York: Wiley, 1984.

Otterstedt, J. E., Ghuzel, M., Sterte, J. P. "Colloidal components in solutions of alkali silicates." *J.Colloid Interface Sci.*, 1987, *115* (1), 95-103.

Park, S.-E., Kim, D. S., Chang, J. S., and Kim, J. M. "Continuous Process and Apparatus for Preparing Inorganic Materials Employing Microwave." (US Patent 2001054549). 2001. USA.

Perez-Pariente, J., Martens, J. A., Jacobs, P. A. "Factors Affecting the Synthesis Efficiency of Zeolite BETA from Aluminosilicate Gels Containing Alkali and Tetraethylammonium Ions." *Zeolites*, 1988, *8* (1), 46-53.

Piccione, P. M., Yang, S., Navrotsky, A., Davis, M. E. "Thermodynamics of Pure-Silica Molecular Sieve Synthesis." *J.Phys.Chem.B*, 2002, *106* (14), 3629-3638.

Rajagopalan, K., Peters, A. W., Edwards, G. C. "Influence of Zeolite Particle Size on Selectivity During Fluid Catalytic Cracking." *Appl.Catal.*, 1986, *23* (1), 69-80.

Ravishankar, R., Kirschhock, C., Schoeman, B. J., De Vos, D., Grobet, P. J., Jacobs, P. A., and Martens, J. A. "Synthesis, isolation and characterization of nano-powder of silicalite-1 type molecular sieves.", *Proc. Int. Conf. Zeolites*, 12th, Baltimore, July 5-10, 1998 (1999), 3, 1825-1832.

Regev, O., Cohen, Y., Kehat, E., Talmon, Y. "Precursors of the zeolite ZSM-5 imaged by cryo-TEM and analyzed by SAXS." *Zeolites*, 1994, *14* (5), 314-319.

Rollmann, L. D. and Valyocsik, E. W. "Continuous-Stream Upflow Zeolite Crystallization Apparatus." (US Patent 4,374,093). 1983.

Saha, S. K., Kubota, Y., Sugi, Y. "A convenient synthesis of MAPO-36 (ATS) by dry-gel conversion (DGC) technique." *Chem.Lett.*, 2003, *32* (11), 1026-1027.

Schmidt, I., Madsen, C., Jacobsen, C. J. H. "Confined space synthesis. A Novel Route to Nanosized Zeolites." *Inorg.Chem.*, 2000, *39* (11), 2279-2283.

Schoeman, B. J., Sterte, J., Otterstedt, J.-E. "Colloidal Zeolite Suspensions." *Zeolites*, 1994, *14* (2), 110-116.

Schoeman, B. J. "A spectroscopic study of the initial stage in the crystallization of TPA-silicalite-1 from clear solutions." *Stud.Surf.Sci.Catal.*, 1997, *105A* (Progress in Zeolite and Microporous Materials, pt. A), 647-654.

Serrano, D. P., Van Grieken, R. "Heterogeneous Events in the Crystallization of Zeolites." *J.Mater.Chem.*, 2001, *11* (10), 2391-2407.

Slangen, P. M., Jansen, J. C., van Bekkum, H. "Induction Heating: A Novel Tool for Zeolite Synthesis." *Zeolites*, 1997, *18* (1), 63-66.

Subotic, B., Bronic, J., and Antonic, T. "On the real significance of the "induction period" of zeolite crystallization.", *Proc. Int. Conf. Zeolites*, 12th, Baltimore, July 5-10, 1998 (1999), 3, 2057-2064.

Subotic, B., Graovac, A. "Kinetic Analysis of Autocatalytic Nucleation During Crystallization of Zeolites." *Stud.Surf.Sci.Catal.*, 1985, *24* 199-206.

Subotic, B., Skrtic, D., Smit, I., Sekovanic, L. "Transformation of Zeolite A into Hydroxysodalite. I. An Approach to the Mechanism of Transformation and its Experimental Evaluation." *J.Crys.Growth*, 1980, *50* (2), 498-508.

Subotic, B., Tonejc, A. M., Bagovic, D., Cizmek, A., Antonic, T. "Electron Diffraction and Infrared Spectroscopy of Amorphous Aluminosilicate Gels." *Stud.Surf.Sci.Catal.*, 1994, *84* 259-266.

Szostak, R. *Molecular Sieves*. London. UK: Blackie Academic & Professional, 1998.

Tatsumi, T., Xia, Q., Jappar, N. "Synthesis of Ti-Beta Zeolite with High Oxidation Activity by a Dry-Gel Conversion Technique." *Chem.Lett.*, 1997, (7), 677-678.

Thoma, S. G., Nenoff, T. M. "Vapor Phase Transport Synthesis of Zeolites From Sol-Gel Precursors." *Microporous Mesoporous Mater.*, 2000, *41* (1-3), 295-305.

Thompson R.W. "Comments of the Autocatalytic Nucleation of (Na, TPA)-ZSM 5." *Zeolites*, 1992, *12* (7), 837-840.

Thompson, R. W. "Population balance analysis of zeolite crystallization." *Modell. Struct. React. Zeolites*, 1992, 231-255.

Thompson, R. W., Dyer, A. "A modified population balance model for hydrothermal molecular sieve zeolite synthesis." *Zeolites*, 1985a, *5* (5), 292-301.

Thompson, R. W., Dyer, A. "Mathematical analyses of zeolite crystallization." *Zeolites*, 1985b, *5* (4), 202-210.

Thompson, R. W., Dyer, A. "Nucleation of zeolite Na-A crystals in hydrothermal systems." *Zeolites*, 1985c, *5* (5), 302-308.

Tsuruta, Y., Satoh, T., Yoshida, T., Okumura, O., Ueda, S. "Studies on the initial product in the synthesis of zeolite A from concentrated solutions." *Stud.Surf.Sci.Catal.*, 1986, *28* (New Dev. Zeolite Sci. Technol.), 1001-1007.

Ueda, S., Murata, H., Koizumi, M., Nishimura, H. "Crystallization of mordenite from aqueous solutions." *Am.Mineral.*, 1980, *65* (9-10), 1011-1018.

Valyocsik, E. W. "Apparatus for a continuous down-flow zeolite production." (US Patent 4,368,174). 1983.

Van Santen, R. A., Ooms, G., Den Ouden, C. J. J., Van Beest, B. W., Post, M. F. M. "Computational studies of zeolite framework stability." *ACS Symp.Ser.*, 1989, *398* (Zeolite Synth.), 617-633.

Verduijn, J. P. "Manufacture of uniform MFI-type zeolites, and the adsorbents and catalysts obtained." (Exxon Chemical Patents, Inc. 92-EP2330(9308124), 32. 4-29-1993. WO. 10-8-1992.

Walton, R. I., O'Hare, D. "An X-ray absorption fine structure study of amorphous precursors of a gallium silicate zeolite." *J.Phys.Chem.Solids*, 2001, *62* (8), 1469-1479.

Wang, X. and Jacobson, A. J. "Synthesis of Large ZSM-5 Crystals Under High Pressure." *Mat.Res.Soc.Symp.*, 2001, 658, GG8.1.1.-GG8.1.6.

Warzywoda, J., Edelman, R. D., Thompson, R. W. "Thoughts on the induction time in zeolite crystallization." *Zeolites*, 1989, *9* (3), 187-192.

Watson, J. N., Brown, A. S., Iton, L. E., White, J. W. "Detection of TPA-silicalite precursors nucleated during the room temperature aging of a clear homogeneous synthesis solution." *J.Chem.Soc., Faraday Trans.*, 1998, *94* (15), 2181-2186.

Watson, J. N., Iton, L. E., Keir, R. I., Thomas, J. C., Dowling, Trevor L., White, John W. "TPA-Silicalite Crystallization from Homogeneous Solution: Kinetics and Mechanism of Nucleation and Growth." *J.Phys.Chem.B*, 1997, *101* (48), 10094-10104.

Xu, H. H., Shah, D. B., Talu, O. "Synthesis of ZSM-5 Films at Elevated Gravity." *Zeolites*, 1997, *19* (2-3), 114-122.

Xu, W., Dong, J., Li, J., Li, J., Wu, F. "A Novel Method for the Preparation of Zeolite ZSM-5." *J.Chem.Soc., Chem.Commun.*, 1990, (10), 755-756.

Xu, W., Li, J., Li, W., Zhang, H., Liang, B. "Nonaqueous Synthesis of ZSM-35 and ZSM-5." *Zeolites*, 1989, *9* (6), 468-473.

Yamazaki, S., Tsutsumi, K. "Synthesis of A-type zeolite membrane using a plate heater and its formation mechanism." *Microporous Mesoporous Mater.*, 2000, *37* (1-2), 67-80.

Yang, H., Walton, R. I., Antonijevic, Sasa, Wimperis, Stephen, Hannon, Alex C. "Local Order of Amorphous Zeolite Precursors from 29Si{1H} CPMAS and 27Al and 23Na MQMAS NMR and Evidence for the Nature of Medium-Range Order from Neutron Diffraction." *J.Phys.Chem.B*, 2004, *108* (24), 8208-8217.

Zhdanov, S. P. "Problems of zeolite crystallization." *Advan.Chem.Ser.*, 1971, *101* 20-43.

Zhdanov, S. P. and Samulevich, N. N. "Nucleation and crystal growth of zeolites in crystallizing aluminosilicate gels.", *Proc. Int. Conf. Zeolites*, 5th (1980), 75-84.

CHAPTER 3: SYNTHESIS OF NaY ZEOLITE IN PRESHAPED AMORPHOUS SILICA PARTICLES THROUGH DRY PROCESS

3.1 INTRODUCTION

Zeolites are generally synthesized by a hydrothermal method, which is a solution mediated process, requiring an excess water. Bibby and Dale in 1985 (Bibby and Dale 1985) were the pioneers who reported the synthesis of ZSM-5 zeolites using ethylene glycol media instead of water. Later, studies were conducted by Huo et al. and Xu et al. (Xu *et al.* 1989; Huo *et al.* 1988) who synthesized various types of zeolites including MFI and FER using organic solvents without additional water. These results suggested that water is not an essential media for synthesizing a variety of zeolites.

In 1990, the results of these studies were further bolstered by Xu and coworkers (Xu *et al.* 1990) who reported the transformation of dry aluminosilicate gel into MFI by contacting with vapors of water and volatile amines. Since then, several studies have been conducted to transform the dry gel into zeolites using water vapor and/or structure directing agents (SDA). Such studies have discovered a lot of applications for synthesizing microporous zeolites with new compositions and structures.

Figure 3.1 provides a schematic understanding of the methods that are used to synthesize microporous zeolites (Xu *et al.* 1990; Matsukata *et al.* 1993; Matsukata *et al.* 1999; Kim *et al.* 1993). Figure 3.1(a) represents the conventional hydrothermal synthesis method in which a hydrogel containing all the chemicals, for example, alumina, silica, sodium cation and water, are converted to a zeolite phase. Organic structure directing agents (SDA) are frequently used in the hydrogel to assist in transforming the amorphous phase into zeolite phase. Crystallization is carried out in a confined space, e.g. an autoclave, in order to maintain autogeneous pressure when crystallization is carried out above 373 K. Once the crystals start to grow, they settle at the bottom of container due to higher density. The crystals are finally removed from the mother liquor through centrifugation or filtration. Figure 3.1(b) and 3.1(c) represent the schematic diagrams of reactors used in the literature for dry gel conversion. While using a volatile SDA such as ethylenediamine (EDA), a mixture of water and SDA is placed in the bottom of the
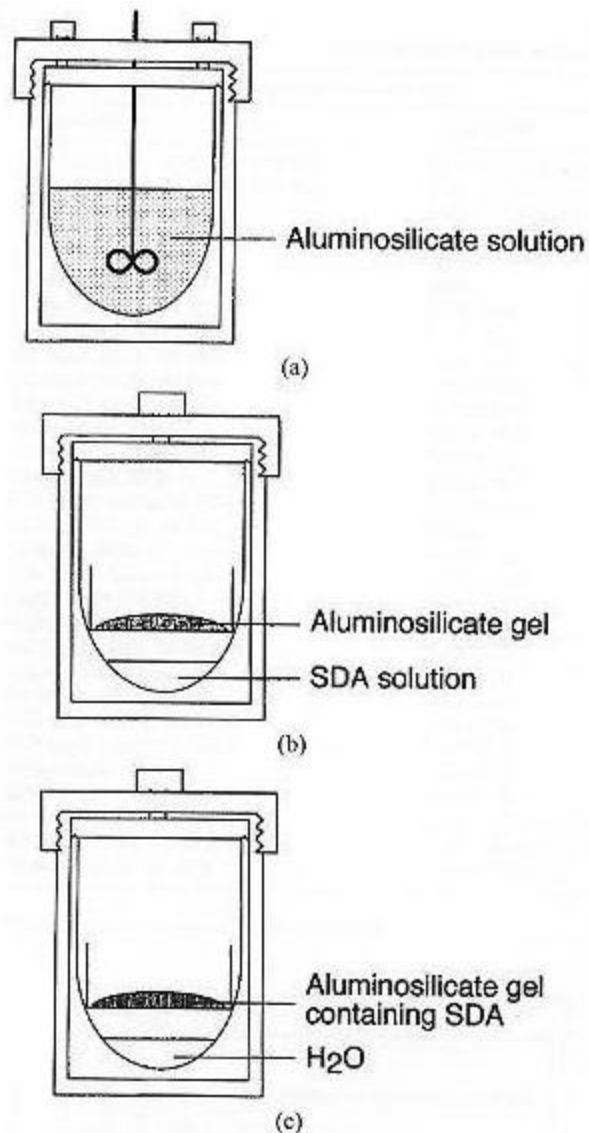
Figure 3.1: Schematic diagram of the synthesizing methods for microporous crystal systems. (a) Hydrothermal method, (b) Vapor-phase transport (VPT) method, and (c) Steam-assisted crystallization (SAC) method. The latter two are the dry gel conversion (DGC) methods (M. Matsukata *et al.* 1999).

autoclave. The dry gel that does not contain the SDA is placed above the mixture, in the middle of autoclave. The support, which holds the amorphous dry gel, is perforated so that the rising vapors of the mixture can make contact with the dry gel upon heating. Water and SDA mixture vaporizes as a result of heating, and make contact with the amorphous dry gel bringing about crystallization. Kim and coworkers (Kim *et al.* 1993) reported this synthesis method as "vapor phase transport (VPT)". Non-volatile quaternary amines such as tetrapropylamines (TPA) are also used as SDA. When such SDAs are used, they are incorporated in the amorphous dry gel during the process of dry gel preparation. Figure 1(c) shows that only water is added to the bottom of the reactor as SDA is already being added to the dry gel. Upon heating, only water vaporizes and forms the steam that is used to bring about crystallization. Matsukata and coworkers (Matsukata *et al.* 1999) called this method "steam assisted conversion (SAC)".

The catalytic applications of nanosized zeolites have received much attention because of their large surface area and reduced diffusion limitation as compared to ordinary zeolite crystals in the size range of micrometers. Fluid catalytic cracking (FCC) (Camblor *et al.* 1989; Rajagopalan *et al.* 1986), hydrocracking of gas oil (Camblor *et al.* 1998), hydroxylation of phenol with H_2O_2 (Notari 1988), and hydration of cyclohexene to cyclohexanol (Mitsui and Yohei 1985) are some examples of important zeolite catalyzed processes where small crystals have been reported as having an edge over large crystals. Among several types of zeolites reported through dry gel conversion, NaY zeolite stands out as a potent zeolite that can be used for several applications in the petroleum industry. One of its applications is in the area of fluid catalytic cracking (FCC) where it can be used as a cracking catalyst after going through a desired ion-exchange and dealumination process in order to make it a stable Y-zeolite. Generally, the Y-zeolite is not used as is for FCC application due to its small size in the range of sub-micrometer to a few micrometers. However, it is loaded on an inert matrix of silica/alumina using spray drying technique to make it suitable for FCC application.

In this study, we have attempted to synthesize nanosized NaY zeolite within pre-shaped silica particles of an average size of $50 \mu m$. Our technique is different from the conventional techniques in the sense that the synthesis is carried out within the silica particles which eliminates the process of loading of zeolite particles on the inert matrix of

silica/alumina through spray drying. Also, the mesopores of silica particles provide channels for crystals to grow in a controlled way. The synthesis in confined space has been reported for ZSM-5, X and A type of zeolites in order to have a better control over crystal size distribution using mesoporous carbons as the inert matrices (Schmidt *et al.* 2000). Our method is different as the narrow channels of silica particles not only provide a confined space but also are consumed during the reaction. The process used is similar to dry gel conversion, which not only reduces the consumption of chemicals but also at the same time, makes the synthesis process simpler and more time efficient. However, it is different from dry gel conversion in the sense that instead of keeping the dry gel reagents separated from the solution of SDA and water, the solution is added to the silica particles in such a way that the overall gel remains in solid form and the solution occupies the volume inside the pores of the silica particles.

3.2 EXPERIMENTAL

The basic requirement of chemicals for the synthesis of NaY zeolite is a source of silica, a source of alumina, and a source of sodium to control pH and also to act as a SDA. The source of silica was porous amorphous silica (SiO_2) gel particles (Sylopol 948) of $50\,\mu m$ average size supplied by Grace Davison, USA. The source of alumina (Al_2O_3) was aluminum nitrate nonahydrate $(Al(NO_3)_3 \cdot 9H_2O)$ supplied by VWR, Canada. Control of pH and structure directing agent (SDA) was obtained by using different concentrations of sodium hydroxide $(NaOH)$ supplied by Alphachem Canada, and distilled water (H_2O), whenever any precursor needed to be added to silica particles.

The synthesis method was adapted from a method reported in literature (Murrell *et al.* 1999), after several modifications in order to make it suitable to our operating conditions and equipment. The starting material was silica (SiO_2) gel in which aluminum nitrate nonahydrate $(Al(NO_3)_3 \cdot 9H_2O)$ was added in three steps to adjust the desired ratio of (SiO_2 / Al_2O_3). In the first step, 100 g of silica gel particles (size $50\,\mu m$) were added with 183.3 g of solution of $(Al(NO_3)_3 \cdot 9H_2O)$ in water (19.28wt%) through incipient wetness using a 600ml Teflon container. Then mixing was carried out for 15 min at 500 rpm until all the solution was absorbed in the pores of silica particles. The

particles looked dry and did not form any paste. After mixing, a retention time of 1 h was used at room temperature for complete penetration of solution throughout the pores of silica particles. The water was removed from the pores of the silica particles by drying the particles at $120^{\circ}C$ using a forced air convection oven until constant weight. During the process of drying an intermittent mixing of particles was carried out in order to avoid any formation of agglomerates. After drying, alumina was obtained by carrying out calcination at $500^{\circ}C$ for 2 hr with a heating rate of $4^{\circ}C/\min$ in a furnace, followed by a decrease in temperature to $120^{\circ}C$ with a cooling rate of $4^{\circ}C/\min$. With this step, the SiO_2/Al_2O_3 ratio obtained was about 20. In step two, about 97 g of silica gel particles were taken from step 1 and added with 159.7 g of solution of $Al(NO_3)_3 \cdot 9H_2O$ in water (21.3wt%), followed by mixing at 500 rpm for 15 min and subsequently, a retention time of 1 h at room temperature. Drying was carried out at $120^{\circ}C$ to a constant weight with intermittent mixing. Finally, calcination was carried out at $300^{\circ}C$ for 6 h with a heating rate of $4^{\circ}C/\min$, followed by a decrease in temperature to $120^{\circ}C$ with a cooling rate of $2^{\circ}C/\min$. With this step SiO_2/Al_2O_3 ratio obtained was about 9. In the third step, 97 g of silica gel particles obtained from step 2 were added with 123.95 g of solution of $Al(NO_3)_3 \cdot 9H_2O$ in water (27.44wt%), followed by mixing at 500 rpm for 15 minutes, and a subsequent retention time of 1 h at room temperature. Drying was carried out at $120^{\circ}C$ to a constant weight with intermittent mixing. Subsequently, calcination was carried out at $300^{\circ}C$ for 6 hr with a heating rate of $4^{\circ}C/\min$, followed by a decrease in temperature to $120^{\circ}C$ with a cooling rate of $2^{\circ}C/\min$. With the final step, the SiO_2/Al_2O_3 ratio was adjusted to 6.1.

After adjusting the SiO_2/Al_2O_3 ratio, a solution of NaOH in distilled water was added to the silica particles through incipient wetness. For this purpose, a 2 g of precursor obtained from third step was added with 3.5 g of 20wt% solution of NaOH using a 60mL polypropylene bottle. Hand mixing was carried out in the polypropylene bottle in order to absorb NaOH solution into the pores of precursor particles. The polypropylene bottle served as a batch reactor for the synthesis reaction. The bottle was sealed before the

reaction and a retention time of 1 h was allowed at room temperature before the synthesis reaction. The molar composition of the precursor was:

$$2.05 Na_2O : Al_2O_3 : 6.09 SiO_2 : 36.47 H_2O$$
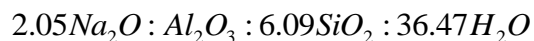
The synthesis reaction was carried out at $100°C$ using the forced air convection oven by placing the sealed bottle for 16-24 h. After the synthesis reaction, the reactor was taken out of the oven and allowed to cool to room temperature. Upon opening the reactor, the product appeared damp. It was washed with water and filtered. The filtered product was then dried in a forced air convection oven at $100°C$.

3.3 CHARACTERIZATION OF NaY ZEOLITE USING PXRD, XRF, EDX, SEM, AND BET

The product was analyzed by Powder X-ray diffraction (PXRD), BET surface area analyzer, scanning electron microscopy (SEM), X-ray florescence (XRF) spectrometer, and energy dispersion X-ray (EDX) analyzer. For determining the crystal structure, a Rigaku diffractometer equipped with $CuK\alpha$ radiations at 40 KV was used. For surface area analysis, Micromeritics ASAP 2010 adsorption instrument equipped with version 5.0 software was used. Prior to analysis, the sample of weight 0.095 g was outgassed in vacuum at $100°C$ for at least 16 h. Brunauer-Emmett-Teller (BET) surface area was determined using nitrogen as the adsorbant. Pore volume distributions and total pore volumes were calculated from the adsorption and desorption branches of the isotherm using the Barett-Joyner-Halenda (BJH) model. Scanning electromicroscopy (SEM) was carried out using Hitachi S-4500 scanning machine capable of producing a spatial resolution of < 2 nm at a high electron beam voltage (> 15 kV). The Hitachi S-4500 field emission SEM is also fully equipped with an EDAXTM EDX system, which provides EDX analyses in parallel with SEM images of the sample. The XRF analysis was conducted on Phillips PW1400 XRF spectrometer using fusion technique to determine the ratio of silica and alumina.

3.4 RESULTS AND DISCUSSION

The identification of the NaY zeolite was carried out through XRD analysis. It was compared with the identification peaks of a commercially available NaY zeolite (CBV-100, $SiO_2 / Al_2O_3 = 5.1$) provided by Zeolyst International USA. Figures 3.2 and 3.3 show that the major peaks of identification are located at $2\theta = 23.6°, 26.9°, and\ 31.3°$.
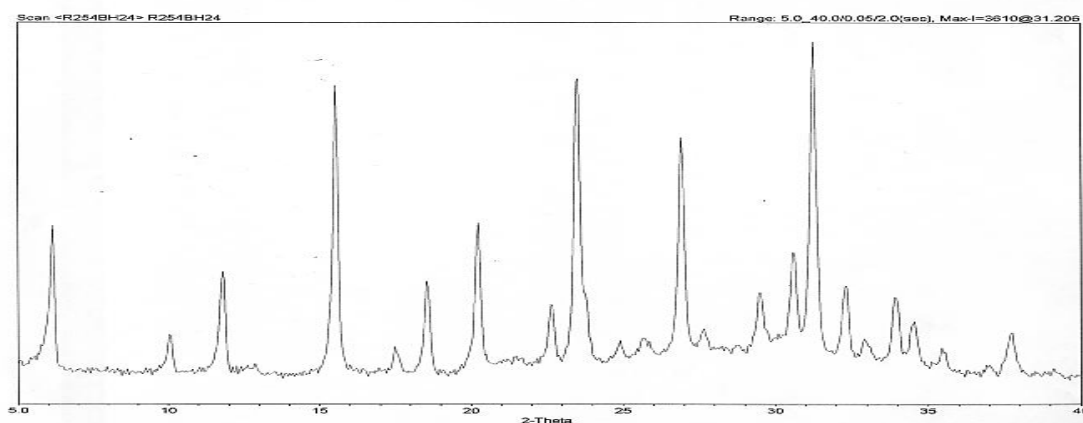
Figure 3.2: X-ray diffraction pattern of NaY zeolite synthesized in pre-shaped silica particles

The pore volume of starting silica gel was very important as it provided the information about how much volume of aluminum nitrate nonahydrate was needed to be gradually added. Also the average pore diameter of the silica particle provided the information about how much the pores narrowed with the gradual addition of aluminum nitrate nonahydrate. The BET surface area of the starting silica gel was found to be 257 m^2 / g . The BJH adsorption pore volume and average pore diameter were found to be 1.56 cm^3 / g and 248 $\overset{\circ}{A}$, respectively. The pore volume and the average pore

diameter of the silica particles gradually started to decrease with the addition of alumina. The average pore diameter was reduced to 146 $\overset{\circ}{A}$ by the third stage of alumina addition.
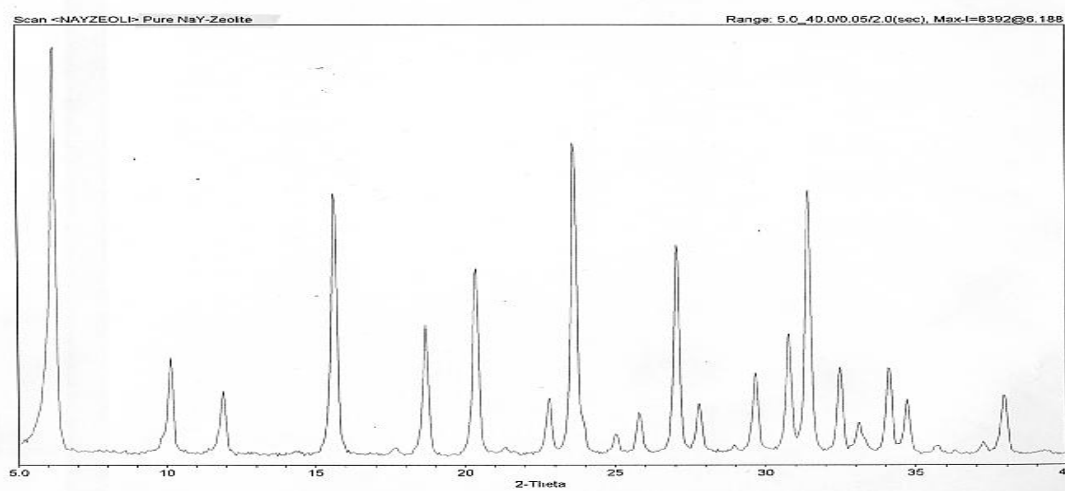
Figure 3.3: X-ray diffraction pattern of commercial NaY zeolite powder

After the synthesis reaction, the BET surface area of the product was found to be 412 m^2/g, and the BJH adsorption pore volume and average pore diameter were found to be 0.024 cm^3/g and 138 $\overset{\circ}{A}$. The change in the surface area is due to the growth of NaY zeolite in the pores of silica gel. However, the decrease in the pore volume and the average pore size is attributed to the space occupation by the growing zeolite crystals within the pore of silica particles. It seems that zeolite particles have grown on and within the walls of the pores and have blocked the pores to some extent. This may be explained in a way that initially, we had an empty glass of water and later it was filled with the crystals of zeolites, thus reducing the volume of the glass. However, the diameter of the glass is not much affected. The small drop in the average pore diameter of the pores before and after the addition of NaOH, and the synthesis reaction further support our hypothesis.

The SiO_2/Al_2O_3 ratio was determined analytically using XRF and EDX methods. It was also determined stoichiometrically while increasing the alumina in silica in several stages. The final stoichiometrical ratio was calculated to be 6.09, while the analytical ratios through XRF and average EDX were found to be 6 and 6.3, respectively. This shows that the bulk ratio determined through XRF and ratios in the crystals determined by EDX were very close to each other. The XRF results covered the bulk of the material and were able to acquire the composition of several layers of the material. Whereas the EDX analysis was more localized and covered a depth of only few layers of the material. The overall observation through both analytical techniques strengthened the concept that in solid-solid transformation the SiO_2/Al_2O_3 ratios of the crystals are not much different from the bulk reagents ratio (Derouane *et al.* 1981).

SEM imaging was carried out for the product in order to visualize the morphology of the NaY zeolite, the crystal size and its distribution. Figures 3.4 and 3.5 represent the SEM images of NaY zeolite and its zoomed view. Since the crystals were imbedded inside the silica particles, the silica particles were cracked opened for visual analysis through SEM equipment. It can be seen that the clusters of zeolites in the range of 1-2 micrometer were formed instead of separated singles crystals which was due to solid-solid transformation (Derouane *et al.* 1981). The size of the crystallites in clusters was in the range of 100-200nm, which exhibited a narrower crystal size distribution. It can also be observed in Figure 3.4 that the crystals were uniformly distributed throughout the silica particles. The growth of crystals on the outer surface of silica particles was not observed, which indicated that the chemicals were uniformly penetrated in the particles and that the alumina was deposited inside the mesopores of silica particles and not accumulated on the surface of the particles.
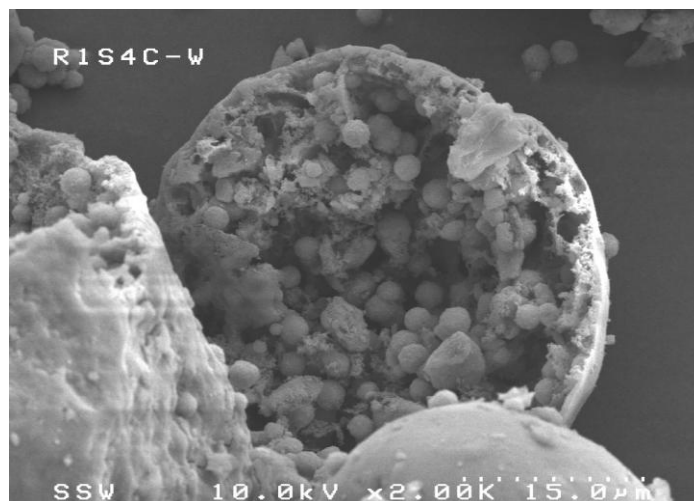
Figure 3.4: SEM image of laboratory synthesized NaY zeolite. The cracked open view of the silica particle ($50\,\mu m$) shows the intact outer crust of the particle with embedded clusters of NaY zeolite ($1-2\,\mu m$).
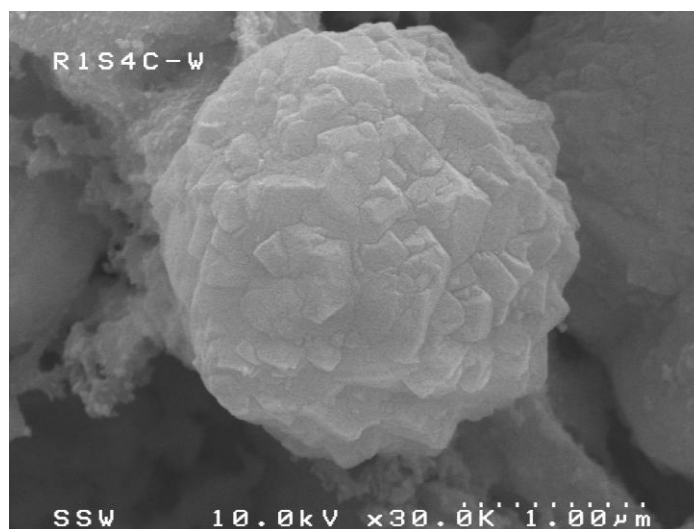
Figure 3.5: Zoomed view of NaY zeolite crystals ($100-200\,nm$) in a cluster within the silica particle.

This observation also strengthened the idea that the remaining outer layer of the silica particle may keep the crystals encapsulated and can be used directly for FCC application after a suitable ion-exchange of NaY zeolite. In this scenario, any further reduction in crystal size may add to its activity, and the nanosized crystals embedded in silica particles may be used for any appropriate application.

3.5 CONCLUSIONS

It can be concluded that a better technique is emerging by using a dry process, which may lead to maximum production of NaY zeolite with reduction in process time. Also, a narrower particle size distribution is achievable with a better control on the crystal size due to their growth in confined space. Due to the size of crystals in the nanometer range, a reduction in diffusion resistance is expected. A saving on consumption of chemicals was obtained in the sense that a negligible chemical waste was generated. Also, using only NaOH solution for the synthesis of NaY zeolite eliminated the use of an organic or inorganic structure directing agent. This also saved on expensive chemicals. Since the nanosized crystals were formed within the silica particles, therefore, their handling would be very easy and may readily be used for any suitable application.

3.6 REFERENCES

Bibby, D. M., Dale, M. P. "Synthesis of Silica-Sodalite From Non-Aqueous Systems." *Nature*, 1985, *317* (6033), 157-158.

Camblor, M. A., Corma, A., Martinez, A., Martinez-Soria, V., Valencia, S. "Mild Hydrocracking of Vacuum Gasoil over NiMo-Beta Zeolite Catalysts: The Role of the Location of the NiMo Phases and the Crystallite Size of the Zeolite." *J.Catal.*, 1998, *179* (2), 537-547.

Camblor, M. A., Corma, A., Martinez, A., Mocholi F.A., Perez Pariente, J. "Benefits in Activity and Selectivity of Small Y Zeolite Crystallites Stabilized by a Higher Silicon-to-Aluminium Ratio by Synthesis." *Appl.Catal.*, 1989, *55* (1), 65-74.

Derouane, E. G., Detremmerie, S., Gabelica, Z., Blom, N. "Synthesis and Characterization of ZSM-5 Type Zeolites. I. Physicochemical Properties of Precursors and Intermediates." *Appl.Catal.*, 1981, *1* (3-4), 201-224.

Huo, Q., Feng, S., Xu, R. "First Syntheses of Pentasil-type Silica Zeolites from Non-aqueous Systems." *J.Chem.Soc., Chem.Commun.*, 1988, 1486-1487.

Kim, M. H., Li, H. X., Davis, M. E. "Synthesis of Zeolites by Water-Organic Vapor-Phase Transport." *Microporous Mater.*, 1993, *1* (3), 191-200.

Matsukata, M., Nishiyama, N., Ueyama, K. "Synthesis of Zeolites Under Vapor Atmosphere. Effect of Synthetic Conditions on Zeolite Structure." *Microporous Mater.*, 1993, *1* (3), 219-222.

Matsukata, M., Ogura, M., Osaki, T., Hari Prasad Rao, P. R., Nomura, M., Kikuchi, E. "Conversion of Dry Gel to Microporous Crystals in Gas Phase." *Topics in Catalysis*, 1999, *9* (1-2), 77-92.

Mitsui, O. and Yohei, K. (DE3441072). 1985.

Murrell, L. L., Overbeek, R. A., Chang, Y.-F., Puil, N. V. D., and Yeh, C. Y. "Method for Making Molecular Sieves and Novel Molecular Sieve Compositions." (6,004,527). 1999. USA.

Notari, B. "Innovation in Zeolite Materials Science." Grobet, P. 37, 413. 1988. Amsterdam, Elsevier Science Publishers B.V. Studies in surface science and catalysis. 1987.

Rajagopalan, K., Peters, A. W., Edwards, G. C. "Influence of Zeolite Particle Size on Selectivity During Fluid Catalytic Cracking." *Appl.Catal.*, 1986, *23* (1), 69-80.

Schmidt, I., Madsen, C., Jacobsen, C. J. H. "Confined space synthesis. A Novel Route to Nanosized Zeolites." *Inorg.Chem.*, 2000, *39* (11), 2279-2283.

Xu, W., Dong, J., Li, J., Li, J., Wu, F. "A Novel Method for the Preparation of Zeolite ZSM-5." *J.Chem.Soc., Chem.Commun.*, 1990, (10), 755-756.

Xu, W., Li, J., Li, W., Zhang, H., Liang, B. "Nonaqueous Synthesis of ZSM-35 and ZSM-5." *Zeolites*, 1989, *9* (6), 468-473.

CHAPTER 4: EFFECTS OF VARIOUS OPERATING CONDITIONS ON THE DRY SYNTHESIS OF NANOSIZED NaY ZEOLITE IN PRE-SHAPED SILICA PARTICLES

4.1 INTRODUCTION

Zeolites are crystalline aluminosilicates which contain pores and cavities at the molecular level. Many types of the zeolites occur naturally, but at the same time a large variety of zeolites are synthesized industrially. Zeolite crystals are porous on a molecular scale and their structures show regular arrays of channels and cavities, which create a nano-scale complex maze that can be filled with water or other guest molecules (Barrer 1982 Breck 1974; Szostak 1998). These properties of zeolites make them vital for many industrial applications, such as adsorption, separation, reaction, and particularly in the field of heterogeneous catalysis. The uniform pore size and the specific adsorption and reactivity of zeolites are the main reasons for the development of adsorptive separation and catalytic reaction processes. In the literature, a variety of work has been reported to adjust the properties of the zeolites according to the requirements for different applications. One of the major applications of the zeolites is in the oil industry, especially in the process of catalytic cracking, where Y zeolite is frequently used in fluid catalytic cracking (FCC) process (Breck and Flanigen 1967; Breck 1974). The majority of the world's gasoline production is obtained through the FFC process which utilizes zeolite catalysts.

The large-scale production of zeolites currently uses batch process and the synthesis procedure takes days to obtain a finished product. Several researchers have devoted their efforts to improve the batch process and tried to make a step towards continuous process (Rollmann and Valyocsik 1983; Valyocsik 1983). Many zeolite synthesis operating variables have been identified and attempted to improve the quality of zeolites and reduce the synthesis time. These parameters include; microwave heating (Arafat *et al.* 1993; Cundy 1998; Jansen *et al.* 1992; Kim *et al.* 2000; Park *et al.* 2001; Slangen *et al.* 1997a), controlling nucleation and crystal growth rates (Cundy *et al.* 1995b; Cundy *et al.* 1995a); and investigating the effect of process variables such as:

temperature, pressure, concentration, composition, gravity, etc. (Wang and Jacobson 2001; Xu *et al.* 1997). Such parametric studies have been generally conducted in solution mediated syntheses employing hydrothermal process using an excess amount of water.

The hydrothermal crystallization is the most common method for synthesizing zeolites. In the conventional hydrothermal synthetic method where a hydrogel containing all sources, for instance, aluminum, silicon and sodium, are converted to a crystalline microporous phase in excess water. Organic structure-directing agents (SDAs) are often included in the hydrogel. The synthesis is performed in a confined system, an autoclave, to maintain autogeneous pressure and temperatures between 373 K and 523 K. In the earlier works on the zeolite synthesis, the general hydrothermal process was described as solution-mediated reaction-crystallization process in presence of a bulk liquid phase. First, the amorphous phase precursor material is dissolved in the solution, and then the zeolite product is crystallized from the resulting solution. Kerr (Kerr 1966; Kerr 1989) demonstrated experimentally the earlier established model, in which the dissolution, solution transport, and crystallization stages were physically separated. His study provided a generally satisfactory mechanism by which the experimental observation of nucleation and crystal growth was explained. At the same time, there were circumstances in which his model was unable to explain the zeolite synthesis phenomena. The solution-mediated process using excess water started to lose its attraction when in 1985 Bibby and Dale (Bibby and Dale 1985) first reported the crystallization of silica sodalite in an ethylene glycol media instead of water as the main source of solution. It has been reported that various types of high silica zeolites including silicalite types MFI and FER were synthesized in organic solvents without additional water (Huo *et al.* 1988; Xu *et al.* 1989). These results suggested that water in excess amount was not always essential as a medium for zeolite synthesis. The final blow to the solution-mediated process using bulk liquid phase was announced in 1990 when Xu and coworkers (Xu *et al.* 1990) introduced a new technique. They converted a dry aluminosilicate gel in contact with steam and vapors of volatile amines (SDA) into zeolite ZSM-5 at an elevated temperature in the range of $180-200\,^{\circ}C$ for 5-7 days. This approach was referred as dry gel conversion (DGC) or vapor-phase transport (VPT) technique. In this technique, a solid precursor in amorphous phase was converted to zeolite phase in the absence of a bulk liquid phase.

This observation led to the postulation of a different mechanism for zeolite synthesis called "solid state transformation". Kim and coworkers (Kim *et al.* 1993) used a similar composition as used by Xu and coworkers (Xu *et al.* 1990) for synthesizing ZSM-5 zeolite with the exception that they did not use any organic structure directing agent. They found that the synthesis of zeolite was a possibility without organic SDA. However, the presence of water was necessary for synthesis reaction. In continuation to Xu and his coworkers' contribution, Matsukata and coworkers in 1999 made a useful distinction between the DGC technique and methods in which the non-volatile SDAs were incorporated into dry aluminosilicate gel and only the steam was supplied from gas phase. The latter technique was designated as steam assisted conversion (SAC) (Matsukata *et al.* 1999). Althoff and coworkers (Althoff *et al.* 1994) prepared zeolite ZSM-5 from completely amorphous aluminosilicate precursors in the presence of a small amount of water formed by the reaction of SiO_2 with NH_4F. Using this procedure, purely siliceous and boron-containing zeolites ZSM-5 were synthesized. The crystallization to ZSM-5 zeolite from the gel containing TPA as SDA in water vapour atmosphere was also carried out by Crea and coworkers (Crea *et al.* 1991). It will be worth pointing out that Mostowicz and Sand (Mostowicz and Sand 1983) reported the synthesis of pentasil zeolites which possessed the properties of flowing powders. A similar study also reported the synthesis of zeolite X in powder form while reaction was carried out for weeks at ambient temperature (Cundy and Cox 2005). All the above studies established a phenomenon that the synthesis of zeolite in the absence of a visible liquid phase was a possibility.

The absence of a visible liquid phase does not mean that there is no water (or any other polar solvent) present in the solid phase reaction mixture. The solid phase reaction mixture, as mentioned in the above studies, generally contained about 20-44% water by weight (Cundy and Cox 2005; Mostowicz and Sand 1983). The water phase within the solid mixture is as bonded as well as adsorbed water. Thus making an environment normally observed in solution based synthesis. It is apparent that the reactions based on solid-solid transformation are fundamentally not different from the solution based reactions having a bulk liquid phase. At the same time, there may be differences due to high concentration gradients, mass transport limitations, and a high surface area to

volume ratio of the mobile phase. Such differences may cause changes in the rate of reaction, crystal morphology, and the state of crystals aggregation (Franklin, and Lowe 1987; Patel and Sand 1977). It may also cause changes in the intermediate or metastable phases (Moretti *et al.* 1985; Padovan *et al.* 1984), or may cause differences in the methods of heating e.g. microwave, or thermal techniques (Cundy 1998; Zhao *et al.* 1999). As a result, a very useful product may be obtained, e.g. the synthesis of zeolite beta leads to a more silicious product when dry synthesis rout is used as compared to more conventional wet gel method with similar starting materials (Matsukata *et al.* 1999; Matsukata *et al.* 2002). Further, the synthesis of zeolitic mesoporous materials can conveniently be obtained by controlled steaming of dried precursor gels (Naik *et al.* 2003).

On the footprints of SAC technique, Murrell et al. (1999) (Murrell *et al.* 1999) used a different approach for the in-situ production of NaY zeolite embedded in silica particles. In this method the starting solid phase was silica gel particles of $50\mu m$ that were gradually loaded with alumina to adjust the SiO_2 / Al_2O_3 ratio followed by drying and calicination. Finally, NaOH solution with or without organic SDA was added through incipient wetness and the solid gel remained in semi-dry form giving a composition of $2.94SiO_2 : 0.49Al_2O_3 : Na_2O : 17.8H_2O$. The reaction was carried out in autoclave or polypropylene bottle and the final product contained 100% crystalline phase. This process was very much like DGC, with the exception that no additional water was added. The water within the gel pores was sufficient to carry out the crystallization. One may utter safely that the phenomena of zeolite synthesis under hydrothermal conditions but in the absence of a visible liquid phase is quite established. All the methods for which the generic term "dry gel conversion" (DGC) has been used, exhibit a number of advantages over the classical hydrothermal crystallization technique requiring excess water. First, they allow the preparation of zeolites which are not accessible via the hydrothermal crystallization route, e.g., all-silica zeolites or zeolites with a relatively high concentration of metal atoms other than silicon in the framework. Secondly, the time required for the synthesis can be reduced, and the consumption of expensive templates (i.e. organic SDA) can be reduced or even be eliminated. Moreover, zeolite membranes

on a broad variety of supports can be prepared via the dry gel conversion method (Matsukata and Kikuchi 1997).

Other studies have improved the zeolite synthesis under solid-solid transformation using dry conversions. Arnold and coworkers (Arnold *et al.* 2003) studied the synthesis of Ga-Beta zeolite using characterization techniques such as SEM, XRD, and multinuclear MAS NMR spectroscopy. They found that during the synthesis the size of the crystal and its morphology not only depended on the breakage and reformation of chemical bonds with the dry-gel particles but also on the redistribution of the solid particles. They termed the redistribution of solid particles "re-crystallization". Their XRD and ^{71}Ga NMR data indicated that the main part of the crystallization reaction, including the incorporation of Ga in the framework, took place over a relatively short period of time (i.e. 16 h). Whereas, other NMR measurements indicated that the local rearrangements in structure e.g. silanol group condensation continued for a longer period of time (i.e. 65 h). Another careful study conducted by Choy, Lee and coworkers (Choy *et al.* 2003; Lee *et al.* 2003) for the conversion of alumina-pillared montmorillonite into sodalite. The pillared clay was mixed with 25wt% water and powdered NaOH with OH/Si ratio of 10. The resulting solid gel mixture was heated to $80°C$ under ambient atmosphere. The samples were intermittently removed and analyzed by XRD, FTIR, MAS NMR, SEM, and HRTEM. They observed through XRD and spectroscopic results that there was a smooth transition from pillared clay to sodalite; whereas, the SEM images indicated a major change in particle size and morphology. Interestingly, the HRTEM images initially indicated layered pillared clay diffraction lines; after 30 minutes, areas of sodalite lattice fringes started to appear randomly throughout the original pattern of pillared clay. Ultimately, in 150 minutes, a long range sodalite fringe pattern became prominent. The authors concluded that the sodalite crystallization took place by the rearrangement of delocalized sodalite nuclei which were formed through solid-solid transformation. It was also noted that the absence of a distinct x-ray amorphous stage implied a short-range molecular-level rearrangement within the solid phase, as compared to synthesis from solution in which transformation takes place through long-range diffusion of dissolved aluminum and silicon species.

For a better understanding of solid-solid transformation, Matsukata and co-workers (Matsukata *et al.* 1999) studied the role of water in the steam assisted conversion (SAC) synthesis of zeolite Beta. They concluded that keeping the water vapours saturated was essential for the zeolite synthesis reaction. A similar study was conducted by Serrano and co-workers (Serrano *et al.* 1996) for the crystallization of titanosilicalite (TS-1 and TS-2) from wetness-impregnated xerogels. They observed that the crystallization was assisted by solid-solid- transformations, but they could not view the entire process as a pure solid-solid mechanism since the liquid phase also played several roles. Therefore, they opined that the origin of this anomalous mechanism was due to the presence of solid material in high concentration as compared to most conventional solution based hydrothermal zeolite synthesis. Similarly, the conversion of kanemite to silicalite by solid state transformation in sealed glass ampoules (Salou *et al.* 1998) showed many similarities to the standard solution based hydrothermal synthesis route, though the solid state route was faster than the solution based route. However, the reaction did not occur at all in an open container when the precursors were heated to temperatures $\geq 100\,^{\circ}C$, indicating that the absorbed water played an important role in carrying out the solid state transformation. The solid-solid transformation can further be understood outside the domain of zeolite synthesis. Let us consider a limiting case of solid-state transformation of ammonium nitrate $(IV) \rightarrow (III)$. The transition of phase IV to III crystal is particularly important because it is a major contributor in caking of the product in the storage at $32°C$ in the presence of moisture. Davey and coworkers (Davey *et al.* 1989) studied the mechanism of this transformation which could be quite relevant to the zeolite solid-solid transformation. Under the employed experimental conditions, the ammonium nitrate $(IV) \rightarrow (III)$ phase transition of crystal does not occur in the absence of water. On the other hand, upon wetting the phase IV crystals with a saturated aqueous solution, a dark line within the crystal was observed which moved through the crystal as it transformed to phase III structure. Further studies (Davey *et al.* 1991) suggested a mechanism depicted in Figure 4.1. The phase transition occurred in a micro layer of ammonium nitrate solution which traveled as an interfacial zone along the transforming crystal surface. Therefore, the transformation may be considered as a solvent-mediated re-crystallization in which a minute amount of water plays the role of a catalyst in

transforming the crystal phase from one to another. Thus, in zeolite synthesis, a similar mechanism may facilitate a solid amorphous phase to a crystalline product.
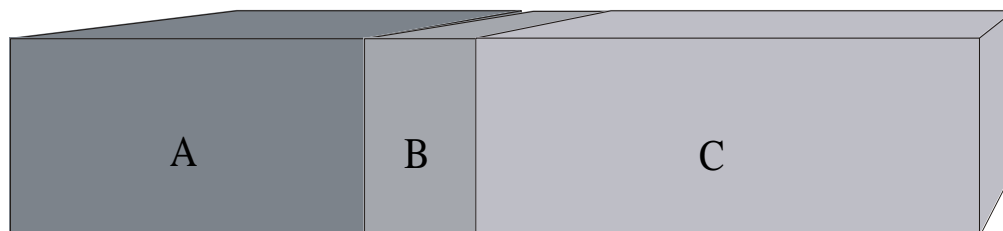
Figure 4.1: A possible model for a localized phase transformation by a solution-mediated mechanism (Cundy and Cox 2005). Initially, phase A dissolves into solution B and crystallizes as less soluble phase C, so that the boundary film migrates across the reaction volume which may not remain constant. In the case of ammonium nitrate (Davey *et al.* 1991), A = Phase IV NH_4NO_3, B = NH_4NO_3 solution, C = Phase III NH_4NO_3, and the transformation takes place within a single crystal. In zeolite system, A could be amorphous precursor, B the reaction solution, and C crystalline zeolite.

Some studies have also indicated that the synthesis of small crystallite size Y zeolite improves its catalytic activity for FCC reaction (Camblor *et al.* 1989; Rajagopalan *et al.* 1986). Studies have been conducted to synthesize nano-size zeolites in colliodal solutions (Li *et al.* 2002; Schoeman *et al.* 1994). Efforts have also been made to produce nano-size zeolite in confined space using inert /amorphous material (Murrell *et al.* 1999; Schmidt *et al.* 2000). Several researchers have successfully reported the synthesis of zeolite in non-aqueous media (Dong *et al.* 1992; Dong *et al.* 1999; Fan *et al.* 1996; Hari Prasad Rao *et al.* 1998; Kim *et al.* 1993; Matsukata *et al.* 1993; Matsukata *et al.* 1996; Xu *et al.* 1989; Xu *et al.* 1990; Yamazaki and Tsutsumi 2000).

The purpose of this study is to combine several aspects of NaY zeolite synthesis under one umbrella, i.e. synthesizing the desired product in nanometer size, using minimal amount of chemicals in order to reduce post treatment of the product. The

synthesis will use the concept of solid-solid transformation thus generating a minimal amount of waste, and reducing the synthesis time. This study also helps in determining the effect of the completion time on the production of any side products. We have attempted to make a parametric study on the synthesis of NaY zeolite using our developed dry synthesis method within porous $50 \mu m$ size silica particles, as described in chapter 3. The synthesis aims at producing the zeolite crystals in a short time, and also to synthesize nanosized crystals up to a size of a few nanomater. This study deals with several operating parameters that can affect the synthesis of zeolite such as the composition of the reagents (precursors), ageing of precursors, synthesis temperature and time, type of reactors, etc. This study leads to an optimum condition that can be used to synthesize nanosized NaY zeolite in a short span of time.

4.2 EXPERIMENTAL

The chemicals used to conduct the parametric study were the same as described in chapter 3, i.e. the source of silica was porous amorphous silica (SiO_2) gel particles (Sylopol 948) with $50 \mu m$ average size supplied by Grace Davison USA. The source of alumina was aluminum nitrate nonahydrate $(Al(NO_3)_3 \cdot 9H_2O)$ supplied by VWR, Canada. pH control was achieved by adding different concentrations of sodium hydroxide $(NaOH)$ supplied by Alphachem Canada that also acted as a structure directing agent (SDA), and distilled water (H_2O). Beside chemicals, two types of reactors were used: polypropylene bottles of 60 mL in size, and stainless steel tubes ($12" \times 0.25"$) with 20.5 mL in size.

The synthesis method was adapted from a report in the literature (Murrell *et al.* 1999), after several modifications in order to make it suitable to our operating conditions and equipment. The starting material was silica gel particles in which aluminum nitrate nonahydrate was added in three steps to adjust the desired ratio of (SiO_2 / Al_2O_3). In the first step, 100 g of Silica gel particles (size $50 \mu m$) were added with different quantities and concentrations of $Al(NO_3)_3 \cdot 9H_2O$ in water in the range from 187.3-215 g of solution (16.4-24.1 wt%) through incipient wetness using a 600ml Teflon container. Then mixing was carried out at 500 rpm using a mixer equipped with a Rushton turbine of $2"$

in diameter. The mixing was carried out for about 15 min until all the solution was adsorbed in the pores of silica particles through incipient wetness. The particles did not form any paste during mixing and remained essentially in flowable powder form. After mixing, a retention time of 1 h was given at ambient temperature for complete penetration of solution throughout the pores of silica particles. The water was then removed from the pores of the silica particles by drying the particles at $120^{\circ}C$ using a forced air convection oven until constant weight. During the process of drying an intermittent mixing of particles was carried out in order to avoid any formation of agglomerates. The drying process allowed the removal of water from the pores and deposition of $Al(NO_3)_3$ inside the pores of silica particles. After drying, alumina was obtained by carrying out calcination at $500°C$ for 2 h with a heating rate of $4°C/\min$ in a furnace, followed by a decrease in temperature to $120°C$ with a cooling rate of $4°C/\min$. The calcination process converted $Al(NO_3)_3$ to Al_2O_3. With this step, SiO_2/Al_2O_3 ratios obtained were in the range from 15-21. In step two, about 97 g of Silica gel particles were taken from step 1 and different quantities and concentrations of $Al(NO_3)_3.9H_2O$ solution in water were added in the range of 145-239 g (9-29.5 wt%), followed by mixing at 500 rpm for 15 min and subsequently, a retention time of 1 h at ambient temperature. Drying was carried out at $120°C$ to a constant weight with intermittent mixing. Finally, calcination was carried out at $300°C$ for 6 h with a heating rate of $4°C/\min$, followed by a decrease in temperature to $120°C$ with a cooling rate of $2°C/\min$. In this step SiO_2/Al_2O_3 ratios obtained were in the range of 7.4-12.5. In the third step, 97 g of Silica gel particles obtained from step 2 were added with different volumes and concentrations of $Al(NO_3)_3.9H_2O$ in water ranging from 114 g to 227 g (9-29.5 wt%), followed by mixing at 500 rpm for 15 min, and a subsequent retention time of 1 h at ambient temperature. Drying was carried out at $120°C$ to a constant weight with intermittent mixing. Subsequently, the calcination was carried out at $300°C$ for 6 h with a heating rate of $4°C/\min$, followed by a decrease in temperature to $120°C$ with a cooling rate of $2°C/\min$. In the third step, the SiO_2/Al_2O_3 ratio was finally adjusted to about 5.1-8.9.

During the three steps of adding Al_2O_3 to SiO_2 particles the pore volume of SiO_2 particles was reduced from $1.56 cm^3/g$ to about $0.67 cm^3/g$, which was due to the occupation of Al_2O_3 in the meso-pores of silica particles. Finally, in the fourth step, the addition of NaOH solution in various concentrations was carried out. The amount of NaOH solution used was in excess in the range of 170-200% to that of the pore volume of the silica particles in order to carry out the synthesis reaction. The particles did not form a paste in the presence of an excess amount of solution; however, they looked apparently wet. To carry out the fourth step, 2 g of material obtained from the third step was added to 10-32 wt% solution of NaOH using a 60 mL size of polypropylene bottle. Hand mixing with the help of a small glass rod was carried out in the polypropylene bottle in order to adsorb NaOH solution into the pores of precursor particles. The reaction was carried out in two types of reactors in order to observe the effects of various parameters on the synthesis of zeolites. The polypropylene bottle and stainless steel tubular reactor served as the batch reactors for the synthesis reaction. The polypropylene bottle and the stainless steel tubular reactor were sealed using Teflon tape before the reaction. An ageing time of 1 h was allowed at room temperature before the synthesis reaction. The molar compositions of the precursor were as:

$$Na_2O : 0.359 - 0.56 Al_2O_3 : 3.2 - 2.86 SiO_2 : 18.77 H_2O$$
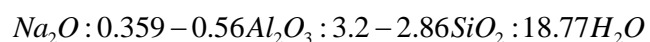
The synthesis reaction was carried out between $100 - 200°C$ using the forced air convection oven by placing the sealed polypropylene bottle/stainless steel tubular reactor between 15 min to 24 h. After the synthesis reaction, the reactors were taken out of the oven and allowed to cool to room temperature under natural convection. Upon opening the reactors, the product appeared damp. It was washed with water, and filtered under vacuum using a $25 \mu m$ size of filter paper. The final product was deposited on the filter paper in the form of a cake, which was then scraped with the help of a spatula and was then dried in the forced air convection oven at $100°C$.

4.3 CHARACTERIZATION OF NaY ZEOLITE USING PXRD, XRF, EDX, SEM, AND BET

The product was analyzed by Powder X-ray diffraction (XRD), BET surface area analyzer, scanning electromicroscopy (SEM), X-ray florescence (XRF) spectrometer, and energy dispersion X-ray (EDX) analyzer. For determining the crystal structure, a Rigaku diffractometer equipped with $CuK\alpha$ radiations at 40 KV was used. For surface area analysis, Micromeritics ASAP 2010 adsorption instrument equipped with version 5.0 software was used. Prior to analysis, the sample of weight $0.095\,g$ was outgassed in vacuum at $100°C$ for at least 16 h. Brunauer-Emmett-Teller (BET) surface area was determined using nitrogen as the adsorbant. Pore volume distributions and total pore volumes were calculated from the adsorption and desorption branches of the isotherm using the Barett-Joyner-Halenda (BJH) model. Scanning electromicroscopy (SEM) was carried out using Hitachi S-4500 scanning machine capable of producing a spatial resolution of < 2 nm at a high electron beam voltage (> 15 kV). The Hitachi S-4500 field emission SEM is also fully equipped with an EDAXTM EDX system, which provides EDX analyses in parallel with SEM images of the sample. The XRF analysis was conducted on Phillips PW1400 XRF spectrometer using fusion technique to determine the ratio of silica and alumina.

4.4 RESULTS AND DISCUSSION

4.4.1 Effect of Si/Al ratio on the crystallization and crystal size

For different batches the SiO_2 / Al_2O_3 ratio was gradually adjusted in three steps by incorporating Al_2O_3 into SiO_2 particles. Several batches were prepared with ratios 5.1, 6.1, 6.6, 7.2, and 8.9. A ratio below 5.1 was not tested, as the lower ratios were more favourable for NaX zeolite. Higher ratios were tried to observe the success rate of NaY zeolite formation. Once the batches were prepared, other operating parameters such as ageing time before reaction, reaction time, and reaction temperature were fixed at 1 h, 16 h, and $100°C$, respectively. Initially started with higher SiO_2 / Al_2O_3 ratios, the Figure 4.2 shows the XRD pattern for SiO_2 / Al_2O_3 ratio of 8.9. The pattern indicates only the amorphous phase for silica from $2\theta = 20 - 35°$ and apparently no peaks were distinguishable from noise that may be an indicative of any crystal formation. This behavior was further confirmed by Figure 4.7(a), which shows SEM images for various SiO_2 / Al_2O_3 ratios. It can be seen that for $SiO_2 / Al_2O_3 = 8.9$, the silica particles were not crystallized and most of the particles remained amorphous within the reaction time of 16 h. A zoomed view shows some zeolite formation at a very small scale, which indicates that the synthesis process was initiated but at a very slow rate. This further shows that the ratio of zeolite/amorphous material was very small making the concentration of zeolite crystals very diluted in the bulk of amorphous silica particles. For this reason XRD results did not show any crystal formation, which was due to the presence of more amorphous phase as compared to crystalline phase.

When the SiO_2 / Al_2O_3 ratio was reduced to 7.2, the XRD pattern in Figure 4.3 started to reveal some peaks but still the amorphous silica was predominant over the zeolite crystal peaks. A similar behavior was observed in Figure 4.7 (b) where SEM images show some zeolite crystals formation on the inner walls of silica particles. The zoomed view also shows that a small portion of the silica particles was converted into zeolite. By further decreasing the SiO_2 / Al_2O_3 ratio to 6.6, the XRD pattern in Figure 4.4 shows more peaks started to appear on top of large hump which was due to the presence of amorphous phase. A similar behavior was also observed for SiO_2 / Al_2O_3 ratio of 6.1

in Figure 4.5. The SEM images in Figure 4.7 (c) and (d) indicate that a large amount of amorphous phase was converted into NaY zeolite. The SEM images also indicate that for a higher ratio of 6.6 the cluster size was between 1-2 micrometer, and the crystallite size varied between $200nm - 1\mu m$. Thus the higher SiO_2 / Al_2O_3 ratio produced larger crystals, which may be because a lesser number of nuclei were initially formed. On the other hand, when SiO_2 / Al_2O_3 ratio of 6.1 was used, the Figure 4.7 (d) shows that the cluster size was in the range of $1 - 2\mu m$ and the crystallite size was in the range of 100-200nm, providing a fairly uniform and small particle size. The lower ratio also indicated that the control on the crystallite size was dependent of SiO_2 / Al_2O_3 ratio. The reason could be due to the formation of a large number of initial nuclei, which leads to a small and uniform particle growth.
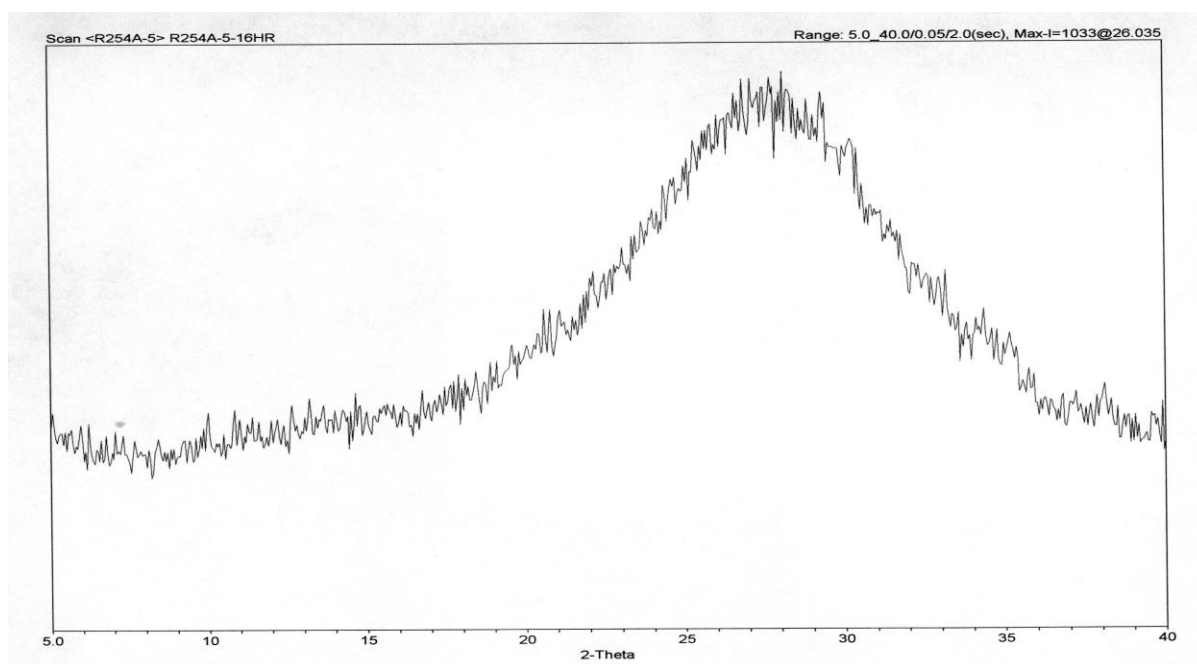
Figure 4.2: XRD pattern of NaY zeolite for SiO_2 / Al_2O_3 ratio of 8.9
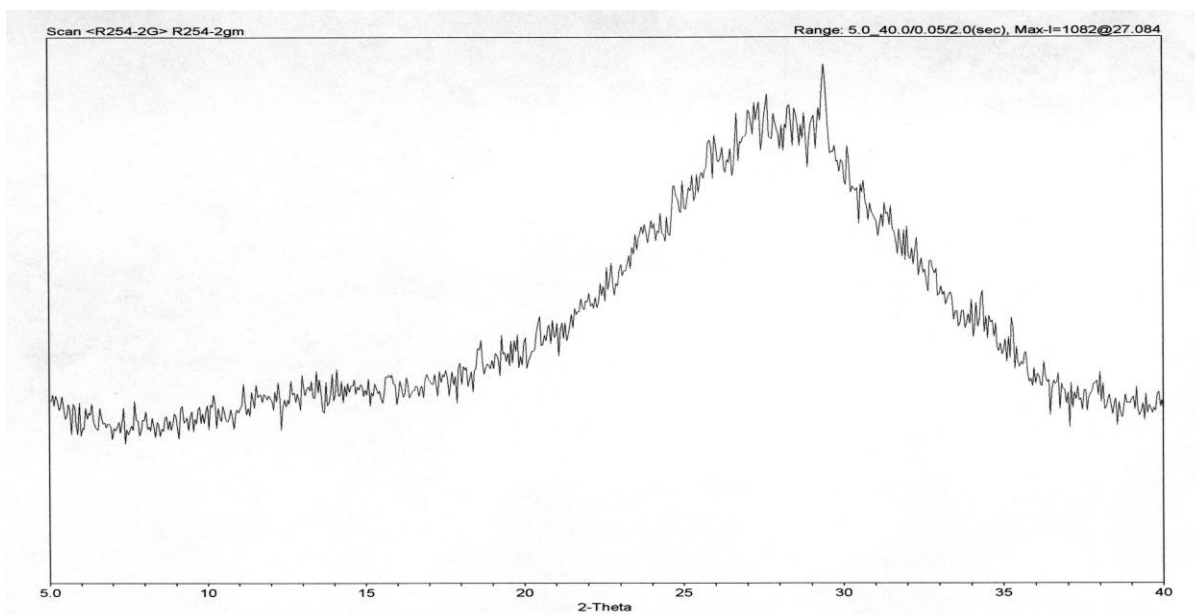
Figure 4.3: XRD pattern of NaY zeolite for SiO_2 / Al_2O_3 ratio of 7.2
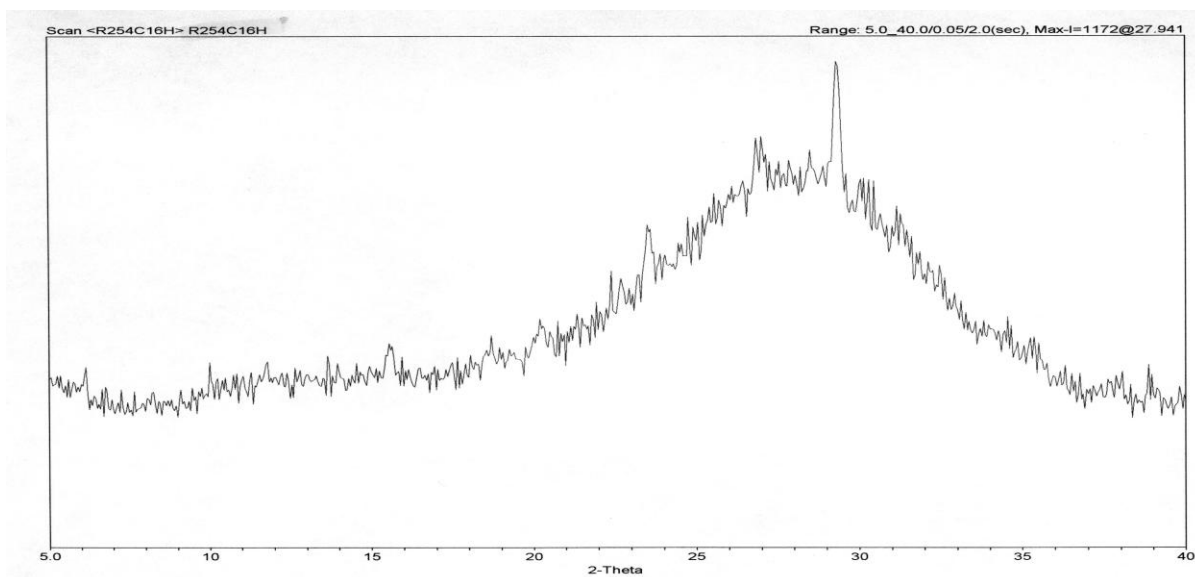
Figure 4.4: XRD pattern of NaY zeolite for SiO_2 / Al_2O_3 ratio of 6.6
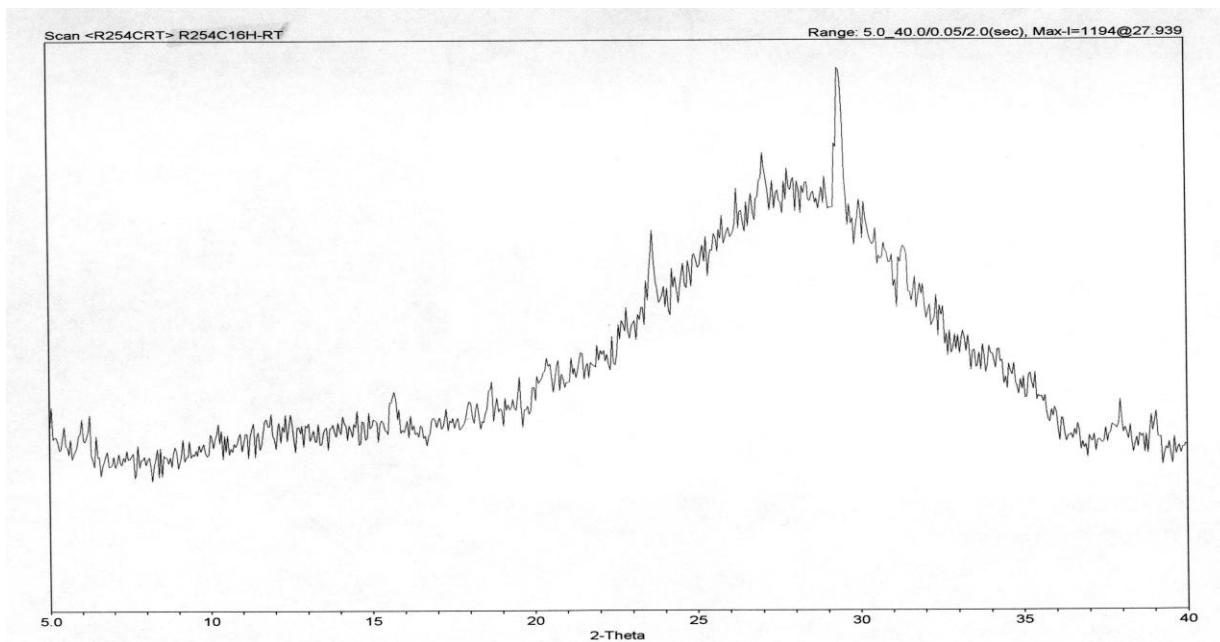
Figure 4.5: XRD pattern of NaY zeolite for SiO_2/Al_2O_3 ratio of 6.1
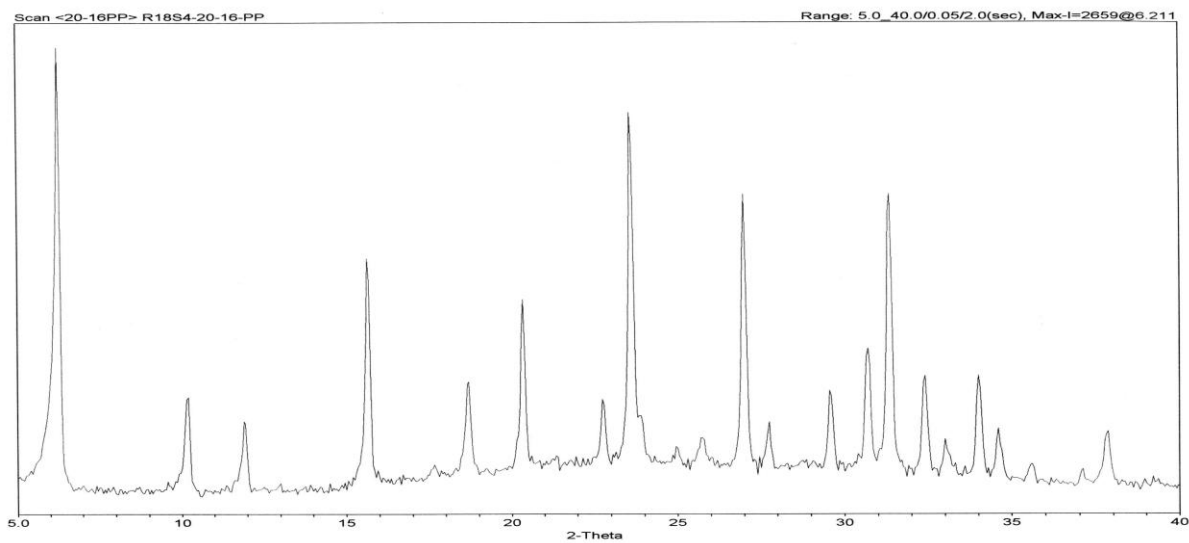
Figure 4.6: XRD pattern of NaY zeolite for SiO_2 / Al_2O_3 ratio of 5.1
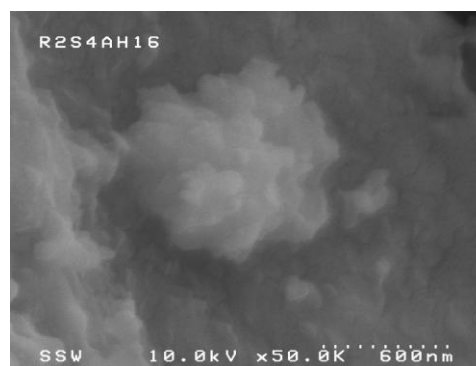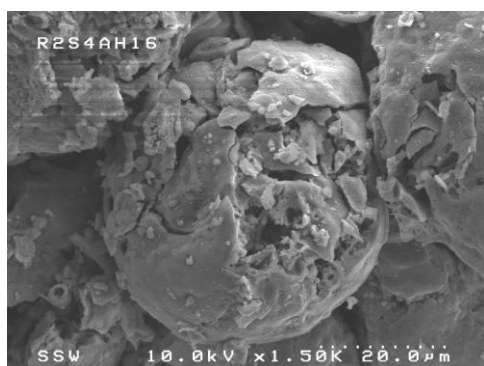
(a) SiO_2 / Al_2O_3 =8.9
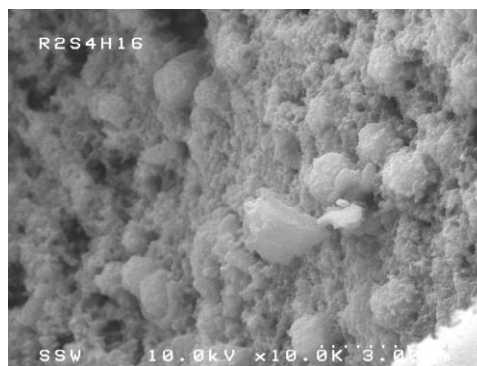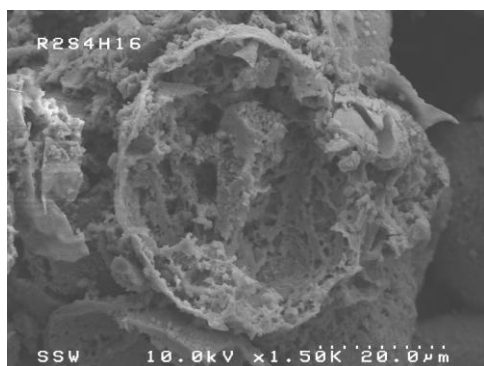
(b) SiO_2 / Al_2O_3 =7.2
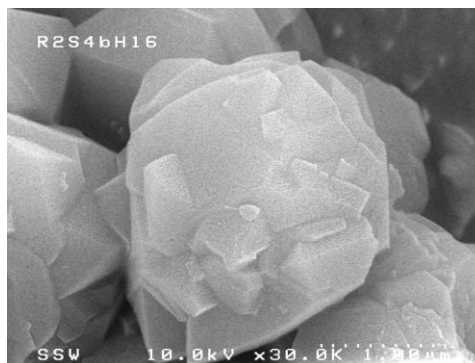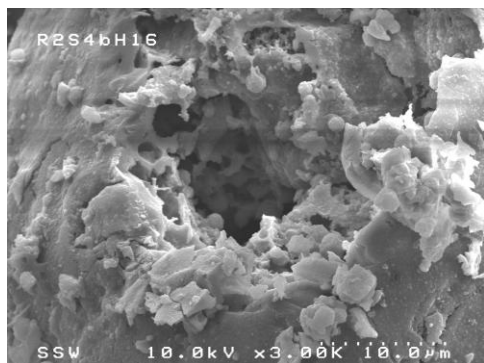
(c) $SiO_2 / Al_2O_3 = 6.6$
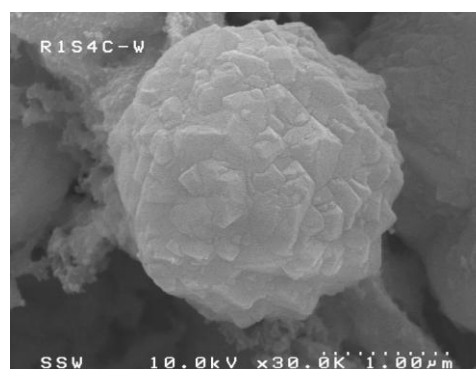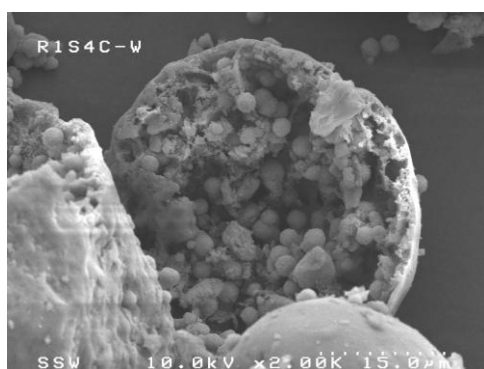
(d) $SiO_2 / Al_2O_3 = 6.1$
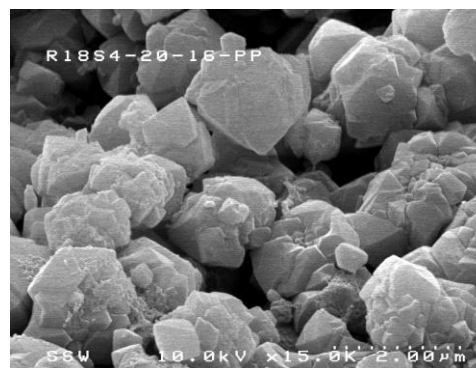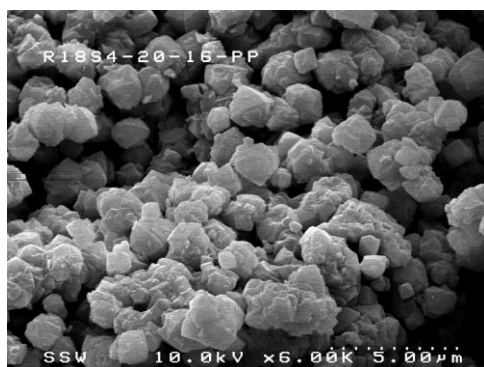
(e) $SiO_2 / Al_2O_3 = 5.1$

Figure 4.7: SEM images of NaY zeolite synthesized using various batch molar ratios of SiO_2 / Al_2O_3

(a) $Na_2O : 0.359Al_2O_3 : 3.2SiO_2 : 18.77H_2O$ (b) $Na_2O : 0.429Al_2O_3 : 3.08SiO_2 : 18.77H_2O$

(c) $Na_2O : 0.46Al_2O_3 : 3.024SiO_2 : 18.77H_2O$ (d) $Na_2O : 0.488Al_2O_3 : 2.97SiO_2 : 18.77H_2O$

(e) $Na_2O : 0.56Al_2O_3 : 2.86SiO_2 : 18.77H_2O$

Upon further decreasing the SiO_2/Al_2O_3 ratio to 5.1, Figure 4.6 clearly indicates the formation of NaY zeolite as the major peaks of identification on XRD pattern were located on $2\theta = 23.6°$, 26.9°, and 31.3°. The XRD pattern also indicates that the peak in the range of $2\theta = 20-35°$, which is an indicative of amorphous silica, was also being reduced. This indicates that the most of amorphous material was being crystallized. The XRD results were further confirmed by the SEM images of the product in Figure 4.7 (e). The SEM images clearly show the formation of zeolite crystals. The images also indicate a great reduction in the amorphous material. The size of the cluster was still in the range of $1-2\mu m$. However, the crystallite size was in the range of $200-500nm$, which was larger than what was observed in Figure 4.7 (d) when SiO_2/Al_2O_3 ratio of 6.1 was employed. The reason for having larger crystallite size may be explained that the formation of NaY zeolite nuclei was smaller in number, which may be due to location and occupation of SiO_2 and Al_2O_3 in the framework of nuclei that lead to the formation of larger crystals. These observations indicated that the SiO_2/Al_2O_3 ratio can be played within the range of 5.1-6.6. However, for a better control on crystal size a ratio of 6.1 was more suited.

In order to support the findings for the effect of Si/Al ratio on the zeolite synthesis, a study carried out by Yan and coworkers was investigated (Yan *et al.* 1995). They carried out the synthesis of ZSM-5 membrane using porous and non-porous $\alpha - Al_2O_3$ supports. When they conducted the study to observe the effects of different quantities of aluminum on zeolite synthesis, they found a better improvement in the intergrowth of zeolite as compared to synthesis reaction carried out without adding any Al in synthesis solution. They found that by using Al in precursor solution the course of zeolite growth was different as compared to what was observed without adding any Al. For the same reason we also observed that higher Si/Al did not help in speeding up the synthesis reaction. Yan and coworkers in their study only described the effects of presence of aluminum in precursor solution. However, they did not provide any effect of using different quantities of aluminum in synthesis mixture, which is contrary to our study. Their study indicated excellent intergrowth of crystals with all the different

quantities of Al in precursor solution. One plausible explanation for not observing any appreciable effects of different aluminum quantities in precursor solution could be that the precursor solution was always in contact with porous or non-porous α-alumina supports inside the reaction vessel. The α-alumina supports provided the necessary quantity of aluminum to carry out the reaction thus somehow shadowing the effect of adding different quantities of aluminum in precursor solution. The aluminum in precursor solution was playing a role in making a uniform amorphous layer and later on uniform growth of crystals but this effect remained the same for all quantities of Al in precursor solution, which left an unexplained observation.

Another study conducted by Inada and coworkers (Inada *et al.* 2005) for the conversion of coal fly ash into zeolite Na-P1 and hydroxy-sodalite under various ratios of Si/Al and concentrations of $NaOH$. The coal fly ash is basically derived from minerals included in coal. During coal combustion, the minerals partially melt to make fly ash particles $(5-10 \mu m)$ in which crystalline phases such as quartz and a silicate mineral mullite remain in the core, whereas a glass phase of aluminosilicate covers the surface of the particle. The glass phase plays an important role in the zeolite formation because of its high solubility into alkaline solution e.g. $NaOH$. The fly ash also includes a small amount of harmful elements such as As, Mn, V, Pb, etc. They are easily separated during the zeolitization since they exist in the glass phase of the particle, dissolve into alkaline solution along with glass phase, and remain in solution and are not incorporated into zeolites. They used two types of fly ash particles with Si/Al ratio of 0.9-1.3. They found that for higher Si/Al ratio at a constant $NaOH$ concentration, zeolite Na-P1 was formed. On the other hand, a lower Si/Al ratio produced hydoxy-sodalite. To further confirm their results they added additional SiO_2 and Al_2O_3 powders to change the Si/Al ratio and found the same trend. These findings support our results that a lower Si/Al may produce NaX zeolite or even further lower ratio may end up with sodalite product. At the same time, a higher Si/Al ratio will produce the desired product. However, Inada did not address the Si/Al ratio changes with reaction time.

On the other hand, Mintova and coworkers (Mintova *et al.* 2006) in a recent investigation on BEA-type nano-size crystalline structure of Beta zeolite from colloidal solution have reported a trend similar to this study during its synthesis using different

Si/Al ratios. They synthesized nanocrystals with a broad range of Si/Al framework compositions by hydrothermal synthesis in basic media with TEA+ cations as a structure-directing agent (SDA). The reactant components were mixed with vigorous stirring and aged on an orbital shaker at ambient temperature for 24 h prior to the hydrothermal treatment. The syntheses were carried out at $100°C$ with duration between 1 and 11 days. The effects of using different Si/Al ratios for Beta zeolite are comparable with our study because a substantial decrease of the Si/Al ratio in the BEA-type structure would provide a material with properties comparable to Y zeolite. They studied the crystallization kinetics of Beta zeolite as a function of aluminum content in a clear mixture (i.e., colloidal solution). They prepared several samples starting from a high aluminum content to zero giving a Si/Al ratio from 25 to ∞. The powder XRD patterns showed that the transformation of aluminosilicate precursors with high aluminum (i.e., Si/Al ratio of 25-83) content into crystalline product took place in about 3 days. Whereas, it took a much longer crystallization time of about 5 days for the precursors with a lower aluminum content $(Si/Al = 250)$ to transform into zeolite. The longest time, 11 days, was recorded for the transformation of pure silica precursor into zeolite. The XRD pattern showed that for lower Si/Al ratios no crystalline product was observed for the first 25 hours. After 40 hours of hydrothermal treatment all characteristic peaks of BEA-type molecular sieve appeared. The intensity of peaks increased with synthesis time and reached to its maximum value at about 65 hours. After that further heating did not improve the peak intensity. With higher Si/Al ratio of 250 and ∞ a further longer heating time was required to obtain similar level of crystallinity. They also observed a broad peak in the range of $2\theta = 6.5 - 8.5°$ that indicated a highly faulted structure due to the presence of two isomorphs in the nanoparticles. This peak became more prominent in solution containing higher Si/Al ratios, which indicated that possibility of impurities increased with higher Si/Al ratio. They concluded that that the presence of aluminum is directly related with the nucleation and crystal growth kinetics of BEA-type zeolite. In other words, the aluminum is necessary for the efficient synthesis of Beta zeolite in a shorter span of time (Mintova *et al.* 2006), as observed in our study.

Mintova and coworkers further employed HRTEM to study the effect of aluminum on the particle size of Beta zeolite. The TEM micrographs revealed that the crystal size and morphology were not substantially influenced by the concentration of aluminum, which is also observed in our study. Although, Mintova et. al found a trend of increase of the crystal size with aluminum concentration was detected, but the difference in the size of nanocrystallites was negligible (Mintova *et al.* 2006). The crystal size in our study more or less agrees with the HRTEM findings of Mintova and coworkers. Though there is a slight change in crystal size observed for the lowest SiO_2 / Al_2O_3 ratio but overall crystal size remained similar. As a whole, this study is in agreement with the study carried out by Mintova et al. Since our objective is to synthesize NaY-zeolite in a shorter span of time, therefore, our XRD patterns and SEM images are in agreement with that of higher SiO_2 / Al_2O_3 ratios used by Mintova but the silica particles did not completely converted to NaY zeolite in 16 h, which agrees with Yan et al. (Yan *et al.* 1995). Also, according to Mintova study the higher Si / Al ratio caused reduction in aluminum content which may reduce the rate of nucleation. Their conclusion further supported our reduction in synthesis as the nucleation rate was low for higher Si / Al ratio and did not provide a sensible synthesis in a short span of time. However, a complete crystallization was achieved due to all suitable conditions of alumina content were met when the SiO_2 / Al_2O_3 ratio was decreased to 5.1.

4.4.1.1 Effect of Time of Reaction

In order to resolve the absence of NaY zeolite characteristic peaks from XRD analysis for higher SiO_2 / Al_2O_3 ratios, the synthesis was carried out for 20-24 h. The XRD results for ratios 8.9 and 7.2 remained indifferent. However, for ratios 6.6 and 6.1 started to show all the peaks for NaY zeolite. Figures 4.8 and 4.9 show the XRD patterns of $SiO_2 / Al_2O_3 = 6.6$ for synthesis time 20 and 24 h, respectively. The pattern also shows the broad peak $2\theta = 20 - 35°$ for amorphous silica but its intensity was very much reduced, which indicates that most of the amorphous silica was converted into zeolite. A further reduction in amorphous peak was observed when synthesis was continued for 24 h, as shown in Figure 4.9.
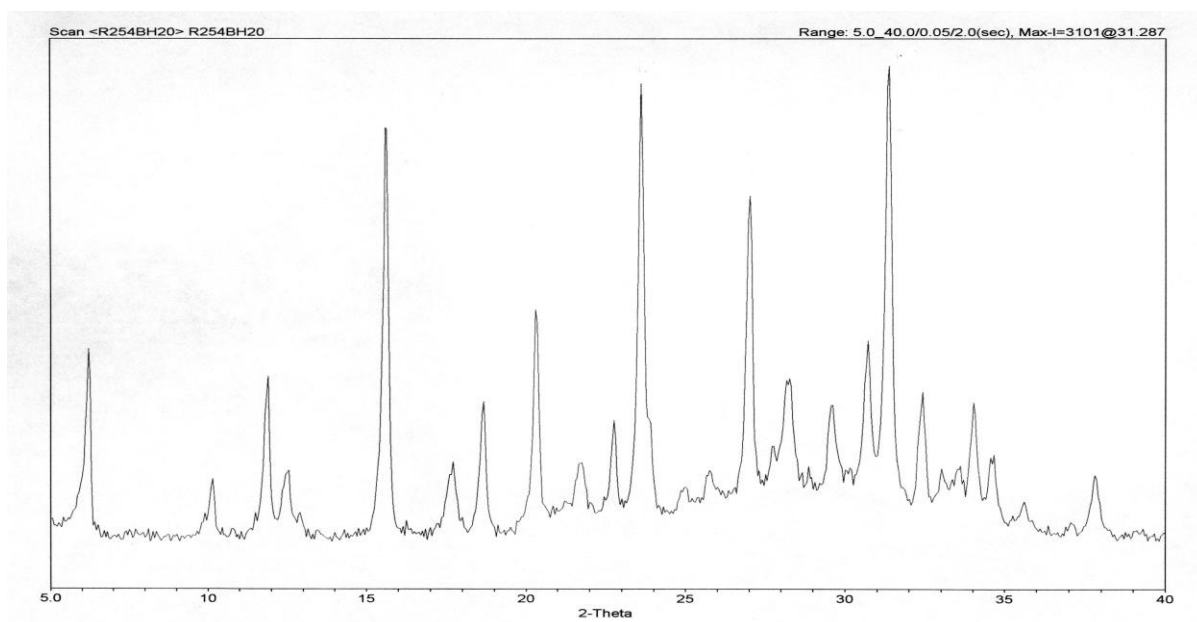
Figure 4.8: XRD pattern for SiO_2 / Al_2O_3 ratio 6.6 after 20 h of Synthesis
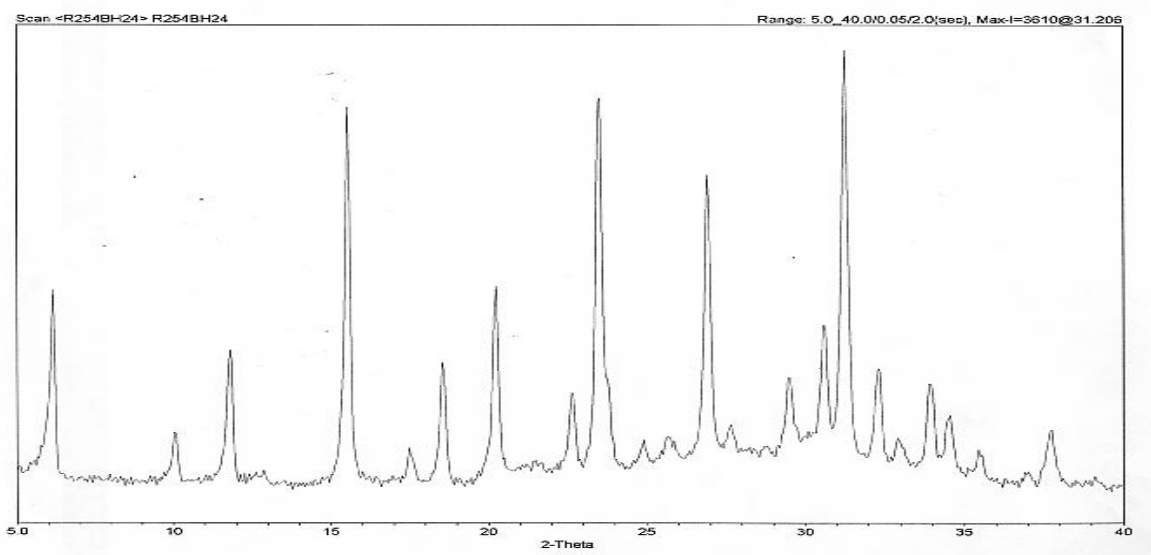
Figure 4.9: XRD pattern for SiO_2 / Al_2O_3 ratio 6.6 after 24 h of Synthesis

A very similar trend was observed when NaY zeolite with SiO_2/Al_2O_3 ratio of 6.1 was synthesized for 20 and 24 h, as shown in Figure 4.10 and 4.11. These observations indicate that a longer synthesis time favored a complete conversion to zeolite using an appropriate SiO_2/Al_2O_3 ratio. The synthesis time in this study was very small as compared to 40-65 h of synthesis time observed during the study conducted by Mintova et al. (Mintova *et al.* 2006). Both studies produced nano-sized crystals; however, the difference in reaction time was due to the hydrothermal synthesis in clear solution in the study of Mintova and coworkers (Mintova *et al.* 2006). The difference between the solution mediated synthesis and dry synthesis using solid-solid transformation may be due to the issue of mobility of reaction species. In case of solution mediated synthesis, the potential growth unit (composed of T-O-T; where T = Si or Al) may detach or dissolve itself from the amorphous particle (composed of polymers or oligomers of Si and Al) and migrates itself through the solution to a potential growth site on a remote developing crystal. This phenomenon is well visualized in Figure 4.12 as depicted by Cundy and Cox (Cundy and Cox 2005). On the other hand, in solid-solid hydrogel phase transformation during the dry synthesis process, the potential growth unit may never escape into solution which fills the pores of amorphous silica particle (as the case in this study). However, it may be transferred in a concerted process from an amorphous region to an immediately adjacent potential crystal growth within the particle. This scenario is not depicted in Figure 4.12, but can be visualized. Therefore, from this perspective the solid-solid transformation may be seen as a limiting case of solution mediated transformation (Derouane *et al.* 1981). The major difference between the two processes is being the distance traveled by the mass-carrying species. The shorter the distance traveled the smaller the zeolite synthesis time. For this reason, it is clear from our study that the dry synthesis process is more efficient as compared to solution mediated synthesis process. The underlying mechanism is still OH^- catalysed T-O-T bond making and bond breaking process. There is sufficient reaction species mobility to continue the equilibration process; however, the mechanism of zeolite formation in dry synthesis basically remains the same as solution mediated synthesis.

It was also observed through SEM image in Figure 4.7(d) and Figure 4.15 (e-f) that the entire silica particle started to convert to NaY zeolite. In Figure 4.7(d), after 16 h

of synthesis time, the cracked opened image of the particle depicts that the most of the silica particle was converted into zeolite, but the outer layer of the particle remained unconverted. At 20 h of synthesis time, the outer layer of the particle was partially consumed, whereas at 24 h of reaction time the outer layer of the particle was completely consumed. A complete conversion of silica particle into zeolite was not desirable in this study, because it consumed undesirably the outer layer of silica particle. The outer layer of silica particle was needed to retain the shape of the particle, so that it may directly be used for any fluidized bed system. Therefore, a shorter synthesis time was required in order to maintain the outer crust of the silica particle intact. This step helped the silica particle to retain its shape and at the same time its macro and meso pores were filled with NaY zeolite. For this reason a shorter synthesis time of 16 h was more favored.
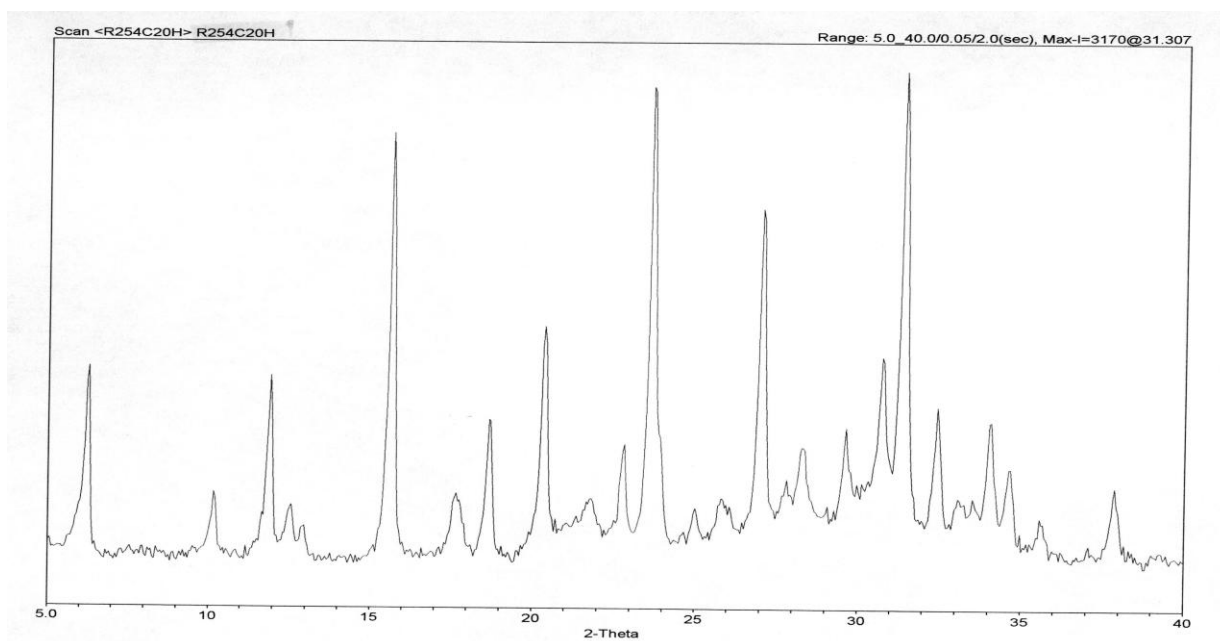
Figure 4.10: XRD pattern for SiO_2 / Al_2O_3 ratio 6.1 after 20 h of Synthesis
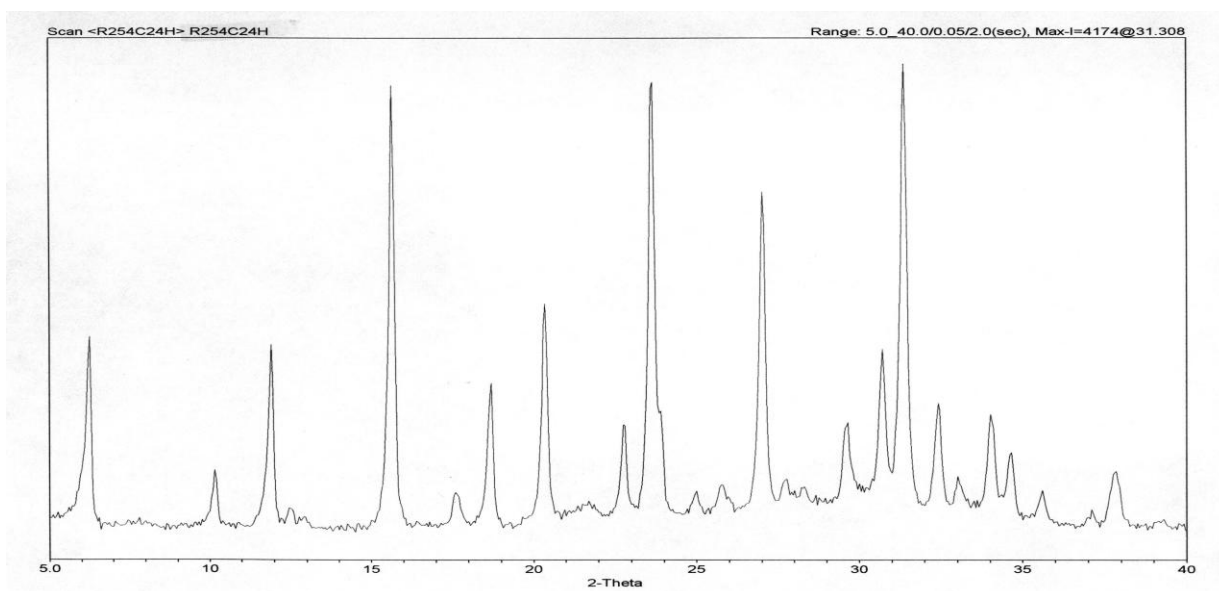
Figure 4.11: XRD pattern for SiO_2 / Al_2O_3 ratio 6.1 after 24 h of Synthesis
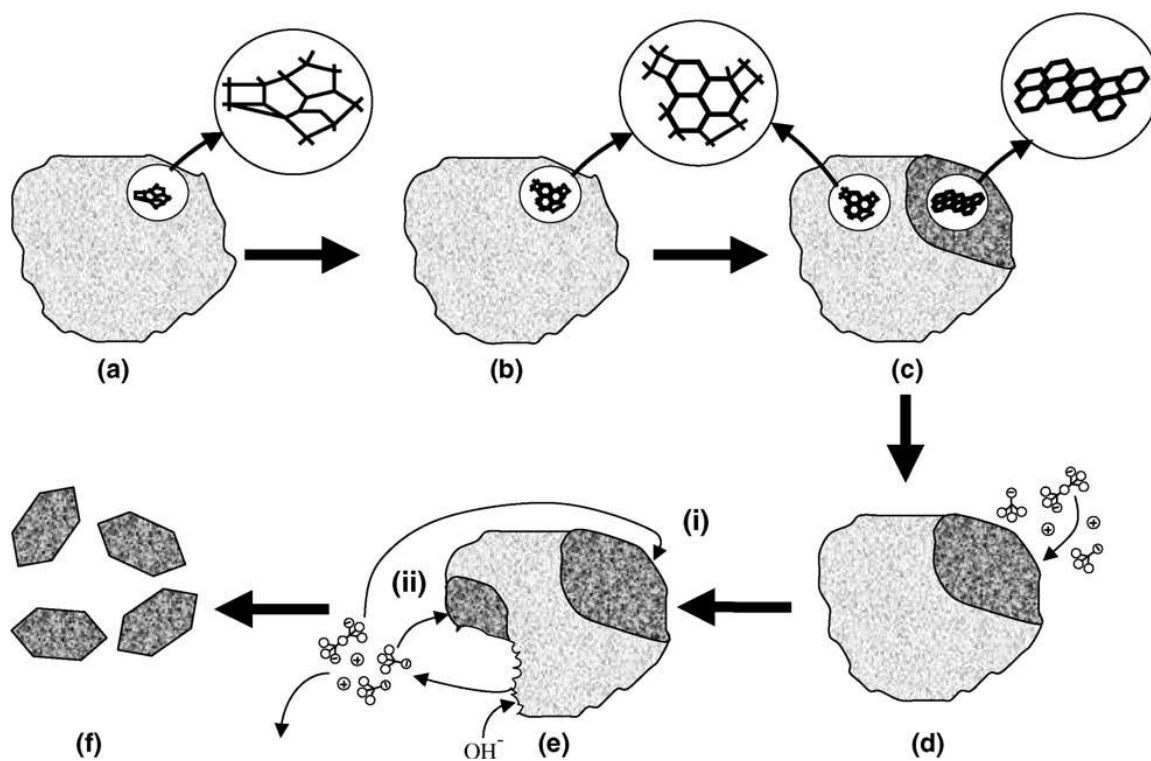
Figure 4.12: Progress from a gel particle to crystalline zeolite from an initially amorphous structure (a), areas of local order are established (b), some of which develop into crystal nuclei (c) and grow by acquisition of building units from solution (d). To provide such growth units, amorphous material is dissolved (e) to supply nutrient to both distant (e-i) and nearby (e-ii) growth sites. The distant site could be located on another gel particle. For the nearby site, crystal growth may reduce in the limit to a local reconstruction of the host gel particle. Eventually, all amorphous material is converted into an approximately equal mass of zeolite crystals (f) (Cundy and Cox 2005).

4.4.2 Effects of Ageing and Synthesis Time on Crystallization

The results from the last section suggested using a SiO_2/Al_2O_3 ratio of 6.1 in order to optimize the precursor composition. This helped to further investigate the effects of precursor ageing before starting synthesis reaction, and also the effect of shorter synthesis time on crystallization. First of all the effect of ageing was investigated by applying various ageing time on a 2 g sample prepared with $SiO_2/Al_2O_3 = 6.1$, adding 3.5 g (20wt%) of $NaOH$ solution, and aged for different times starting from no ageing to 24 h at room temperature. The precursor particles appeared slightly wet due to the addition of $NaOH$ in excess to the pore volume of precursor silica particles. It was found through SEM and XRD analyses that no significant change in the level of crystallization was observed for an ageing time greater that 1 h. However, when the synthesis reaction was carried out at $100°C$ for 16 h without any ageing at room temperature, the crystallization was partially achieved as compared to when an ageing time of 1 h was employed. Figure 4.13 depicts the partial conversion of silica particles.

(a)   (b)
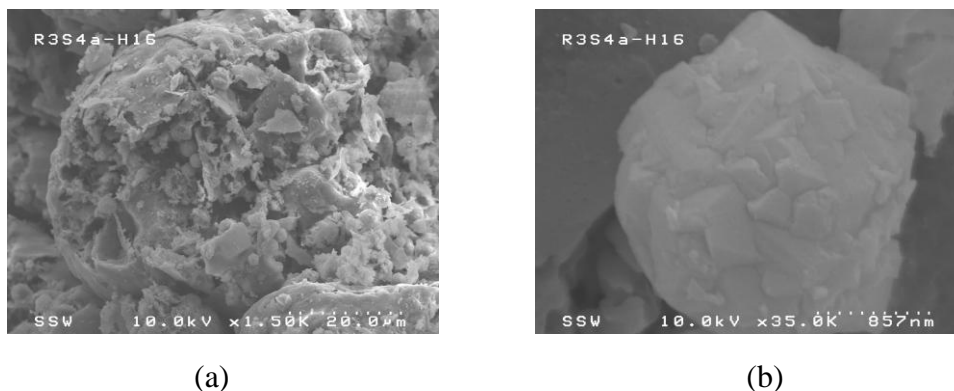
Figure 4.13: SEM images of NaY zeolite synthesis without ageing the precursor at room temperature: (a) silica particle with embedded NaY zeolite clusters, (b) zoomed view of NaY cluster in silica particle with crystals.

The XRD analysis did not show any peak as most of the material was still amorphous. In order to further investigate the formation of zeolite, the synthesis time was increased to 20 h. Figure 4.14 depicts all the majors peaks of NaY zeolite. However, the presence of broad peak $2\theta = 20 - 35°$ for amorphous silica clearly suggests a partial conversion of amorphous silica to NaY zeolite as compared to what is depicted in Figure 4.10.

This study shows that the crystallization behavior of the synthesis reaction mixture is dependant upon ageing at ambient temperature prior to the principle heating step. The first synthesis of Y zeolite from colloidal solution by Breck (Breck 1964; Breck 1974) also required an ageing step prior to hydrothermal crystallization in order to acquire the formation of pure faujasite phase and to avoid contamination by impurities such as zeolite P (gismondine type) or S (gmelinite type). Similar ageing procedures have also been described for other zeolites, for example zeolite L (Vaughan 1984), zeolite omega (ZSM-4) (Nicolas *et al.* 1988), and ZSM-5 (Kacirek 1985).

The ambient temperature ageing is directly related to nucleation of reaction mixture which remains X-ray amorphous in general. However, its seeding potential is time dependant, suggesting the development of structured components during the ageing process. Many attempts (Ginter *et al.* 1992b; Gora and Thompson 1997; Polak and Cichocki 1973) were made to detect the nucleating entities during the ageing of reaction mixtures by using chemical or spectroscopic methods, but very little information was revealed. Though the nuclei are in great number but the mass they occupy is very little as compared to the mass of the reaction mixture which is amorphous. This scenario was well expressed by Cundy and Cox (Cundy and Cox 2005). They concluded that the ratio of the nuclei mass to the mass of the product was $2x10^{-8}$, although the number of nuclei per gram of the nutrient was 10^{11}. This further depicts that the number of nuclei can be estimated using modeling studies e.g. population balance method (Cook and Thompson 1988), but it is generally more helpful with experimental observations. Polak and Cichocki (Polak and Cichocki 1973) found in their early work that the changes in the chemical composition took place during the ageing of faujasite hydrogel precursors.
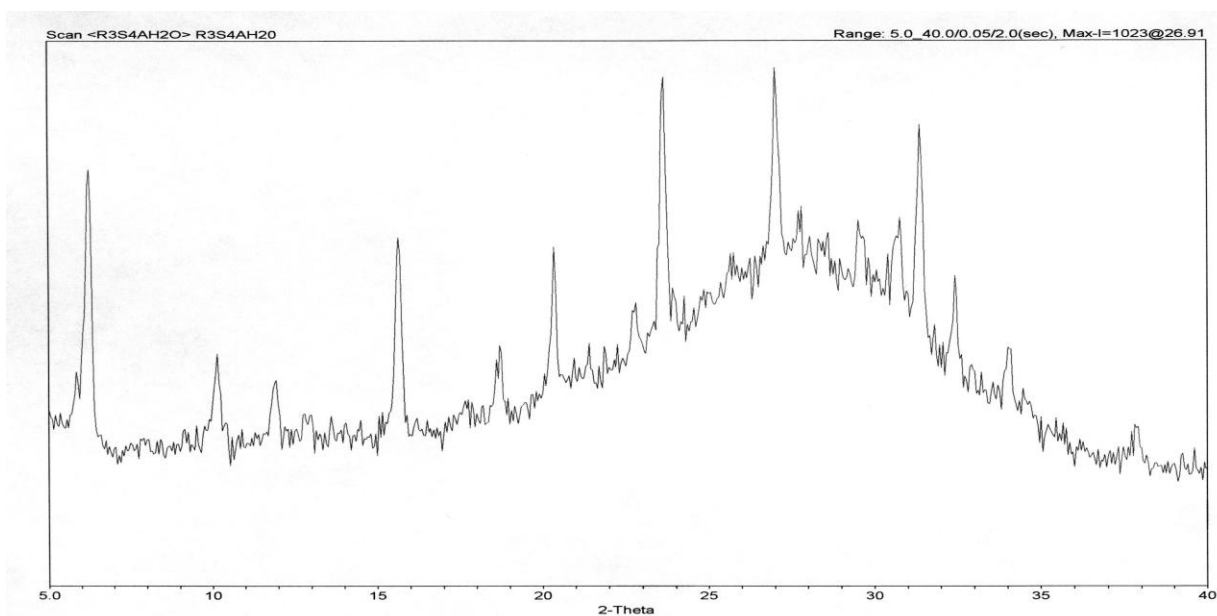
Figure 4.14: XRD pattern of NaY zeolite for SiO_2 / Al_2O_3 ratio 6.1 after 20 h of synthesis, without ageing at room temperature

The change in the chemical composition was attributed to the polycondensation reactions which formed certain groups of species that facilitated crystallization upon final heating process. The water molecules are released as a result of condensation reaction, as shown in equation 2.7. In this study, since the precursor particles appeared wet due to the addition of NaOH solution in excess amount as compared to the pore volume of the silica particle, therefore the effect of release of water molecules was not observed. However, this information was revealed in our another study, as described in chapter 5, where the NaOH solution filled the precursor silica particles approximately 100% of their pore volume.

The phenomenon during ageing process was better explained by Ginter et al. (Ginter *et al.* 1992b; Ginter *et al.* 1992a) who performed different studies on physical and chemical transformations occurring during the room temperature ageing for the synthesis of NaY zeolite from colloidal solutions. They found that upon mixing the silica colloidal sol with sodium aluminate solution, a gel was instantly formed due to the flocculation of the silica particles. The gel was further homogenized by mixing the gel with an agitator, which sheared the gel into small granules. This phenomenon was hard to achieve in our study as all the physical or chemical changes were taking place within the silica precursor particles. Ginter et al. (Ginter *et al.* 1992b; Ginter *et al.* 1992a) also found that there was no chemical transformation of silica colloidal particles took place during mixing, but upon ageing the silica particles slowly dissolved, and released silicate anion species into surrounding solution. These species reacted with aluminate anion species to produce aluminosilicate species, which further precipitated due to their solubility. The precipitated amorphous aluminosilicate solid was rich in Al and hydrated Na^+ cations. The precipitation of the aluminosilicate consumed the dissolved Al and Si from solution. Then after complete consumption of dissolved Al, the remaining colloidal silica dissolved and released silicate anion into the solution. The precipitated aluminosilicate reacted slowly with the dissolved silicate anions in the solution, which resulted in a change of Si/Al and Na/Al ratios. This explanation may hold true in comparison to our study; however, the step of dissolution of silica colloidal particles, traveling through the solution, and get reacted with aluminosilicate precipitate may be eliminated as the entire phenomena is taking place within the silica particle making the whole process

accelerated. For this reason the ageing time indicated no effect on the synthesis reaction after 1 h of ageing. A further possibility, as explained by Cundy and Cox (Cundy and Cox 2005), may be the equilibration process leading to the intermediate semi-ordered state had reached a thermodynamic pseudo-equilibrium i.e. concentration of proto-nuclei had reached a steady-state in 1 h of ageing time. Therefore, after 1 h of ageing time further extended ageing time did not show any change or improvement in zeolite synthesis.

The effect of synthesis time was further investigated by limiting the SiO_2 / Al_2O_3 ratio to 6.1, ageing time 1 h, and reaction temperature at $100°C$. The synthesis was carried out for several time periods starting from 4 h to 24 h. The SEM images depict the effect of reaction time on zeolite synthesis, as shown in Figure 4.15. Apparently no crystal formation was observed during the first 4 h. The XRD analysis also showed amorphous phase. After 8h of synthesis time, SEM images start to show some level of crystal formation; however, major portion of silica particles remained amorphous. Between 12 to 16 hr the right size of clusters were observed with crystal size in the range of 100-200 nm. Upon further heating for 20 to 24 h, the external surface of the silica particle started to transform into zeolite and in 24 h the entire particle was transformed into zeolite. The XRD analysis also confirmed the complete zeolite transformation in Figures 4.9 and 4.10. The synthesis reaction after 20-24 h is not the objective of this study as the outer crust of the silica particles is needed to remain intact, so that the crystals may be used as part of large particle which is easy to handle in bulk quantities. Therefore, a suitable reaction time of 12 h, and to be on the safe side 16 h is more suitable for NaY zeolite synthesis.

Our results may be considered similar to the work of Ginter and coworkers (Ginter *et al.* 1992a) who investigated the effects of ageing at room temperature on the NaY zeolite and synthesis reaction at elevated temperature using powder X-ray diffraction, ^{29}Si MAS NMR, FTIR, and Raman spectroscopy. They found that the room temperature ageing of colloidal silica gels strongly affected the kinetics of NaY crystallization at $100°C$. They also discovered that the maximum crystallization activity was achieved with ageing time of 12 h or less. On the other hand, without ageing, NaY
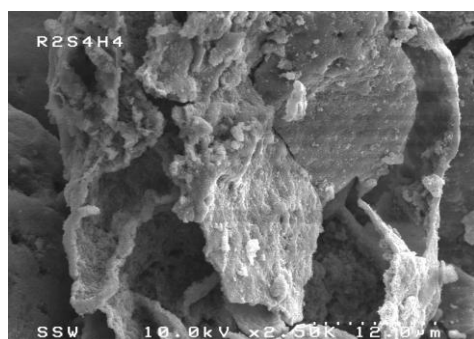
(a) 4 h
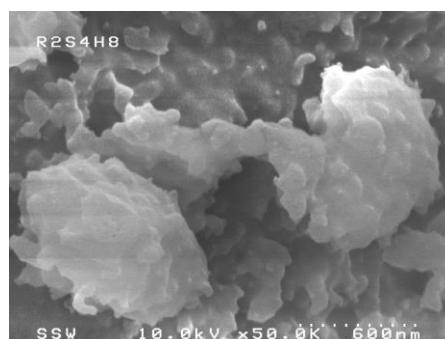
(b) 8 h
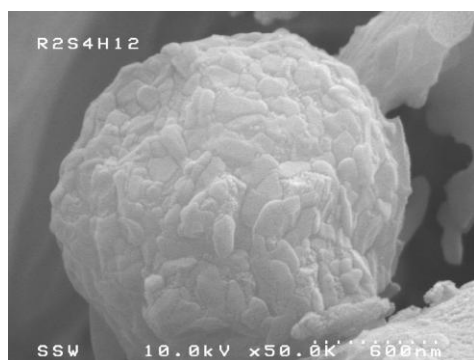
(c) 12 h
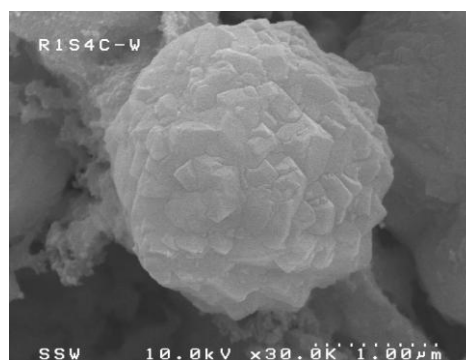
(d) 16 h
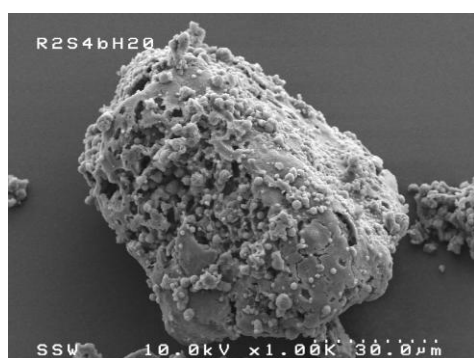
(e) 20 h
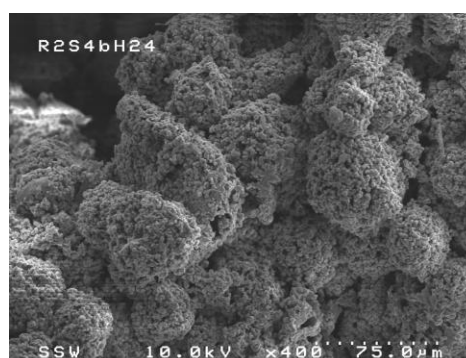
(f) 24 h

Figure 4.15: SEM images for the effect of reaction time on the synthesis of NaY zeolite using a SiO_2 / Al_2O_3 ratio of 6.1 (a)-(f): 4h-24h

crystallization was very slow, and barely yielded any noticeable amounts of NaY after about 100 h reaction time at $100^{\circ}C$. This is contrary to our study where we were able to achieve some level of crystallization without ageing at room temperature, which may be due to the advantage of using the dry process. Ginter and coworkers (Ginter *et al.* 1992a) also found that the crystal size was decreased with the ageing time. The time dependant effects of ageing on the control crystal size may also be linked to earlier studies by Freund (Freund 1976), and Zhdanov and Smulevich (Zhdanov and Samulevich 1980). Their investigations showed that room temperature ageing of aluminosilicate NaA and NaX gels resulted not only in acceleration of crystallization but also a decrease in the crystal size, thus linking the ageing process directly to the number of nuclei formation. A study carried out by Slangen and coworkers (Slangen *et al.* 1997b) sheds further light on the ageing related zeolite A synthesis using microwave heating. They found that the product from short ageing time of 5 min was amorphous after 5 min of microwave heating at $100^{\circ}C$. On the other hand, the zeolite A was crystallized in 1 min at $120^{\circ}C$ after an overnight ageing of synthesis mixture. The product crystal size was decreased with ageing time, suggesting that the structured elements related to nucleation process were being formed during the ageing process. Our study showed a high crystallization activity after 1 h of ageing at room temperature, which may be mainly due to the dry process itself. The effect of dry process can further by visualized that without any ageing our process still yielded the NaY zeolite after 20 h of reaction at $100^{\circ}C$, whereas, Ginter and coworkers (Ginter *et al.* 1992a) did not observed any appreciable product even after 100 h of reaction at $100^{\circ}C$. Also the formation of structured elements, which leads to nuclei formation, is faster that is why after 1 h of ageing the product is synthesize upon heating. However, we did not observe any significant change or decrease in crystal size with ageing, which may be due to the fact that our system was basically a dry process. The time and distance required to assemble all the species prior to nucleation was short because all activities were taking place within the silica particles. Therefore, no significant effect on nucleation and later on size of crystals was observed. This further suggests that these observations are closely connected to colloid, gel, or silica particles (this study) rather than to the actual process of zeolite formation, meaning that they are

related to particles and their aggregation rather than the chemistry taking place within them to form the zeolite lattice.

Our study clearly indicated the dependency of zeolite synthesis on the duration of reaction time. The apparent inactivity for crystal formation for the first 4 h indicated some phenomena occurring beyond the sensitivity of SEM (Figure 4.15 (a)). This phenomena may be related to the ageing that continued even when the reaction mixture was exposed to high temperature or as explained earlier that the equilibration process leading to the intermediate semi-ordered state had reached a thermodynamic pseudo-equilibrium during the first 4 h of synthesis reaction at $100^{\circ}C$. This scenario may, however, alter if there is a change in the reaction temperature.

4.4.3   Effect of Temperature on the crystallization and crystal size

So far, the synthesis reaction was carried out at $100°C$ in polypropylene bottles. In order to observe the effects of synthesis temperature on the crystallization, several temperatures were tested using polypropylene bottles in the range of $90-110°C$ keeping other parameters constant such as, SiO_2/Al_2O_3 ratio at 6.1, $NaOH$ 20wt%, ambient temperature ageing for 1 h, and the synthesis time at 16 h. The synthesis above $110°C$ was not carried out due to the operating temperature limitation for polypropylene. The SEM images in Figure 4.16(a) show that at $90°C$ most of the silica particles remained amorphous. Only a part of the silica particles was transformed into zeolite, and the cluster size was around $1.5\mu m$. This also suggests that the lower temperature was not suitable for zeolite conversion. This observation was further supported by longer synthesis time at $90°C$ for 20 and 24 h but the results remained the same. The XRD analysis in Figure 4.17 shows that a major portion remained as amorphous silica with only few crystal peaks start to show up. On the other hand, when a synthesis temperature of $110°C$ was applied, the silica particles were completely transformed into NaY zeolite, as shown in Figure 4.18 by XRD pattern. However, the size of cluster and the crystal size were quite large. The SEM images in Figure 4.16(b) shows that the clusters were in the range of $2-5\mu m$ and the crystallite size was in the range of $100-300nm$.
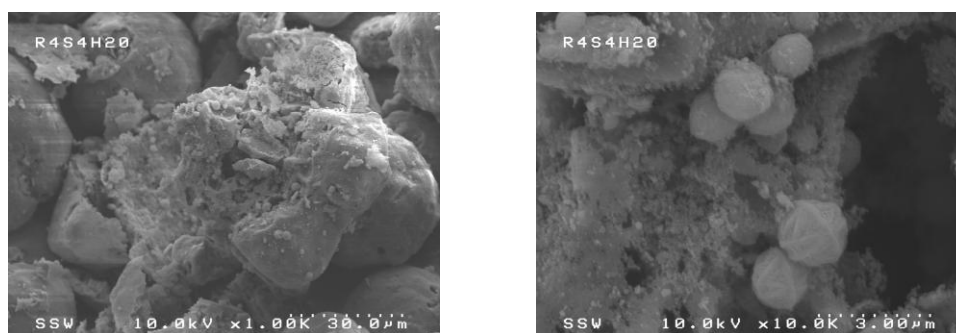
(a) Silica particle and its zoomed view for synthesis at $90°C$
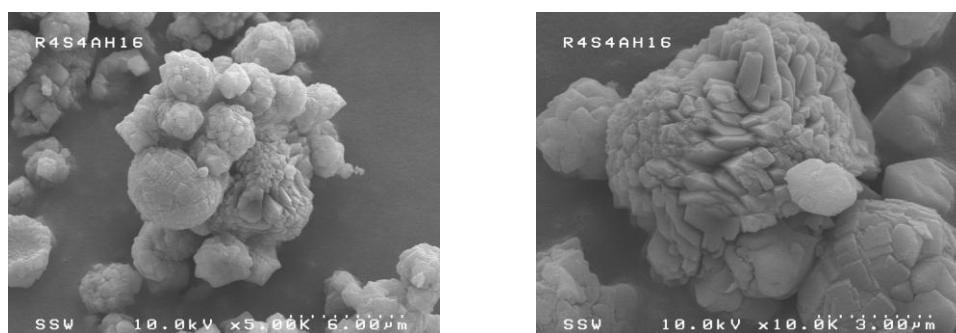
(b) NaY zeolite cluster and its zoomed view for synthesis at $110°C$

Figure 4.16: SEM images for the effect of reaction temperature in polypropylene bottle on the synthesis of NaY zeolite using a SiO_2 / Al_2O_3 ratio of 6.1, (a) $90°C$ (b) $110°C$
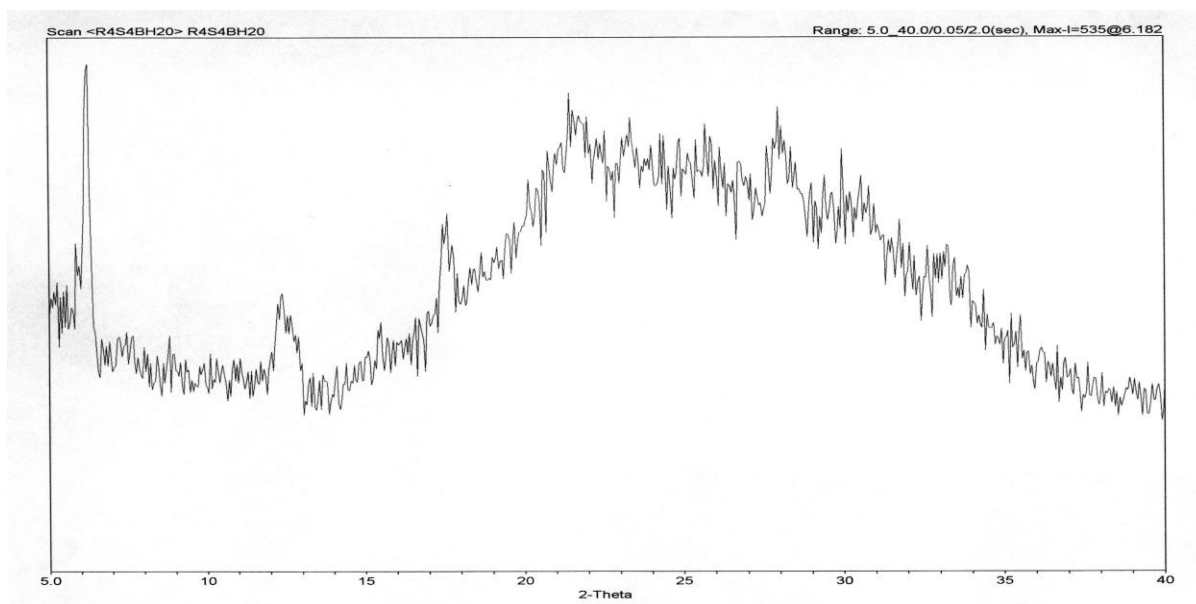
Figure 4.17: XRD pattern of NaY zeolite synthesis at $90°C$ using a SiO_2 / Al_2O_3 ratio of 6.1
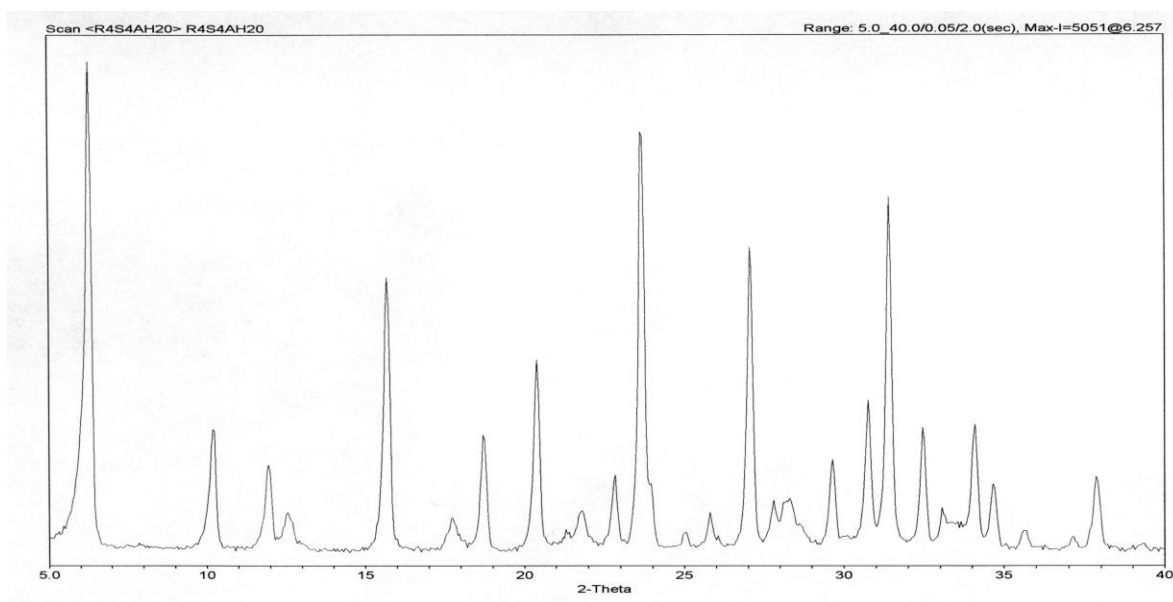
Figure 4.18: XRD pattern of NaY zeolite synthesis at $110°C$ using a SiO_2 / Al_2O_3 ratio of 6.1

The study by Fajula and coworkers (Fajula *et al.* 1987) supported our findings. They synthesized zeolite omega (ZSM-4) at two different reaction temperature of $100-135°C$. A pure zeolite omega was synthesized in 1 day while operating at $135°C$. On the other hand, it took 15 days to synthesize zeolite omega at $100°C$. They also observed that during the reaction at $100°C$ the faujasite crystals were formed first and then subsequently dissolved, and finally a pure zeolite omega was formed in 15 days. These findings indicate high dependency of zeolite synthesis on temperature.

The increase in the cluster size with temperature in our study suggests that though the nucleation was continued throughout the synthesis time, but the higher synthesis temperature suppressed the nucleation rate and enhanced the crystal growth rate. Apparently higher reaction temperatures favored the crystal growth rate as compared to nucleation rate. For this reason larger crystals were observed at $110°C$ making the cluster size around 2-5 micrometer. It was also observed that a higher synthesis temperature caused a complete transformation of silica particles into zeolite in 16 h of synthesis. Figure 4.18 depicts the XRD analysis of the NaY zeolite without any amorphous peak of silica. This observation suggests that a shorter synthesis time could be achievable with higher synthesis temperature.

4.4.4 Effect of type of reactor and temperature on the crystal synthesis time and size

In order to optimize the operating conditions and to reduce the synthesis time, the polypropylene bottles were replaced by a stainless steel tubular reactor $(0.25^{"} \times 12^{"})$. The stainless steel has a higher thermal conductivity $(k = 16.3 \, W/m\text{-}K)$ as compared to polypropylene $(k = 0.12 \, W/m\text{-}K)$. The replacement of polypropylene bottle by the stainless steel tubular reactor provided the capacity of operating at higher temperature, which was not possible with the polypropylene bottle due to its operating temperature limitation of $120°C$. In order to achieve rapid heat transfer to the centre of the tube reactor, a diameter of $0.25^{"}$ was chosen, which also provided ease in filling the tube with silica particles for reaction, and later on removing the product and cleaning the tube. For this study, a batch composition of $2.05Na_2O : Al_2O_3 : 6.09SiO_2 : 36.47H_2O$ was used. In

the first set, the synthesis was carried out at 100 ºC for $2\text{-}16h$. It was observed that the crystals started to appear after 4 h of reaction. The SEM image in Figure 4.19 (a) shows that after 8 h, the same level of synthesis was achieved which was observed in polypropylene bottles after 16 h of reaction. After 12 h, the silica particles were completely crystallized into zeolites in stainless steel tubular reactor, as shown in Figure 4.19 (b). These findings clearly indicate the advantage of using stainless steel tubular reactor over the polypropylene bottles. This observation further supported the idea (Jansen *et al.* 1992) that a rapid heat transfer also reduces the zeolite synthesis time while carrying out synthesis on almost dry basis.

In order to observe the effect of temperature on the time of synthesis reaction, a higher temperature of $125°C$ was used for 2-6 h. It was found that the crystals started to appear after 2 h. Figure 4.20 (a) shows that after 5 h of synthesis time, the same level of crystallization was achieved which was observed after 6 h of synthesis at $100°C$. After 6 h, the entire silica particle was converted into zeolite, as shown in Figure 4.20 (b). These findings clearly show that the higher synthesis temperature supported the reduction in synthesis time. In order to observe further reduction in synthesis time, the synthesis was carried out at $150°C$ for 2-4 h. It was observed, as shown in Figure 4.21 (a), that the NaY zeolite crystals started to appear after 2 h of reaction, and the entire silica particle was transformed to zeolite in 4 h. The SEM image in Figure 4.21 (b) depicts that the crystal size was increased to 1-2 µm and the cluster size was around 10-12 µm, which holds true for the reason given for synthesis at $110°C$ using polypropylene bottles. The difference between the two observations is that at a synthesis reaction temperature of $150°C$ the crystal and cluster size was increased around two fold. This observation led to the idea that the higher synthesis temperature was suppressing the nucleation rate, and favoring the crystal growth rate.

Another observation was also made; that for a certain synthesis reaction temperature there was always a time period in the beginning of synthesis that did not show any crystal formation when images were taken by SEM. However, this inactive period was reduced to 4 h to 2 h.

(a)   (b)
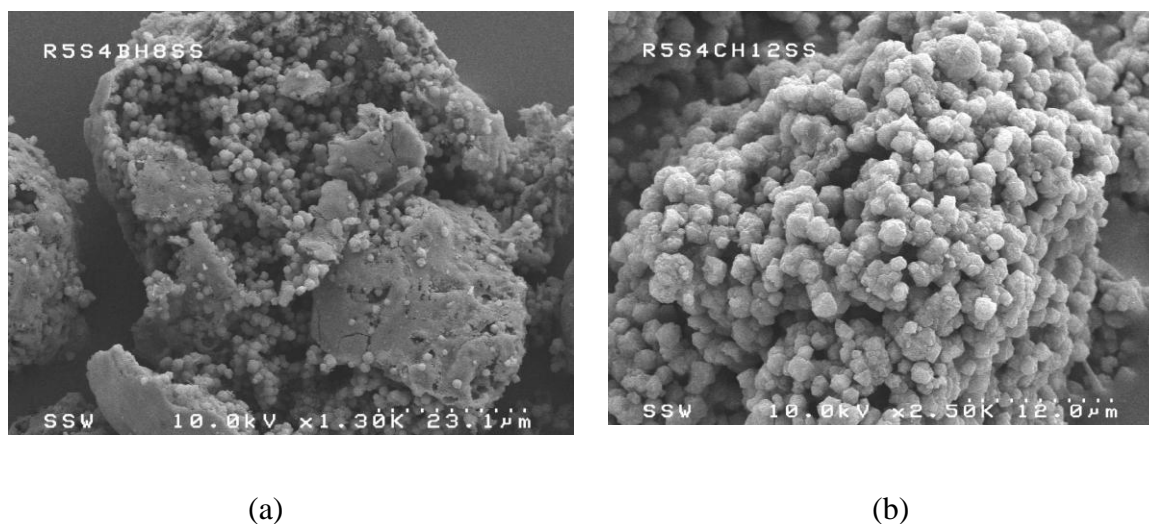
Figure 4.19: SEM images of NaY zeolite synthesized in stainless steel tubes at 100 ℃ : (a) partial conversion of silica particle to NaY zeolite in 8h (b) complete conversion of silica particle to NaY zeolite in 12 h

(a)   (b)
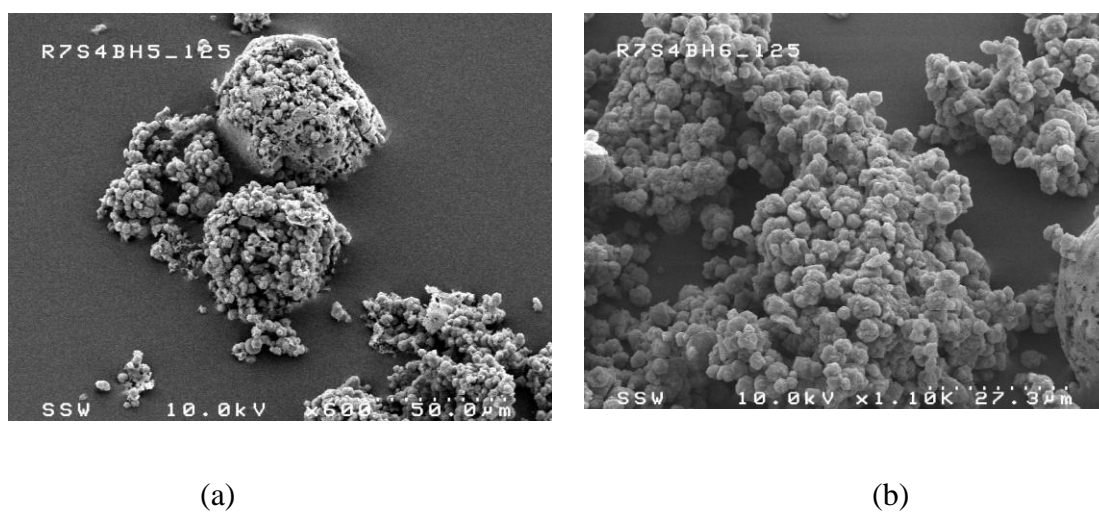
Figure 4.20: SEM images of NaY zeolite synthesized in stainless steel tubes at 125 ℃: (a) partial conversion of silica particle to NaY zeolite in 5 h (b) complete conversion of silica particle to NaY zeolite in 6 h

(a)   (b)
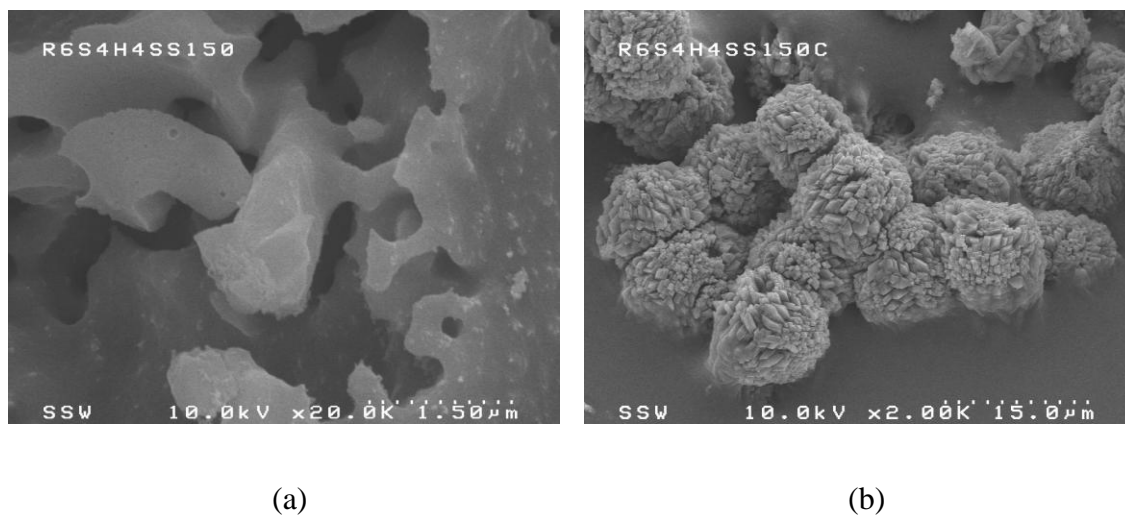
Figure 4.21: SEM images of NaY zeolite synthesized in stainless steel tubes at 150 ºC: partial conversion of silica particle in 2 h (b) complete conversion of silica particle in 4 h

Cizmek and coworkers (Cizmek *et al.* 1997) examined the time and temperature effects of gel ageing on the properties of silicalite-1 synthesized at $170°C$. They aged the gel at ambient temperature for 0 to 192 h, and at different temperatures from $20-80°C$ for 12-24 h. They did not find any crystals in the aged gel prior to the final heating step. Li and coworkers in a series of papers (Li *et al.* 1999; Li *et al.* 2000; Li *et al.* 2001) used a two-stage-varying-temperature synthesis procedure to investigate the nucleation period in colloidal TPA-silicalite synthesis. They applied single stage heating for the entire period of synthesis for both lower and higher temperatures in the range of $60-100°C$, and also the combination of the two temperatures with the lower temperature was set for a definite time. They found that for the single set of temperature at $60°C$ produced smaller size crystals, about $55nm$, but the synthesis time was around 400 h. On the other extreme end of $100°C$, the crystal size was around $95nm$ for the synthesis time of 50 h. This indicated that crystal number concentration was increased and the ultimate crystal size was decreased for the lower temperature synthesis. They also observed an induction period, which was larger (170 h) for lower temperature synthesis and smaller (<10 h) for higher temperature synthesis during which only nucleation took place and no crystal was observed. The authors pointed out two processes that could be taking place during induction/ageing period before any crystal was observed: one was the depolymerization of colloidal particle and the second was the formation of nuclei. These findings very closely match with our results, the only difference being the process of hydrothermal treatment. In our study, two phenomena are taking place simultaneously: ambient temperature ageing followed by high temperature ageing for the initial few hours of synthesis, and high temperature crystal growth. It can be seen that for lower temperature of $100°C$, the crystal size was <300nm. On the other hand at higher temperature of $150°C$, the crystal size was increased to 1-2 µm meaning that the nucleation process was being taken over by crystal growth. To further support our point of view, Cundy and coworkers (Cundy *et al.* 2003) investigated the effects of room temperature ageing followed by synthesis of colloidal silicalite at temperatures between $90°C$ and $175°C$ using both thermal and microwave heating. They found that the largest particle sizes were seen for the shortest ageing time and fastest heating rate. As the ageing time was increased or heating rate or final temperature was reduced, the particle size was

decreased. They also found that even after ageing the reaction mixture sol for about 200 days, no crystalline material was detected by conventional XRD methods in samples isolated from the unheated sol. They concluded that during ageing only proto-nuclei were accumulated and remained dormant under prevailing conditions, maturing into viable nuclei, and initiating crystal growth when exposed to crystallization temperature. These proto-nuclei may be taken as islands of order, as described earlier. This order continues to grow till reach the nucleation stage, which basically happens by the constant reversible T-O-T bond making and bond breaking equilibration reactions. This process was continued in our case during ageing and initial synthesis temperature when no crystals were observed.

We were interested to know whether the above phenomena further continued before 2 h or less, if the synthesis temperature was further increased. For this purpose, the temperature for synthesis was increased to $170°C$ for 15 min to 1 h. It was observed that the crystals started to appear in 15 min, but then started to disappear after 1 h of synthesis, as shown in Figure 4.22. In order to understand more about the new occurring of crystal disappearance either due to dissolution or due to some other reason, a further higher synthesis temperature of $180°C$ was tried for 15 min to 1 h. It was observed that crystals were formed during the first 15 min of synthesis, but they started to disappear after 45 min of synthesis, and then they were converted to analcime after 1 h of synthesis. The change in phase is depicted in Figure 4.23, and is also revealed in XRD result in Figure 4.25. This change in phase is due to the fact that NaY zeolite is a metastable state and is sensitive to synthesis temperature. A high synthesis temperature leads the NaY zeolite crystals towards a more stable state, which is analcime in this study. A further higher synthesis temperature of $200°C$ additionally supported the change in phase phenomena. It can be seen in Figure 4.24 that the crystals appeared in 15 min and were transformed into analcime in 45 min. These observations showed that higher synthesis temperature accelerates the phase transformation of NaY zeolite. The metastability of NaY zeolite may explained from Ostwald Law of Successive Transformations (also called as Rule of Stages) which states that an unstable system does not directly transforms into the most stable system.

(a)   (b)
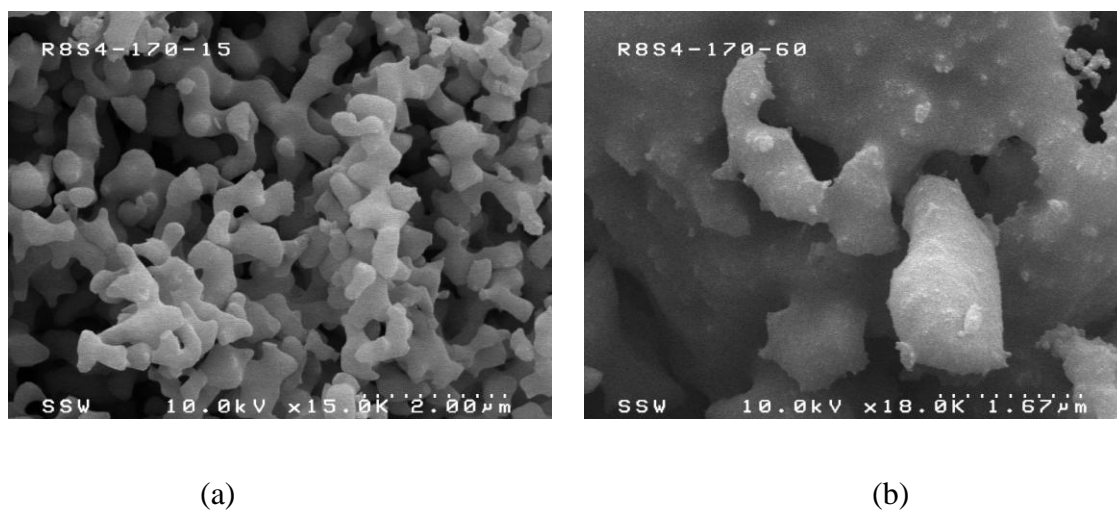
Figure 4.22: SEM images of NaY zeolite synthesized in stainless steel tubes at 170 ºC for (a) crystals in 15 min (b) transformation/disappearance of crystals in 1 h

(a)   (b)
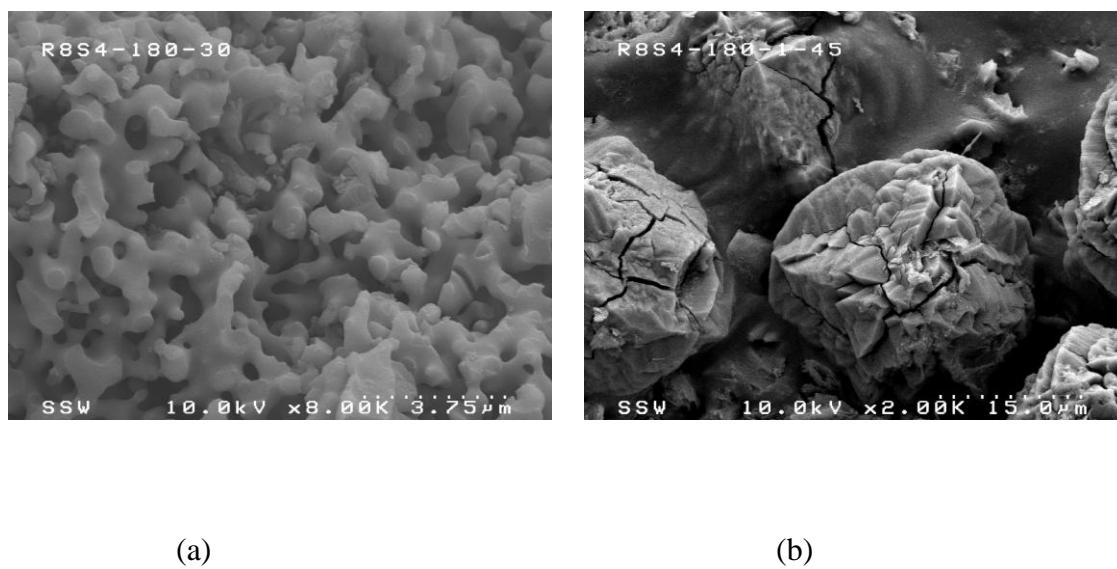
Figure 4.23: SEM images of NaY zeolite synthesized in stainless steel tubes at 180 ºC for (a) crystals in 30 min (b) transformation to analcime zeolite in 1 h

(a)   (b)
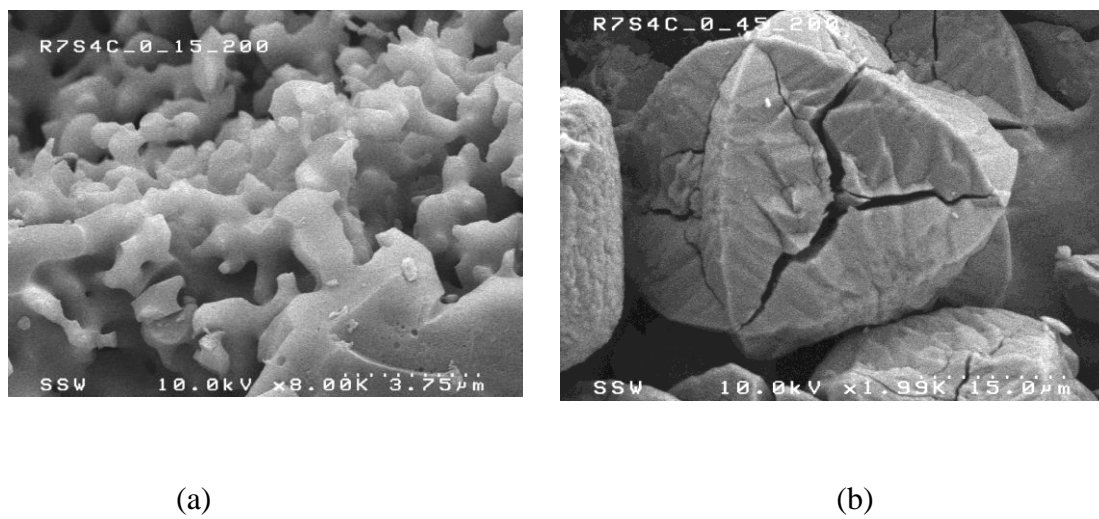
Figure 4.24: SEM images of NaY zeolite synthesized in stainless steel tubes at 200 ºC for (a) crystals in 15 min (b) transformation to analcime zeolite in 45 min
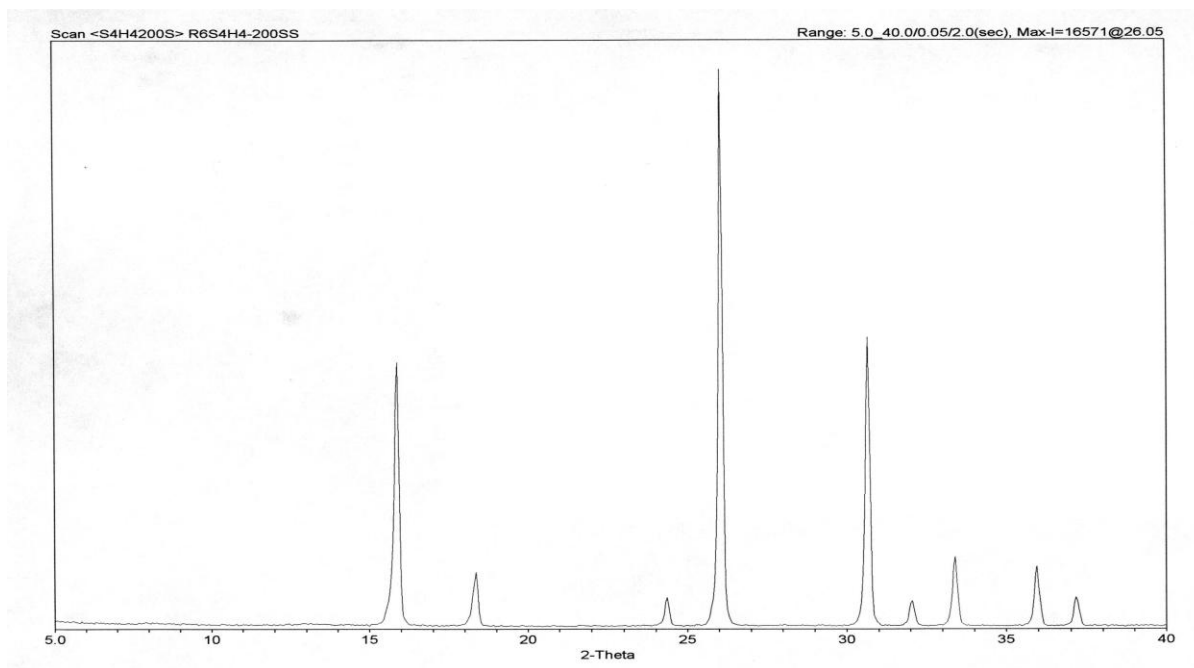
Figure 4.25:XRD pattern of analcime zeolite formation at $200°C$ using a ratio of 6.1

It initially undergoes a transient state whose formation from the original state is accompanied by a smallest loss of free energy (Mullin 2001; Ostwald 1897). In case of zeolite, a number of kinetic products may form from this transient state on the way to the final thermodynamically stable product. The transient state may be called precursors which are partially structured. These precursors or secondary amorphous phase (as described earlier in chapter 2) are essential for zeolite formation. The target zeolite product from these precursors may be a metastable product at certain reaction conditions and may not be a true thermodynamically stable product. The zeolite metastability mostly occurred in the phenomena of reaction over-run, in which the zeolite product is decomposed into a more dense phase under certain operating conditions. Aluminous zeolites such as A, X, or Y give way to sodalite, analcime, modenite, or cristobalite (Fajula *et al.* 1987), while siliceous zeolites may end up with dense silica phase, or quartz (Cundy and Cox 2005). Sometimes NaY zeolite may also decompose to zeolite P or ZSM-4 (Dwyer and Chu 1979; Perrotta *et al.* 1978) depending upon the operating conditions. For these reasons, temperatures beyond $170°C$ we ended up with more thermodynamically stable product of analcime. These findings set a temperature limitation to our method of dry synthesis. This study indicates that a rapid heat transfer and higher temperature reduce the synthesis time, but an optimum temperature is always needed in order to retain desired zeolite phase.

4.4.5 Effect of NaOH concentration on zeolite synthesis

The addition of NaOH into the silica particles through incipient wetness is the most important step to initiate the entire process of nucleation followed by crystal growth. As mentioned earlier in chapter 2, all the dissolved species gather around Na^+ cation after OH^- participation in bond-breaking and bond-making of oligomers of silica, which leads to a primary amorphous phase, then a secondary amorphous phase followed by nucleation and crystal growth. A 20 wt% concentration of NaOH was generally used for all the above-mentioned studies as this is the usual concentration that is reported in literature.

Using the optimum SiO_2/Al_2O_3 ratio and synthesis time, the effect of different concentrations of NaOH on the zeolite synthesis was studied. For this purpose, the

SiO_2 / Al_2O_3 ratio was kept constant at 6.1, and synthesis temperature and time were kept at $100°C$ and 16 h, respectively. Initially, a 15 wt% (Na_2O/Al_2O_3 = 1.53) of NaOH was used through incipient wetness. After 16 h of reaction at $100°C$, the results did not show any appreciable crystal growth. Figure 4.26 shows the SEM images of the silica particles. It can be seen that the major portion of silica particle remained amorphous while only a small portion was crystallized. However, when the NaOH concentration was increased to 20 wt% (Na_2O/Al_2O_3 = 2.05), the amorphous silica particles were transformed into crystals with cluster size in the range of 1-2 µm and crystallite size in the cluster was in the range of 100-200 nm, as shown in Figure 4.27. It can also be seen that the outer crust of the silica particle was intact though the particle was cracked opened to reveal crystals inside. Upon further increasing the NaOH concentration to 27 wt% (Na_2O/Al_2O_3 = 2.76), the silica particles were completely transformed into crystals. It should be noted that the cluster size was reduced to 500 nm-1µm and the crystallite size was in the range of 50-100 nm, as shown in Figure 4.28 through SEM images. The reduction in size may be due to higher nucleation rate as compared to crystal growth rate which was due to using higher concentration NaOH. This argument was further strengthened by using a further higher NaOH concentration of 32wt% (Na_2O/Al_2O_3 = 3.27). It can be distinctly seen in Figure 4.29 that the cluster size was further reduced to less than 500 nm with the crystallite size less than 50nm. The reduction in the crystal size with increase in NaOH concentration is summarized in Figure 4.30. These observations indicate that using higher concentration of NaOH could be helpful in reducing the crystal size. A further higher concentration of NaOH was not tried due to the reason that higher concentration of NaOH tends to dissolve the silica particles. In this study the concentration above 32 wt% started to dissolve the silica particles which severely reduced the shape and pore volume of the particles.

(a)   (b)
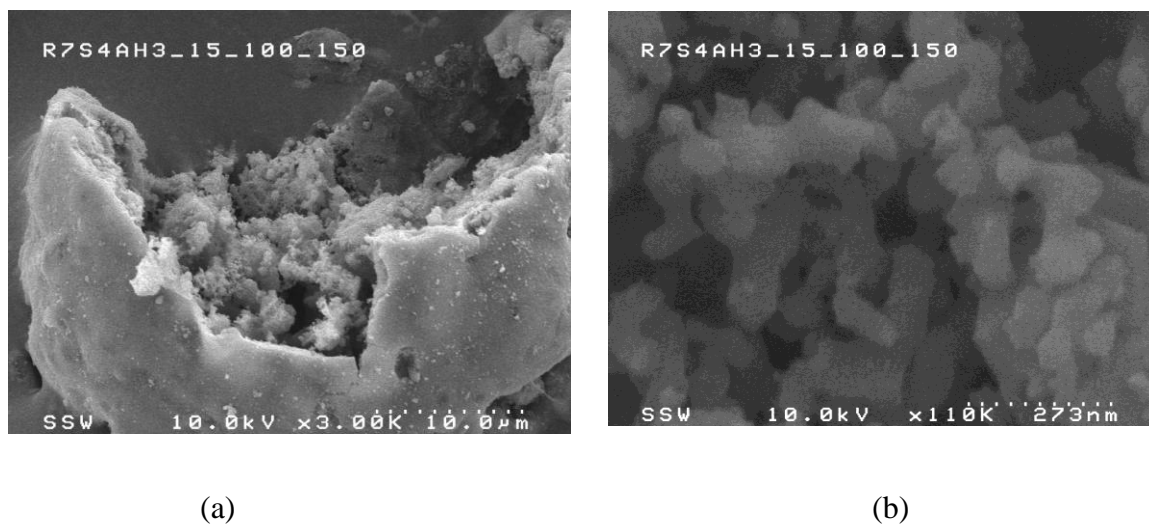
Figure 4.26: SEM images of NaY zeolite synthesis using NaOH = 15% (Batch Comp: 1.53Na$_2$O:Al$_2$O$_3$:6.09SiO$_2$:40.17H$_2$O) (a) silica particle mostly amorphous (b) zoomed view of silica particle with crystals

(a)   (b)
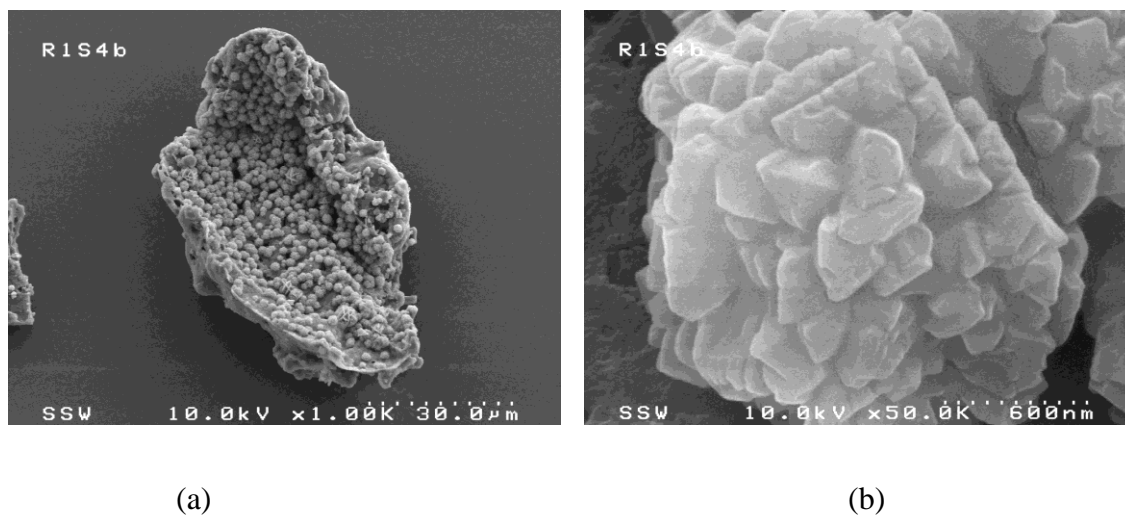
Figure 4.27: SEM images of NaY zeolite synthesis using NaOH = 20% (Batch Comp: 2.05Na$_2$O:Al$_2$O$_3$:6.09SiO$_2$:36.47H$_2$O) (a) silica particle embedded with NaY zeolite clusters (b) zoomed view of embedded cluster of NaY zeolite in silica particle
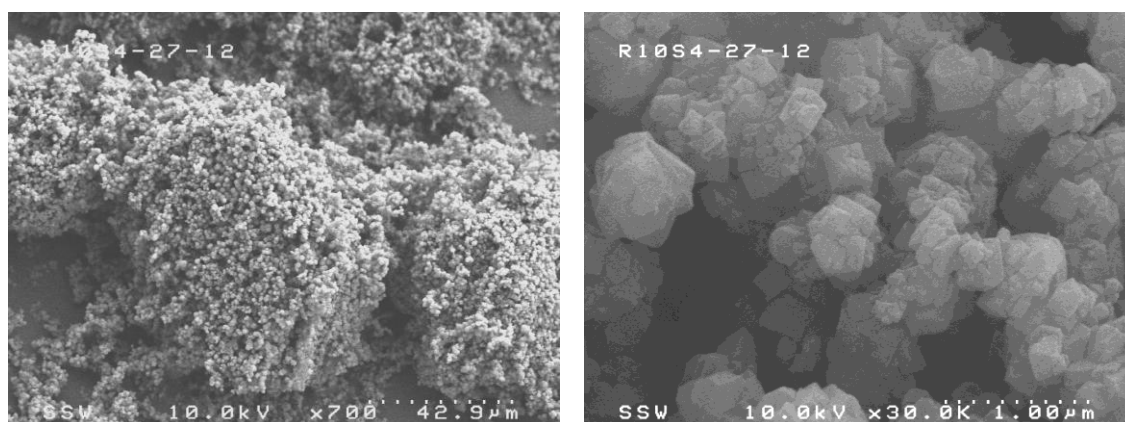
<center>(a)   (b)</center>

Figure 4.28: SEM images of NaY zeolite synthesis using NaOH = 27% (Batch
Comp: 2.76Na$_2$O:Al$_2$O$_3$:6.09SiO$_2$:35.94H$_2$O) (a) silica particle with embedded
NaY zeolite clusters (b) zoomed view of NaY zeolite clusters
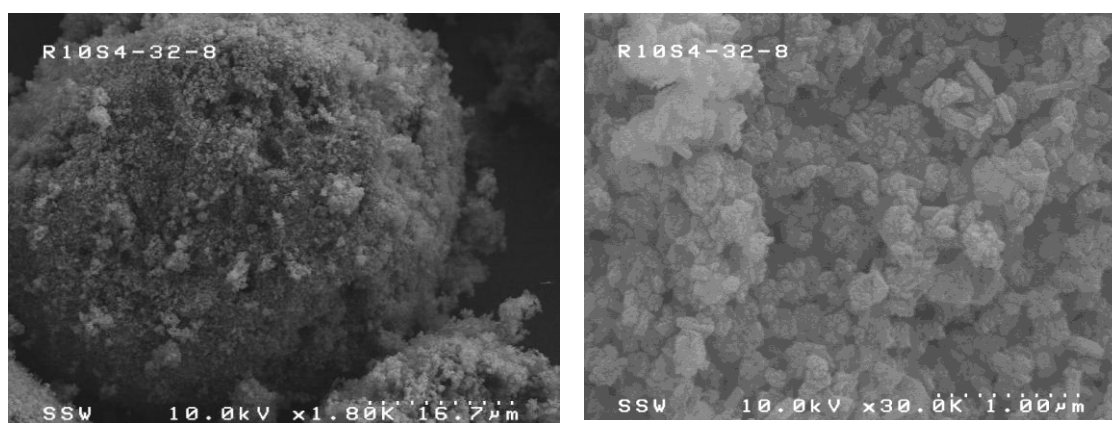
<center>(a)   (b)</center>

Figure 4.29: SEM images of NaY zeolite synthesis using NaOH = 32% (Batch Comp:
3.27Na$_2$O:Al$_2$O$_3$:6.09SiO$_2$:34.2H$_2$O) (a) silica particle with embedded NaY zeolite
(b) zoomed view NaY zeolite crystals
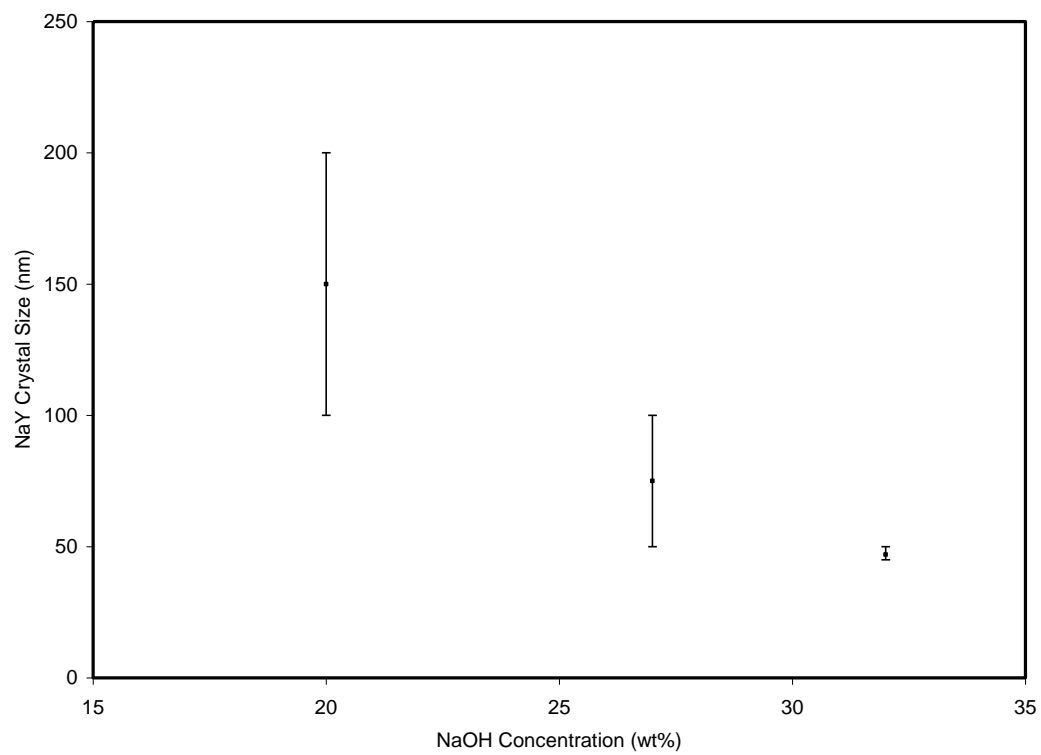
Figure 4.30: Effect of NaOH concentration on the crystal size of NaY zeolite

Our argument is supported by the work of Fegan and Lowe (Fegan and Lowe 1986) who studied the behavior of silicalite synthesis system by changing NaOH concentration. They conducted the study at $95°C$ using different alkalinity in the range of mol 0.25 to mol 6.5. They found that 100% crystallinity was obtained in a shorter period of time (from 8 to less than 4 days) as the alkalinity was increased from mol 2 to 5. This finding also supports our results as the conversion of silica particle increases by increasing NaOH concentration. Their SEM results also showed that the size of the zeolite crystal was decreased as the alkalinity was increased, which corresponds to our findings. They also converged to the argument that increasing the alkalinity increased the nucleation rate which formed smaller crystal size. However, they made another observation that for a very high alkalinity mol 6.5, they were expecting further reduction in crystal size but instead they found an increase in crystal size. They concluded that further increasing the alkalinity caused a reduction or disappearance of solid gel phase resulting in production fewer nuclei and hence larger crystals. The effect of very high alkalinity to reduce the nucleation and increase the crystal size was not observed in our study. This was because when the NaOH concentration higher than 32 wt% was applied the silica particle completely dissolved and lost its shape and integrity.

The above findings of Fegan and Lowe (Fegan and Lowe 1986) were further scrutinized by Cundy and Cox (Cundy and Cox 2005) who took their data and further refined it. They obtained a relationship between nucleation and crystal growth by increasing the alkalinity. According to this relationship, both nucleation and crystal growth rates vary as a function of the alkalinity of the reaction mixture, and reached a maximum value. However, the maxima for the crystal growth and nucleation did not coincide. The crystal growth reached its maximum while alkalinity was still on the lower side (i.e. $mol \approx 1.5$) and then continued to decrease with increasing alkalinity. Nucleation, however, continued to increase till it reached its maximum at alkalinity around $mol \approx 4.5$ indicating that the nucleation was still taking place at a higher base level. They rationalized this scenario that the nucleation was considered in terms of a collision mechanism in which the soluble species were coming together and separating in a dynamic way. In this perspective, the nucleation rate was proportional to the alkalinity

and flux of the soluble species which was generated from the solid gel phase. Therefore at low alkalinity, the deficit of OH^- may lead to reduced nucleation and growth, while at maximum a balance may be maintained between the competing addition and dissolution reactions. However, both nucleation and crystal growth start to fall down as the dissolution of the reaction species reaches its limit at the highest value of alkalinity. For this reason we observed that the silica particle was completely dissolved for NaOH concentration greater than 32 wt%.

4.5 CONCLUSIONS

It can be seen that the reactant composition, especially, the SiO_2/Al_2O_3 ratio plays a vital role in synthesis reaction. A ratio higher than 6.6 does not lead to desired synthesis reaction in a set interval of time. Conversion may start at much longer synthesis time. This was the reason that with a SiO_2/Al_2O_3 ratio lower than 6.6 complete crystallization occurred when synthesis time was increased from 16 h to 24 h. Therefore an optimum batch composition was obtained as $3.27Na_2O : Al_2O_3 : 6.09SiO_2 : 34.2H_2O$. Ageing for 1 h helps in internal rearrangement of precursors within the silica particles before the reaction. However, a longer ageing time leads to little improvement in the synthesis reaction. Increased synthesis temperature reduces the synthesis time but at the same time the crystal size also increases. Use of a stainless steel tubular reactor reduces the synthesis time even at a lower temperature of $100°C$, as compared to polypropylene bottles. Higher synthesis temperature in stainless steel tubular reactor not only reduces the synthesis time but also affects the crystal size. Also, it may cause changes in the phase composition from NaY zeolite to analcime when operating above $170°C$. An optimal synthesis temperature of $170°C$ may be suitable within 15 minute of reaction time without transforming to an undesirable phase. The technique of solid phase transformation may be more suitable for fast synthesis as compared with liquid phase transformation. The various concentrations of NaOH can be helpful in controlling the size of the crystals. For nano sized crystals smaller than $50nm$, a concentration greater than 30wt% of NaOH may be more suitable.

4.6 REFERENCES

Althoff, R., Unger K., Schuth, F. "Is the Formation of a Zeolite From a Dry Powder Via a Gas Phase Transport Process Possible?" *Microporous Mater.*, 1994, *2* (6), 557-562.

Arafat, A., Jansen, J. C., Ebaid A.R., van Bekkum, H. "Microwave Preparation of Zeolite Y and ZSM 5." *Zeolites*, 1993, *13* (3), 162-165.

Arnold, A., Steuernagel, S., Hunger, M., Weitkamp, J. "Insight into the dry-gel synthesis of gallium-rich zeolite [Ga]Beta." *Microporous Mesoporous Mater.*, 2003, *62* (1-2), 97-106.

Barrer, R. M. *Hydrothermal Chemistry of Zeolites*. New York: Academic Press, 1982.

Bibby, D. M., Dale, M. P. "Synthesis of Silica-Sodalite From Non-Aqueous Systems." *Nature*, 1985, *317* (6033), 157-158.

Breck, D. W. "Crystalline molecular sieves." *J.Chem.Educ.*, 1964, *41* (12), 678-689.

Breck, W. D. *Zeolite Molecular Sieves*. New York: Wiley, 1974.

Breck, W. D., Flanigen, E. M. "Synthesis and Properties of Union Carbide Zeolites L, X, and Y." *Molcular Sieves Pap.Conf.*, 1967, 47-61.

Camblor, M. A., Corma, A., Martinez, A., Mocholi F.A., Perez Pariente, J. "Benefits in Activity and Selectivity of Small Y Zeolite Crystallites Stabilized by a Higher Silicon-to-Aluminium Ratio by Synthesis." *Appl.Catal.*, 1989, *55* (1), 65-74.

Choy, J. H., Lee, S. R., Han, Y. S., Park, M., Park, G. S. "Solid-solid transformation mechanism for nanocrystalline sodalite from pillared clay." *Chem.Commun.(Cambridge, U.K.)*, 2003, (15), 1922-1923.

Cizmek, A., Subotic, B., Kralj, D., Babic-Ivancic, V., Tonejc, A. "The influence of gel properties on the kinetics of crystallization and particulate properties of MFI-type zeolites. I. The influence of time and temperature of gel ageing on the particulate properties of silicalite-1 microcrystals." *Microporous Mater.*, 1997, *12* (4-6), 267-280.

Cook, J. D., Thompson, R. W. "Modeling the effect of gel aging." *Zeolites*, 1988, *8* (4), 322-326.

Crea, F., Aiello, R., Nastro, A., Nagy, J. B. "Synthesis of ZSM-5 Zeolite from very Dense Systems: Formation of Pelleted ZSM-5 Zeolite from (Na, Li, TPA, Si, Al) Hydrogels." *Zeolites*, 1991, *11* (5), 521-527.

Cundy, C. S. "Microwave Techniques in the Synthesis and Modification of Zeolite Catalysts. A Review." *Collect.Czech.Chem.Commun.*, 1998, *63* (11), 1699-1723.

Cundy, C. S., Henty, M. S., Plaisted, R. J. "Zeolite Synthesis Using a Semicontinuous Reactor. Part 1. Controlled Nucleation and Growth of ZSM-5 Crystals Having Well-Defined Morphologies." *Zeolites*, 1995a, *15* (4), 353-372.

Cundy, C. S., Henty, M. S., Plaisted, R. J. "Zeolites Synthesis Using a Semicontinuous Reactor. 2. Synthesis at High Nucleation Rates." *Zeolites*, 1995b, *15* (2), 400-407.

Cundy, C. S., and Cox, P. A. "The hydrothermal synthesis of zeolites: Precursors, intermediates and reaction mechanism." *Microporous Mesoporous Mater.*, 2005, *82* (1-2), 1-78.

Cundy, C. S., Forrest, J. O., Plaisted, R. J. "Some observations on the preparation and properties of colloidal silicalites. Part I: synthesis of colloidal silicalite-1 and titanosilicalite-1 (TS-1)." *Microporous Mesoporous Mater.*, 2003, *66* (2-3), 143-156.

Davey, R. J., Ruddick, A. J., Guy, P. D., Mitchell, B., Maginn, S. J., Polywka, L. A. "The IV-III polymorphic phase transition in ammonium nitrate: a unique example of solvent mediation." *J.Phys.D: Appl.Phys.*, 1991, *24* (2), 176-185.

Davey, R. J., Guy, P. D., Mitchell, B., Ruddick, A. J., Black, S. N. "The growth of phase IV ammonium nitrate crystals and their transformation to the phase III structure." *J.Chem.Soc., Faraday Trans.1*, 1989, *85* (7), 1795-1800.

Derouane, E. G., Detremmerie, S., Gabelica, Z., Blom, N. "Synthesis and Characterization of ZSM-5 Type Zeolites. I. Physicochemical Properties of Precursors and Intermediates." *Appl.Catal.*, 1981, *1* (3-4), 201-224.

Dong, J., Dou, T., Zhao, X., Gao, L. "Synthesis of Membranes of Zeolites ZSM-5 and ZSM-35 by the Vapor Phase Method." *J.Chem.Soc., Chem.Commun.*, 1992, (15), 1056-1058.

Dong, W.-Y, Sun, Y.-J., He, H.-Y., Long, Y.-C. "Synthesis and Structural Characterization of B-Al-ZSM-5 Zeolite From Boron-Silicon Porous Glass in the Vapor Phase." *Microporous Mesoporous Mater.*, 1999, *32* (1-2), 93-100.

Dwyer, F. G., Chu, P. "ZSM-4 crystallization via faujasite metamorphosis." *J.Catal.*, 1979, *59* (2), 263-271.

Fajula, F., Vera-Pacheco, M., Figueras, F. "Synthesis of zeolite omega. Influence of the temperature and the reagents on the crystallization kinetics." *Zeolites*, 1987, *7* (3), 203-208.

Fan, W., Li, R., Fan, B., Ma, J., Cao, J. "Effects of Introduction of Different Alkali Metal Halides on Crystallization and Characteristics of ZSM-48 in a Solid Reaction Mixture System Effects of Alkali Metal Chlorides[1]." *Appl.Catal.A:General*, 1996, *143* (2), 299-308.

Fegan, S. G., Lowe, B. M. "Effect of alkalinity on the crystallization of silicalite-1 precursors." *J.Chem.Soc., Faraday Trans.1*, 1986, *82* (3), 785-99, 2.

Franklin, K. R., Lowe, B. M. "Preparation and properties of gel particle silicalite." *Zeolites*, 1987, *7* (2), 135-142.

Freund, E. F. "Mechanism of the crystallization of zeolite X." *J.Cryst.Growth*, 1976, *34* (1), 11-23.

Ginter, D. M., Bell, A. T., Radke, C. J. "The Effects of Gel Aging on the Synthesis of NaY Zeolite From Colloidal Silica." *Zeolites*, 1992a, *12* (6), 742-749.

Ginter, D. M., Went, G. T., Bell, A. T., Radke, C. J. "A physicochemical study of the aging of colloidal silica gels used in zeolite Y synthesis." *Zeolites*, 1992b, *12* (6), 733-741.

Gora, L., Thompson, R. W. "Controlled addition of aged mother liquor to zeolite NaA synthesis solutions." *Zeolites*, 1997, *18* (2/3), 132-141.

Hari Prasad Rao, P. R., Ueyama, K., Matsukata, M. "Crystallization of High Silica BEA by Dry Gel Conversion." *Appl.Catal.A*, 1998, *166* (1), 97-103.

Huo, Q., Feng, S., Xu, R. "First Syntheses of Pentasil-type Silica Zeolites from Non-aqueous Systems." *J.Chem.Soc., Chem.Commun.*, 1988, (22), 1486-1487.

Inada, M., Tsujimoto, H., Eguchi, Y., Enomoto, N., Hojo, J. "Microwave-assisted zeolite synthesis from coal fly ash in hydrothermal process." *Fuel*, 2005, *84* (12-13), 1482-1486.

Jansen, J. C., Arafat, A., Barakat, A. K., and van Bekkum, H. "Microwave techniques in zeolite synthesis.", Synthesis of Microporous Materials: Molecular Sieves. (1), 507-521. 1992. New York, Van Nostrand Reinhold.

Kacirek, H., Crystalline zeolitic aluminosilicates. (Sued-Chemie A.-G., Fed. Rep. Ger. 84-3402842(3402842), 19. 1985. DE. 1-27-1984.

Kerr, G. T. "Chemistry of crystalline aluminosilicates. I. Factors affecting the formation of zeolite A." *J.Phys.Chem.*, 1966, *70* (4), 1047-1050.

Kerr, G. T. "Crystallization of sodium zeolite A." *Zeolites*, 1989, *9* (5), 451.

Kim, D. S., Park S.-E., Kang, S. O. "Microwave Synthesis of Micro-Mesoporous Composite Material." *Stud.Surf.Sci.Catal.*, 2000, *129* 107-116.

Kim, M. H., Li, H. X., Davis, M. E. "Synthesis of Zeolites by Water-Organic Vapor-Phase Transport." *Microporous Mater.*, 1993, *1* (3), 191-200.

Lee, S. R., Han, Y. S., Park, M., Park, G. S., Choy, J. H. "Nanocrystalline Sodalite from Al2O3 Pillared Clay by Solid-Solid Transformation." *Chem.Mater.*, 2003, *15* (25), 4841-4845.

Li, Q., Creaser, D., Sterte, J. "The nucleation period for TPA-silicalite-1 crystallization determined by a two-stage varying-temperature synthesis." *J.Microporous Mesoporous Mater*, 1999, *31* (1-2), 141-150.

Li, Q., Creaser, D., Sterte, J. "An Investigation of the Nucleation/Crystallization Kinetics of Nanosized Colloidal Faujasite Zeolites." *Chem.Mater.*, 2002, *14* (3), 1319-1324.

Li, Q., Mihailova, B., Creaser, D., Sterte, J. "The nucleation period for crystallization of colloidal TPA-silicalite-1 with varying silica source." *Microporous Mesoporous Mater.*, 2000, *40* (1-3), 53-62.

Li, Q., Mihailova, B., Creaser, D., Sterte, J. "Aging effects on the nucleation and crystallization kinetics of colloidal TPA-silicalite-1." *Microporous Mesoporous Mater.*, 2001, *43* (1), 51-59.

Matsukata, M., Kikuchi, E. "Zeolitic Membranes: Synthesis, Properties, and Prospects." *Bull.Chem.Soc.Jpn.*, 1997, *70* (10), 2341-2356.

Matsukata, M., Nishiyama, N., Ueyama, K. "Synthesis of Zeolites Under Vapor Atmosphere. Effect of Synthetic Conditions on Zeolite Structure." *Microporous Mater.*, 1993, *1* (3), 219-222.

Matsukata, M., Nishiyama, N., Ueyama, K. "Crystallization of FER and MFI Zeolites by a Vapor-Phase Transport Method." *Microporous Mater.*, 1996, *7* (2-3), 109-117.

Matsukata, M., Ogura, M., Osaki, T., Hari Prasad Rao, P. R., Nomura, M., Kikuchi, E. "Conversion of Dry Gel to Microporous Crystals in Gas Phase." *Topics in Catalysis*, 1999, *9* (1-2), 77-92.

Matsukata, M., Osaki, T., Ogura, M., Kikuchi, E. "Crystallization behavior of zeolite beta during steam-assisted crystallization of dry gel." *Microporous Mesoporous Mater.*, 2002, *56* (1), 1-10.

Mintova, S., Valtchev, V., Onfroy, T., Marichal, C., Knoezinger, H., Bein, T. "Variation of the Si/Al ratio in nanosized zeolite Beta crystals." *Microporous Mesoporous Mater.*, 2006, *90* (1-3), 237-245.

Moretti, E., Leofanti, G., Padovan, M., Solari, M., De Alberti, G., and Gatti, F. "A new route to ZSM-5 zeolite: crystal properties and catalytic activity evolution during the synthesis." *Int. Congr. Catal., [Proc.]*, 8th (1985), 4, IV713-IV723.

Mostowicz, R., and Sand, L. B. "Morphological study of ZSM-5 grown in the 12Na2O/4.5(TPA)2O system." *Zeolites*, 1983, *3* (3), 219-225.

Mullin, J. W. *Crystallization*. Butterworth-Heinemann Ltd., Oxford, 1993.

Murrell, L. L., Overbeek, R. A., Chang, Y.-F., Puil, N. V. D., and Yeh, C. Y. "Method for Making Molecular Sieves and Novel Molecular Sieve Compositions." (6,004,527). 1999. USA.

Naik, S. P., Chiang, A. S. T., Thompson, R. W. "Synthesis of Zeolitic Mesoporous Materials by Dry Gel Conversion under Controlled Humidity." *J.Phys.Chem.B*, 2003, *107* (29), 7006-7014.

Nicolas, S., Massiani, P., Vera Pacheco, M., Fajula, F., Figueras, F. "New synthesis route to zeolite omega." *Stud.Surf.Sci.Catal.*, 1988, *37* (Innovation Zeolite Mater. Sci.), 115-122.

Ostwald, W. "The formation and changes of solids." *Zeit.physikal.Chem.*, 1897, *22* 289-330.

Padovan, M., Leofanti, G., Solari, M., Moretti, E. "Studies on the ZSM-5 zeolite formation." *Zeolites*, 1984, *4* (3), 295-299.

Park, S.-E., Kim, D. S., Chang, J. S., and Kim, J. M. "Continuous Process and Apparatus for Preparing Inorganic Materials Employing Microwave." (US Patent 2001054549). 2001. USA.

Patel, A. K., Sand, L. B. "Mechanisms of synthesizing pseudomorphic zeolite particulates using high concentration gradients." *ACS Symp.Ser.*, 1977, *40* (Mol. Sieves-2, Int. Conf., 4th), 207-218.

Perrotta, A. J., Kibby, C., Mitchell, B. R., Tucci, E. R. "The synthesis, characterization, and catalytic activity of omega and ZSM-4 zeolites." *J.Catal.*, 1978, *55* (2), 240-249.

Polak, F., Cichocki, A. "Mechanism of formation of X and Y zeolites." *Advan.Chem.Ser.*, 1973, *121* (Mol. Sieves, Int. Conf., 3rd), 209-216.

Rajagopalan, K., Peters, A. W., Edwards, G. C. "Influence of Zeolite Particle Size on Selectivity During Fluid Catalytic Cracking." *Appl.Catal.*, 1986, *23* (1), 69-80.

Rollmann, L. D. and Valyocsik, E. W. Continuous-Stream Upflow Zeolite Crystallization Apparatus. (US Patent 4,374,093). 1983.

Salou, M., Kiyozumi, Y., Mizukami, F., Nair, P., Maeda, K., Niwa, S. "Influence of solid-state transformation time on the nucleation and growth of silicalite 1 prepared from layered silicate." *J.Mater.Chem.*, 1998, *8* (9), 2125-2132.

Schmidt, I., Madsen, C., Jacobsen, C. J. H. "Confined space synthesis. A Novel Route to Nanosized Zeolites." *Inorg.Chem.*, 2000, *39* (11), 2279-2283.

Schoeman, B. J., Sterte, J., Otterstedt, J.-E. "Colloidal Zeolite Suspensions." *Zeolites*, 1994, *14* (2), 110-116.

Serrano, D. P., Uguina, M. A., Ovejero, G., Van Grieken, R., Camacho, M. "Crystallization of TS-1 and TS-2 zeolites with contribution of solid-solid transformations." *Chem.Commun.(Cambridge)*, 1996, (10), 1097-1098.

Slangen, P. M., Jansen, J. C., van Bekkum, H. "Induction Heating: A Novel Tool for Zeolite Synthesis." *Zeolites*, 1997a, *18* (1), 63-66.

Slangen, P. M., Jansen, J. C., van Bekkum, H. "The effect of ageing on the microwave synthesis of zeolite NaA." *Microporous Mater.*, 1997b, *9* (5,6), 259-265.

Szostak, R. *Molecular Sieves*. London. UK: Blackie Academic & Professional, 1998.

Valyocsik, E. W. "Apparatus for a continuous down-flow zeolite production." (US Patent 4,368,174). 1983.

Vaughan, D. E. W. "A zeolite of the L type using organic templates." (Exxon Research and Engineering Co., USA. 84-307759(142348), 26. EP. 11-9-1984.

Wang, X. and Jacobson, A. J. "Synthesis of Large ZSM-5 Crystals Under High Pressure.", 2001, *Mat.Res.Soc.Symp.*, 658, GG8.1.1.-GG8.1.6.

Xu, H. H., Shah, D. B., Talu, O. "Synthesis of ZSM-5 Films at Elevated Gravity." *Zeolites*, 1997, *19* (2-3), 114-122.

Xu, W., Dong, J., Li, J., Li, J., Wu, F. "A Novel Method for the Preparation of Zeolite ZSM-5." *J.Chem.Soc., Chem.Commun.*, 1990, (10), 755-756.

Xu, W., Li, J., Li, W., Zhang, H., Liang, B. "Nonaqueous Synthesis of ZSM-35 and ZSM-5." *Zeolites*, 1989, *9* (6), 468-473.

Yamazaki, S., Tsutsumi, K. "Synthesis of A-type zeolite membrane using a plate heater and its formation mechanism." *Microporous Mesoporous Mater.*, 2000, *37* (1-2), 67-80.

Yan, Y., Davis, M. E., Gavalas, G. R. "Preparation of Zeolite ZSM-5 Membranes by In-Situ Crystallization on Porous α-Al$_2$O$_3$." *Ind.Eng.Chem.Res.*, 1995, *34* (5), 1652-1661.

Zhao, J. P., Cundy, C. S., Plaisted, R. J., and Dwyer, J. "The potential of microwave heating in [Al]ZSM-5 synthesis.", *Proc. Int. Conf. Zeolites*, 12th, Baltimore, July 5-10, 1998 (1999), 3, 1591-1594.

Zhdanov, S. P. and Samulevich, N. N. "Nucleation and crystal growth of zeolites in crystallizing aluminosilicate gels.", *Proc. Int. Conf. Zeolites*, 5th (1980), 75-84.

CHAPTER 5: A NOVEL REACTOR SYSTEM FOR THE RAPID PRODUCTION OF NaY ZEOLITE WITHIN PRESHAPED SILICA PARTICLES

5.1 INTRODUCTION

The growing applications of synthetic zeolites make them an integral part of today's industrial world since its laboratory synthesis in 1942. The zeolites were originally recognized as a new type of minerals in 1756 by a Swedish minerlogist A. Cronstedt. He named this mineral "zeolite" (Greek word: meaning boiling stone) as it seemed to boil at high temperature due to high water content (Othmer 1984). Since then, many types were found naturally like, chabazite, erionite, faujasite, mordenite, etc. (Serrano and Grieken 2001). It was found that the zeolites were composed of crystalline aluminosilicates and possessed properties of adsorption, reaction, and ion-exchange. Since 1942 many types of industrially important zeolites were commercially produced. So far more than 150 synthetic zeolites have been reported. Currently, however, a few are of commercial importance, like, type A, X, Y, Z, L, ZSM-5, etc. (Corma and Wojciechowski 1985), but this number is growing fast as more avenues in industrial applications are opening. In principle, zeolites are prepared from alumina silicate gels, which in turn are prepared from aqueous solutions of sodium aluminate, sodium silicate, and sodium hydroxide. The process employed is called hydrogel process.

One of the major applications of the zeolites is in the oil industry, especially in the process of catalytic cracking, where Y zeolite is frequently used in fluid catalytic cracking (FCC) process (Breck and Flanigen 1967; Breck 1974). Another potential area, among several other applications, is the desulfurization of gasoline (Babich and Moulijn 2003; de Lasa *et al.* 2006; Gong *et al.* 2009; Hernandez-Maldonado *et al.* 2005; Jayaraman *et al.* 2006; Jiao *et al.* 2006; King and Li 2006; Kong *et al.* 2006; Ma *et al.* 2002; Ma *et al.* 2005; Reut and Prakash 2006; Shan *et al.* 2002; Yang *et al.* 2003). The large-scale production of zeolites currently uses batch process and the synthesis procedure takes days to obtain a finished product. A general method to improve the zeolite synthesis is to test the sensitivity of the reaction to different synthesis parameters

and to optimize the procedure. As the operating conditions are varied the synthesis reaction may appear to occur faster or slower as it progresses towards or away from the optimum conditions depending upon the criteria applied and the starting point. A large number of publications have been concentrated on developing such strategies. Several researchers have devoted their efforts to improve the batch process and tried to make a step towards continuous process (Rollmann and Valyocsik 1983).   Many zeolite synthesis operating variables have been identified and attempted to improve the quality of zeolites and reduce the synthesis time. These parameters include; microwave heating (Arafat *et al.* 1993; Cundy 1998; Jansen *et al.* 1992; Kim *et al.* 2000; Park *et al.* 2001; Slangen *et al.* 1997), controlling nucleation and crystal growth rates (Cundy *et al.* 1995b; Cundy *et al.* 1995a); process variables such as: temperature, pressure, concentration, composition, gravity, etc. (Wang and Jacobson 2001; Xu *et al.* 1997).

Among the several methods tried and tested for rapid production of zeolite, the microwave dielectric heating technique has shown a significant improvement in a variety of chemical syntheses (Elander *et al.* 2000; Gabriel *et al.* 1998; Loupy 2002; Mingos and Baghurst 1991; Strauss 1999). A review has discussed the benefits of zeolite synthesis using microwave technique (Cundy 1998). In conventional thermal heating, the reaction is generally influenced by the rate of heat transfer through the walls of the containing vessel, which results in a thermal gradient across the reaction volume. These limitations are generally modified when a different form of energy is applied. Microwaves are electromagnetic waves with wavelengths in the range of 1 mm to 1 m, with frequencies between 300 GHz to 0.3 GHz, respectively. Figure 5.1 shows an electromagnetic spectrum of all types of waves. Since the electromagnetic waves travel at the speed of light, therefore, the transfer of energy from the source to the material to be heated overcomes all the energy transport limitations offered by conventional thermal heating (Schiffmann 2007).
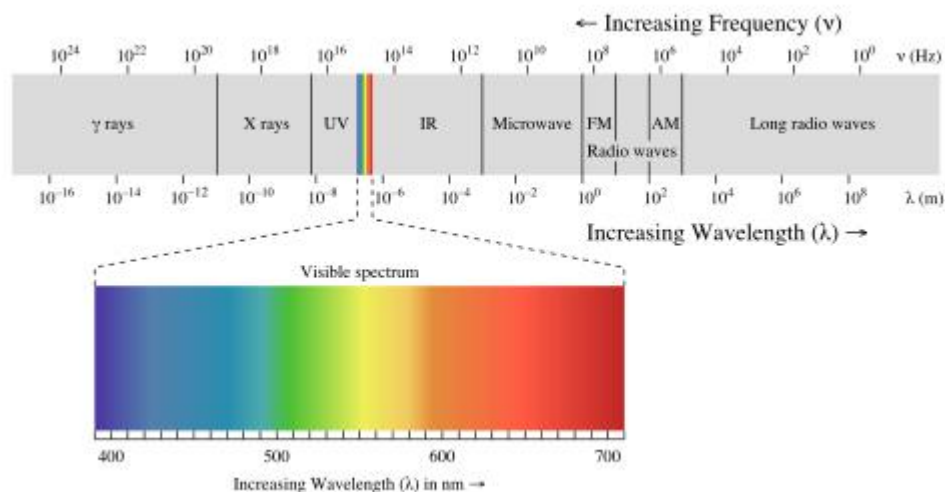
Figure 5.1: Electromagnetic Spectrum

The dielectrics or microwaves are not a form of heat but rather forms of energy which is transformed into heat by interaction with materials (Schiffmann 2007). There are many mechanisms to convert the energy into heat, but primarily important mechanisms in dielectric heating phenomena are ionic conduction and dipolar rotation of molecules. In ionic conduction, the ions, which are charged units, are accelerated by electrical fields. In a basic solution, e.g. NaOH solution as in the case of zeolite synthesis, the sodium and hydroxyl ions tend to move in opposite direction with respect to their own polarity when exposed to electromagnetic field. In doing so, they tend to collide with unionized water molecules, transferring kinetic energy and causing water molecules to accelerate which in turn collide with other water molecules in a billiard ball way, and when the polarity of the electromagnetic field changes, the ions accelerate in the opposite direction. Since this phenomenon happens many million times per second, therefore, a large number of collisions and transfer of energy take place. In short, the electromagnetic energy is transformed into disordered kinetic energy, which appears as an increase in the heat of the system. On the other hand, the polar molecules in a material, e.g. water in case of zeolite synthesis, tend to rotate as they have electrical dipole movement. The electrical dipole movement in a polar molecule keeps it aligned in an electromagnetic field. If the electromagnetic field oscillates, as in the case of

electromagnetic wave, the molecules also start to rotate in order to keep themselves aligned with the electromagnetic field. As the electromagnetic field alternates, the polar molecules also reverse their direction. The rotating molecules collide, push or pull other molecules through electrical and gravitational forces. This perturbation of molecules help in distributing the energy to the other molecules and atoms in the material hence causes increase in kinetic energy of material, which in turn increase the temperature of the material. The microwave dielectric effect can be seen in a home microwave oven (2.45 GHz) which operates more efficiently on liquid water as compared to fats, sugars, or frozen water (Schiffmann 2007; Wikipedia 2010a).

The apparent advantage of microwave heating is the shortening of reaction time, which is found in all the cases of zeolite synthesis using microwave technique. The factors that reduced the synthesis time were analyzed by Cundy and coworkers (Cundy 1998; Cundy and Zhao 1998) in terms of thermal lag, induction period, and crystal growth. They found that the major acceleration was caused in thermal lag and induction period due to the rapid heating rate to the working temperature. However, under pseudo-steady state, they did not find any significant difference in the linear crystal growth between the two techniques of conventional thermal heating and microwave heating (Cundy *et al.* 2003). Another advantage of microwave heating may be the selectivity of the product, where the components of the system are sensitive to microwave energy or heating rate. Such situation has been observed in case of heterogeneous reaction mixture containing components of different dielectric properties, or difference in rates of nucleation and growth of competing phases. One such effect was observed by Arafat and coworkers (Arafat *et al.* 1993) who demonstrated the phase selectivity in zeolite Y synthesis by suppressing the undesired side-products by using microwave heating. Microwave heating may thus be considered an alternative to conventional thermal heating methods in zeolite synthesis. It is, however, generally effective for solution based system. For solution based systems, a significant reduction in synthesis time is generally observed and also a possibility of phase purity. However, no evidence of a thermal microwave effect is observed (Cundy and Cox 2005).

Thermal radiation, on the other hand, may be a good substitute for conventional thermal and microwave heating, especially when the zeolite synthesis system is based on a dry synthesis process. The electromagnetic spectrum for the wavelength in the range of $0.1\mu m - 100\mu m$ is responsible for thermal radiation. This range includes visible light, and some part of the infrared, ultraviolet, and X-ray radiation spectrum, as shown in Figure 5.1 (Holman 1990). The thermal radiation is also electromagnetic radiation, which is emitted from the surface of an object due to the temperature of the object. Any object at a temperature above absolute zero emits thermal radiation. Thermal radiation is generated when the heat from the movement of charged particles within atoms is transformed into electromagnetic radiation. One good example is the radiation from sun, which heats up the earth during the day, and at night the earth becomes a heat radiator (Wikipedia 2010b). The advantage of thermal radiation over microwaves is that whenever they come in contact with solid or liquid material, it is transmitted, reflected, or absorbed. The absorbed energy of thermal radiation is directly converted into heat by imparting kinetic energy to atoms and molecules of the material, which may provide a clear advantage for the dry synthesis process, which is mainly composed of solid material. Among thermal radiation, the infrared radiation is increasingly used in industrial heating especially in drying of paints, food, etc. (Blanc *et al.* 1997; Dhib 2007; Hashimoto and Kameoka 1999; Raghavan *et al.* 2005; Ricks 1998). In industry, drying is considered to be the most common and most energy consuming operation with several variants used in drying particulate solids, pastes, continuous sheets, slurries, or solutions. Drying thus provides most diversified unit operations in chemical engineering. Use of IR (infrared) radiation for drying is one of the increasingly popular but not yet common drying methods. In the past the IR radiation was used incidentally in conjunction with other types of heating/drying methods, but now it is primarily used as a source of heating/drying (Williams-Gardner 1971). The literature is full of common applications of IR heating/drying in the areas of dehydration of coated films, drying of paper and board, paints, ink, adhesives, textiles etc. (Navarri *et al.* 1992; Therien *et al.* 1991; Williams-Gardner 1971). IR drying/heating is also applied to other products like foodstuff, wood or sand (Hallstro"m *et al.* 1988) but these applications are not common as yet. Sandu (Sandu 1986) pointed out the advantages of IR radiation in the drying of

food, the versatility of IR heating, simplicity of equipment needed, easy accommodation of IR heating with convective, conductive, and microwave heating, fast transient response, and also considerable energy savings.

In general the IR radiation is used in rapid heating or drying processes. So far we have not come across any study in which IR radiation is used for zeolite synthesis purposes. In this study, our objective is to produce NaY zeolite within the preshaped silica particles ($50 \mu m$) using a dry process. The ultimate goal is to use the zeolite embedded in silica particles for any industrial application. For this purpose we have focused on FCC reaction and desulfurization of gasoline, where it can be directly used in a fluidized bed system. Since our process is almost a dry process, we have chosen a fluidized bed system in conjunction with IR radiation as the primary source of heat. In order to facilitate the uniform temperature distribution within the fluidized bed, we have further added perforated vibrated baffles. Our designed system is thus called vibrated baffles fluidized bed (VBFB) reactor heated by IR radiation. In this study, we will elaborate on the IR radiation and its use in zeolite synthesis, design of a novel vibrated baffles fluidized bed reactor heated by IR radiation, and testing of the system for NaY zeolite synthesis.

5.2 PRINCIPLE BEHIND INFRARED HEATING

The electromagnetic radiation does not require any medium for its transmission. The wavelength of the radiation depends upon the nature and the temperature of heat source. Every body, which is at a temperature above absolute zero emits thermal radiation. IR radiation is generally classified as near/short IR ($0.75 - 3.00 \mu m$), medium IR ($3.00 - 25 \mu m$), and far IR ($25 - 100 \mu m$) (Sandu 1986).

The incident thermal radiation upon a body may be absorbed and its energy converted into heat, transmitted through the material, or reflected from the surface of the material. The reflectivity (ρ), absorptivity (α), and transmissivity (τ) are related as:

$$\rho + \alpha + \tau = 1 \qquad\qquad (5.1)$$

For monochromatic incident radiation the angle of incident is equal to angle of reflection and the reflection of radiation is called "spectral". For polychromatic radiation the incident beam is distributed uniformly in all directions after reflection and the reflection is called "total or diffuse" (Holman 1990; Sandu 1986). The materials on which the radiation impinges are classified according to their transmissivity. Those materials, which do not allow transmission of radiation are called opaque and are characterized by $\tau = 0$. Most solids fall under this category. On the other hand, liquids and some solids like rock salt, glass, or quartz have a defined transmissivity and are somewhat transparent to radiation. The reflection from the surface of the material may be spectral (also called regular) or diffuse depending upon the finish of the surface of the material. The former case holds true in the case of highly polished surfaces or smooth surfaces when the incident radiation angle is equal to the angle of reflection. The latter case occurs when the roughness of the surface becomes larger than the wavelength of the radiation and radiation is reflected diffusively in all directions (Ratti and Mujumdar 2007).

In general all of the incident radiation is absorbed by the solid body in a very narrow layer near the surface of the body. This consideration becomes important in modeling the heat transfer process as mathematically this concept transforms a term into a boundary condition in energy balance. Thus an ideal body that absorbs all the incident energy without reflecting or transmitting is called a black body for which $\alpha = 1$. Thus, the total amount of radiation emitted by a body per unit area and time is called total emissive power (E) (Kreith 1973), and it depends upon the temperature and surface condition of the body. This energy is emitted in all directions and at all wavelengths from the surface of the body. The black body is an ideal case, which emits maximum radiation per unit area in any direction. Therefore, the emissive power of a black body (E_b) depends only on its temperature. At the same time the emissivity (ε) of a body other than the black body is defined as the ratio of its total emissive power to that of a black body at the same temperature ($\varepsilon = E / E_b$) (Ratti and Mujumdar 2007).

The monochromatic emissive power (E_λ), on the other hand, is the radiant energy contained between wavelengths λ and $\lambda + d\lambda$ (Welty et $al.$ 1984). Therefore,

the monochromatic emissive power for a black body is expressed by Planck's law of radiation as:

$$E_{b,\lambda} = \frac{2\pi c^2 h \lambda^{-5}}{\exp\left(\dfrac{ch}{k\lambda T}\right) - 1}$$

(5.2)

and the monochromatic emissivity of a body is defined as $\varepsilon_\lambda = E_\lambda / E_{b,\lambda}$, where $E_{b,\lambda}$ is the monochromatic emissive power of black body at wavelength λ at the same temperature. The monochromatic absorptivity (α_λ) may be defined in the same way as monochromatic emissivity. According to Kirchhoff's rule, the monochromatic absorptivity and emissivity of a body are equal (i.e. $\varepsilon_\lambda = \alpha_\lambda$) under thermodynamic equilibrium which requires all the surfaces to be at the same temperature (Welty *et al.* 1984). The $E_{b,\lambda}$ in Eq. 5.2 has a maximum with respect to temperature and is related by Wien's displacement law:

$$\lambda_{max} T = 2897.6 \mu m.K$$

(5.3)

Equation 5.2 may be integrated over the entire wavelengths to get the total emissive power of a black body called the Stefan-Boltzmann law:

$$E_b = \int_0^\infty E_{b,\lambda} d\lambda = \sigma T^4$$

(5.4)

where, $\sigma = 5.669 \times 10^{-8} W/m^2.K^4$ is the Stefan-Boltzmann constant (Holman 1990). The emissivity of a grey body, on the other hand, does not change over the entire wavelength spectrum. Thus, the Kirchhoff's law may be applied to a grey body independent of its temperature.

The heat transfer by radiation between two black bodies, which are at different temperatures may be obtained by using the Stefan-Boltzmann law as follows:

$$Q_r = A_i F_{ij} \sigma (T_i^4 - T_j^4)$$

(5.5)

where F_{ij} is the shape or view factor between surfaces i and j. The shape factor is defined as the fraction of the energy leaving surface i which reaches surface j. The view factors of most common geometries are available in literature (Holman 1990; Siegel and Howell 2002). The shape factor for concentric cylinders of finite length

shown in Figure 5.2 represents the infrared heating elements employed in our fluidized bed. The shape factors and the areas of the radiation exchanged surfaces can be related to each other by using the reciprocity theorem as follows:

$$A_i F_{ij} = A_j F_{ji} \qquad (5.6)$$

If the radiation energy exchange takes place between N bodies, then the shape factor will follow the following relation:

$$\sum_{j=1}^{N} F_{ij} = 1 \qquad (5.7)$$

It may be noted that very few bodies behave as black body, therefore, it is more realistic to assume grey bodies. In this scenario, the total heat exchange between two grey bodies may be obtained as follows (Holman 1990):

$$Q_r = \frac{\sigma(T_i^4 - T_j^4)}{\left(\dfrac{\rho_i}{\varepsilon_i A_i} + \dfrac{1}{A_i F_{ij}} + \dfrac{\rho_j}{\varepsilon_j A_j} \right)} \qquad (5.8)$$

Some of the thermal radiation that impinges on a body may be attenuated by scattering inside the body during absorption. The scattering of the radiation inside the body may undergo a change in direction of electromagnetic radiation which may cause a partial loss or gain in energy (Siegel and Howell 2002). If I_λ represents the spectral radiation impinging normally on a layer of material where some of it is absorbed and a part is scattered, then the intensity of the monochromatic radiation attenuated is obtained by the following relationship:

$$I_\lambda(z) = I_\lambda(0) \exp\left[-\int_0^z K_\lambda(z^*) dz^* \right] \qquad (5.9)$$

which is called Bougher-Lambert law, where K_λ is the extinction coefficient, z the distance, and $I_\lambda(0)$ is the radiation at the surface of the body. The extinction coefficient in Eq. (5.9) depends upon temperature, pressure, composition, and the wavelength of the incident radiation.
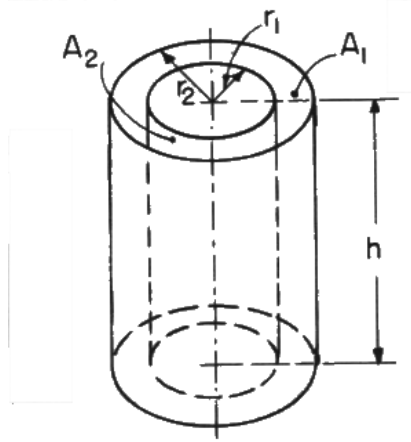
Figure 5.2 Shape factor calculations for concentric cylinders with finite length (Siegel and Howell 2002).

$$F_{1-2} = \frac{1}{\pi R_2} \left[\begin{array}{l} \frac{1}{2}\left(R_2^2 - R_1^2 - 1\right)\cos^{-1}\frac{R_1}{R_2} + \pi R_1 - \frac{\pi}{2}AB \\[2mm] - 2R\tan^{-1}\left(R_2^2 - R_1^2\right)^{\frac{1}{2}} + \left\{\left(1 + A^2\right)\left(1 + B^2\right)\right\}^{\frac{1}{2}}\tan^{-1}\left\{\frac{\left(1 + A^2\right)B}{\left(1 + B^2\right)A}\right\}^{\frac{1}{2}} \end{array} \right]$$

$$where\ R_1 = {r_1}/{h}\ ;\ R_2 = {r_2}/{h}\ ;\ A = R_2 + R_1;\ B = R_2 - R_1$$

Besides all the above theory behind IR heating, the knowledge about material used for IR heating plays an important role for radiation heat exchange between the bodies. The key properties are emissivity, absorptivity, reflectivity, and transmissivity. The relative magnitude of α, ρ, and τ depends upon material itself, its thickness and surface finish, and also on the wavelength of the radiation. On the other hand, ε is only the property of material. For non-conducting materials ε shows directional properties i.e. the emissivity of actual surfaces is not constant in all directions. Its magnitude decreases as the direction of emission deviates from normal. However, the opposite is true for metals (Ratti and Mujumdar 2007; Welty *et al.* 1984). For practical purposes, only the average value of emissivity or absorptivity over the direction is used. The radiation properties of metals and non-metals can be found in literature (Welty *et al.* 1984).

A high reflectivity of material is required especially when it is used as the source of radiation. The total reflectivity of polished pure gold at high temperature is around 0.98. That is why the IR radiation lamps are sometimes coated with gold to provide intense and directional source of heat. On the other hand, the material to be heated by IR radiation should have a low reflectivity in order to absorb most of the incident radiation. This reduces the power requirement to heat it. Therefore, e.g., drying of paints or coatings, a high absorptivity of material is needed. However, drying foodstuff containing high moisture content requires a material with high transmissivity in order to avoid extreme intense heating and thermal damage of the surface. The absorptivity and transmissivity of moist materials is not readily available in literature; however, some experimental data on radiation properties of agriculture and food products is reported (Ginzburg 1969; Mohsenin 1984; Ratti and Mujumdar 2007).

5.3 DESIGN OF NOVEL VIBRATED BAFFLES FLUIDIZED BED (VBFB) REACTOR COUPLED WITH *IR* HEATERS

The idea of novel vibrated baffles fluidized bed (VBFB) reactor coupled with IR heaters was aroused from the limitations of the available technology of using microwaves as a source of fast heat transfer for the rapid production of zeolites. Microwaves are efficient in solution-based systems due to their property of rotating water molecules by change in polarity. For dry synthesis of zeolite, other than conventional heating techniques, using IR radiation heating was found to be an efficient way of heating solid particles for zeolite synthesis. This is primarily due to the reason that the thermal radiation is directly converted into heat upon absorption in solid material and is not dissipated into medium (i.e. air in our case) between the source and the object. The IR heaters are generally used for heating buildings efficiently or drying different chemicals such as dyes, paints etc. and foodstuff (Blanc *et al.* 1997; Dhib 2007; Hashimoto and Kameoka 1999; Raghavan *et al.* 2005; Ricks 1998). This is the first time that an attempt is made to use IR heating for the synthesis of zeolites.

In this study, our technique was based on using porous amorphous SiO_2 particles with an average size of $50 \mu m$, which is suitable for use in any fluidized bed system. The silica particles were added with different quantities of Al_2O_3 in different stages in order

to adjust SiO_2 / Al_2O_3 to a desired ratio. Finally, a solution of $NaOH$ was added to the SiO_2 particles to fill their pores to 100%. The SiO_2 particles filled with $NaOH$ solution appeared dry as the surface of the particles was almost dry. This made the particles fluidizable in a fluidized bed system.

The concept of this design was evolved from the idea of using the solution filled SiO_2 particles in a fluidized bed system so that during heating a uniform temperature may be achieved. A rapid heat transfer was ensured by using IR heaters in order to obtain the desired reaction temperature of the particles in a very short time. The combination of the two was pivotal in achieving a rapid and uniform heat transfer thus making the synthesis time shorter. Since the particles were not completely dry, the use of the vibrated baffles helped in fluidizing the particles. The heating was carried out with the help of ring shaped IR heaters, which surrounded the fluidized bed in order to obtain uniform heating. The air was used for fluidization of the particles in a closed loop fashion. The recirculation of air was needed in order to maintain the vapours of the reaction mixture within the system ensuring constant reaction conditions. Initially, this design was based on a batch process, which may further be modified to a continuous process. Figure 5.3 shows the schematic diagram of the VBFB reactor system.

5.3.1   Description of Vibrated Baffle Fluidized Bed (VBFB) Reactor System

Figure 5.3(c) depicts a detailed drawing of the VBFB reactor system, which was fabricated at the University of Western Ontario Engineering Machine Services. The reactor system is composed of stainless steel with a quartz window 5 cm in diameter and a total height of 97 cm. The initial bed height for the SiO_2 particles is 10 cm. The heated section is composed of quartz to visually observe the fluidized particles, to provide minimum absorption or maximum transmittance to infrared radiation, and to withstand fairly high reaction temperature within the reactor. The source of heat is ring-shaped infrared emitters, which are four in number to cover the entire bed height for uniform heating. The heaters are coated with pure gold on the one side for maximum reflection of radiation in order to direct the IR radiation into the fluidized bed.
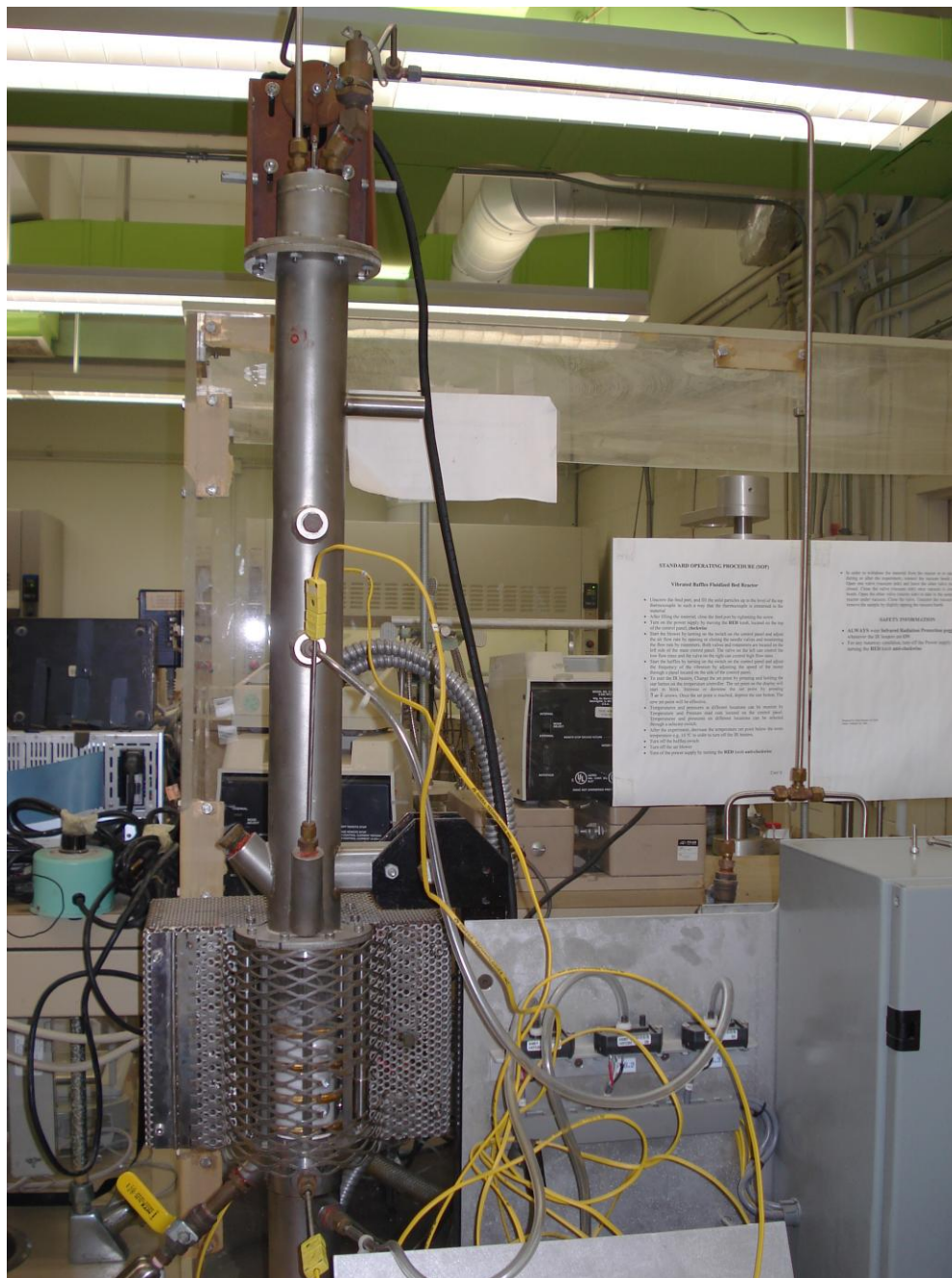
(a)

(b)
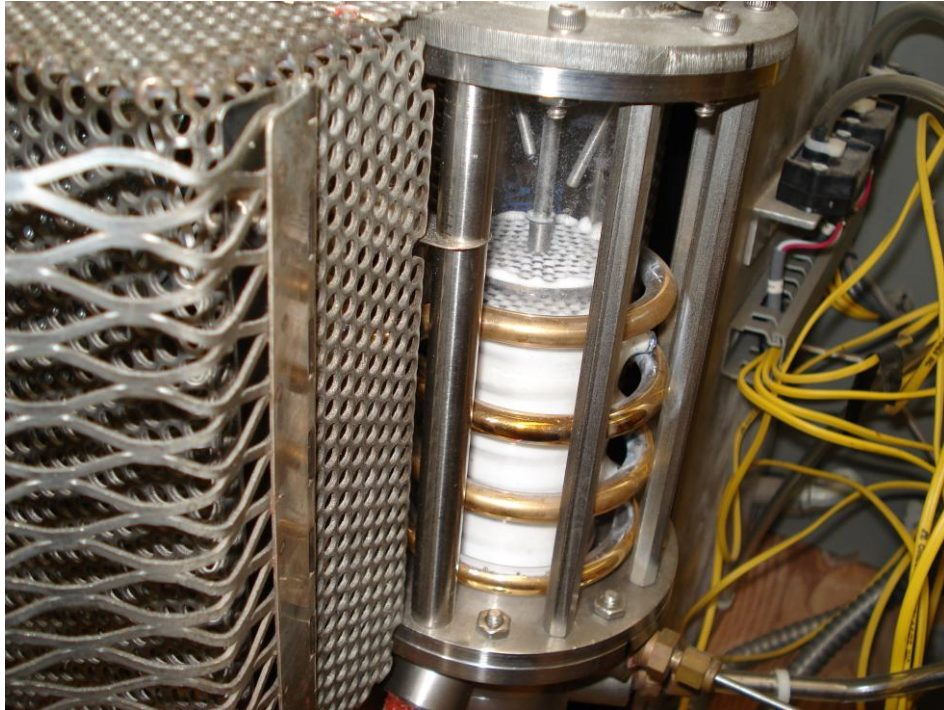
Schematic Diagram of Vibrated Baffle Fluidized Bed (VBFB) Reactor

(c)
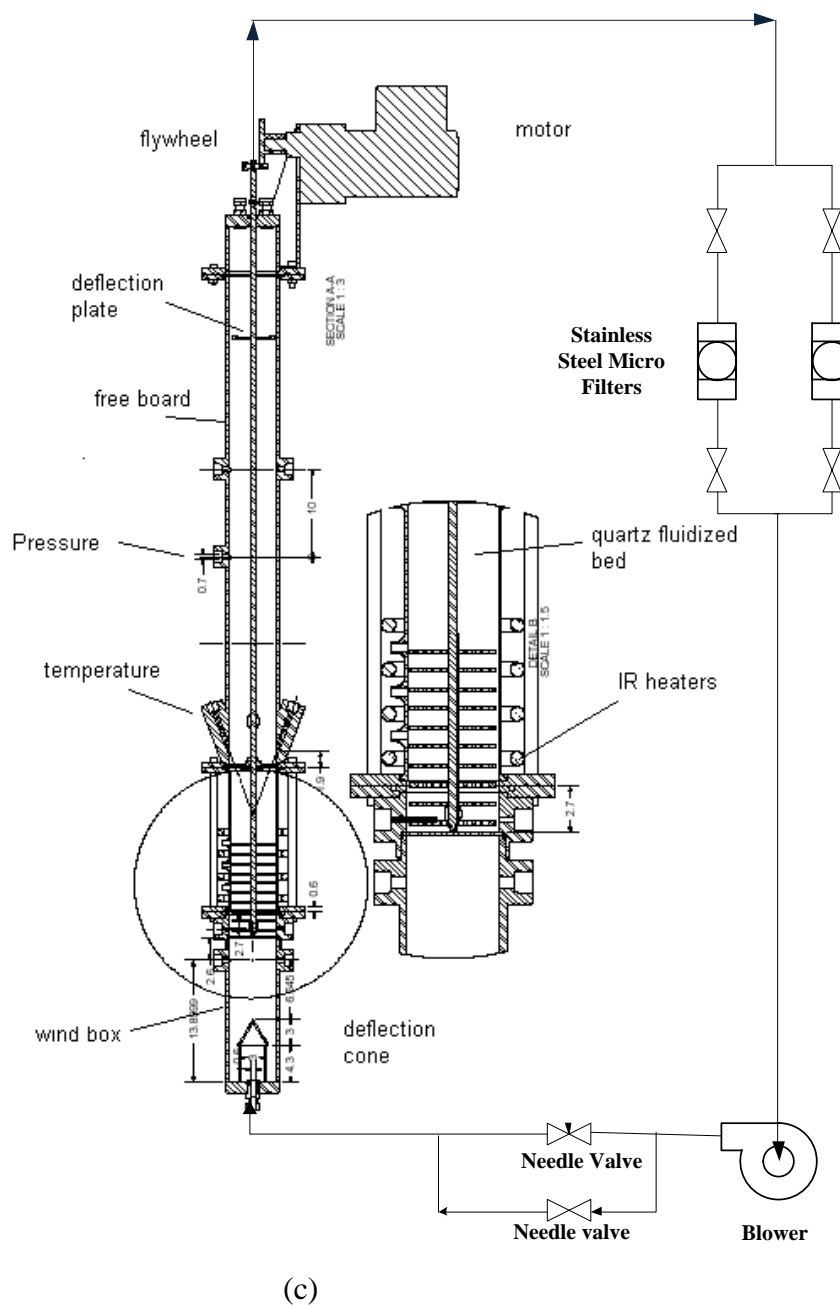
Figure 5.3: Schematic of vibrated baffle fluidized bed (VBFB) reactor; (a) The fluidized bed reactor system, (b) zoomed view of fluidized bed section with IR heaters, (c) a detailed drawing of VBFB reactor system.

A porous plate is provided at the bottom of the bed to provide uniform distribution of air throughout the bed. A cone is designed and located in the wind box to facilitate the uniform distribution of air. Several pressure taps are located in wind box, fluidized bed, and the freeboard to study the pressure drop in different locations. This is helpful in determining the minimum fluidization velocity (u_{mf}), particle size, etc. A deflection plate is located near the top of the freeboard in order to stop majority of fine particles entrained in the gas leaving the fluidized bed. Further capturing of fine particles is ensured by the micro filters located in the recycle line.

Since the reaction temperature is very important for the desired synthesis, a set of thermocouples is provided at the base of the bed, top of the bed with adjustable height, and one in the freeboard to measure the leaving gas stream temperature. The thermocouple with adjustable height on the top of the bed is used to control the temperature of the bed. The top thermocouples are inclined at an angle of $60°$ from horizontal in order to reach the top of the bed. This was needed as it was difficult to drill hole and make space for thermocouple in quartz tube. One of the thermocouples on the top of the bed is connected to a PI controller. The PI controller is used to control the temperature of the bed by turning on and off the IR emitters in order to achieve the desired temperature in the bed.

The reactor is equipped with five perforated baffles, which are mounted on a central shaft attached to a flywheel. The flywheel is drilled with holes in different locations, which is used to change the amplitude of vibrations. The flywheel is connected to a variable speed electrical motor to drive it at variable frequencies. Inter-baffle distance is adjustable with the help of variable size sleeves in between the baffles. The hot moist air leaving the bed is recycled by using a diaphragm blower, after passing through micro filters, in order to preserve the reaction conditions inside the reactor. The purpose of using diaphragm blower is to minimize the escape of fine particles from the micro filter, and keep the blower operational under severe operating conditions.

5.3.2   Internals of Vibrated Baffle Fluidized Bed (VBFB) Reactor System

The fluidized bed reactor system composed of several sections including the bed, freeboard, windbox, perforated baffles, ring shaped infrared emitters, temperature and pressure sensors, etc. The VBFB reactor system is designed for a maximum operating temperature of $200°C$.

5.3.2.1 The Bed

The bed section is composed of quartz tube with diameter of 5 cm and total height of 15 cm. The quartz tube was manufactured and supplied by Pegasus Industrial Specialties Inc. Ontario. The quartz tube was chosen for maximum transmission of IR radiation and to withstand fairly high temperatures. The bed height of the silica particles was kept around 10 cm. The additional height of the quartz tube provided a visual observation for any rise in the bed height during fluidization. The fluidized bed was designed based on the minimum fluidization velocity (u_{mf}) of 2.83 mm/s of the SiO_2 particles with an average particle size of $50\,\mu m$. The calculations for u_{mf} are shown in Appendix A. The bed section contains five perforated baffles 2 cm apart covering the entire height of the bed section. The reciprocating motion of the perforated baffles further aids in fluidization. The diameter of the perforated disc was chosen as 4.8 cm in order to allow free movement of the baffles inside the quartz tube. The size and number of holes on each perforated disc were $3mm$ and 102, respectively. The calculations are shown in Appendix A with the assumption that the open area on the perforated disc is about 40% of the disc area. The addition of vibrated perforated baffles in the fluidized bed was to facilitate the fluidization of the particles at u_{mf} in order to keep the size of freeboard small and to minimize the escaping fine particles from the freeboard.

Since it was difficult to make connections for thermocouples and any other accessories at the top and the bottom of the quartz tube, therefore, the bottom of the bed was connected with a stainless steel section of 5 cm in diameter and 1.8 cm height. This section was fitted with a commercially available stainless steel perforated porous plate of $0.2\,\mu m$ in size and 5 cm in diameter in order to distribute air uniformly at u_{mf}. The porous plate was provided by Mott Corporation, USA. The bottom section of the bed also

contains two K-type thermocouples to measure the temperature at the bottom of the bed. The outside of the quartz tube is surrounded by four ring shaped IR emitters, each is 2 cm apart. The ring shaped IR emitters are 80 mm in size with a heating capacity of 1500W each (total 6000W for four heaters). The IR emitters are composed of quartz tube for maximum transmission of IR radiation, and are coated with gold on one side for directional radiation focused on the bed. The IR emitters were supplied by Heraeus Noblelight LLC, USA.

5.3.2.2 The Freeboard

The freeboard is a 5 cm diameter stainless steel tube, with a total height of 61.8 cm. The freeboard contains connectors for temperature and pressure measurements at different locations. It also contains a deflection plate of 4 cm in diameter located 12.7 cm from the top of the freeboard. The calculations for the position of the deflection plate are shown in Appendix A. A hole is drilled on the top of the freeboard to install the reciprocating rod connected to the perforated baffles in the fluidized bed section. A guide hole is also provided near the bottom of the freeboard in order to overcome any radial displacement or vibrations produced by the reciprocating rod. The purpose of the reciprocating rod is to induce vibrations in the fluidized bed with the help of five perforated baffles mounted at the end of the rod. The frequency and the amplitude of the vibrations are controlled by the speed of the motor and the flywheel with holes in different positions on which the reciprocating rod is mounted. The position of hole on the flywheel controls the amplitude of the vibrations in the range of 0.25-2.5 cm. The frequency of the vibrations is controlled by adjusting the speed of the motor in the range of 0.5-5 Hz (30-300 rpm on the scale of 1-10).

Two air outlet connections of 0.6 cm in size are provided on the top. The top of the freeboard is also equipped with a pop-up safety valve set at 15 psig. Two connections are made at the bottom of the freeboard to facilitate for retractable thermocouples. The angle of each connection is 60° from horizontal in order to access the top of the bed. The position of inclined thermocouples is set such that it does not hinder the reciprocating motion of perforated baffles.

5.3.2.3 The Windbox

The windbox is made of stainless steel with 5 cm in diameter and a total height of 13.9 cm. The windbox contains an air inlet of 0.6 cm at the centre of its bottom. A deflection cone is placed inside the windbox for a uniform distribution of air before it passes through the porous plate. The cone is located 7.3 cm from the bottom of the windbox, with a length of 3 cm and a diameter on the wider side of 3 cm. The calculations for the design of cone, its location in the windbox, and the height of the windbox are shown in Appendix A.

5.4 EXPERIMENTAL

The chemicals used to conduct the parametric study for the synthesis of zeolite in the fluidized system were the same as described in Chapter 3. The source of silica was the porous amorphous silica (SiO_2) gel particles (Sylopol 948) of $50\,\mu m$ average size supplied by W. R. Grace & Co. (Columbia, Maryland, USA). The source of alumina was aluminum nitrate nonahydrate $(Al(NO_3)_3 \cdot 9H_2O)$ supplied by VWR, Canada. The structure directing agent (SDA) was different concentrations of sodium hydroxide $(NaOH)$ solution supplied by Alphachem Canada, and distilled water (H_2O) which also adjusted the pH. Beside chemicals, two types of reactors were used: vibrated baffles fluidized bed (VBFB) reactor, and stainless steel tubular reactor $(12" \times 0.25")$ with 20.5mL in size. The stainless steel tubular reactor was used for comparison purpose.

The synthesis method was adapted from a method reported in literature (Murrell *et al.* 1999), after several modifications in order to make it suitable to our operating conditions and equipment.

The starting material was silica gel particles in which aluminum nitrate nonahydrate was added in three steps to adjust the desired ratio of (SiO_2 / Al_2O_3). In the first step, 100 g of silica gel particles (size $50\,\mu m$) were added with different quantities and concentrations of $Al(NO_3)_3 \cdot 9H_2O$ in water in the range from 187.4 - 197.3 g of solution (17.9 - 24.1 wt%) through incipient wetness using a 600 ml Teflon container. Then mixing was carried out at 500 rpm using a mixer equipped with a Rushton turbine of $2"$ in diameter. The mixing was carried out for about 15 min until all the solution was

adsorbed in the pores of silica particles through incipient wetness. The particles did not form any paste during mixing and remained essentially in flowable powder form. After mixing, a retention time of 1 hr was given at room temperature for complete penetration of solution throughout the pores of silica particles. The water was then removed from the pores of the silica particles by drying the particles at $120^{\circ}C$ using a forced air convection oven until constant weight was achieved. During the process of drying intermittent mixing of particles was carried out in order to avoid formation of agglomerates. The drying process allowed the removal of water from the pores and deposition of $Al(NO_3)_3$ inside the pores of silica particles. After drying, alumina was obtained by carrying out calcination at $500°C$ for 2 hr with a heating rate of $4°C/\min$ in a furnace, followed by a decrease in temperature to $120°C$ with a cooling rate of $4°C/\min$. The calcination process converted $Al(NO_3)_3$ to Al_2O_3. With this step, SiO_2/Al_2O_3 ratios obtained were in the range from 14.9-20.1. In step two, about 97 g of silica gel particles were taken from step 1 and different quantities and concentrations of $Al(NO_3)_3.9H_2O$ solution in water were added in the range of 155.8-160.7 g (21.8-26.6 wt%), followed by mixing at 500 rpm for 15 min and subsequently, a retention time of 1 h at ambient temperature. Drying was carried out at $120°C$ to a constant weight with intermittent mixing. Finally, calcination was carried out at $300°C$ for 6 h with a heating rate of $4°C/\min$, followed by a decrease in temperature to $120°C$ with a cooling rate of $2°C/\min$. In this step SiO_2/Al_2O_3 ratio was in the range of 7.4-9.7. In the third step, 97 g of silica gel particles obtained from step 2 were added with different volumes and concentrations of $Al(NO_3)_3.9H_2O$ in water ranging from 116 g to 130 g (9-29.5 wt%), followed by mixing at 500 rpm for 15 min, and a subsequent retention time of 1 h at ambient temperature. Drying was carried out at $120°C$ to a constant weight with intermittent mixing. Subsequently, the calcination was carried out at $300°C$ for 6 h with a heating rate of $4°C/\min$, followed by a decrease in temperature to $120°C$ with a cooling rate of $2°C/\min$. With the third step, the SiO_2/Al_2O_3 ratio was finally adjusted to about 5.1-6.2. During the three steps of adding Al_2O_3 into SiO_2 particles the pore volume of SiO_2

particles was reduced from $1.56 cm^3/g$ to about $0.64 - 0.78 cm^3/g$, which was due to the occupation of Al_2O_3 in the meso-pores of silica particles.

Finally, in the fourth step, the addition of *NaOH* solution to the SiO_2 particles obtained from third step was carried out. Since the material was to be used in the VBFB reactor, therefore the amount of *NaOH* solution used was estimated to be in the range of 97-100% of the pore volume of the silica particles in order to carry out the synthesis reaction. The particles did not form a paste, and apparently looked dry. To carry out the fourth step, a 4-5 g of material obtained from the third step was added with 32 wt% solution of *NaOH* using a 60 ml size of polypropylene bottle. Hand mixing with the help of a small glass rod was carried out in the polypropylene bottle in order to adsorb *NaOH* solution into the pores of precursor particles. The reaction was carried out in two types of reactors in order to observe the effects of various parameters on the synthesis of zeolites. The VBFB reactor and stainless steel tubular reactor served as the batch reactors for the synthesis reaction. The stainless steel tubular reactor was sealed using Teflon tape before the reaction. An ageing time of 1 h was allowed at ambient temperature before the synthesis reaction. The molar compositions of the precursor were as:

$$Na_2O : 0.518 - 0.711 Al_2O_3 : 3.211 - 3.629 SiO_2 : 10.444 H_2O$$

The synthesis reaction was carried out at $100°C$ using the forced air convection oven by placing the sealed stainless steel tubular reactor for 24 h. In case of the VBFB reactor, the material obtained from forth step was loaded in the reactor from the feed port. It took about 155 g of material to fill the reactor. The recirculation of air was started with a flow rate in the range of 400-800 cm^3/min. The vibrated baffles were started and kept in the range of 150 rpm with amplitude of 0.5 cm. The set point of temperature in the bed was gradually increased to $100°C$ which started the IR heaters in on-off mode. The synthesis was carried out between 5-20 min.

After the synthesis reaction, the set point for the VBFB reactor was reduced to ambient temperature, and the products were removed from the reactor partly through sample valve and the remaining amount by opening the reactor. Several samples of

product were collected from different locations of the bed to verify the consistency of the product composition. On the other hand, the stainless steel tube reactor was taken out of the oven and allowed to cool to ambient temperature under natural convection. The product from both reactors was washed with water, and filtered under vacuum using a $25 \mu m$ size of filter paper. The final product was deposited on the filter paper in the form of a cake, which was then scrapped with the help of a spatula and was then dried in forced air convection oven at $100°C$.

5.4.1 Two-step method

A key modification made in the synthesis method as compared to our previous syntheses in polypropylene bottles and stainless steel tubular reactor, was that the number of stages was reduced from three to two for the gradual addition of $Al(NO_3)_3 \cdot 9H_2O$ into SiO_2 particles. This method was adopted, as it was necessary to load SiO_2 particles into the VBFB reactor with pores filled approximately up to 100%. In our previous studies, the pores were filled around 170 - 200%. The particles having more than 100% filled pores were from slightly wet to dry but did not form any paste. However, the extra moisture for the VBFB reactor was a hindrance in fluidization. At the same time the pore volume of the SiO_2 particles was reduced from $1.56 cm^3/g$ to about $0.67 cm^3/g$ in three stages of adding $Al(NO_3)_3 \cdot 9H_2O$. The reduced pore volume of $0.67 cm^3/g$ for the SiO_2 particles filled with 100% $NaOH$ solution did not initiate any reaction in stainless steel tube reactors in 24 hours; however, the crystals were formed in the VBFB reactor. Therefore, a two-stage preparation of SiO_2 particles was developed in order to adjust the (SiO_2/Al_2O_3) ratio and to acquire a larger pore volume.

The starting material was silica gel particles in which aluminum nitrate nonahydrate was added in two steps to adjust the desired ratio of (SiO_2/Al_2O_3). In the first step, 75 g of silica gel particles (size $50 \mu m$) were added with 147.89 g of $Al(NO_3)_3 \cdot 9H_2O$ solution in water (27.3 wt%) through incipient wetness using a 600 ml Teflon container. Then mixing was carried out at 500 rpm using a mixer equipped with a Rushton turbine of $2^{"}$ in diameter. The mixing was carried out for about 15 min until all

the solution was adsorbed in the pores of silica particles through incipient wetness. The particles did not form any paste during mixing and remained essentially in flowable powder form. After mixing, a retention time of 1 h was given at ambient temperature for complete penetration of solution throughout the pores of silica particles. The water was then removed from the pores of the silica particles by drying the particles at $120^{\circ}C$ using a forced air convection oven until no detectable change in the weight was observed. During the process of drying an intermittent mixing of particles was carried out in order to avoid any formation of agglomerates. The drying process allowed the removal of water from the pores and deposition of $Al(NO_3)_3$ inside the pores of silica particles. After drying, alumina was obtained by carrying out calcination in a furnace at $300°C$ for 6 hr with a heating rate of $3°C/\text{min}$ which was preceded by increasing the furnace temperature to $160°C$ for 3 hr with a heating rate of $3°C/\text{min}$, followed by a decrease in temperature from $300°C$ to $170°C$ at a cooling rate of $1.5°C/\text{min}$ for 5 h. The calcination process converted $Al(NO_3)_3$ into Al_2O_3. With this step, a SiO_2/Al_2O_3 ratio of 13.17 was obtained. In step two, about 74 g of Silica gel particles were taken from step 1 and added with 120.87 g of $Al(NO_3)_3.9H_2O$ solution in water (32.85 wt%) were added, followed by mixing at 500 rpm for 15 min and subsequently, a retention time of 1 hr at ambient temperature. Drying was carried out at $120°C$ to a constant weight with intermittent mixing. Finally, calcination was carried out at $300°C$ for 6 h with a heating rate of $3°C/\text{min}$ which was preceded by increasing the furnace temperature to $160°C$ for 3 hr with a heating rate of $3°C/\text{min}$, followed by a decrease in temperature from $300°C$ to $170°C$ at a cooling rate of $1.5°C/\text{min}$ for 5 h. With this step a SiO_2/Al_2O_3 ratio of 6.2 was obtained.

During the two steps of adding Al_2O_3 into SiO_2 particles the pore volume of SiO_2 particles was reduced from $1.56 cm^3/g$ to about $0.85 cm^3/g$. Finally, in the third step, the addition of $NaOH$ solution to the SiO_2 particles obtained from the second step was carried out. Since the material was to be used in VBFB reactor, therefore the amount of $NaOH$ solution used was in the range of 97-100% of the pore volume of the silica particles in order to carry out the synthesis reaction. The particles did not form a paste,

and apparently looked dry. To carry out the third step, a 4-5 g of material obtained from the second step was added with 32wt% solution of *NaOH* using a 60 ml size of polypropylene bottle. Hand mixing with the help of a small glass rod was carried out in the polypropylene bottle in order to adsorb *NaOH* solution into the pores of precursor particles. The reaction was carried out in two types of reactors in order to observe the effects of various parameters on the synthesis of zeolites. The VBFB reactor and stainless steel tubular reactor served as the batch reactors for the synthesis reaction. The stainless steel tubular reactor was sealed using Teflon tape before the reaction. An ageing time of 1 h was allowed at ambient temperature before the synthesis reaction. The molar compositions of the precursor were as:

$$Na_2O : 0.4609 Al_2O_3 : 2.858 SiO_2 : 10.444 H_2O$$

The synthesis reaction was carried out at $100°C$ using the forced air convection oven by placing the sealed stainless steel tube for 24 h. In case of VBFB reactor, the material obtained from third step was loaded in reactor from the feed port. It took about 155 g of material to fill the reactor. The recirculation of air was started at a flow rate in the range of 400-800 cm^3/min. The vibrated baffles were started and kept in the range of 150 rpm with amplitude of 0.5 cm. The set point of temperature in the bed was gradually increased to $100°C$ which started the IR heaters in an on-off mode. The VBFB reactor was operated for 5-20 min. After the synthesis reaction, the set point for VBFB reactor was reduced to ambient temperature, and the product was removed from the reactor. The processing of the product after its removing from the reactor was the same as described earlier.

5.5 CHARACTERIZATION OF NaY ZEOLITE USING PXRD, XRF, EDX, SEM, and BET

The product was analyzed by powder X-ray diffraction (PXRD), BET surface area analyzer, scanning electromicroscopy (SEM), X-ray florescence (XRF) spectrometer, and energy dispersion X-ray (EDX) analyzer. For determining the crystal

structure, a Rigaku diffractometer equipped with $CuK\alpha$ radiations at 40 KV was used. For surface area analysis, Micromeritics ASAP 2010 adsorption instrument equipped with version 5.0 software was used. Prior to analysis, the sample of weight $0.095\,g$ was outgassed in vacuum at $100°C$ for at least 16 h. Brunauer-Emmett-Teller (BET) surface area was determined using nitrogen as the adsorbent. Pore volume distributions and total pore volumes were calculated from the adsorption and desorption branches of the isotherm using the Barett-Joyner-Halenda (BJH) model. Scanning electromicroscopy (SEM) was carried out using Hitachi S-4500 scanning machine capable of producing a spatial resolution of < 2 nm at a high electron beam voltage (> 15 kV). The Hitachi S-4500 field emission SEM is fully equipped with an EDAXTM EDX system, which provides EDX analyses in parallel with SEM images of the sample. The XRF analysis was conducted on Phillips PW1400 XRF spectrometer using fusion technique to determine the ratio of silica and alumina.

5.6 RESULTS AND DISCUSSION

5.6.1 Effect of Si/Al ratio on Synthesis using Three-Step Preparation Method

Initially the synthesis material was prepared by our regular method in which the SiO_2/Al_2O_3 ratio was adjusted in three steps. The three-step procedure resulted in a lower pore volume in the range of $0.64 - 0.78\,cm^3/g$. We used this pore volume and filled the pores of the silica particles by 32wt% NaOH solution up to 100% instead of around 170% that we used in our previous studies. We selected two SiO_2/Al_2O_3 ratios of 5.1 and 6.2 in order to observe any changes in the synthesis reaction. We did not use a ratio lower than 5.1 as it may tend to form NaX instead of NaY zeolite, also a lower Si/Al ratio is not preferred in industry. We also did not try to obtain higher SiO_2/Al_2O_3 ratio than 6.2 as our previous studies and other studies have reflected that the synthesis time increases with increasing SiO_2/Al_2O_3 ratio (Kacirek and Lechert 1975; Kacirek and Lechert 1976).

Two types of reactors were simultaneously utilized i.e. the VBFB reactor and stainless steel tubular reactor to synthesis zeolite with a SiO_2/Al_2O_3 ratio of 5.1. This strategy was used to observe what type of product was obtained in two different reactors.

Since the silica particles were only filled up to 100% with 32wt% *NaOH* solution in order to maintain the flowability of the particles, it was found that the stainless steel tubular reactor did not show any sign of crystal formation for duration of 24 hr and at a temperature of $100°C$ using PXRD analysis; however, some crystal formation was observed through SEM images which can be seen in Figure 5.4. Figure 5.4 (a) shows the silica particles, which have retained their shape. The higher magnification is depicted in Figure 5.4 (b), which shows the crystals were in the range of 100-200 nm. It is also noted that the cluster size was in the range of 500 nm. One reason that may support this observation could be the reduction in nucleation rate which may be due to the location and occupation of SiO_2 and Al_2O_3 in the framework of nuclei that led to the formation of larger but fewer crystals. For this reason the crystals were larger than 50 nm. In our previous study where the 32wt% *NaOH* solution filled the pores of the silica particles by 170%, we observed smaller crystals. The same reason may hold true for the smaller cluster size as reduction in nucleation rate caused fewer and larger crystals. Generally the crystals may grow in size in two ways i.e. by the addition of growth units and by aggregation. There is abundant evidence in literature which indicates the aggregation of crystals during their growth (Cundy *et al.* 1995a; Gonthier and Thompson 1994). This phenomenon has been observed in our previous studies that larger crystals lead to smaller clusters. It seems that the amount of *NaOH* solution was not enough to carry out an observable synthesis reaction for the chosen reaction duration. Apparently the smaller pore volume plays a role. Since the pores were filled up to 100% as compared to around 170% in previous studies, therefore a sufficient vapor pressure was not produced in order to carry out the reaction in the tubular reactor, which was maintained at indigenous pressure for the duration of 24 h.

(a)

(b)

Figure 5.4: SEM images of NaY zeolites in stainless steel reactor with 100% pores filled with 32 wt% NaOH solution: (a) silica particle in stainless steel tubular reactor with SiO_2/Al_2O_3 ratio of 5.1 (b) zoomed view of silica particle.

On the other hand, when the same reaction was conducted in the VBFB reactor for 5 min at $100°C$, it produced crystals. The SEM images can be seen in Figure 5.5. A marked difference is discernable when a comparison is made between Figure 5.4 and 5.5. In the VBFB reactor, the silica particle has retained its shape and crystals are observed on its surface, as shown in Figure 5.5 (a). However, the zoomed view clearly indicates that the crystal size in Figure 5.5 (b) is in the range of 500 nm to $1 \mu m$, which is very large as compared to the 100-200 nm crystals in stainless steel tube reactor. The shape of the crystals in the VBFB reactor was more cylindrical as compared to cubical shape observed in stainless steel tube reactor. The large crystal size in the VBFB reactor clearly indicates that there may be a change in the crystal growth rate. A linear growth rate has been reported in many studies depending upon the synthesis conditions e.g. Si/Al ratio, temperature, ageing etc. (Cundy *et al.* 1995a; Gonthier and Thompson 1994; Grebner *et al.* 1993; Kacirek and Lechert 1976; Wiersema and Thompson 1996; Zhdanov and Samulevich 1980). One plausible reason could the acceleration of surface integration of the crystals, which has caused a rapid growth in a short span of time i.e. 5 min. The literature has shown that surface integration is a rate limiting step in view of other parameters for crystal growth including crystal linear growth rate, formation of covalent bond to form a polymeric structure piece by piece for T-O-T bonds, activation energy $\left(\approx 45 - 90 kJmol^{-1} \right)$ (Barrer 1982; Cournoyer *et al.* 1975; Cundy *et al.* 1993; Garside and Shah 1980; Mostowicz and Sand 1982; Mullin 1993; Thompson 1998). The reduction in nucleation rate is reasonable in the VBFB as fewer crystals were observed and at the same time no clusters of crystals were found. Mostly single crystals were observed with some inter growth in other crystals. In the literature, claims have been made for the acceleration of surface integration but in the end mostly rejected (Cundy and Cox 2005). Based on our observation we are not sure whether the surface integration was playing any role or not. We were able to produce large single crystals in a very short reaction time of 5 min in the VBFB reactor using IR radiation as the heat source.
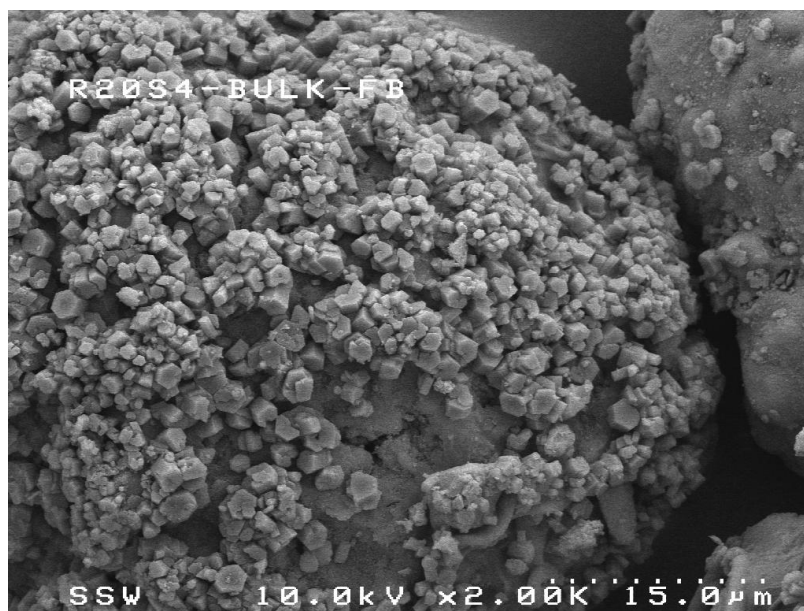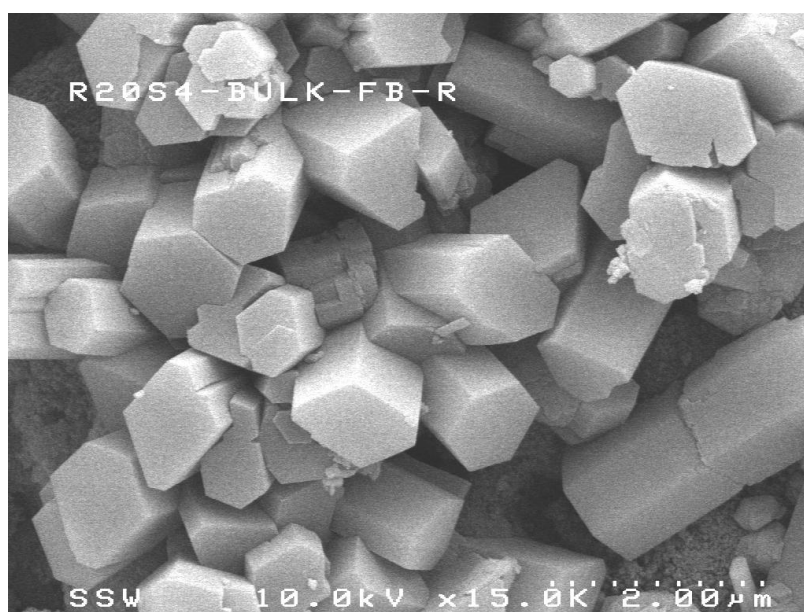
(a)

(b)

Figure 5.5: SEM images of NaY zeolite using VBFB reactor with pores 100% filled with 32 wt% NaOH solution: (a) silica particle with SiO_2 / Al_2O_3 ratio of 5.1 (b) a zoomed view of crystals.

Such large crystals were not observed in the stainless steel tubular reactor running for 24 hr in parallel to the VBFB reactor. In fact, in all our previous studies we did not find any results similar to the VBFB reactor in 5 min of reaction time. The high rate of heat transfer in the form of IR radiation was playing a role. The emitting radiation from the IR heaters was directly absorbed by the silica particles, with the absorbtivity of approximately 0.9. On the other hand, reaction with microwaves does accelerate the synthesis time but microwaves do not directly transform into heat (Arafat *et al.* 1993; Cundy and Zhao 1998; Jansen *et al.* 1992; Kim *et al.* 2000; Park *et al.* 2001; Slangen *et al.* 1997). It rotates the polar solvent and water molecules, and the rotation causes heat to generate. This rapidly generated heat causes synthesis reaction to speed up. One can comment that there may be a lag in microwave heating as the heat reaches the desired synthesis level in two steps. On the other hand, in the IR radiation the desired heat is generated in one step. Though the lag may be extremely small but a clear difference was observed in the VBFB reactor.

Both the stainless steel tubular reactor and VBFB reactor were further utilized for the synthesis reaction by using SiO_2 / Al_2O_3 ratio of 6.2. In stainless steel tube reactor no change in morphology of crystals was observed using SEM images, and XRD results again showed an amorphous phase. The reason may be due to the reduced nucleation rate leading to the formation of fewer crystals. One observation was also made during the preparation of precursors for the synthesis using especially the VBFB reactor. Generally it was observed that when the NaOH was added to the silica particles before they were charged to the reactors, there was a rise in temperature of silica particles. This rise in temperature was attributed to the making of primary amorphous aluminosilicate phase into a secondary amorphous phase through polymerization and depolymerization reactions, and condensation reaction, i.e.

$$T - OH + {}^{-}O - T \Leftrightarrow T - O - T + OH^{-}$$

$$T - OH + HO - T \Leftrightarrow T - O - T + H_2O$$
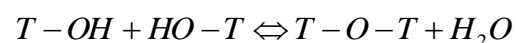
where T=Si or Al

This may have further caused the onset of the crystal growth process to an extremely small extent at ambient temperature (Cundy and Cox 2005). The condensation reaction was evident in the case of VBFB reactor as the dry silica particles appeared slightly wet after 1 h of ageing at ambient temperature. Though this wetness did not affect the flowability of the particles but it reflected the transformation of the phase from primary to secondary amorphous phase, which remained amorphous to x-ray detection. Apparently the preconditions were met for the synthesis but the insufficient quantity of NaOH solution may have caused the final product to remain amorphous. The VBFB reactor also depicted a similar scenario. It produced similar shape and size of crystals which were observed in the study using SiO_2/Al_2O_3 ratio of 5.1, as shown is Figure 5.6. The synthesized crystals with SiO_2/Al_2O_3 ratio of 6.2 are preferred as a higher SiO_2/Al_2O_3 ratio is looked more favorably in industry.

5.6.2 Synthesis of NaY Zeolite using Two-Step Preparation Method

From the results of experiments, based upon the three steps preparation method, it was found that the pore size might be a cause of incomplete synthesis as the XRD results were not conclusive; however, SEM images did show crystals. In order to further investigate the issue, a two steps preparation method was designed, as discussed earlier, in order to acquire a bigger pore volume of the silica particle in the range of $0.80 - 0.84\, cm^3/g$. Since the results from the previous runs using SiO_2/Al_2O_3 ratio of 5.1 and 6.2 produced similar results, therefore, further tests were conducted using SiO_2/Al_2O_3 ratio of 6.2.

The silica particles, which were obtained as a result of the two-step preparation method, were filled with 32 wt% NaOH solution so that the pores of the silica particles were filled up to 100% only. By doing this the flowability of the silica particles was also maintained in order to fulfill the requirements of the VBFB reactor. The synthesis reaction was simultaneously conducted in the stainless steel tubular reactor and the VBFB reactor in order to observe any changes in the product as a result of using different types of reactors. It was found that the stainless steel tubular reactor clearly showed the formation of NaY zeolite crystals for the synthesis reaction at $100°C$ for the duration of

24 hr. The XRD pattern is shown in Figure 5.7 (a) and (b), where a comparison is also made with the commercial NaY zeolite. It can be seen in Figure 5.7 (a) that all the required x-ray diffraction peaks were visible for our synthesized NaY zeolite. No additional or missing peaks were detected indicating that the synthesized product was of pure nature and no by-products were present. An overlapping pattern in Figure 5.7 (b) further suggests that our synthesized zeolite was of similar quality as compared to the commercial zeolite as there was no shift in the diffraction pattern. The results clearly indicate that the increase in the pore volume from $0.64 - 0.78 cm^3/g$ range to $0.82 - 0.84 cm^3/g$ range made a difference in the synthesis reaction as we were able to inject more amount of NaOH solution by 100% filling the pores of the silica particles while maintaining the flowability of the silica particles. Apparently a minimum but sufficient amount of NaOH was available to carry out the synthesis reaction to completion within the time frame of 24 hr.

On the other hand, when the same material was injected in the VBFB reactor and the synthesis reaction was carried out for 5 min under IR radiations, it did not produce crystals that may be detected under XRD analysis. However, SEM images indicated that some crystallization took place. Figure 5.8 depicts such scenario. The silica particle mainly remained amorphous, as seen in Figure 5.8 (a), but at the same time single crystals in the range of 300-600 nm were observed. The smaller crystal size, as seen in zoomed view in Figure 5.8 (b), clearly indicates the effect of pore volume of the silica particles. A larger pore volume may hold more quantity of NaOH solution resulting in a higher rate of nucleation, which in turn is responsible for smaller crystals as compared to our previous study. However, no agglomeration of the crystals was noted contrary to all our previous studies. The formation of single crystals suggests that the nucleation rate was not up to that level which may have triggered the formation of clusters of zeolites with smaller crystallites. At the same time the formation of larger crystal size in a short span of time of 5 minutes suggested that acceleration in surface integration might have been a factor. The single crystal formation also suggests that though the nucleation rate was not very high, but at the same time species for surface integration were available near the surface and rapidly integrated with the surface under the influence of IR radiation.
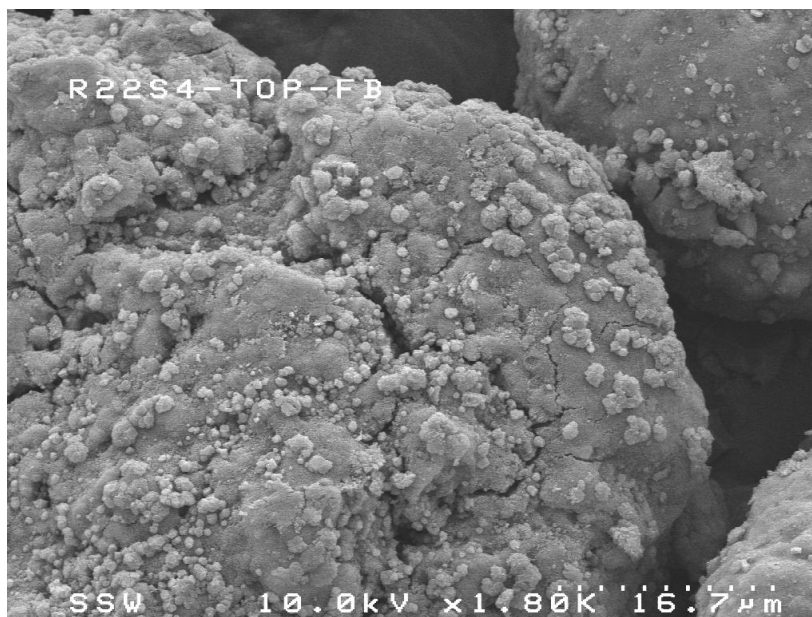
(a)
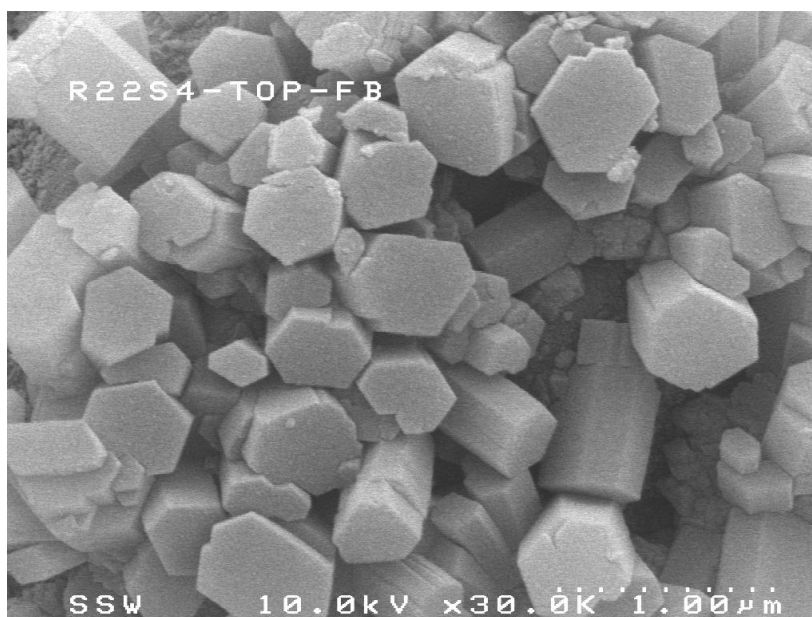
(b)

Figure 5.6: SEM images of NaY zeolite using VBFB reactor with pores 100% filled with 32 wt% NaOH solution: (a) silica particle with SiO_2 / Al_2O_3 ratio of 6.2 (b) zoomed view of crystals.
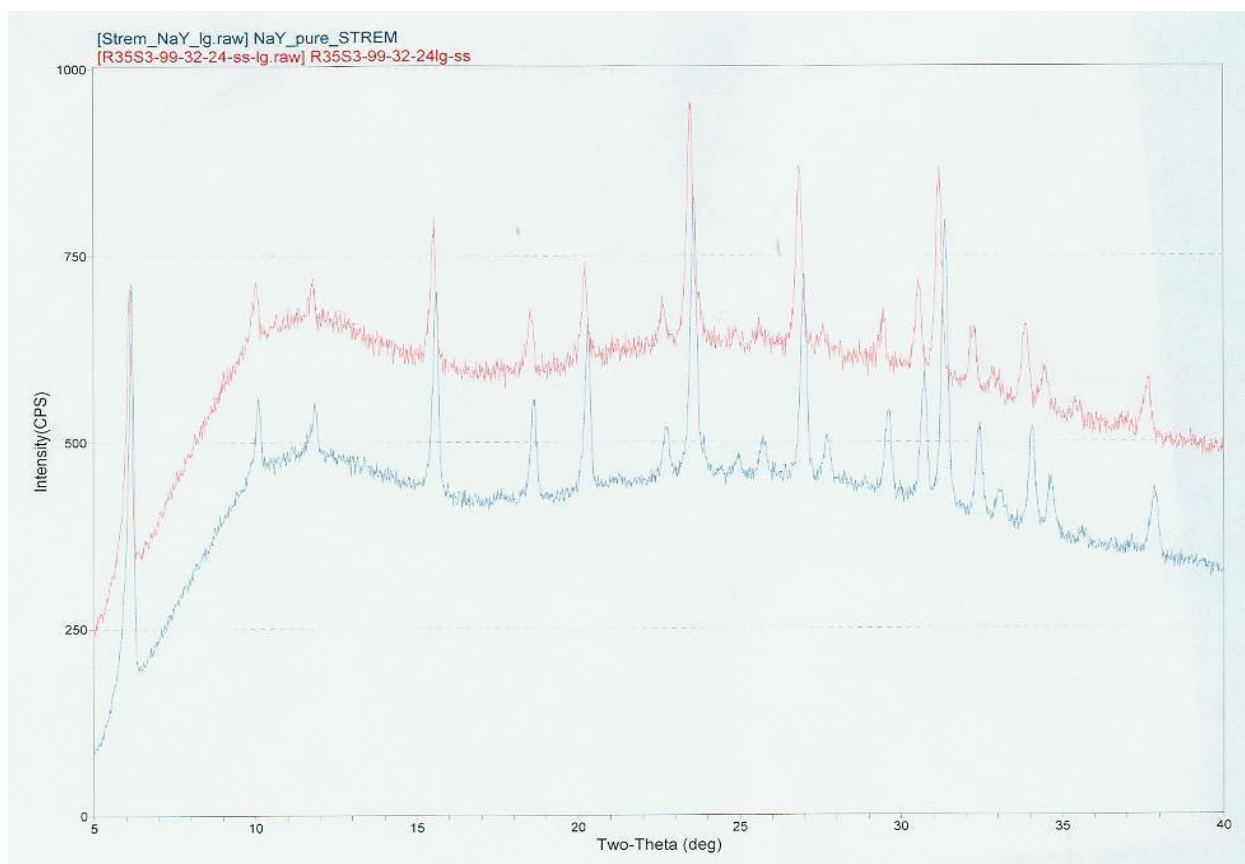
Figure 5.7 (a): XRD patterns of NaY zeolite using stainless steel tube reactor (pattern in red), and commercially available NaY zeolite (pattern in blue) obtained by STREM chemicals.
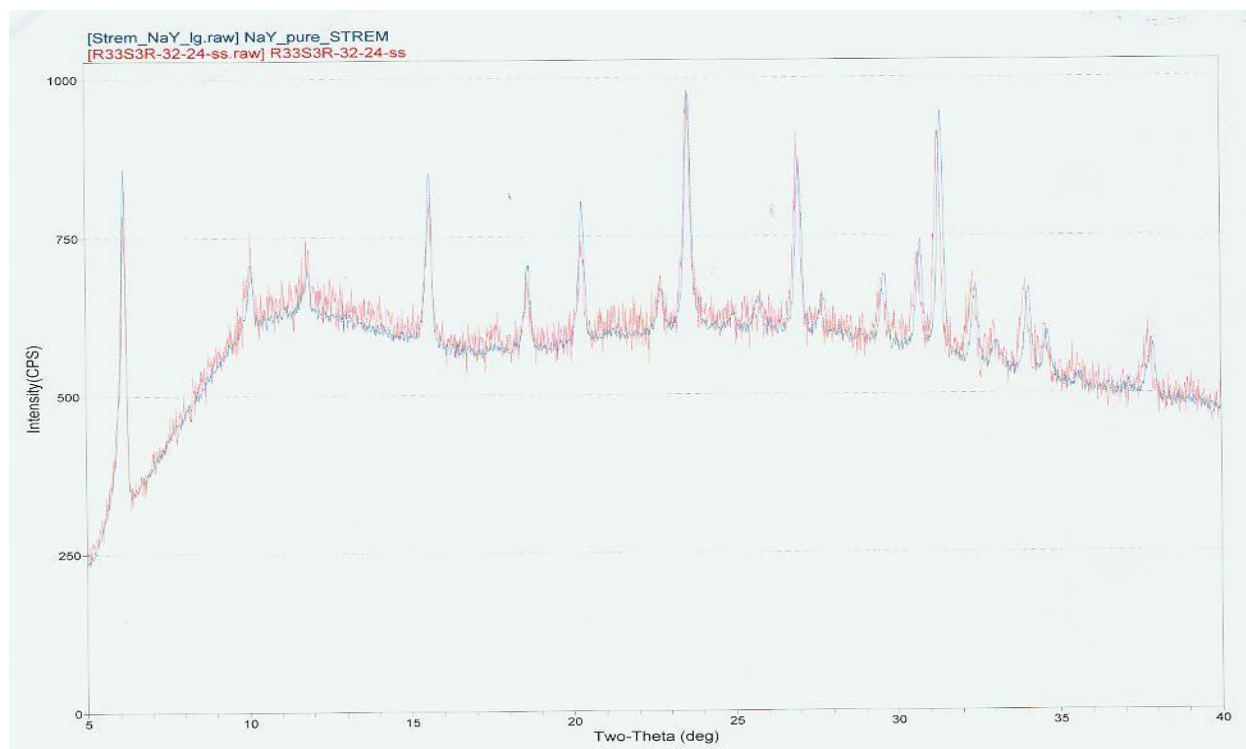
Figure 5.7 (b): A comparison of XRD patterns of NaY zeolite using stainless steel tubular reactor (pattern in red), and commercially available NaY zeolite (pattern in blue) obtained by STREM chemicals.

(a)
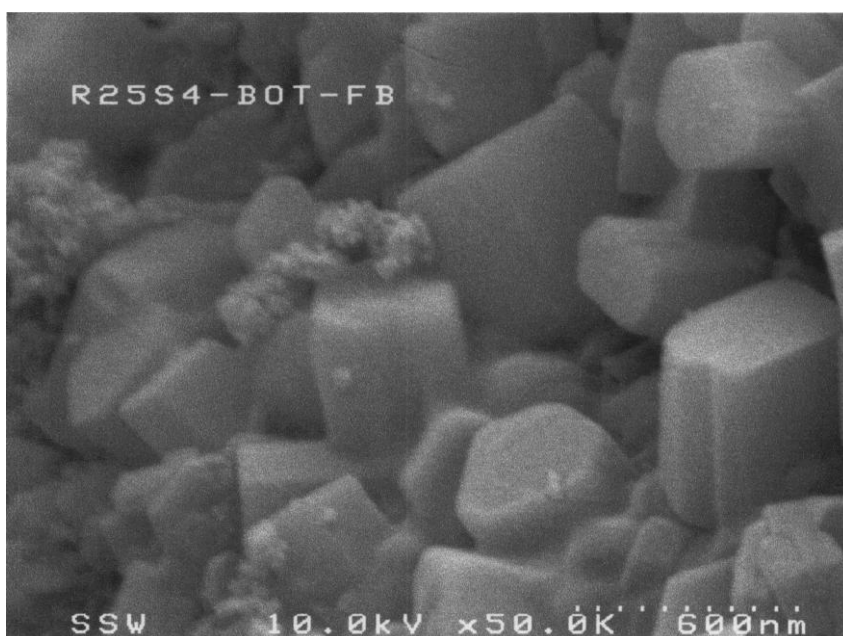
(b)

Figure 5.8: SEM images of NaY zeolite using VBFB reactor with pores 100% filled with 32 wt% NaOH solution using two-step preparation method: (a) silica particle with SiO_2 / Al_2O_3 ratio of 6.2 (b) zoomed view of crystals.

5.6.3　Effect of Reaction Time on Synthesis

In order to visualize the effects of synthesis time on the product quality in the VBFB reactor, we conducted synthesis reaction for duration in the range of 5-20 min. The results of the synthesis reaction for 5 min are depicted in Figures 5.5, 5.6., and 5.8. On the other hand, the results of the synthesis reaction of 20 min are shown in Figure 5.9. The chemical composition of the reactants was kept the same for Figures 5.5, and 5.9. It can be seen from both these figures that there is no apparent change in the size or shape of the crystals. The SEM images in both Figures 5.5, and 5.9 show the crystals in the size range of 500 nm to $1 \mu m$, and in both cases the zeolite is seen as single crystals.

It seems that the increase in the synthesis reaction time did not make any change in the size or shape of the crystals. Apparently the reaction did not proceed further at the prolonged reaction time. A comparison of the Figure 5.5 and 5.9 further suggested that the reaction might have reached its completion by exhausting the available reacting species. However, there may be a possibility that after reaching a certain size of the crystal the further surface integration of species was slowed down due to their lack of availability in the vicinity of the reaction site. In Figure 5.9 some smaller size single crystals are also visible, which may further suggest that some islands of active species were formed, in addition to growing large crystals.

5.6.4　Effect of Quantity of NaOH Solution in the Pores of Silica Particles

Two different amounts of NaOH solution were tried in our study. The solution was added by filling the pores of the silica particles from 95% to 100%. The synthesis material was prepared by using a two-step method in order to achieve pore volume in the range of $0.82 - 0.84 \, cm^3 / g$. The reaction was carried out in the stainless steel tubular reactor and the VBFB reactor. The reaction with 95%-100% filled pore using the VBFB did not show any crystal formation by using PXRD analysis. On the other hand the SEM images showed the crystal formation for the 100% filled pore, as shown in Figures 5.5, 5.6, 5.8 and 5.9. However, the pores filled with 95% of NaOH solution did not show any sign of crystal formation even on the SEM micrographs. This was a clear indication that the amount of NaOH solution was very critical in order to start the formation of nuclei

and further crystal growth. However, when stainless steel tubular reactor was used to carry out the synthesis using two quantities of NaOH solution i.e. 95-100% pores of silica particles filled. The PXRD patterns in both cases showed very clear formation of NaY zeolites, as depicted in Figure 5.7 (a) and (b), respectively. Both patterns were compared with commercial NaY zeolite and did not indicate any by-product formation, and also there was no sign of shift in the diffraction patterns that is shown in the overlapping pattern in Figure 5.7 (b). These observations clearly indicate that the amount of NaOH in filling the pores of silica particles is not very critical, which was observed in the VBFB reactor. One plausible reason could be the length of synthesis time. The short span of 5 min in the VBFB reactor did not allow any flexibility in quantity of NaOH solution. However, the longer reaction time of 24 hr in stainless steel tubular reactor was enough to allow synthesis reaction to proceed to completion.
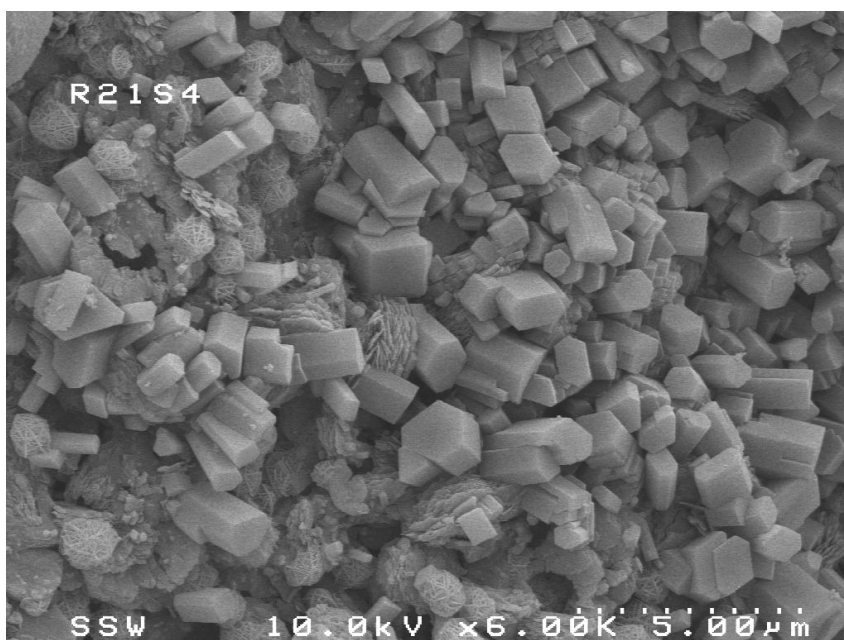
(a)
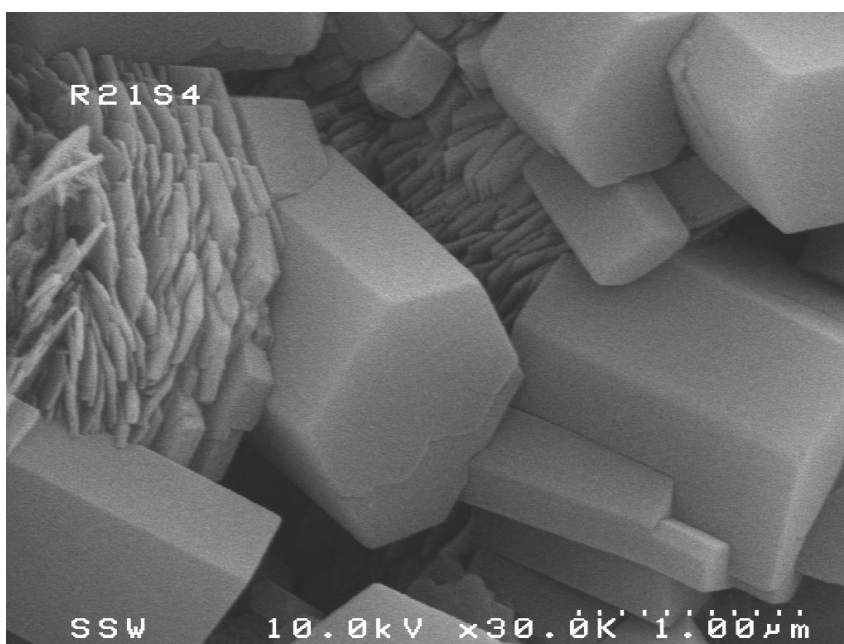
(b)

Figure 5.9: SEM images of NaY zeolite using VBFB reactor with pores 100% filled with 32 wt% NaOH solution for synthesis time of 20 min: (a) silica particle with SiO_2 / Al_2O_3 ratio of 5.1 (b) a zoomed view of crystals

5.7 CONCLUSIONS

The effect of the SiO_2 / Al_2O_3 ratio over the range of 5.1 to 6.2 was not significant; therefore, the higher ratio of 6.2 was preferred. The novel VBFB reactor was able to produce crystals in a short span of time of 5 min at a synthesis temperature of $100°C$ using two methods of preparation. However, the two-step preparation method was found to be more effective for the VBFB reactor when using silica particles pores 100% filled with NaOH solution as it produced pore volume in the range of $0.82 - 0.84 cm^3 / g$. With the two-step preparation method in the VBFB reactor the large single crystals were obtained in the range of 300-600 nm. A smaller nucleation rate was apparent which led to the production of large crystals. The synthesis of large size crystals suggested a significant effect of the surface integration mechanism for the crystal growth for a short span of time of 5 min. The stainless steel tubular reactor produced pure NaY zeolite in 24 hr while filling the pores of silica particles between 95-100% by using two-step preparation method.

Appendix A

Design Equations for the Vibrated Baffle Fluidized Bed (VBFB) Reactor

A.1   Minimum Fluidization Velocity (u_{mf})

(Bergougnou 2005; Briens 1999; Kunii and Levenspiel 1991; Kwauk 1992; Nedderman 1999)

Density of air:

$$\rho_{air} = D = 1.2929\left(\frac{273.13}{T}\right)\left[\frac{B - 0.3783 \times e}{760}\right] \qquad (A.1)$$

Where,

$T = Temperature, K$

$B = Barometric\ \mathrm{Pr}essure\ (mmHg)$

$e = vapour\ pressure\ of\ moisture\ in\ air\ (mmHg)$

Considering conditions at room temperature $(T = 25°C)$

$\therefore e = 23.75mmHg$

Assuming

$B = 760mmHg$

$$\rho_{air} = D = 1.2929\left(\frac{273.13}{298.13}\right)\left[\frac{760 - 0.3783 \times 23.756}{760}\right]$$

$\rho_g = 1.1704\,kg/m^3$

kinematic viscosity of air

$$\left(\frac{\mu}{\rho}\right) = \nu_{air} = -1.1555 \times 10^{-14}T^3 + 9.5728 \times 10^{-11}T^2 + 3.7604 \times 10^{-8}T - 3.4484 \times 10^{-6}\ m^2/s$$

$$(A.2)$$

Taking T = 298.13*K*

$$\left(\frac{\mu}{\rho}\right) = \nu_{air} = 1.5964 \times 10^{-5} \ m^2/s$$

$$\mu_g = 1.5964 \times 10^{-5} \times 1.1704$$

$$\mu_g = 1.8685 \times 10^{-5} \ kg/m.s$$

Bulk Density of particle $= \rho_{bulk} = 647.4 \ kg/m^3$

Assuming $\varepsilon = 0.5$

Approximate ρ_p

$$\rho_p = \frac{\rho_{bulk}}{\varepsilon} = 1294.8 \ kg/m^2$$

Using Ergun Equation to calculate minimum fluidization velocity:

$$\frac{\Delta P}{H_{bed}} = 150\left(\frac{(1-\varepsilon)^2}{\varepsilon^3}\right)\left(\frac{\mu_g u_{mf}}{(\phi d_p)^2}\right) + 1.75\left(\frac{(1-\varepsilon)}{\varepsilon^3}\right)\left(\frac{\rho_g u_{mf}^2}{\phi d_p}\right) \tag{A.3}$$

Also,

$$\Delta P = \frac{W_{bed}}{A} = g\,H_{mf}(1-\varepsilon_{mf})(\rho_p - \rho_g) \tag{A.4}$$

combining equations A.3 and A.4

$$\frac{g\,H_{mf}(1-\varepsilon_{mf})(\rho_p - \rho_g)}{H_{bed}} = 150\left(\frac{(1-\varepsilon)^2}{\varepsilon^3}\right)\left(\frac{\mu_g u_{mf}}{(\phi d_p)^2}\right) + 1.75\left(\frac{(1-\varepsilon)}{\varepsilon^3}\right)\left(\frac{\rho_g u_{mf}^2}{\phi d_p}\right)$$

$$g\,(1-\varepsilon_{mf})(\rho_p - \rho_g) = 150\left(\frac{(1-\varepsilon)^2}{\varepsilon^3}\right)\left(\frac{\mu_g u_{mf}}{(\phi d_p)^2}\right)\left(\frac{\rho_g d_p \mu_g}{\rho_g d_p \mu_g}\right) + 1.75\left(\frac{(1-\varepsilon)}{\varepsilon^3}\right)\left(\frac{\rho_g u_{mf}^2}{\phi d_p}\right)\left(\frac{d_p^2 \mu_g^2 \rho_g}{d_p^2 \mu_g^2 \rho_g}\right)$$

$$g\,(1-\varepsilon_{mf})(\rho_p - \rho_g) = 150\left(\frac{(1-\varepsilon)^2}{\varepsilon^3}\right)\left(\frac{\rho_g u_{mf} d_p}{\mu_g}\right)\left(\frac{\mu_g^2}{\phi^2 d_p^3 \rho_g}\right) + 1.75\left(\frac{(1-\varepsilon)}{\varepsilon^3}\right)\left(\frac{\rho_g u_{mf} d_p}{\mu_g}\right)^2\left(\frac{\mu_g^2}{\phi d_p^3 \rho_g}\right)$$

$$g\,(\rho_p - \rho_g)\left(\frac{d_p^3 \rho_g}{\mu_g^2}\right) = 150\left(\frac{(1-\varepsilon)}{\varepsilon^3}\right)\left(\frac{\text{Re}_{mf}}{\phi^2}\right) + 1.75\left(\frac{\text{Re}_{mf}^2}{\varepsilon^3 \phi}\right)$$

L.H.S. of above equation becomes Archimedes Number

$$Ar = \frac{\rho_g(\rho_p - \rho_g)g\,d_p^3}{\mu_g^2} \tag{A.5}$$

$\therefore$

$$Ar = \frac{1.1704\left((1294.8 - 1.1704)9.81(50 \times 10^{-6})^3\right)}{(1.8685 \times 10^{-5})^2}$$

$Ar = 5.3178$

therefore:

$$\text{Re}_{mf} = -C_1 + \left[C_1^2 + C_2\, Ar\right]^2 \qquad (A.6)$$

where,

$$C_1 = 42.86\frac{(1 - \varepsilon_{mf})}{\phi}\ , \quad C_2 = 0.5714\,\phi\,\varepsilon_{mf}^3$$

Assuming

$\varepsilon_{mf} \approx 0.5$, $\phi \approx 1$

then

$C_1 = 21.43$
$C_2 = 0.071425$

if $Ar < 1000$

$$\text{Re}_{mf} = 0.5\, Ar\left(\frac{C_2}{C_1}\right) \qquad (A.7)$$

$\text{Re}_{mf} = 8.86 \times 10^{-3}$

$\sin ce$

$$\text{Re}_{mf} = \frac{\rho_g u_{mf} d_p}{\mu_g}$$

$\therefore$

$$u_{mf} = \frac{8.86 \times 10^{-3} \times 1.8685 \times 10^{-5}}{1.1704 \times 50 \times 10^{-6}}$$

$u_{mf} = 2.8257 \times 10^{-3}\, m/s$

or

$u_{mf} = 0.28257\, cm/s = 2.8257\, mm/s$

A.2 Terminal Velocity of the smaller particles (size 27 μm)

From equation A.5

$$Ar = \frac{\rho_g(\rho_p - \rho_g)g\,d_p^3}{\mu_g^2}$$

$$Ar = \frac{1.1704(1294.8 - 1.1704)9.81(27 \times 10^{-6})^3}{(1.8685 \times 10^{-5})^2}$$

$$Ar = 0.83737$$

$$C_D\,\mathrm{Re}_t^2 = \frac{4}{3}Ar \qquad\qquad\qquad (A.8)$$

or

$$\mathrm{Re}_t = \frac{u_t d_p \rho_g}{\mu_b} = \left[\frac{4}{3}\frac{Ar}{a}\right]^{1/(2-b)} \qquad (A.9)$$

first get Re

$\sin ce\ Ar < 1000,$

$\therefore from\ A.7$

$$\mathrm{Re}_{mf} = 0.5\,Ar\left(\frac{C_2}{C_1}\right)$$

$$C_1 = 42.86\frac{(1 - \varepsilon_{mf})}{\phi}, \quad C_2 = 0.5714\phi\varepsilon_{mf}^3$$

assuming

$\varepsilon_{mf} \approx 0.5$, $\phi \approx 1$

then,

$C_1 = 21.43$

$C_2 = 0.071425$

$$\mathrm{Re}_{mf} = 0.5 \times 0.83737\left(\frac{0.071425}{21.43}\right)$$

$$\mathrm{Re}_{mf} = 1.395 \times 10^{-3}$$

since Re < 2, therefore, it is in stokes regime

therefore,

$a = 24, b = 1$

from equation A.9

$$\text{Re}_t = \left[\frac{4}{3} \times \frac{0.83737}{24}\right]^{1/(2-1)}$$

$$\text{Re}_t = 0.04652$$

$$u_t = 0.04652 \times \frac{1.8685 \times 10^{-5}}{27 \times 10^{-6} \times 1.1704}$$

$$u_t = 0.0275 m/s$$

or

$$u_t = 27.5 mm/s$$

A.3   Pressure Drop (ΔP) across the Bed at Minimum Fluidization Velocity (u_{mf})

From Equation A.3 or A.4, the general equation for pressure drop across the bed is:

$$\frac{\Delta P}{H_{bed}} = \frac{W_{bed}}{H_{mf} A} = g(1 - \varepsilon_{mf})(\rho_p - \rho_g) = 150\left(\frac{(1-\varepsilon)^2}{\varepsilon^3}\right)\left(\frac{\mu_g u_{mf}}{(\phi d_p)^2}\right) + 1.75\left(\frac{(1-\varepsilon)}{\varepsilon^3}\right)\left(\frac{\rho_g u_{mf}^2}{\phi d_p}\right)$$

or

$$\Delta P = \frac{W_{bed}}{A} = g H_{mf}(1 - \varepsilon_{mf})(\rho_p - \rho_g)$$

Taking $u_{mf} = v_g$, assuming $\varepsilon_{mf} = 0.5$

$$\frac{\Delta P}{H_{mf}} = g(1 - \varepsilon_{mf})(\rho_p - \rho_g)$$

$$\frac{\Delta P}{H_{mf}} = 9.81(1 - 0.5)(1294.8 - 1.1704)$$

$$\frac{\Delta P}{H_{mf}} = 6345.25 \frac{N}{m^2.m}$$

if $H_{mf} = 10 cm = 0.1 m$

then

$$\Delta P = 634.525 N/m^2 \text{ or } Pa$$

if $H_{mf} = 15 cm = 0.15 m$

then

$$\Delta P = 951.78 N/m^2 \text{ or } Pa$$

A.4   Design of Windbox and Deflection Cone below the Perforated Distributor Plate

Design of Deflection Cone Below Distributor
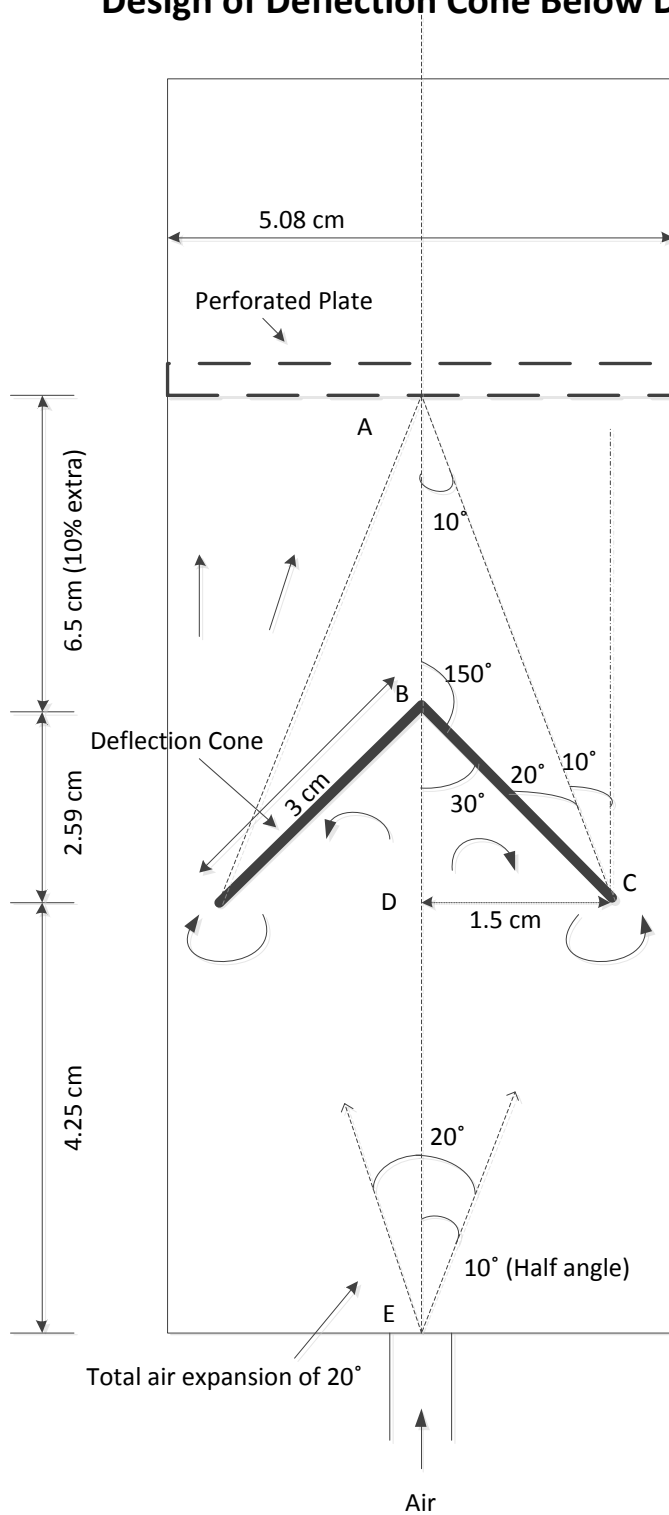
Given:

Total angle of the cone $= 60°$

Half angle of the cone $= 30°$

Length of the cone ($\overrightarrow{BC}$) $= 3.0$ cm

The angle at with the air moving up leaving the cone (point C) $= 10°$

Total angle at which the air enters the windbox (point E) $= 20°$

The half angle at which the air enters the windbox (point E) $= 10°$

Calculating all the lengths of the cone:

$$\sin\theta = \frac{\overrightarrow{CD}}{\overrightarrow{BC}}$$

$$\overrightarrow{CD} = \sin 30 \times 3.0 = 0.5 \times 3.0$$

$$\overrightarrow{CD} = 1.5 \; cm$$

$$\cos\theta = \frac{\overrightarrow{BD}}{\overrightarrow{BC}}$$

$$\overrightarrow{BD} = \cos 30 \times \overrightarrow{BC} = 0.866 \times 3.0$$

$$\overrightarrow{BD} = 2.598 \; cm$$

To find length $\overrightarrow{AB}$

$$\tan\theta = \frac{\overrightarrow{CD}}{\overrightarrow{AD}}$$

$$\overrightarrow{AD} = \frac{\overrightarrow{CD}}{\tan 10} = \frac{1.5}{0.1763}$$

$$\overrightarrow{AD} = 8.5 \; cm$$

$$\overrightarrow{AB} = \overrightarrow{AD} - \overrightarrow{BD} = 8.5 - 2.598$$

$$\overrightarrow{AB} = 5.905 \; cm$$

taking 10% extra length

$$\overrightarrow{AB} = 6.5 \; cm$$

Calculating the length $\overrightarrow{DE}$

Assuming that the air stream will reach half of $\overrightarrow{CD}$ with a half angle of $10°$

$$\tan\theta = \frac{\overrightarrow{CD}/2}{\overrightarrow{DE}}$$

$$\overrightarrow{DE} = \frac{1.5/2}{\tan 10} = \frac{0.75}{0.1763}$$

$$\overrightarrow{DE} = 4.25 \ cm$$

A.5   Location of Top Deflection Disc

Top Deflection Disc
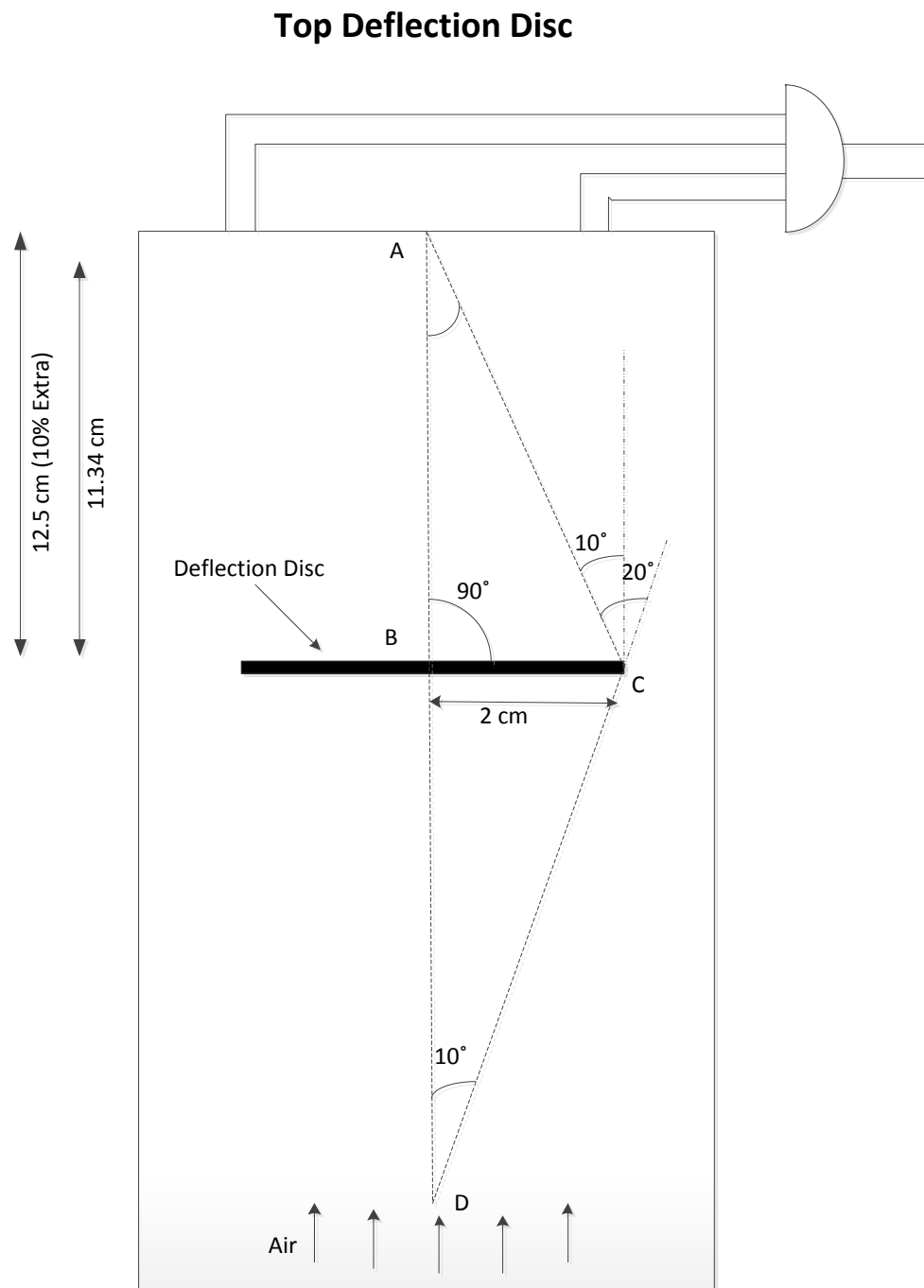
Diameter of top deflection disc = 4 cm

Thickness of top deflection disc = 2 mm

Calculating distance of the disc from the top of the column

Air leaving the at an angle of 10° from point C

$$\tan \theta = \frac{\overrightarrow{BC}}{\overrightarrow{AB}}$$

$$\overrightarrow{AB} = \frac{\overrightarrow{BC}}{\tan 10} = \frac{2.0}{0.1763}$$

$$\overrightarrow{AB} = 11.34 \; cm$$

taking 10% extra length

$$\overrightarrow{AB} = 12.5 \; cm$$

A.6 Design of Vibrated Baffle

Diameter of the Disc = 4.8 cm

Thickness of the Disc = 2 mm

Diameter of the hole in the Disc = 3 mm

Open Area on the perorated Disc = 40% of the diameter of the disc (Assumption)

$$\text{area of the disc } = \frac{\pi}{4}(4.8)^2 = 18.095 \, cm^2$$

$$\text{area available for holes } = 18.095 \times 0.4 = 7.238 \, cm^2$$

$$\text{Area of the hole} = \frac{\pi}{4}(3/10)^2 = 0.07068 \, cm^2$$

$$\text{Number of holes needed } = \frac{7.238}{0.070685} = 102.4$$

5.8 REFERENCES

Arafat, A., Jansen, J. C., Ebaid, A. R., van Bekkum, H. "Microwave Preparation of Zeolite Y and ZSM 5." *Zeolites*, 1993, *13* (3), 162-165.

Babich, I. V. and Moulijn, J. A. "Science and technology of novel processes for deep desulfurization of oil refinery streams: a review." *Fuel*, 2003, 82(6), 607-631.

Barrer, R. M. *Hydrothermal Chemistry of Zeolites*. New York: Academic Press, 1982.

Bergougnou, M. Fluidised Bed Designing, Personal Communication, 2005.

Blanc, D., Laurent, P., Gerard, J. F., and Andrieu, J. "Experimental infrared drying study of a model water-based epoxy-amine painting coated on iron support." *Drying Technol.*, 1997, 15(6-8), 1787-1799.

Breck, W. D. *Zeolite Molecular Sieves*. New York: Wiley, 1974.

Breck, W. D., Flanigen, E. M. "Synthesis and Properties of Union Carbide Zeolites L, X, and Y." *Molcular Sieves Pap.Conf.*, 1967, 47-61.

Briens, C., "Fluidized bed Design.", 1999. Lecture Notes.

Corma, A., Wojciechowski, B. W. "The chemistry of catalytic cracking." *Catal.Rev.-Sci.Eng.*, 1985, *27* (1), 29-149.

Cournoyer, R. A., Kranich, W. L., Sand, L. B. "Zeolite crystallization kinetics related to dissolution rates of quartz reactant." *J.Phys.Chem.*, 1975, *79* (15), 1578-1581.

Cundy, C. S. "Microwave Techniques in the Synthesis and Modification of Zeolite Catalysts. A Review." *Collect.Czech.Chem.Commun.*, 1998, *63* (11), 1699-1723.

Cundy, C. S., Henty, M. S., Plaisted, R. J. "Zeolite Synthesis Using a Semicontinuous Reactor. Part 1. Controlled Nucleation and Growth of ZSM-5 Crystals Having Well-Defined Morphologies." *Zeolites*, 1995a, *15* (4), 353-372.

Cundy, C. S., Henty, M. S., Plaisted, R. J. "Zeolites Synthesis Using a Semicontinuous Reactor. 2. Synthesis at High Nucleation Rates." *Zeolites*, 1995b, *15* (2), 400-407.

Cundy, C. S., and Cox, P. A. "The hydrothermal synthesis of zeolites: Precursors, intermediates and reaction mechanism." *Microporous Mesoporous Mater.*, 2005, *82* (1-2), 1-78.

Cundy, C. S., Forrest, J. O., Plaisted, R. J. "Some observations on the preparation and properties of colloidal silicalites. Part I: synthesis of colloidal silicalite-1 and titanosilicalite-1 (TS-1)." *Microporous Mesoporous Mater.*, 2003, *66* (2-3), 143-156.

Cundy, C. S., Lowe, B. M., Sinclair, D. M. "Crystallization of zeolitic molecular sieves: direct measurements of the growth behavior of single crystals as a function of synthesis conditions." *Faraday Discuss.*, 1993, *95* 235-252.

Cundy, C. S., Zhao, J. P. "Remarkable synergy between microwave heating and the addition of seed crystals in zeolite synthesis - a suggestion verified." *Chem.Commun.(Cambridge)*, 1998, (14), 1465-1466.

de Lasa, H., Enriquez, R. Hernandez, and Tonetto, G. "Catalytic Desulfurization of Gasoline via Dehydrosulfidation." *Ind.Eng.Chem.Res.,*2006, 45(4), 1291-1299.

Dhib, R. "Infrared drying: from process modeling to advanced process control." *Drying Technol.*, 2007, 25(1-3), 97-105.

Elander, N., Jones, J. R., Lu, S. Y., Stone-Elander, S. "Microwave-enhanced radiochemistry." *Chem.Soc.Rev.*, 2000, *29* (4), 239-249.

Gabriel, C., Gabriel, S., Grant, E. H., Halstead, B. S. J., Mingos, D. M. "Dielectric parameters relevant to microwave dielectric heating." *Chem.Soc.Rev.*, 1998, *27* (3), 213-224.

Garside, J., and Shah, M. B. "Crystallization kinetics from mixed suspension mixed product removal (MSMPR) crystallizers." *Ind.Eng.Chem.Process Des.Dev.*, 1980, *19* (4), 509-514.

Ginzburg, A. S. *Application of infra-red radiation in food processing*. London: Leonard Hill Books, 1969.

Gong, Y., Dou, T., Kang, S., Li, Q., and Hu, Y. "Deep desulfurization of gasoline using ion-exchange zeolites: Cu(I)- and Ag(I)-beta." *Fuel Process.Technol.,*2009, 90(1), 122-129.

Gonthier, S., Thompson, R. W. "Effects of seeding on zeolite crystallization, and the growth behavior of seeds." *Stud.Surf.Sci.Catal.*, 1994, *85* (Advanced Zeolite Science and Applications), 43-73.

Grebner, M. D., Reich, A., Schueth, F., Unger, K. K., Franz, K. D. "Influence of synthesis conditions on the morphology of Dodecasil 1H." *Zeolites*, 1993, *13* (2), 139-144.

Hallstro"m, B., ldebrand, C., gaørdh, C. *Heat Transfer and Food Products*. London: Elsevier Applied Science, 1988.

Hashimoto, A. and Kameoka, T., "Effect Of Infrared Irradiation On Drying Characteristics Of Wet Porous Materials." *Drying Technol.*, 1999, 17(7), 1613-1626.

Hernandez-Maldonado, A. J., Yang, F. H., Qi, G., and Yang, R. T. "Desulfurization of transportation fuels by π-complexation sorbents: Cu(I)-, Ni(II)-, and Zn(II)-zeolites," *Appl.Catal., B* , 2005, 56(1-2), 111-126.

Holman, J. P. "Radiation Heat Transfer," *Heat Transfer*. New York: McGraw-Hill, Inc., 1990, 385-483.

Jansen, J. C., Arafat, A., Barakat, A. K., and van Bekkum, H. Microwave techniques in zeolite synthesis. (1), 507-521. 1992. New York, Van Nostrand Reinhold.

Jayaraman, A., Yang, F. H., and Yang, R. T. "Effects of Nitrogen Compounds and Polyaromatic Hydrocarbons on Desulfurization of Liquid Fuels by Adsorption via π-Complexation with Cu(I)Y Zeolite", *Energy Fuels*, 2006, 20(3), 909-914.

Jiao, H. Y., Yang, L. N., Shen, J., Li, J., and Qi, Y. T. "Desulfurization of FCC gasoline over mordenite modified with Al2O3", *Pet.Sci.Technol.*,2006, 24(11), 1301-1306.

Kacirek, H., and Lechert, H. "Growth of the zeolite type NaY." *J.Phys.Chem.*, 1975, *79* (15), 1589-1593.

Kacirek, H., and Lechert, H. "Rates of crystallization and a model for the growth of sodium-Y zeolites." *J.Phys.Chem.*, 1976, *80* (12), 1291-1296.

Kim, D. S., Park, S.-E., Kang, S. O. "Microwave Synthesis of Micro-Mesoporous Composite Material." *Stud.Surf.Sci.Catal.*, 2000, *129,* 107-116.

King, David L. and Li, Liyu. "Removal of sulfur components from low sulfur gasoline using copper exchanged zeolite Y at ambient temperature", *Catal.Today*, 2006, 116(4), 526-529.

Kong, L., Li, G., Wang, X., and Wu, B. "Oxidative Desulfurization of Organic Sulfur in Gasoline over Ag/TS-1", *Energy Fuels*, 2006, 20(3), 896-902.

Kreith, F. *Principles of heat transfer*. New York: Intext Educational Publishers, 1973.

Kunii, D., Levenspiel, O. *Fluidization engineering*. Boston ; Toronto: Butterworth-Heinemann, 1991.

Kwauk, M. *Fluidization : idealized and bubbleless, with applications*. Beijing ; New York ; Toronto: Science Press ; Ellis Horwood, 1992.

Loupy, A. *Microwaves in organic synthesis*. Weinheim : Wiley-VCH, 2002.

Ma, X., Sun, L., and Song, C. "A new approach to deep desulfurization of gasoline, diesel fuel and jet fuel by selective adsorption for ultra-clean fuels and for fuel cell applications", *Catal.Today*, 2002, 77(1-2), 107-116.

Ma, X., Velu, S., Kim, J. H., and Song, C. "Deep desulfurization of gasoline by selective adsorption over solid adsorbents and impact of analytical methods on ppm-level sulfur quantification for fuel cell applications", *Appl.Catal., B*, 2005, 56(1-2), 137-147.

Mingos, D. M., Baghurst, D. R. "Applications of microwave dielectric heating effects to synthetic problems in chemistry." *Chem.Soc.Rev.*, 1991, *20* (1), 1-47.

Mohsenin, N. N. *Electromagnetic radiation properties of foods and agricultural products*. New York: Gordon and Breach, 1984.

Mostowicz, R., and Sand, L. B. "Crystallization of ZSM-5 with relatively high (Me2/n)2O/(TPA)2O reactant ratios." *Zeolites*, 1982, *2* (2), 143-146.

Mullin, J. W. *Crystallization*. Oxford ; Boston: Butterworth-Heinemann, 1993.

Murrell, L. L., Overbeek, R. A., Chang, Y. F., Puil, N. V. D., and Yeh, C. Y. "Method for Making Molecular Sieves and Novel Molecular Sieve Compositions", (6,004,527). 1999. USA.

Navarri, P., Gevaudan, A., and Andrieu, J. "Preliminary study of drying of coated film heated by infrared radiation", *Drying '92 Proc.Int.Drying Symp., 8th Pt. A*, 1992, 722-728.

Nedderman, R. M. "Fluidised Bed Reactors," Winterbottom, J. M., King, M. B., *Reactor design for chemical engineers*. 1999, 312-343.

Othmer, K. *Encyclopaedia of Chemical Technology*. New York: Wiley, 1984.

Park, S. E., Kim, D. S., Chang, J. S., and Kim, J. M. "Continuous Process and Apparatus for Preparing Inorganic Materials Employing Microwave", (US Patent 2001054549), 2001. USA.

Raghavan, G. S. V., Rennie, T. J., Sunjka, P. S., Orsat, V., Phaphuangwittayakul, W., and Terdtoon, P. "Overview of new techniques for drying biological materials with emphasis on energy aspects", *Braz.J.Chem.Eng.*, 2005, 22(2), 195-201.

Ratti, C., and Mujumdar, A. S. "Infrared Drying," Mujumdar, A. S., *Handbook of Industrial Drying*. Boca Raton, FL : CRC/Taylor & Francis, 2007, 423-437.

Reut, S. and Prakash, A. "Evaluation of sorbents for thiophene removal from liquid hydrocarbons", *Fuel Process.Technol.*, 2006, 87(3), 217-222.

Ricks, M. R. "High density fast-response (HDF) gas infrared drying: a new level of drying performance: evaluates the state of gas infrared technology available today", *Pulp & Paper Canada*, 1998, 99(6), 64.

Rollmann, L. D. and Valyocsik, E. W. "Continuous-Stream Upflow Zeolite Crystallization Apparatus", (US Patent 4,374,093). 1983.

Sandu, C. "Infrared radiative drying in food engineering: a process analysis", *Biotechnol Prog*, 1986, 2(3), 109-119.

Schiffmann, R. F. "Microwave and dielectric drying," Mujumdar, A. S., *Handbook of industrial drying*. Boca Raton, FL : CRC/Taylor & Francis, 2007, 286-305.

Serrano, D. P., and Van Grieken, R. "Heterogeneous Events in the Crystallization of Zeolites." *J.Mater.Chem.*, 2001, *11* (10), 2391-2407.

Shan, H. H., Li, C. Y., Yang, C. H., Zhao, H., Zhao, B. Y., and Zhang, J. F. "Mechanistic studies on thiophene species cracking over USY zeolite", *Catal.Today*, 2002, 77(1-2), 117-126. "

Siegel, R., and Howell, J. R. *Thermal radiation heat transfer*. New York ; London: Taylor & Francis, 2002.

Slangen, P. M., Jansen, J. C., van Bekkum, H. "Induction Heating: A Novel Tool for Zeolite Synthesis." *Zeolites*, 1997, *18* (1), 63-66.

Strauss, C. R. "A combinatorial approach to the development of environmentally benign organic chemical preparations." *Aust.J.Chem.*, 1999, *52* (2), 83-96.

Therien, N., Cote, B., and Broadbent, A. D. "Statistical analysis of a continuous infrared dryer." *Textile Research Journal* , 1991, 61, 193-202.

Thompson, R. W. "Recent advances in the understanding of zeolite synthesis." *Mol.Sieves*, 1998, *1* (Synthesis), 1-33.

Wang, X. and Jacobson, A. J. "Synthesis of Large ZSM-5 Crystals Under High Pressure.", *Mat.Res.Soc.Symp.*, (2001), 658(Solid-State Chemistry of Inorganic Materials III), GG8.1.1-GG8.1.6.

Welty, J. R., Wicks, C. E., Wilson, R. E. *Fundamentals of momentum, heat, and mass transfer*. New York: Toronto Wiley, 1984.

Wiersema, G. S., Thompson, R. W. "Nucleation and crystal growth of analcime from clear aluminosilicate solutions." *J.Mater.Chem.*, 1996, *6* (10), 1693-1699.

Wikipedia. "Dielectric heating." *http://en.wikipedia.org/wiki/Dielectric_heating*., 2010a.

Wikipedia. "Thermal Radiation." *http://en.wikipedia.org/wiki/Thermal_radiation*.,2010b.

Williams-Gardner, A. *Industrial Drying*. London, L. Hill, 1971.

Xu, H. H., Shah, D. B., Talu, O. "Synthesis of ZSM-5 Films at Elevated Gravity." *Zeolites*, 1997, *19* (2-3), 114-122.

Yang, R. T., Hernandez-Maldonado, A. J., and Yang, F. H. "Desulfurization of Transportation Fuels with Zeolites Under Ambient Conditions." *Science (Washington, DC, U.S.),* 2003, 301(5629), 79-81.

Zhdanov, S. P. and Samulevich, N. N. "Nucleation and crystal growth of zeolites in crystallizing aluminosilicate gels.", *Proc. Int. Conf. Zeolites*, 5th (1980), 75-84.

CHAPTER 6: APPLICATIONS OF LAB SYNTHESIZED NaY ZEOLITE

6.1 INTRODUCTION

The zeolite was first discovered around 250 years ago as a natural occurring mineral called stilbite (Bhatia 1990). Since then several natural occurring zeolites were discovered like chabazite, erionite, faujasite, mordinite, etc., and found their applications in areas of adsorption, ion-exchange, and reaction. The first industrially important zeolite was synthesized in laboratory in 1942. Since then more than 150 types of zeolites have been reported in literature. However, a lesser number of synthetic zeolites have been adopted in major industrial applications such as, type A, X, Y, Z, L, ZSM-5, etc. (Corma and Wojciechowski 1985). The petroleum industry has become one of the major consumer of zeolites, especially in the process of catalytic cracking, where Y zeolite is frequently used in fluid catalytic cracking (FCC) process (Breck 1974). The use of zeolite containing catalyst in fluid catalytic cracking reaction started in mid-1960s by replacing the acid leached clays and amorphous silica-alumina catalysts, which greatly increased the conversion and gasoline yield and reduced the formation of coke and dry gas formation. The first high-octane yielding FCC catalyst was commissioned in United States in mid-1970. Since then more than one third of the gasoline sold in North America and Europe originates in FCC units (Scherzer 1989). The process of fluid catalytic cracking (FCC) involves a hot and almost carbon-free catalyst, which is intimately mixed with a petroleum-derived feedstock. It is then transported through a turbulent reaction zone with a reactant residence time of 1-4 s. The vapor products from the cracking reaction are separated from the catalyst utilizing a variety of devices, then cooled and fractionated in a distillation column. After the reaction the catalyst which is partially deactivated by coke formed during the cracking reaction is regenerated by combustion in a separate regenerator. The benefits of modern reaction systems are improved selectivity towards desirable products. However, due to reduced reaction time and the elimination of non-selective conversion, an increase in reaction severity is required in order to maintain

adequate conversion. This can be achieved by increasing reaction temperature, catalyst-to-oil ratio, or catalyst activity. The higher catalyst activity is achieved by increasing the content of active ingredients in the catalyst. In general the commercial FCC catalysts are manufactured using $1-2\,\mu m$ zeolites dispersed on an amorphous silica–alumina matrix forming an average of $60\,\mu m$ particles (Scherzer 1993). The zeolites are very active in hydrocarbon conversion reactions as their pore dimensions make them selective where the molecules are adsorbed or converted. Y-zeolite plays an important role among all the components of FCC catalyst because of its activity as it provides the major part of the surface area and the active sites (Pine *et al.* 1984; Scherzer 1989). Thus, it is a major component in FCC catalyst which controls catalyst activity and selectivity (Arribas *et al.* 1987; Pine *et al.* 1984). Studies have indicated that having smaller crystallites Y zeolite introduces less diffusion resistance and hence improves the catalytic activity for FCC reaction (Camblor *et al.* 1989).

Another potential application of zeolites is the removal of sulfur compounds from liquid hydrocarbons as they cause several problems such as catalyst poisoning, corrosion, and toxic atmospheric emissions. Sulfur containing compounds released into atmosphere after the combustion of transportation fuels are the major contributors in the formation of smog, affecting the ozone layer, and acid rain. In the early 1990s, some regulations were enforced to reduce the sulfur content in liquid fuels and are becoming more stringent with time. According to new US Environmental Protection Agency (EPA 1999) regulations, added to the Clean Air Act in 2004, the sulfur content in American gasoline has been reduced from its average of 300 ppmw (parts per million by weight) to 30 ppmw in 2007, and for the diesel fuel the limit is set at 15ppmw (EPA Tier 2; 2010) (Avidan *et al.* 2001; Fredrick 2002; Hernandez-Maldonado, and Yang 2003a). The European Union Directives approved regulations lowering gasoline sulfur content from 150 ppm to 50 ppm in 2005 with a mandatory 10 ppmw limit by 2009 (EUER 2010). The traditional process to remove sulfur from gasoline and other hydrocarbons is hydrotreating or hydrodesulfurization (HDS). The HDS process adequately desulfurizes aliphatic and acyclic sulfur compounds but is not very efficient in removing thiophenes, and their derivatives in order to meet the new specifications (Bianchini and Meli 1998).

Following the HDS process, the predominant remaining sulfur compounds are thiophene, benzothiophene, dibenzothiophene.

In modern refineries, the major pool for gasoline comes from naphtha, which is obtained through FCC process. The FCC naphtha contains olefinic compounds, which are generated from cracking reactions. During hydrotreating, these olefinic compounds are hydrogenated in parallel with the HDS reaction. Thus, the olefin saturation not only reduces the octane rating of gasoline but also significantly increases the hydrogen consumption (Furimsky 1998). High operational costs and the inherent chemical limitations of the HDS process lead the petroleum industry to look for alternative ways to desulfurize gasoline to meet the new environmental and regulatory challenges. Recently, several processes have been introduced to effectively reduce the sulfur content in gasoline without dropping the octane number and reduction in hydrogen consumption. These methods are called non-HDS methods, which either do not involve the use of hydrogen for the catalytic decomposition of organo-sulfur compounds or use hydrogen in very limited quantities. Such methods involve following approaches that are considered to be attractive for attaining high levels of sulfur removal by shifting the boiling point of sulfur-containing compounds, separating by extraction or adsorption, and decomposition via selective oxidation (Babich and Moulijn 2003). Under selective adsorption one technique is commercially available which a propriety sorbent to reduce sulfur. Another promising method is called extractive mass transfer but it is in experimental state (Fredrick 2002).

In this study, attempts were made to observe the efficiency of our synthesized zeolite as submicron-size (100-200 nm) NaY zeolite crystals inside the micro/meso pores of amorphous silica using a dry process. Our synthesized zeolite was used as a FCC catalyst, and also as an adsorbent for desulfurization of hydrocarbons. We have also tried to focus on the impact of our technique on the desulfurization of hydrocarbons in petroleum industry where our technique of sulfur removing may be added as a finishing touch to the currently used hydrotreating or hydrodesulfurization (HDS) process. With the addition of our technique the removal of thiophene and its derivates may become much easier and more economical. The requirement of sulfur content down to 30 ppmw for gasoline could easily be met. This will not only reduce the

sulfur content in the exhaust gases of transportation vehicles but also help in reducing the environmental pollution due to sulfur emission.

6.2   EXPERIMENTAL

6.2.1   Synthesis of NaY Zeolite

The chemicals that were used for this study were the same as described in Chapter 3, i.e. the source of silica was obtained by porous amorphous silica (SiO_2) gel particles (Sylopol 948) with $50 \mu m$ average size supplied by W.R. Grace and Co., USA. The source of alumina was aluminum nitrate nonahydrate $(Al(NO_3)_3 \cdot 9H_2O)$ supplied by VWR, Canada. The control of pH was achieved by adding of sodium hydroxide $(NaOH)$ supplied by Alphachem Canada that also acted as a structure directing agent (SDA), and distilled water (H_2O). Beside chemicals, two types of reactors were used: polypropylene bottles of 60 ml in size, and stainless steel tube reactor $(12^{"} \times 0.25^{"})$ with an internal volume of 20.5 mL.

The synthesis method was adapted from a report in literature (Murrell *et al.* 1999), after several modifications, as reflected in experimental procedure, in order to make it suitable to our operating conditions and equipment. The starting material was silica gel particles in which aluminum nitrate nonahydrate was added in three steps to adjust the desired ratio of (SiO_2 / Al_2O_3). In the first step, 100 g of silica gel particles (size $50 \mu m$) were added with 215 g of solution of $Al(NO_3)_3 \cdot 9H_2O$ in water through incipient wetness using a 600 ml Teflon container, which provided 16.4wt% of $Al(NO_3)_3$ to silica particles. Then mixing was carried out at 500 rpm using a mixer equipped with a Rushton turbine of $2^{"}$ in diameter. The mixing was carried out for about 15 min until all the solution was adsorbed in the pores of silica particles through incipient wetness. The particles did not form any paste during mixing and remained essentially in flowable powder form. After mixing, a retention time of 1 h was given at ambient temperature for complete penetration of solution throughout the pores of silica particles. The water was then removed from the pores of the silica particles by drying the particles at $120^{\circ}C$ using a forced air convection oven until constant weight. During the process of

drying an intermittent mixing of particles was carried out in order to avoid any formation of agglomerates. The drying process allowed the removal of water from the pores and deposition of $Al(NO_3)_3$ inside the pores of silica particles. After drying, alumina was obtained by carrying out calcination at $500°C$ for 2 hr at a heating rate of $4°C/min$ in a furnace, followed by a decrease in temperature to $120°C$ with a cooling rate of $4°C/min$. The calcination process converted $Al(NO_3)_3$ to Al_2O_3. With this step, SiO_2/Al_2O_3 ratio obtained was 21. In step two, about 97 g of silica gel particles were taken from step 1, and 241 g of $Al(NO_3)_3.9H_2O$ solution in water was added to the particles, which provided 14.8 wt% of $Al(NO_3)_3$ to the silica particles. Then, the mixing was carried out at 500 rpm for 15 min and subsequently, a retention time of 1 h at ambient temperature. Drying was carried out at $120°C$ to a constant weight with intermittent mixing. Finally, calcination was carried out at $300°C$ for 6 h with a heating rate of $4°C/min$, followed by a decrease in temperature to $120°C$ with a cooling rate of $2°C/min$. In this step SiO_2/Al_2O_3 ratio obtained was as 9.6. In the third step, 97 g of silica gel particles obtained from step 2 were finally added with 222 g of $Al(NO_3)_3.9H_2O$ solution in water providing 15.9 wt% of $Al(NO_3)_3$ to silica particles, followed by mixing at 500 rpm for 15 min, and a subsequent retention time of 1 h at ambient temperature. Drying was carried out at $120°C$ to a constant weight with intermittent mixing. Subsequently, the calcination was carried out at $300°C$ for 6 h with a heating rate of $4°C/min$, followed by a decrease in temperature to $120°C$ with a cooling rate of $2°C/min$. In the third step, the SiO_2/Al_2O_3 ratio was finally adjusted to about 6.1.

During the three steps of adding Al_2O_3 to SiO_2 particles the pore volume of SiO_2 particles was reduced from $1.56cm^3/g$ to about $0.67cm^3/g$, which was due to the occupation of Al_2O_3 in the meso-pores of silica particles. Finally, in the fourth step, the addition of NaOH solution was carried out. The amount of NaOH solution used was in excess in the range of 200% to that of the pore volume of the silica particles in order to carry out the synthesis reaction. The particles did not form a paste in the presence of an excess amount of solution; however, they looked apparently wet. To carry out the fourth

step, 2 g of material obtained from the third step was added to 20wt% solution of NaOH using a 60 ml size of polypropylene bottle. Hand mixing with the help of a small glass rod was carried out in the polypropylene bottle in order to adsorb NaOH solution into the pores of precursor particles. The polypropylene bottle and stainless steel tubular reactor served as the batch reactors for the synthesis reaction. The polypropylene bottle and the stainless steel tubular reactors were sealed using Teflon tape before the reaction. An ageing time of 1 h was allowed at ambient temperature before the synthesis reaction. The molar composition of the precursor was:

$$Na_2O : 0.49Al_2O_3 : 2.98SiO_2 : 18.77H_2O$$
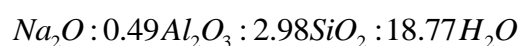
The synthesis reaction was carried at $100°C$ using the forced air convection oven by placing the sealed polypropylene bottle/stainless steel tubular reactors for 16 h and 8 h, respectively. After the synthesis reaction, the reactors were taken out of the oven and allowed to cool to room temperature under natural convection. Upon opening the reactors, the product appeared damp. It was washed with water, and filtered under vacuum using a $25\mu m$ size of filter paper. The final product was deposited on the filter paper in the form of a cake, which was then scraped with the help of a spatula and was then dried in the forced air convection oven at $100°C$.

6.2.2 Preparation and Testing of Y zeolite for FCC Reaction

Though NaY zeolite prepared by our method has several potential applications, its immediate use is in the FCC unit where the small crystal size (in submicrometer range) offers reduced diffusion resistance and aids in increasing the reaction rate. The product that we used for FCC reaction was synthesized in stainless steel tubular reactor, which was maintained at $100°C$ for 8 h. In order to prepare and test our synthesized NaY zeolite for FCC reaction, the ion exchange was carried out first to transform the NaY zeolite into HY zeolite in order to make it suitable for FCC reaction.

The ion exchange was carried out using 1M NH_4NO_3 solution which replaced the Na^+ with NH_4^+ cation. First of all a 500 ml 1M NH_4NO_3 solution was prepared and

its stirring was carried out in Rotavap at $80^{\circ}C$ for 1 h. Then 5 g of NaY zeolite was added to it. The solution was maintained at $80^{\circ}C$ under constant stirring for 6 h. After this the zeolite was recovered through washing with water and filtration. The product was further washed with ethanol and filtered. This process was repeated three times to ensure removal of Na^{+} cation. After this step the zeolite was air dried at $120^{\circ}C$ with the heating rate of 0.5-1.0 $^{\circ}C/\min$ and staying at $120^{\circ}C$ for 6 h for complete drying. Finally, calcination in air was carried out at $400^{\circ}C$ for 4-5 h. The calcination step removed NH_3 and the resulting zeolite was HY zeolite.

Since our product was composed of $50\,\mu m$ amorphous silica particles embedded with Y zeolite, therefore any further step was not required in order to make it suitable to be fed to FCC reactor. The reactor used for testing our catalyst was the RISER simulator (CREC-RISER simulator, The University of Western Ontario) using a model compound of 1,3,5-tri-isopropylbenzene (1,3,5-TIPB). Figure 6.1 provides a schematic of the RISER simulator. The reactor was loaded with 0.8 g of our synthesized catalyst. The catalyst/feed ratio was 5 i.e. for 0.8 g of catalyst 0.16 g of feed was injected. The RISER simulator was first purged with argon gas at the reaction temperature for 3 h followed by the reaction, which was carried out at 530 °C and 450 °C, respectively. The reaction time was kept at 5 s.
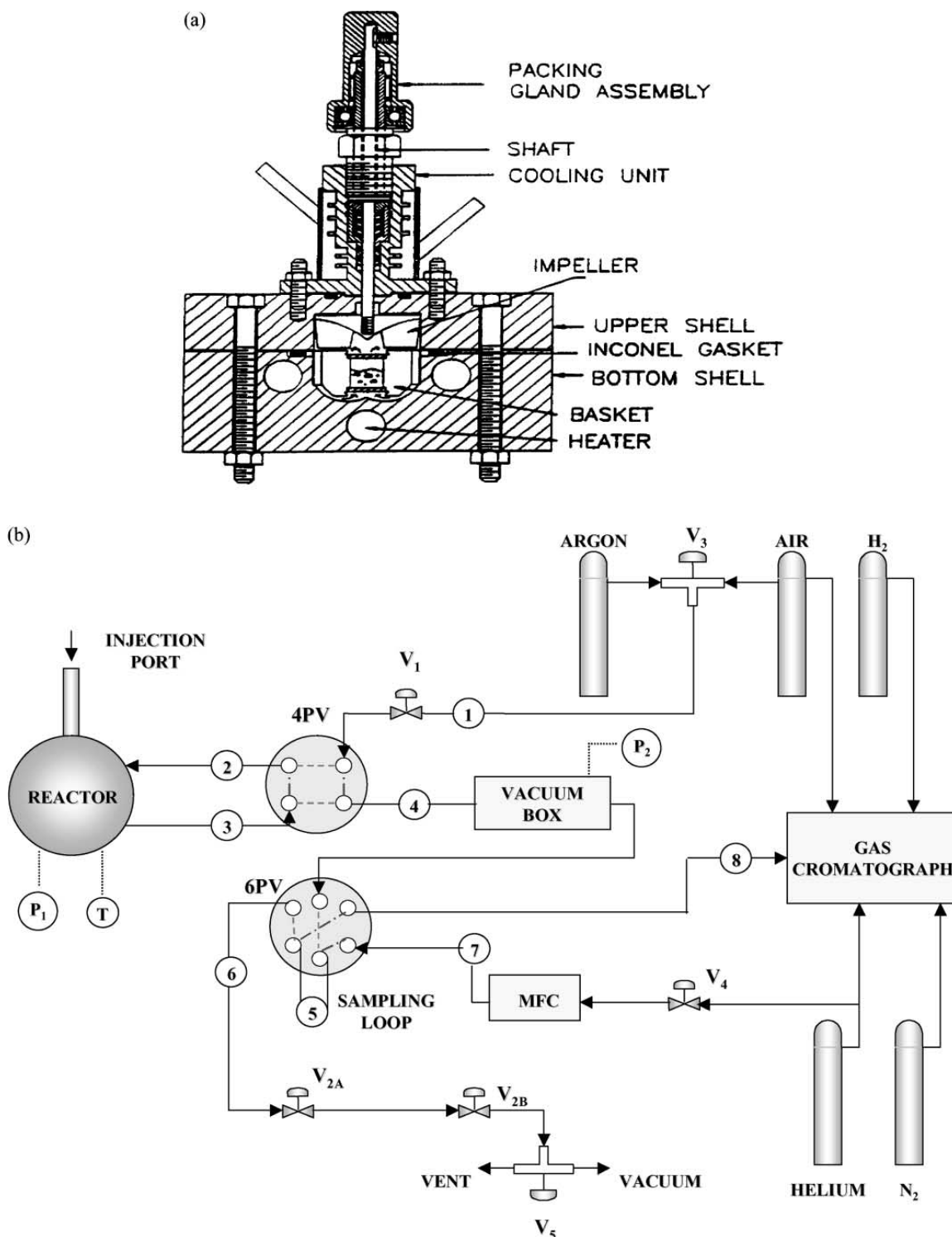
Figure 6.1: (a) Schematic description of the CREC Riser Simulator. (b) Schematic diagram of the Riser Simulator experimental set-up. (Al Khattaf and de Lasa 2002)

6.2.3   Testing of As-synthesized NaY zeolite for Desulfurization of Hydrocarbons

Another potential application is in the area of desulfurization of hydrocarbons. We used our product that was synthesized in the polypropylene bottles, which were maintained at $100°C$ for 16 h. We used the as-synthesized NaY zeolites embedded in $50\mu m$ amorphous silica particles. The purpose of using the as-synthesized NaY zeolite was to check its activity for the adsorption of sulfur compounds from hydrocarbons. In HDS processes the removal of thiophene is more challenging. That is why in this study we chose the removal of thiophene from hydrocarbons.

The preparation of NaY zeolite for desulfurization was carried out by drying the zeolite at $120°C$ for 12 h in a forced aird convection oven. This allowed removal of any traces of non-structural water from the pores of silica particles and the embedded NaY zeolite. The product after the drying was immediately transferred to a desiccator to avoid any moisture absorption. The absence of moisture absorption was checked by weighing the product before and after putting in the desiccator. The desulfurization setup consisted of a 250 ml standard flask. A rubber cork was placed on the mouth of the flask to prevent the vapors from escaping during the adsorption process. Due to the high volatility of the material, all the runs were carried out in a vacuum hood. The material was prepared by dissolving different concentrations of thiophene, ranging from 500 ppmw to 1500 ppmw, in $50\,cm^3$ of hydrocarbons including hexanes, p-xylene, and toluene. For adsorption, different quantities ranging from 2-10 g and types of adsorbents were used. The adsorbents selected were $50\mu m$ amorphous silica particles, lab synthesized NaY zeolite embedded in $50\mu m$ amorphous silica particles, commercially available NaX zeolite (Molsiv 13X 1/16" pellets), NaY zeolite (NaY-MHSZ-128 1/16" pellets), and commercial NaY zeolite fine powder $(1-2\mu m)$. Also, for certain runs the commercial pellets were reduced to $53-125\mu m$ powder for a better comparison with lab synthesized product. The size reduction of commercial pellets was carried out in a grinder and the average size of $53-125\mu m$ was achieved through sieving.

The method of adsorption consisted of taking the desired quantity of thiophene with the help of a precision pipette and added to $50\,cm^3$ of hydrocarbon solution. The

freshly dried adsorbent cooled to room temperature was added to the solution in desired quantity. A magnetic stirrer was added to the flask containing all the ingredients, and then the flask was plugged with rubber cork to avoid any escaping vapors. The ingredients in the flask were constantly stirred magnetically throughout the adsorption process. A small sample was withdrawn from the flask every 5 min, and the adsorption process was carried out for a maximum time of 105 min at ambient temperature.

6.3   ANALYTICAL METHODS

The analysis of the product from the RISER simulator was carried out by a gas Hewlett Packard 5890A Gas Chromatograph (GC). The flame ionization detector (FID) and a HP-1 25m capillary column of cross-linked silicone were used to quantify the reaction products.

The samples from desulfurization through adsorption process were analyzed in a gas chromatograph (GC) in order to determine the thiophene concentration in hydrocarbons. The gas chromatograph was equipped with a sulfur-specific flame photometric detector (FPD). A Hewlett-Packard model HP-1 (cross-linked methyl silicone) capillary column (50 m, 0.2mmID) was used. A sample of $2\mu L$ was injected in the GC apparatus using a $5\mu L$ needle injector. Table 6.1 describes the various parameters that were used for the GC analysis.

6.4   RESULTS AND DISCUSSION

6.4.1   Analysis of FCC Reaction

The FCC reaction was carried out at two different operating temperatures in order to investigate the conversion of the reactants. The reaction was carried out at 530 °C and 450 °C, respectively. The preliminary tests showed some promising results. The reaction at 530 °C exhibited a 55-65% hydrocarbon conversion and the reaction at 450 °C showed a 30-48% conversion. In order to check the reproducibility of data, when the entire procedure was repeated, the conversion at 530 °C was dropped to around 50%, which indicated fairly reproducible results. Mahgoub and Al-Khattaf (Mahgoub and Al Khattaf 2005) reported the conversion of 1,3,5-TIPB using FCC catalyst

Table 6.1: Operating Parameters Used with Gas Chromatography (GC)

Parameter	Value
Inlet	
injection temperature	$150^{\circ}C$
Pressure	25 psi
split ratio	50:1
Detector (FPD)	
detector temperature	$300^{\circ}C$
He flow rate	100 mL/min
Oven	
initial temperature	$45^{\circ}C$ for 3 min
heating condition	Ramp $15^{\circ}C/\min$, up to $100^{\circ}C$, and then held for 1 min

containing dealuminated Y zeolite for the similar conditions at $450^{\circ}C$ was less than 15%. The higher conversion in this study indicated a potential of our catalyst.

6.4.2 Desulfurization of hydrocarbons

In order to test the desulfurization of hydrocarbons using as-synthesized NaY zeolite, different parameters were addressed. These parameters included $hydrocarbon : silica$ ratio, different concentrations of thiophene, mixture of hydrocarbons, and different types of adsorbents.

6.4.2.1 Hydrocarbon to Silica ratio

When we started the testing of our zeolite we were not sure what hydrocarbon:zeolite ratio would be optimum. For this purpose we worked with 2 g, 5g, and 10 g of $50\,\mu m$ amorphous silica particles prior to NaY synthesis in $50\,cm^3$ of hexanes. These quantities corresponded $hydrocarbon : silica$ ratios of 25, 10, and 5, respectively. Figure 6.2 depicts our findings. It can be seen that the higher $hydrocarbon : silica$ ratio does not show any sign of adsorption, similar to the case of using 2 g of silica for adsorption of thiophene in hexanes. However, a lower ratio of 5 showed better results and the silica particle were considerably more effective to bring down the thiophene concentration from 500 ppmw to around 300 ppmw. Though these figures were not encouraging from silica point of view, it provided a trend of effectiveness of using lower $hydrocarbon : silica$ ratio.

6.4.2.2 Role of Lab Synthesized NaY zeolite for Desulfurization of Hydrocarbons

From the trends of using different $hydrocarbon : silica$ ratios, we selected a $hydrocarbon : zeolite$ ratio of 5 and used the same ratio throughout subsequent studies. Figure 6.3 depicts the outcome of using 10 g of lab synthesized NaY zeolite embedded in $50\,\mu m$ amorphous silica particles for the removal of 500 ppmw of thiophene from $50\,cm^3$ of hexanes. It can be seen that the lab synthesized NaY zeolite was very effective in removing thiophene from hexanes.
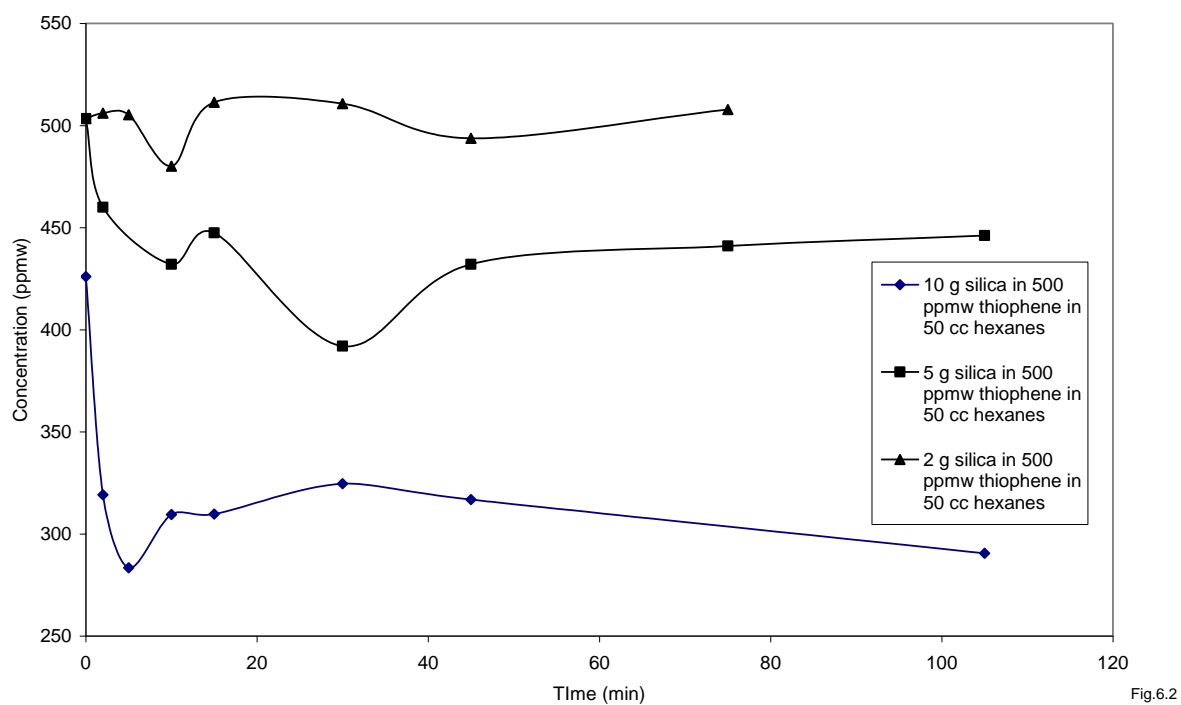
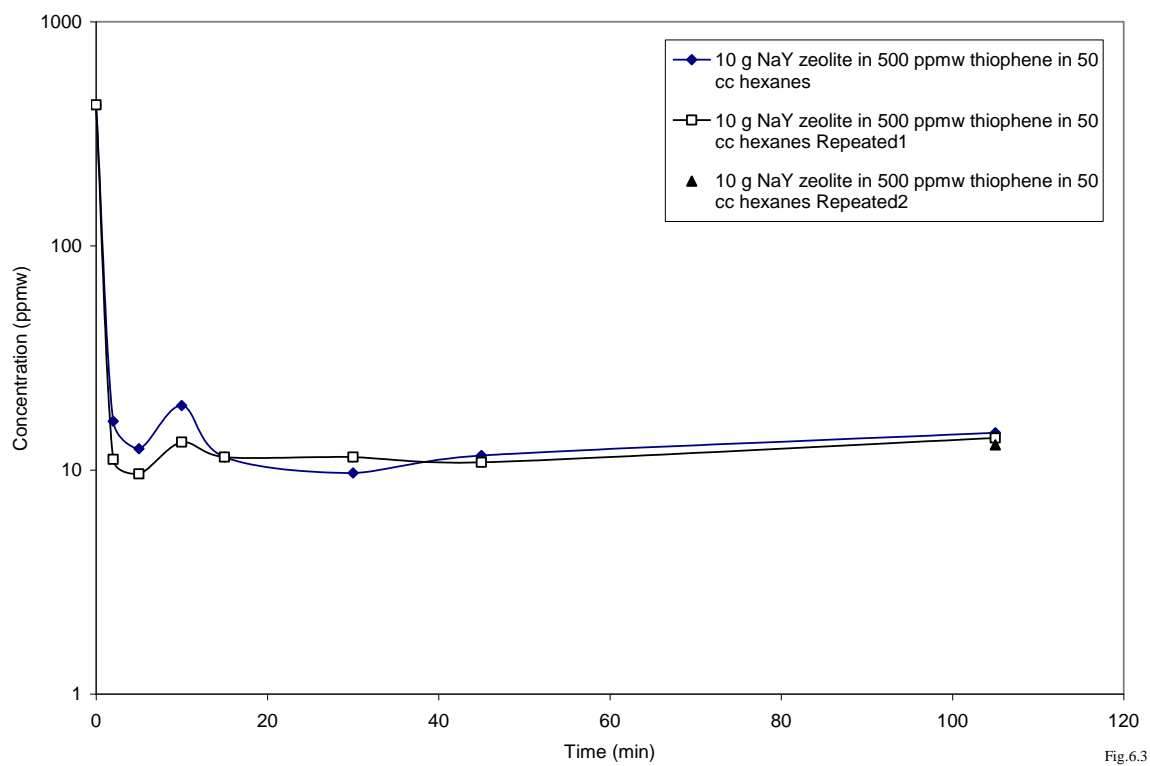Figure 6.2: Effect of hydrocarbon:silica ratio on the adsorption of thiophene in silica particles

Figure 6.3: Effect of lab synthesized NaY zeolite on the removal of 500 ppmw thiophene in 50 cc hexanes

It was found that the thiophene removal was very fast and within 5 min the concentration of thiophene dropped down to less than 15 ppmw. In order to check the reproducibility of data, three runs were carried out at the same operating conditions. It can be seen in Figure 6.3 that all the runs produced the similar results. The fluctuations in data could be attributed to sampling and analysis. The effective thiophene removal was due to its ring structure as NaY zeolite had an affinity to adsorb cycloalkenes due to having double bonds in the structure. Hexanes were either in normal or iso- forms did not pose any competition with thiophene for adsorption. Probably the crystal size played a role in removal of thiophene as the size of the crystal was in the range of $100 - 200 nm$. The advantage of using submicron size crystals, which were synthesized within the amorphous silica particles, was that the overall particle was large about $50 \mu m$ and at the same time submicron crystals were effective in removing thiophene. This scenario suggested that using these crystals in fluidized bed system would be more effective as compared to packed bed system where pressure drop is a concern with smaller particle size.

6.4.2.3 Effects of Different Concentrations of Thiophene in Hexanes on Lab Synthesized NaY Zeolite

The lab synthesized NaY zeolite was also tested for different concentrations of thiophene ranging from 500 to 1500 ppmw in haxanes. Figure 6.4 depicts the outcome of thiophene removal at different concentrations in hexanes. A similar trend was found that within the first 5 min the adsorption of thiophene reached more than 90% of the total adsorption in the entire run. The 1500 ppmw concentration of thiophene was dropped to around 100 ppmw. Whereas, the 1000 ppmw concentration of thiophene touched the 50 ppmw mark upon its adsorption in the lab synthesized NaY zeolite. All the three runs were repeated for reproducibility of data and conformed to the results.

These results also suggest that the thiophene removal was subjected to its initial concentration in the hydrocarbon. The higher initial concentration reached the thiophene saturation in zeolite early that is why the adsorption in the zeolite did not proceed below 100 ppmw. This phenomenon was reflected in other two runs using initial concentrations of 1000 and 500 ppmw, respectively.
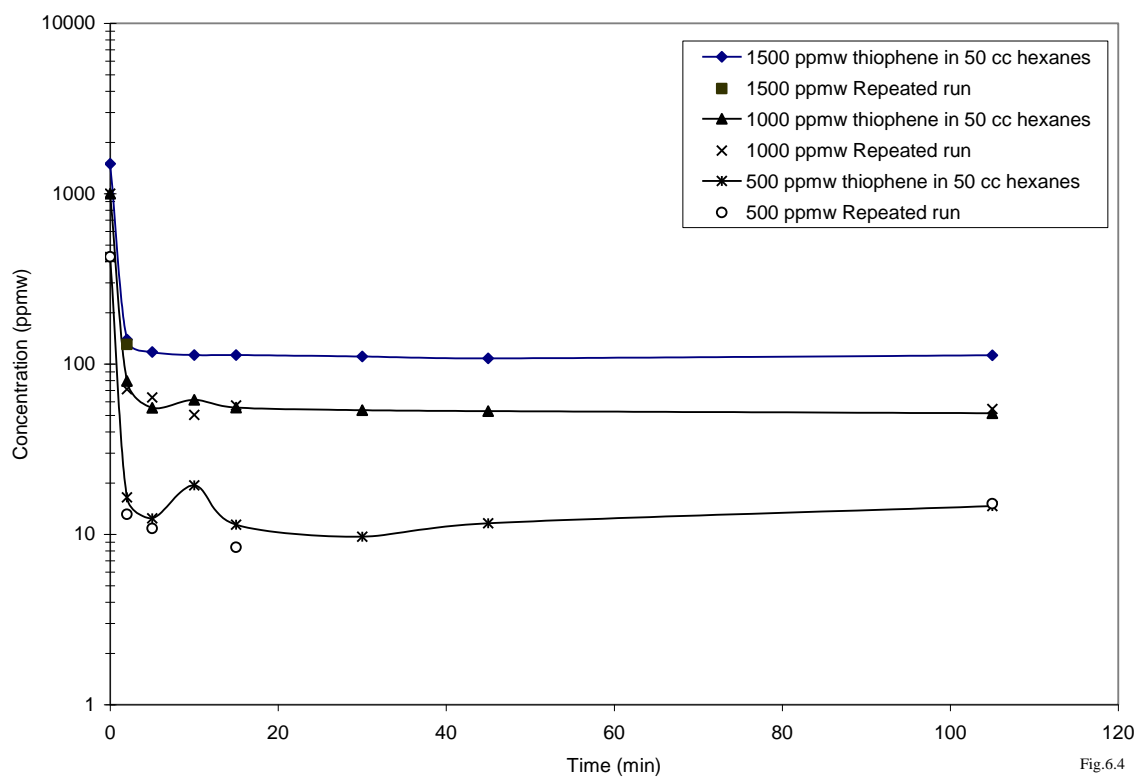
Figure 6.4: Adsorption of 500-1500 ppmw of thiophene by using lab synthesized NaY zeolite in 50 cc of hexanes

The saturation point was not reached in first case until concentration dropped down to 50 ppmw. Similar trend was observed for initial concentration of 500 ppmw that the end point reached below 15 ppmw. These results suggest a higher adsorption capacity for lab synthesized NaY zeolite.

6.4.2.4 Effects of using Different Adsorbents for the Removal of Thiophene from Hexanes

A comparison was made using different types of adsorbents to observe their effects on the removal of 500 ppmw of thiophene from $50 cm^3$ of hexanes. Figure 6.5 depicts the results of the comparison. The most inefficient adsorbent was found to be the $50 \mu m$ amorphous silica particles, which were unable to remove thiophene below 300 ppmw. However, one observation was also made that rate of removal of thiophene was very fast in the first 5 min of adsorption process. This observation suggested that the meso pores in the silica particle pose a minimal resistance for diffusing thiophene. On the other hand when commercially available NaX zeolite (Molsiv $13X 1/16"$) pellets were used, it indicated a diffusion resistance as the removal of thiophene was gradual with time. The thiophene removal rate was not as fast as amorphous silica particles, as shown in Figure 6.5. This suggested a requirement of minimal diffusion resistance for adsorption. In order to overcome the diffusion resistance, the pellets of commercial NaX zeolites were ground and the particles with an average size in the range of $53-125 \mu m$ were selected. Figure 6.5 showed that the initial thiophene removal rate was faster as compared to NaX pellets, and at the same it was similar to amorphous silica particles. However, the overall thiophene removal by NaX zeolite remained similar in both cases. This suggested that the NaX zeolite was not a suitable candidate for sulfur removal because of its lower affinity for thiophene adsorption. However, the size reduction was helpful in minimizing diffusion resistance for thiophene compound. A comparison of NaX zeolite was made by Reut and Prakash (Reut and Prakash 2006) in which NaX performed better than many other adsorbents, however, this preliminary study suggested potential prospects for our lab synthesized zeolite.
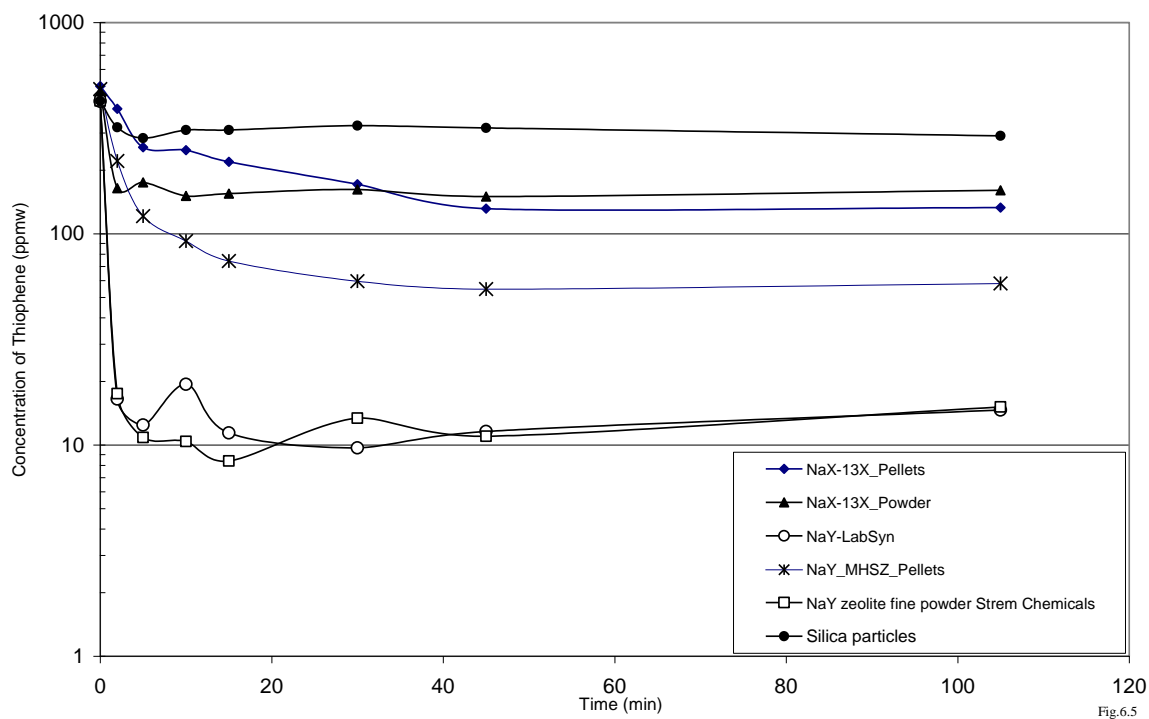
Figure 6.5: A comparison of amorphous silica particles, NaX zeolite (Molsiv 13X 1/16" comm. pellets, and 53-125 micron powder), NaY-MHSZ-128 1/16" comm. Pellets, STREM NaY comm. fine powder, and lab synthesized NaY zeolite) using 10 g of adsorbent for adsorbing 500 ppmw thiophene in 50 cc hexanes

Commercially available NaY zeolite $(MHSZ-1281/16'')$ pellets were also tested for thiophene removal. Though it was more efficient than NaX zeolite as it lowered down the thiophene concentration to about 80 ppmw; it also posed the diffusion resistance. That is why the slope of the curve was brought to zero in 45 min. This suggested that commercial NaY was effective but it took a long time to reach its saturation point. On the other hand when a commercially available NaY zeolite in fine powder (supplied by Strem Chemicals) was used, it produced the similar results that were obtained by lab synthesized NaY zeolite. The major difference between the two was that the fine powder was pure zeolite with particle size of $1-2\mu m$. Such a small size is not feasible to be used in any type of adsorption bed either fixed bed or fluidized bed. The size limitation was overcome in our lab synthesized NaY zeolite as the zeolite carrier particle was $50\mu m$ in size, which made it a suitable candidate for a fluidized bed system. A comparison of the slopes of both NaY zeolites suggested that the lab synthesized NaY zeolite was fully capable of behaving like pure zeolite and at the same time its embedded arrangement in amorphous silica particles made it viable for industrial use.

6.4.2.5 Effects of using Aromatic Mixtures on the thiophene Removal using Lab Synthesized NaY Zeolite

Since the petroleum products contain different types of aromatic compounds, two types of aromatic compounds were selected for this study to observe their effects on thiophene removal capabilities of lab synthesized NaY zeolite. For this purpose two solutions were prepared and calibrated for thiophene concentrations. The first solution was a 10wt% p-xylene in hexanes and the second solution was 10wt% toluene in hexanes. Figure 6.6 shows the effects of removal of 500 ppmw thiophene from these solutions. It can be seen that the presence of p-xylene posed no competition with thiophene for adsorption on the zeolite. For this reason the thiophene removal was swift and more than 90% of thiophene was removed in first 5 min of adsorption process.
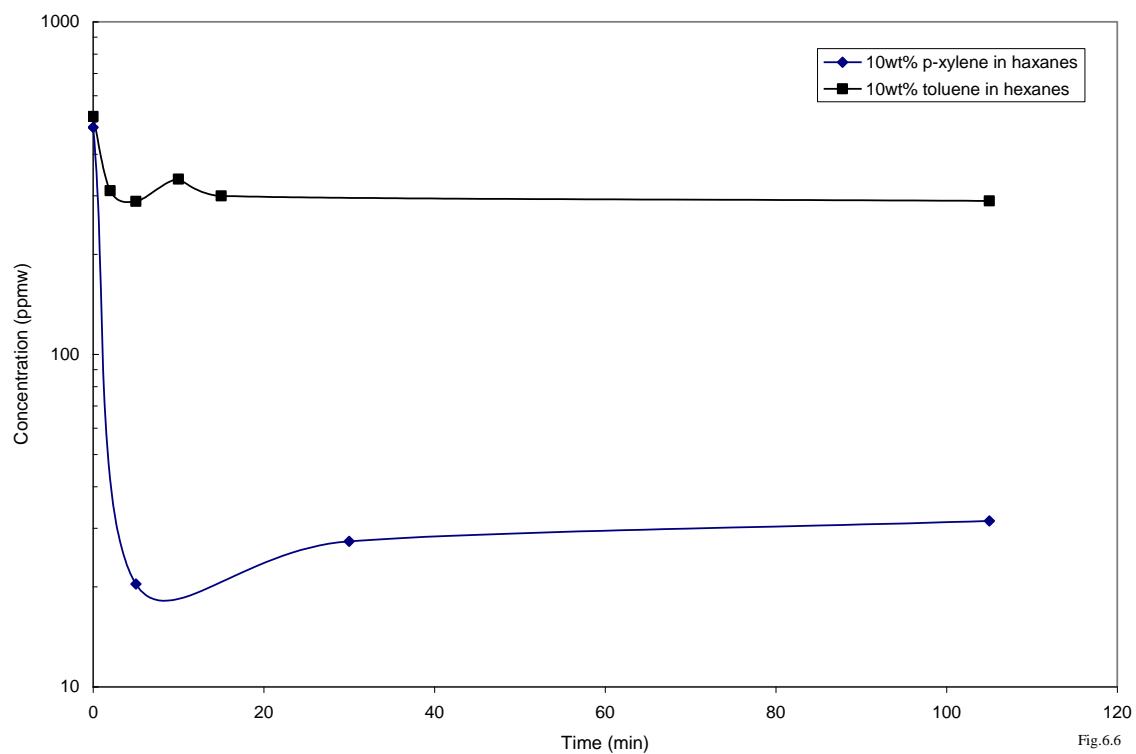
Figure 6.6: Removal of 500 ppmw thiophene from 10wt% p-xylene and 10wt% toluene in 50 cc hexanes using 10 g of lab synthesized NaY zeolite

On the other hand, when the mixture of 10 wt% toluene was subjected to adsorption, a sort of competition started to come in place, which may be explained by the $\pi-complexation$ bond nature of NaY. Thus, toluene may have a higher tendency for making $\pi-complexation$ bond with zeolite (Takahashi *et al.* 2002). For this reason the thiophene removal dropped in presence of toluene. In this case the first 5 min were still important as the most of the adsorption took place during this time and afterwards it leveled off. This scenario suggested that Na^+ cation was not capable to selectively adsorbing the thiophene. The drop in adsorption capabilities could be revived by replacing the Na^+ cation with other potential metals such as $Cu^+, Ag^+, Co^{+2}, La^{+2}$ etc. (Hernandez-Maldonado and Yang 2003a; Hernandez-Maldonado and Yang 2003b; Hernandez-Maldonado *et al.* 2005; Jayaraman *et al.* 2006; Li *et al.* 2006; Takahashi *et al.* 2002; Yang *et al.* 2003).

6.5   CONCLUSIONS

Our lab synthesized NaY zeolite converted to HY zeolite after ion exchange and used as a catalyst without any further processing resulted a higher conversion for FCC reaction for the model compound 1,3,5-TIPB. The conversion obtained was in the range of 55-65% at $530°C$ with a reproducibility error of 10%. The synthesis of NaY zeolite within the amorphous silica particles of $50 \mu m$ in size eliminated the step of loading the zeolite in an inert matrix. A further study is thus suggested to explore the potential of our synthesized catalyst. The preliminary results of as-synthesized NaY zeolite for thiophene removal from hydrocarbons were very encouraging since the adsorption was achieved in a short span of time of 5 min at ambient temperature. The lab synthesized zeolite was found to be most effective as compared to other adsorbents i.e silica particles of size $50 \mu m$, commercially available NaX and NaY zeolite pellets. The performance of commercial NaY zeolite fine powder was compatible with our synthesized NaY zeolite. However, the small size of crystals for commercial NaY zeolite made it unsuitable for any direct application in industry. Whereas, our synthesized zeolite has a potential for fluidized bed applications since the overall silica particle size is $50 \mu m$ which is embedded with NaY zeolite. The thiophene reduction to a low concentration of 15

ppmw was obtained successfully, while removing 500 ppmw of thiophene from hexanes and mixture of p-xylene in hexanes. However, the thiophene removal from the mixture of toluene in hexane was not up to the mark as the affinity of Na^+ was more for toluene than thiophene, which was due to $\pi-complexation$ bond nature of NaY zeolite. It is therefore suggested to use other metals cations $Cu^+, Ag^+, Co^{+2}, La^{+2}$ etc. to replace Na^+ for further studies. The lab synthesized NaY zeolite after some modifications may be added to oil industry as a finishing step in desulfurization process.

6.6   REFERENCES

EPA (US Environmental Protection Agency). Report EPA420-F-99-051. 1999.

EPA (US Environmental Proetection Agency)., Internet Source, http://www.dieselnet.com/standards/us/ld_t2.php 2010.

EUER (European Union emission regulations), Internet Source, http://www.dieselnet.com/standards/eu/ld.php 2010

Al Khattaf, S. and de Lasa, H. "The role of diffusion in alkyl-benzenes catalytic cracking." *Appl.Catal., A*, 2002, 226(1-2), 139-153.

Arribas, J., Corma, A., Fornes, V., and Melo, F. "Influence of framework aluminum gradients on the catalytic activity of Y zeolites: cracking of gas-oil on Y zeolites dealuminated by different procedures." *J.Catal.*, 1987, 108(1), 135-142.

Avidan, A., Klein, B., Ragsdale, R. "Improved planning can optimize solutions to produce clean fuels." *Hydrocarbon Process., Int.Ed.*, 2001, *80* (2), 47-50, 53.

Babich, I. V. and Moulijn, J. A. "Science and technology of novel processes for deep desulfurization of oil refinery streams: a review." *Fuel*, 2003, 82(6), 607-631.

Bhatia, S. *Zeolite Catalysis Principles and Applications*. Fla.: CRC Press Boca Raton, 1990.

Bianchini, C., and Meli, A. "Hydrogenation, Hydrogenolysis, and Desulfurization of Thiophenes by Soluble Metal Complexes: Recent Achievements and Future Directions." *Acc.Chem.Res.*, 1998, *31* (3), 109-116.

Breck, W. D. *Zeolite Molecular Sieves*. New York: Wiley, 1974.

Camblor, M. A., Corma, A., Martinez, A., Mocholi, F. A., Perez Pariente, J. "Benefits in Activity and Selectivity of Small Y Zeolite Crystallites Stabilized by a Higher Silicon-to-Aluminium Ratio by Synthesis." *Appl.Catal.*, 1989, *55* (1), 65-74.

Corma, A., Wojciechowski, B. W. "The chemistry of catalytic cracking." *Catal.Rev.-Sci.Eng.*, 1985, *27* (1), 29-149.

Fredrick, C. "Sulfur reduction: What are the options?" *Hydrocarbon Process.*, 2002, 81(2), 45-46,48,50.

Furimsky, E. "Selection of catalysts and reactors for hydroprocessing." *Appl.Catal., A*, 1998, *171* (2), 177-206.

Hernandez-Maldonado, A. J., Yang, F. H., Qi, G., and Yang, R. T. "Desulfurization of transportation fuels by π-complexation sorbents: Cu(I)-, Ni(II)-, and Zn(II)-zeolites." *Appl.Catal., B*, 2005, 56(1-2), 111-126.

Hernandez-Maldonado, A. J. and Yang, R. T. "Desulfurization of Commercial Liquid Fuels by Selective Adsorption via π-Complexation with Cu(I)-Y Zeolite." *Ind.Eng.Chem.Res.*, 2003a, 42(13), 3103-3110.

Hernandez-Maldonado, A. J., and Yang, R. T. "Desulfurization of Liquid Fuels by Adsorption via I_ Complexation with Cu(I)-Y and Ag-Y Zeolites." *Ind.Eng.Chem.Res.*, 2003b, 42(1), 123-129.

Jayaraman, A., Yang, F. H., and Yang, R. T., Effects of Nitrogen Compounds and Polyaromatic "Hydrocarbons on Desulfurization of Liquid Fuels by Adsorption via π-Complexation with Cu(I)Y Zeolite." *Energy Fuels*, 2006, 20(3), 909-914.

Li, Y., Yang, F. H., Qi, G., and Yang, R. T. "Effects of oxygenates and moisture on adsorptive desulfurization of liquid fuels with Cu(I)Y zeolite." *Catal.Today*, 2006, 116(4), 512-518.

Mahgoub, K. A. and Al Khattaf, S. "Catalytic Cracking of Hydrocarbons in a Riser Simulator: The Effect of Catalyst Accessibility and Acidity." *Energy Fuels*, 2005, 19(2), 329-338.

Murrell, L. L., Overbeek, R. A., Chang, Y. F., Puil, N. V. D., and Yeh, C. Y. "Method for Making Molecular Sieves and Novel Molecular Sieve Compositions." (6,004,527). 1999. USA.

Pine, L. A., Maher, P. J., and Wachter, W. A. "Prediction of cracking catalyst behavior by a zeolite unit cell size model." *J.Catal.*, 1984, 85(2), 466-476.

Reut, S. and Prakash, A. "Evaluation of sorbents for thiophene removal from liquid hydrocarbons." *Fuel Process.Technol.*, 2006, 87(3), 217-222.

Scherzer, J. "Correlation between catalyst formulation and catalytic properties." *Stud.Surf.Sci.Catal.*, 1993, 76(Fluid Catalytic Cracking: Science and Technology), 145-182.

Scherzer, J. "Octane-enhancing, zeolitic FCC catalysts: scientific and technical aspects." *Catal.Rev.- Sci.Eng.*, 1989, 31(3), 215-354.

Takahashi, A., Yang, F. H., and Yang, R. T. "New sorbents for desulfurization by π-complexation: Thiophene/benzene adsorption." *Ind.Eng.Chem.Res.*, 2002, 41(10), 2487-2496.

Yang, R. T., Hernandez-Maldonado, A. J., and Yang, F. H. "Desulfurization of Transportation Fuels with Zeolites Under Ambient Conditions." *Science (Washington, DC, U.S.)*, 2003, 301(5629), 79-81.

CHAPTER 7: CONCLUSIONS AND RECOMMENDATIONS

7.1 CONCLUSIONS

This Ph.D. dissertation is a research study based on an experimental work to explore the synthesis of nano-sized NaY zeolite within $50\,\mu m$ silica particles using a dry synthesis process. The synthesis arrangement of NaY zeolite embedded in silica particles was achieved by using three different types of reactors including polypropylene bottles, stainless steel tubular reactors, and a novel vibrated baffles fluidized bed (VBFB) reactor coupled with infrared (IR) radiation emitters as a source of thermal radiations for a fast zeolite synthesis reaction rate. The product analysis was carried out using several analytical methods including PXRD, BET, SEM, EDX, and XRF. A systematic parametric study was conducted to observe the effects of several operating conditions on the synthesis of the desired product. The shift from polypropylene bottles to stainless steel tubular reactor concluded that a faster synthesis rate was possible in the stainless steel reactors due to better heat transfer. This led to the idea of using IR radiations for a faster synthesis rate due to the possibility of higher heat transfer rates by thermal radiations. The synthesized product was further tested for its performance for fluid catalytic cracking (FCC) process in riser simulator (CREC-RISER simulator, The University of Western Ontario) using a model compound 1,3,5-tri-isopropylbenzene (1,3,5-TIPB). The conversion was compared with other studies and found to be 100% more under the similar operating conditions. Also, the as-synthesized product was tested for the desulfurization of hydrocarbons using model compounds, i.e. thiophene in hexanes and mixtures of hexanes with aromatic compounds such as p-xylene and toluene. Our lab synthesized zeolite removed thiophene from 500ppmw to less than 15ppmw in 5 min in most of the cases.

The most relevant conclusions of this thesis work are as follows:

1.   A thorough literature review revealed prevalence of heterogeneous transformation mechanism over the homogeneous mechanism in zeolite synthesis. The solid-solid transformation shifted the generally used solution based hydrothermal process towards dry synthesis mechanism. The dry synthesis mechanism showed several advantages over

the solution based hydrothermal process including the purity of the desired zeolite phase, and a reduction in chemical waste generation. During the synthesis, the composition of the starting gel and the final crystal remained the same. A reduction in the use of expensive structure directing agents, and a better control of the desired phase of zeolite were reported.

2.   The promising findings from the literature review triggered the idea of using a technique which was not only based on a dry synthesis method but also was able to produce NaY zeolites within pre-shaped silica particles. The study revealed that such synthesis can be obtained within 24 h of reaction time at a temperature of $100^{\circ}C$ using $60 mL$ polypropylene bottles as reactor. A pure NaY zeolite was obtained as revealed by the PXRD results. The zeolite crystals were embedded inside the silica particles with the cluster size of about 1-2 micrometer and crystal size was in the range of 100-200 nm. The dry synthesis process did not produce any chemical waste as all the reactants were completely utilized while reacting and transforming to zeolite product within the silica particles.

3.   The effects of different operating conditions were also tried on the synthesis of NaY zeolite embedded in silica particles. The use of different SiO_2 / Al_2O_3 ratios showed that a ratio above 6.6 did not produce any considerable crystallization for a synthesis time of 24 h. It was due to the reduction in the rate of nucleation which required the presence of Al in the vicinity of Si species. The SiO_2 / Al_2O_3 ratio of 6.1 was found to be optimum for duration of 24 h. The ageing of 1 h before the synthesis reaction helped the internal rearrangement of precursors within the silica particles, which caused the formation of structured elements related to nucleation process. However, the increase in ageing time did not make any improvement in synthesis process. The synthesis time between 16-24 h at $100^{\circ}C$ produced the desirable results using polypropylene bottles. A reduction in synthesis time below 16 h using polypropylene bottles did not reveal the desired product due to incomplete synthesis process. Increase in the synthesis temperature reduced the synthesis time but at the same time increased the crystal size, which was due to the increase in crystal growth rate. The 20.5 mL $(12^{"} X 0.25^{"})$ stainless steel tubular reactor produced the desired product in almost half the time required by the

polypropylene bottles. The higher thermal conductivity of the stainless steel tubular reactor as compared to polypropylene bottle played a role. This confirmed that a higher rate of heat transfer was essential for reduction in synthesis time. The use of higher temperature in the range of $100-170^{\circ}C$ in the stainless steel tubular reactor effectively reduced the synthesis time from 8 h to 15 min, but it caused an increase in crystal size while operating at temperatures above $100^{\circ}C$ as explained for the polypropylene bottles. The synthesis temperature above $170^{\circ}C$ showed a transformation from NaY zeolite to analcime after 15 min of synthesis reaction. The transformation was due to the metastable property of NaY zeolite which was triggered at higher temperatures and caused the NaY zeolite to transform to a more stable phase which was analcime. Thus a maximum synthesis temperature of $170^{\circ}C$ was suggested for NaY zeolite in order to achieve synthesis in 15 min. An NaOH concentration above 20 wt% affected the crystal size. The higher NaOH concentration not only reduced the crystal size but also a reduction in the cluster size was observed. A concentration more than 30 wt% was suitable for producing crystals smaller than 50 nm in size, however, a concentration beyond 32 wt% was not recommended as the dissolution of silica particles commenced and the particles lost their shape and integrity.

4.   The VBFB reactor required the pores of silica particles to be filled up to 100% in order to achieve fluidization of the silica particles and to avoid any agglomeration of silica particles. The change in NaY zeolite synthesis procedure from three-step to two-step produced silica particle pore volume in the range of $0.82-0.84\,cm^3/g$, which allowed accumulation of sufficient $32wt\%$ NaOH solution inside the pores to carry out the synthesis reaction. The effect of SiO_2/Al_2O_3 ratio in the range of 5.1 to 6.2 did not show any significant change in crystal growth, therefore, the higher ratio of 6.2 was preferred. The VBFB reactor produced crystals in the range of $300-600nm$ using the two-step zeolite synthesis procedure. The larger single crystals suggested a smaller nucleation rate. However, acceleration in surface integration mechanism was apparent as the single crystal grew at a very fast rate in the first 5 min of synthesis time. The use of IR radiation as the source of thermal radiation produced significant results with the synthesis of large single crystals, however, to acquire a better control on crystal size

remained inconclusive. The stainless steel tubular reactor produced pure NaY zeolite in 24 hr while filling the pores of silica particles between 95-100% by using two-step preparation method.

5.   The applications of laboratory synthesized NaY zeolite produced promising results. The testing of laboratory synthesized NaY zeolite was carried out in riser simulator for FCC reaction using a model compound of 1,3,5-tri-isopropylbenzene (1,3,5-TIPB) after a suitable ion-exchange of Na^+ with H^+. The product from the riser simulator for the reaction at 530 °C exhibited a 55-65% hydrocarbon conversion and the reaction at 450 °C showed a 30-48% conversion. The conversion at 450 °C was found to be 100% more than a study conducted under similar conditions. The reproduced results indicated a reduction in conversion by 10%.

6.   The desulfurization of thiophene from model compounds i.e hexanes, and mixture of p-xylene and toluene in hexanes by using as-synthesized NaY zeolite at ambient temperature showed interesting results. The optimum hydrocarbon:zeolite ratio was determined to be 5. The adsorption of 500ppmw thiophene in 50mL of hexanes using 10 g of as-synthesized NaY zeolite brought down the thiophene concentration in hexanes to below 15 ppmw in 5 min. Such finding was compared with other potential adsorbents like, amorphous $50 \mu m$ silica particles, commercially available NaX and NaY zeolite pellets of $1/16"$ in size, and a commercial pure NaY zeolite fine powder $(1-2 \mu m)$. It was found that the performance of as-synthesized NaY zeolite for thiophene removal was only matched with NaY zeolite fine powder. However, the small particle size of commercial NaY zeolite fine powder made it unsuitable for any type of adsorbing system whether a fixed bed or a fluidized bed. On the other hand the laboratory synthesized NaY zeolite was found to be suitable for fluidized bed system. The other adsorbents could not remove thiophene below 80 ppmw. The adsorption of 500 ppmw thiophene from model compounds of $10 wt\%$ p-xylene in hexanes and $10 wt\%$ toluene in hexanes showed that the presence of p-xylene did not pose any competition with thiophene. On the other hand, toluene started to compete with thiophene for adsorption which was depicted in results as removal of thiophene could not be dropped down below 300 ppmw. The affinity of toluene for making $\pi-complexation$ bond with zeolite made it difficult for thiophene to be adsorbed on zeolite.

7.2   RECOMMENDATIONS

Based on this research the following recommendations are made for future work:

1.   One-step synthesis of NaY zeolite may further reduce the synthesis time. This may be achieved by injecting the aluminum nitrate nonahydrate $(Al(NO_3)_3 \cdot 9H_2O)$ solution under saturated or super-saturated condition into silica particles. This may allow the desired SiO_2 / Al_2O_3 ratio in one step.

2.   During the preparation steps of NaY zeolite for large quantities in the range of 100 g or more, it was observed that in the final step, the addition of NaOH solution was difficult even in gradual form. That is why the addition of NaOH was carried out in steps using a smaller quantity of silica particles in the range of 5 g at a time. The dropwise addition of NaOH in 5 g of silica particles did not cause any agglomeration. However, the addition of NaOH in larger quantities of silica particle caused partial agglomeration and loss of fluidization. Thus, it is recommended that the system may be devised to overcome this challenge.

3.   During the experiments using VBFB reactor it was observed that some condensate was accumulated in the freeboard section of the fluidized bed system. The condensation of the vapors may be avoided by insulating the freeboard and by providing heating coils to maintain a constant temperature as observed in the fluidized bed section. A constant temperature throughout fluidized bed system may avoid any condensation.

4.   The synthesis in VBFB reactor produced large single crystals in the range of $300 - 600 nm$ which indicated a fast reaction coupled with accelerated surface integration mechanism. In order to achieve synthesis of smaller crystals in the range of $50 - 100 mn$ or less, a control on the crystal size in VBFB reactor may be needed.

5.   The tests on riser simulator for FCC reaction indicated promising results due to higher conversion rates. A detailed investigation is suggested to explore the full potential of laboratory synthesized NaY zeolite when used as a catalyst after suitable ion-exchange, and dealumination if required. A comprehensive product selectivity investigation is recommended.

6.   The as-synthesized NaY zeolite performed very well for the removal of thiophene from hydrocarbons through adsorption. In order to improve the adsorption capabilities of

the zeolite, the Na^+ cation may be ion-exchanged with other metal cations such as $Cu^+, Ag^+, Co^{+2}, La^{+2}$ etc. This way a better adsorbent may emerge which can handle a variety of complex aromatic compounds.

7.   The present study tested the working of as-synthesized NaY zeolite for desulfurization of hydrocarbons. It did not cover the regeneration of the zeolite. In order to fully evaluate the potentials of the zeolite, a further study including the regeneration of the spent adsorbent is needed.

8.   Since the as-synthesized zeolite was composed of $50\,\mu m$ silica particle embedded with NaY zeolite, its size made it suitable for fluidized bed system. It is therefore suggested that a fluidized bed system may be used for further unlocking the potentials of laboratory synthesized NaY zeolite as an effective adsorbent.

VITA

Name:	Syed Sameen Ali Zaidi
Post-secondary Education and Degrees:	N.E.D. University of Engineering & Technology Karachi, Pakistan 1987 B. E. Chemical Engineering
	King Fahd University of Petroleum & Minerals Dhahran, Saudi Arabia 1992 M.S. Chemical Engineering
	The University of Western Ontario London, Ontario, Canada 2010 Ph.D. Chemical Engineering
Honours and Awards:	Research Assistanceship for M.S. Research / Teaching Assistanceship for Ph.D.
Related Work Experience:	Teaching Assistant King Fahd University of Petroleum & Minerals 1989-1992
	Lecturer King Fahd University of Petroleum & Minerals 1992-2001
	Teaching Assistant The University of Western Ontario 2001-2005

Publications:
- Syed Sameen Ali Zaidi and Sohrab Rohani, "Progress Towards a Dry Process for the Synthesis of Zeolite - A Review", Reviews in Chemical Engineering, 2005, 21(5), pp. 265-306.
- S.S.A. Zaidi, and S. Rohani, "Synthesis and Characterization of NaY Zeolite", the 15th International Symposium on Industrial Crystallization (ISIC), Sorrento, Italy, 15-18 September 2002
- Mazen A. Shalabi, Sameen A. Zaidi, and Muhammad A. Al-Saleh, "Effect of Reduction Conditions on the Activity of $Ni/\gamma Al_2O_3$ Catalyst for Methanation Reaction", Chem. Eng. Comm., 1997, vol.157, pp. 23-33

Conference Presentations:
- S. Zaidi, and S. Rohani , "Synthesis and Characterization of NaY Zeolite in Pre-shaped Amorphous Silica Particles: A Parametric Study", the 55th Canadian Chemical Engineering Conference, Toronto, Ontario, 16-19 October 2005

- S. Zaidi, and S. Rohani, "Synthesis and Characterization of NaY Zeolite in an Inert Matrix: A Parametric Study", the 53rd Canadian Chemical Engineering Conference, Hamilton, Ontario, 26-29 October 2003
- S. Zaidi, and S. Rohani, "Synthesis and Characterization of NaY Zeolite in an Inert Matrix", the 52nd Canadian Chemical Engineering Conference, Vancouver, 20-23 October 2002